

Towards Turaev-Viro topological field theories on
stratified manifolds
Evaluation at vertices and local moves

Dissertation with the aim of achieving a doctoral degree at the
Department of Mathematics
Faculty of Mathematics, Informatics and Natural Sciences
University of Hamburg

submitted by
Julian Farnsteiner

Hamburg, 2023

Supervisor and first referee

Prof. Dr. Christoph Schweigert, Universität Hamburg

Second referee

Prof. Dr. Alexis Virelizier, Université de Lille

Submitted

08 May, 2023

Fachbereich Mathematik, Universität Hamburg

Defended

12 July, 2023

Erklärung

Hiermit erkläre ich an Eides statt, dass ich die vorliegende Dissertationsschrift selbst verfasst und keine anderen als die angegebenen Quellen und Hilfsmittel benutzt habe.

Hamburg, 29.09.2023

Julian Farnsteiner

Summary.

In the definition of 3-dimensional topological field theories of state-sum type, the evaluation of certain graphs on spheres that surround vertices of a triangulation is a crucial ingredient. For the definition of a topological field theory on manifolds with stratifications, such an evaluation has been known only for specific geometric configurations. For general configurations, an extruded graph on a sphere has to be evaluated to a scalar.

In this thesis, we define such an evaluation for extruded graphs labeled by spherical fusion categories and traced bimodule categories over them. We prove that this evaluation is invariant under a set of local moves, which makes the evaluation explicitly computable. We show that the definition specializes to known evaluation procedures in specific situations. The results pave the way towards a construction of topological field theories on stratified manifolds.

Zusammenfassung.

Die Evaluation bestimmter Graphen auf Sphären, die die Vertizes einer Triangulierung umschließen, ist ein wesentlicher Bestandteil der Definition von dreidimensionalen topologischen Feldtheorien, die auf Zustandssummen basieren. Eine solche Evaluation, die für die Definition einer topologischen Feldtheorie auf stratifizierten Mannigfaltigkeiten geeignet ist, ist bislang nur für spezielle geometrische Konfigurationen bekannt. Um allgemeinere Konfigurationen einzuschließen, muss ein extrudierter Graph auf der Sphäre evaluiert werden können.

In dieser Dissertation definieren wir eine solche Evaluation für extrudierte Graphen, die mit sphärischen Fusionskategorien und Bimodulkategorien mit Spur beschriftet sind. Wir beweisen, dass die Evaluation unter einem Satz lokaler Transformationen invariant bleibt, was die Evaluation explizit berechenbar macht. Wir zeigen außerdem, dass sich die Definition in Spezialfällen auf bekannte Evaluationsvorschriften spezialisiert. Diese Ergebnisse ebnen den Weg für die Konstruktion einer topologischen Feldtheorie auf stratifizierten Mannigfaltigkeiten.

CONTENTS

1	Introduction	7
2	Algebraic Preliminaries	14
2.1	Calabi-Yau Categories	15
2.2	Monoidal Categories	15
2.3	Diagrammatic Notations	16
2.4	Hom-Space Contractions	17
2.5	Ends and Coends	18
2.6	Computing with Components	20
2.7	Traced Bimodule Categories	23
2.8	Centers of Bimodule Categories	26
2.9	Balanced Functors and Functorial Diagrams	28
2.10	(Split) Equalizers of Bi-Balanced Functors	31
2.11	Shifting Actions under (Co-)Ends	35
2.12	Relative Deligne Products and Schaumann’s Tricategory.	40
2.13	Eilenberg-Watts-Equivalences.	45
2.14	Silent and Cosilent Objects	46
2.15	Generalized Yoneda Lemmas for Balanced Functors	47
2.16	Contraction Operations	51
2.17	Module (Co-)Ends	53
3	Extruded Graphs and their Evaluation	58
3.1	Defect Manifolds and Extruded Graphs	58
3.2	The Modular State-Sum Functor	65
3.3	Definition of the Evaluation	71
3.4	Lasso Graphs	74
3.5	Loop Graphs	79
4	Moves of Invariance	83
4.1	Overview of Moves	84
4.2	Elementary Moves	96
4.2.1	Proof Strategy for Elementary Moves	96
4.2.2	OR – Orientation Reversal	97
4.2.3	C – Contraction	98
4.2.4	EF – Edge Fusion	100
4.2.5	SV – Subside Vertex	104
4.2.6	Fun – Functoriality	106
4.3	Composite Moves	106
4.3.1	DV – Dissolve Vertex	106
4.3.2	L – Loop Move	107
4.3.3	DE – Dissolve Edge	108
4.3.4	IH – Internal Hom-Move	112

5	Towards a Turaev-Viro TFT with Defects	114
5.1	The Lego-Teichmüller Game	115
5.2	Relating Extruded Graphs to Knotted Nets	116
5.3	Relation to Polygon Diagrams	132
5.4	State-sums with Defects	134

1 INTRODUCTION

The idea to associate to topological or geometric objects algebraic invariants pervades many fields of mathematics, ranging from differential geometry to algebraic topology. In quantum topology, the notion of a topological field theory has received much attention: it assigns invariants not only to manifolds, but also to (extended) cobordisms, thus ensuring locality of the manifold invariants, which take values in a field \mathbb{K} .

The modern notion of state-sum models on 3-manifolds dates back to the Ponzano-Regge model [PR68] of 3-dimensional quantum gravity. This theory is prone to divergence issues as the "sum" refers to a sum over isomorphism classes of irreducible $SU(2)$ -representations – which there are infinitely many of. In what can be described as a regularization of the model, Turaev and Viro [TV92] took the quantum group $U_q\mathfrak{sl}(2)$ instead of $SU(2)$ as the input datum for their construction. Nowadays, one often uses a *category* instead of a Hopf algebra as the algebraic ingredient for the construction of a state-sum model. More concretely, Barrett and Westbury [BW96] showed that a *spherical fusion category* is the appropriate structure for this purpose.

A spherical fusion category is, in particular, a \mathbb{K} -linear monoidal category. *Fusion* is a finiteness and semisimplicity property for \mathbb{K} -linear monoidal categories, while *spherical* refers to a structure that ensures particularly well-behaved dualities. These qualities of spherical fusion categories are essential for the definition of a state-sum invariant, which we now recall, loosely following the formulation of [TV17].

State-sums are defined not for closed 3-manifolds, but for closed 3-manifolds with an embedded auxiliary substructure, which for the moment the reader might imagine as a triangulation. In a second step, it has to be proven that the value of the state-sum does not depend on the choice of triangulation – only then is it an invariant of 3-manifolds. Given a spherical fusion category \mathcal{A} and a 3-manifold M with triangulation, one assigns to each face of the triangulation a simple object of \mathcal{A} to label it with. These simple objects are the "states" over which a sum will be performed. The sum will be finite because \mathcal{A} is a *fusion* category, which implies that up to isomorphism, \mathcal{A} only has finitely many simple objects. Now consider a small, ball-shaped neighborhood around a vertex v of the triangulation of M . The boundary of the neighborhood is a 2-sphere which intersects the edges and faces adjacent to v . This intersection is a graph on a sphere, whose edges stem from the faces of the triangulation, and whose vertices stem from the edges of the triangulation. The edges of the graph inherit a labeling with simple objects of \mathcal{A} from the faces. To such a graph on a sphere, the graphical calculus of a spherical category assigns a linear form on a finite-dimensional vector space associated with the graph. The vector space in question is a tensor product over hom-spaces: one for each vertex of the graph. Having obtained a linear form for each vertex of the triangulation, a vector is needed on which the linear forms can be evaluated. Indeed, a natural choice for such a vector exists due to the semisimplicity of \mathcal{A} , which is again part of the *fusion* property. This defines a scalar for each labeling of faces by simple objects on \mathcal{A} . The state-sum is defined as the sum of the scalars for all choices of labels, adjusted by some weighting and normalization factors.

A feature of state-sum invariants of manifolds is that they are local: The construction can not only be defined for manifolds, but for cobordisms, making it a *topological field theory* (TFT). This means in particular that the state-sum invariant of a given manifold can be computed by

cutting the manifold into pieces, and performing the state-sum for each piece. For the state sum models of interest in this thesis, it is believed that this construction be iterated so that they even define a fully extended TFT.

DEFECT STRUCTURES. In state-sum models with *defects*, one considers an invariant not for manifolds, but stratified manifolds, which might in particular have boundaries. We refer to the stratification as a *defect structure*, in which each stratum is a defect – a substructure embedded in a manifold, labeled with additional algebraic data. An invariant of manifolds with defects provides a geometric tool to study the algebraic data which label the defects.

State-sums for manifolds with (framed) 1-dimensional defects (or *defect lines*) are well-understood [BK10], even when they, together with 0-dimensional defects, form a network of defect lines in the manifold [TV10; TV17]. A first example of a 2-dimensional defect is the boundary of a compact 3-manifold. It is possible to define a state-sum for compact 3-manifolds with boundary and defect lines [FS22]. Defect lines are then embedded either in the boundary or in the interior of the 3-manifold, and their algebraic labels are distinct. If we consider the state-sum with respect to a spherical fusion category \mathcal{A} , then boundary defect lines have to be labeled by objects of \mathcal{A} (or a Morita equivalent spherical fusion category), while interior defect lines are labeled by objects of the Drinfeld center $\mathcal{Z}(\mathcal{A})$.

Such a structure may seem contrived, but there are relevant examples: The Frobenius-Schur indicator is a classical quantity from representation theory, which assigns a number to a complex representation of a finite group, and is, among other qualities, capable of detecting whether an irreducible representation is (a) a complexification of a real representation, can (b) be obtained by restriction of scalars from a quaternionic representation, or is (c) not self-dual. A modern generalization of the Frobenius-Schur indicator takes as input datum a pair (a, x) , where $a \in \mathcal{A}$ is an object of a spherical fusion category, and $x \in \mathcal{Z}(\mathcal{A})$ is an object of its Drinfeld Center. This Frobenius-Schur indicator can be obtained as the state-sum for a solid torus, with an x -labeled defect loop embedded in its interior and a configuration of a -labeled defect lines embedded on the boundary, revolving around the torus [FS22]. Moreover, this description allows for reasoning about the indicator, as some of its properties can be understood in geometric terms. State-sums for other manifolds with defects have been associated with representation-theoretic quantities in [Meu22].

A state-sum invariant for closed 3-manifolds with an embedded defect structure consisting of 2-, 1-, and 0-dimensional cells has been developed by Meusburger [Meu22] under the requirement that the defect structure as a whole forms a 2-manifold. This thesis aims to develop some of the tools that are necessary for a further generalization eliminating this restriction. If we want to propose a state-sum construction for 3-manifolds with defects in all codimensions, there are two important questions to be answered.

1. Which types of algebraic data should label the defects of various dimension?
2. How do we evaluate at vertices?

The first question has essentially been answered in the literature. The point of the thesis is to provide a solution to the second question. We present the following answers:

1. The algebraic labeling of the defect structure is composed of:

3-cells	Spherical fusion categories.
2-cells (Defect surfaces)	Finite semisimple bimodule categories over the spherical fusion categories that label the adjacent 3-cells. The bimodule categories are equipped with the additional structure of a bimodule trace, which is equivalent to a pivotal structure.
1-cells (Defect lines)	Objects in the relative Deligne product over all bimodule categories that label the adjacent 2-cells. In the case of a defect line is adjacent to precisely two 2-cells, these objects may be described as bimodule functors between the bimodule categories that label the 2-cells.
0-cells (Vertices)	Linear forms on the <i>block space</i> of the vertex, which is a vector space assigned to the vertex that takes into account the geometry of its neighborhood, as well as all the algebraic labels for the adjacent defect strata of higher dimension.

That bimodule categories are suitable labels for defect surfaces has been observed for some time [KK12; FSV13]. Bimodule traces as additional structures on bimodule categories originate in [Sch13b]; they equip the higher Morita category of spherical fusion categories and traced bimodule categories with duals [Sch13a]. Traced module categories have been used as labels for boundaries in state-sum models implicitly, see e.g. [LFHSV21], and defect surfaces labeled with traced bimodule categories appear in [Meu22]. The labeling of defect lines with bimodule functors is in agreement with [Meu22]. It is established [FSS22] that objects in the relative Deligne product are the appropriate generalization for the labels of defect lines with more than two adjacent defect surfaces. The labeling of vertices by linear forms on block spaces is new to this thesis. In other approaches, bimodule natural transformations [Meu22] or morphisms in a Drinfeld center [TV17] are used to label 0-dimensional defects. Block spaces in our sense were introduced in [FSS22] and can be thought of as generalized, symmetric versions of vector spaces of natural transformations.

2. Sufficiently small closed ball neighborhoods of a vertex have the structure of an *extruded graph*, as illustrated, for instance, in (3.44). Extruded graphs can be evaluated to a scalar without the need to resort to projections or a pre-determined set of local moves.

Having provided a definition for how extruded graphs are to be evaluated, we owe a convincing argument for why our proposition is a good, or even *the correct* evaluation procedure for the purpose of building a state-sum model. The following main results of the thesis substantiate this claim:

- (a) Loop graphs as depicted in (3.61) evaluate to traces, as would be expected in a graphical calculus. This is the content of Theorem 3.28.
- (b) We specify a set of local moves which any reasonable evaluation should be invariant under. We prove this invariance property for our evaluation procedure in Theorem 4.4.

- (c) Our method of evaluation is the unique evaluation procedure which satisfies (a) and (b), as shown in Theorem 4.5.
- (d) The evaluation of extruded graphs specializes to the ordinary graphical calculus of a spherical fusion category. This statement is made precise in Theorem 5.12.

Let us now shed some light into the two "black boxes" that appeared in the discussion so far: The block space associated to a vertex, and the evaluation procedure for extruded graphs.

BLOCK SPACES AND PRE-BLOCK SPACES. To this end, we need to gain a better understanding of the neighborhood of a vertex v in a defect structure. We can describe it as follows: The surface of a small ball neighborhood is a sphere, and the intersection of the surface with the surrounding defect structure is a graph on the sphere. The edges of this graph inherit a labeling by bimodule categories from the defect surfaces. To differentiate the graph's vertices from the vertices of the defect structure, such as v , we refer to the former as *nodes*. Within the interior of the neighborhood, there are defect lines that connect the vertex v radially with the nodes. These lines are also labeled by algebraic data, namely objects in relative Deligne products. To this graph on a sphere, along with its associated algebraic labels, we need to assign a vector space. There is a natural candidate for such a vector space: the *block space* constructed in [FSS22]. It can be seen as a result of this thesis that this block space is an appropriate space of labels for the vertices of a defect structure.

Recall from [FSS22] that the block space is defined as a subspace of a larger vector space known as the pre-block space, which is a common construction in state-sum models. Roughly speaking, the pre-block space is a hom-space in a large Deligne product, whose arguments are the objects that label the defect lines adjacent to v , but without balancings. We can think of the pre-block space as storing information about which adjacent defect lines are linked by a defect surface. The block space is a subspace of the pre-block space, consisting of those vectors that satisfy a set of conditions, one for each of the 3-cells adjacent to v . These conditions are expressed through an equalizer diagram into which in particular the balancings of the objects labeling the defect lines enter, and the block space is defined as its equalizer in Section 3.2.

EXTRUDED GRAPHS. In a state-sum model without defects, the neighborhood of a vertex in a triangulation defines a graph. A choice of objects (state-sum variables) for edge labels and morphisms for vertex labels turns this graph into a string diagram on the sphere.

Similarly, the neighborhood of a vertex v in a defect structure, as described earlier, needs additional algebraic labels to constitute an *extruded graph* as pictured in (3.44). The graph on the boundary sphere of the neighborhood has edges labeled by bimodule categories. A secondary label is needed for each of the edges: a choice of object in the corresponding bimodule category. To each node (vertex of this graph), we associate a vector space, which is a hom-space that couples the objects labeling the adjacent edges to the object in the relative Deligne product which labels the adjacent defect line. Each node must be labeled with a vector from the corresponding vector space. Lastly, recall that the vertex v is labeled with a linear form on the block space. All of these data combined endow the neighborhood of v with the structure of an extruded graph,

which, through our evaluation procedure, yields a scalar invariant. The notion of an extruded graph will be made precise in Section 3.1.

THE EVALUATION. The evaluation of extruded graphs can be seen as an extension of the graphical calculus on spheres. Usually, a graphical calculus is defined by first choosing a projection of the diagram in question. For instance, string diagrams for braided categories are embedded in 3-dimensional space, but to be able to evaluate them, they have to be projected onto a standard plane. It is then a theorem that the evaluation does not differentiate between different choices of projection; see [JS91, Thm. 3.5] for one formulation of this statement. While working with string diagrams for braided categories in this way is manageable, the projection-based approach has disadvantages. In the case of extruded graphs, the combinatorics involved in transforming one choice of projection into another are unknown to us. For us, defining a projection-based evaluation is therefore neither feasible nor desired.

Indeed, the evaluation procedure for extruded graphs we present in Section 3.3 is defined without resorting to projections. It involves three steps. In the first step, the labels of the nodes are used to define a vector in the pre-block space. From this vector, a corresponding vector in the block space is then constructed. Finally, in the third step, the linear form that labels the vertex v is evaluated on the obtained element of the block space. The first and third steps of the evaluation procedure are relatively tame. It is the second step which is most significant. It involves a distinguished linear map from the pre-block space to the block space, which was, however, only a subspace by definition. The key insight needed here is that in the semisimple setting, the spherical structure on the involved fusion categories exhibits the equalizer from the definition of the block space as a *split equalizer*. This means that the block space is not merely a subspace of the pre-block space, but a retract. Consequently, any vector in the pre-block space comes with a distinguished projection provided by the spherical structures into the block space, as is required in the second step of the evaluation procedure.

LOCAL MOVES. Since we defined the evaluation without choosing any projection, it evidently provides a well-defined quantity associated to the extruded graph. No theorem is necessary that ensures the independence of a projection. This feature comes with a drawback: It is hard to use the definition we give to directly compute the evaluation of an extruded graph. We address this problem by providing tools for practical calculations in Section 4. Namely, we introduce a set of local moves for extruded graphs, which leave the evaluation invariant. Evaluating an extruded graph using local moves is then a process of gradually simplifying the extruded graph, until it is of a standard form, called a *loop graph*. We show that loop graphs, pictured in (3.61), evaluate to a trace.

The set of local moves includes generalizations of standard moves for string diagrams. We briefly mention two of them: A strand connecting two vertices of a string diagram, can be *contracted* into a single vertex. The new vertex needs to be labeled with a morphism, which is obtained by composing the labels of the old vertices. We call the corresponding move on extruded graphs the **C**-move. It also consists of a topological transformation, in which two nodes are replaced by one, and an algebraic prescription detailed in Section 2.16 to obtain the label of the new node from the two labels of the nodes that have been contracted. In string diagrams for

monoidal categories, the juxtaposition of strands represents the monoidal product of the objects that label them. As a consequence, a pair of parallel strands can always be replaced with a single strand labeled with a monoidal product. The **EF**-move for extruded graphs is similar, though a relative Deligne product has to be taken instead of a monoidal product.

That the corresponding local moves for string diagrams leave the evaluation invariant follows immediately from the projection-based definition. We prove the invariance of the evaluation under these moves and others for extruded graphs, which is a main result of the thesis.

RELATION TO OTHER KNOWN EVALUATIONS. Specific extruded graphs can be reduced to string diagrams in a spherical fusion category \mathcal{A} on the surface of a ball, with additional strands, labeled by objects in the Drinfeld center $\mathcal{Z}(\mathcal{A})$, pointing radially inwards towards the center of the ball. This type of diagram is encountered in state-sum models with at most 1-dimensional defect structure [BK10; TV17]. In Section 5.2, we show that the evaluation of such specific extruded graphs reproduces the usual, projection-based evaluation of these diagrams.

In the state-sum model with defects introduced in [Meu22], yet another class of diagrams appeared, called *polygon diagrams*. Like extruded graphs, polygon diagrams involve a labeling of edges by objects of different traced bimodule categories. They are, however, planar in nature. This is appropriate for the model: because the defect structure in [Meu22] is required to be a 2-manifold, graphs on the surface of a ball neighborhood of a vertex in the defect structure come with a distinguished plane on which they can be projected. Some extruded graphs can be compared to polygon diagrams. In these cases, the respective evaluations agree as well, see Section 5.3.

TOWARDS DEFINING A STATE-SUM. Having developed a theory of extruded graphs, and shown that their evaluation specializes to known evaluation procedures, we are in a position to propose a state-sum model with defects in Section 5.4, though proving the independence of triangulation remains beyond the scope of this thesis. Looking forward, it seems likely that extruded graphs can be used to further simplify the definition of state-sum models. This is because while the extruded graphs we considered so far are of spherical shape, higher-genus extruded graphs can be considered as well. It is then feasible, as outlined in Remark 5.15, that the state-sum of a triangulated 3-manifold with defects can be computed as from the evaluation of a single extruded graph, whose topology is a tubular neighborhood of the 1-skeleton of the triangulation. This has, however, to be relegated to future work.

ACKNOWLEDGEMENTS I am thankful to my advisor Christoph Schweigert, who spent many hours with me discussing extruded graphs, pointing me towards new literature, and explaining ideas; leaving me with new problems to solve each time. When I was ready to get lost in details, I could rely on him to always have the bigger picture in mind, and to bring me back on track. I always left our discussions with more motivation than I entered them with.

I thank Catherine Meusburger for various discussions during her visit to Hamburg, which contributed to my understanding of state-sum models. I am also grateful to Alexis Virelizier, who inspired me to rethink in how far extruded graphs are 2- or 3-dimensional.

At the university, I was lucky to share an office with David Jaklitsch. His understanding of pivotal module categories has also helped this thesis at various points.

Most of the work on this thesis, however, was done in home-office. In this environment, I must thank Katrin Suchowski not only for creating the many pictures scattered through the following pages, but even more for putting up with the ups and downs of accompanying me on this endeavor over the past years. She and the rest of my family are a constant source of support for me, which I am grateful to have.

2 ALGEBRAIC PRELIMINARIES

Before we can introduce extruded graphs, the objects of interest in this thesis, in Section 3, we need to develop some algebraic machinery that is necessary to work with them. Some of this section is spent fixing notation, and recalling standard concepts, such as bimodule categories, categorical centers and the relative Deligne product. Lesser-known structures which are reviewed include bimodule traces in Section 2.7. More importantly though, we lay out some specific algebraic tools that are necessary to work with extruded graphs, such as the piecewise module coend in Section 2.17.

Throughout this paper, let us fix an algebraically closed field \mathbb{K} of characteristic 0. We will mainly work with \mathbb{K} -linear categories, using standard terminology that can be found in [EGNO15]. When not stated otherwise, all linear categories are also assumed finite and semisimple.

The following notational conventions serve to shorten and clarify the presentation:

- Given any category \mathcal{C} with objects $x, y \in \mathcal{C}$, we denote hom-sets by angled brackets:

$$\langle x, y \rangle := {}_{\mathcal{C}}\langle x, y \rangle := \text{Hom}_{\mathcal{C}}(x, y). \quad (2.1)$$

- Lowercase bold letters $(\mathbf{x}, \mathbf{y}, \dots)$ are used for objects that are necessarily simple. In a finite semisimple category \mathcal{C} , the notation

$$\sum_{\mathbf{x} \in \mathcal{C}} \dots \quad (2.2)$$

stands for a sum over the set of isomorphism classes of simple objects of \mathcal{C} , with \mathbf{x} assuming the value of a representative for each class in the sum.

- We denote the opposed category to any category \mathcal{C} by an overline:

$$\overline{\mathcal{C}} := \mathcal{C}^{\text{op}}. \quad (2.3)$$

If $x \xrightarrow{g} y \xrightarrow{f} z$ are objects and morphisms in \mathcal{C} , then we also denote the corresponding objects and morphism in $\overline{\mathcal{C}}$ by an overline:

$$\overline{z} \xrightarrow{\overline{f}} \overline{y} \xrightarrow{\overline{g}} \overline{x}. \quad (2.4)$$

Using this overline-notation, the relation between composition in \mathcal{C} and composition in $\overline{\mathcal{C}}$ can be written out concisely as

$$\overline{f \circ g} = \overline{g} \circ \overline{f}. \quad (2.5)$$

- If \mathcal{X} and \mathcal{Y} are linear categories, we frequently consider the Deligne product $\mathcal{X} \boxtimes \mathcal{Y}$. We treat the Deligne product as strictly associative and use tacitly that the equivalence $\mathcal{X} \boxtimes \mathcal{Y} \cong \mathcal{Y} \boxtimes \mathcal{X}$ is symmetric. In practice this means that we can identify any two orderings of a multiple Deligne product via a distinguished equivalence: Let $\mathcal{X}_1, \dots, \mathcal{X}_n$ be linear

categories, and let σ be a permutation of $\{1, \dots, n\}$. By the universal property of the Deligne product, the functor

$$\begin{aligned} \mathcal{X}_1 \times \dots \times \mathcal{X}_n &\rightarrow \mathcal{X}_{\sigma(1)} \boxtimes \dots \boxtimes \mathcal{X}_{\sigma(n)} \\ (x_1, \dots, x_n) &\mapsto x_{\sigma(1)} \boxtimes \dots \boxtimes x_{\sigma(n)} \end{aligned} \quad (2.6)$$

defines an equivalence $\mathcal{X}_1 \boxtimes \dots \boxtimes \mathcal{X}_n \cong \mathcal{X}_{\sigma(1)} \boxtimes \dots \boxtimes \mathcal{X}_{\sigma(n)}$. If throughout this work the ordering of a Deligne product is changed, it will always be via this equivalence.

2.1 CALABI-YAU CATEGORIES

A linear category \mathcal{C} equipped with a *trace* $\mathrm{Tr}_{\mathcal{C}}$, that is, a collection of maps $\mathrm{Tr}_{\mathcal{C}} : \mathcal{C}\langle x, x \rangle \rightarrow \mathbb{K}$ for each object $x \in \mathcal{C}$ satisfying

- Symmetry: $\mathrm{Tr}_{\mathcal{C}}(f \circ g) = \mathrm{Tr}_{\mathcal{C}}(g \circ f)$, and
- Non-Degeneracy: The assignment $f \mapsto \mathrm{Tr}_{\mathcal{C}}(f \circ -)$ defines an isomorphism $\mathcal{C}\langle x, y \rangle \cong \mathcal{C}\langle y, x \rangle^*$ for each $f : x \rightarrow y$ in \mathcal{C} ,

is called a *Calabi-Yau Category*. For any object $x \in \mathcal{C}$, the scalar $d_x := \mathrm{Tr}_{\mathcal{C}}(\mathrm{id}_x)$ is called the *dimension* of x . This notion can, for example, be found in [Cos04] or [Sch13b].

Lemma 2.1 ([Sch13b, Prop. 5.2]). *The trace of a (finite semisimple) Calabi-Yau category \mathcal{C} is determined by its dimension vector $(d_{\mathbf{x}})$, that is, the finite list of dimensions $d_{\mathbf{x}}$ of (representatives of) simple objects $\mathbf{x} \in \mathcal{C}$. The entries of the dimension vector are non-zero, $d_{\mathbf{x}} \neq 0$. Conversely, any list of non-zero scalars for each isomorphism class of simple objects defines a trace.*

The "squared norm"

$$\mathcal{D}_{\mathcal{C}} := \sum_{\mathbf{x}} d_{\mathbf{x}}^2 \quad (2.7)$$

of the dimension vector is called the *dimension* of the Calabi-Yau category \mathcal{C} . If \mathcal{C} and \mathcal{D} are two Calabi-Yau categories, then the Deligne product $\mathcal{C} \boxtimes \mathcal{D}$ is a Calabi-Yau category with trace

$$\mathrm{Tr}_{\mathcal{C} \boxtimes \mathcal{D}}(f \otimes g) := \mathrm{Tr}_{\mathcal{C}}(f) \mathrm{Tr}_{\mathcal{D}}(g) \quad (2.8)$$

for endomorphisms f in \mathcal{C} and g in \mathcal{D} . This product category's dimension is the product of the dimensions of the factors:

$$\mathcal{D}_{\mathcal{C} \boxtimes \mathcal{D}} = \sum_{\mathbf{z} \in \mathcal{C} \boxtimes \mathcal{D}} d_{\mathbf{z}}^2 = \sum_{\substack{\mathbf{x} \in \mathcal{C} \\ \mathbf{y} \in \mathcal{D}}} d_{\mathbf{x} \boxtimes \mathbf{y}}^2 = \sum_{\substack{\mathbf{x} \in \mathcal{C} \\ \mathbf{y} \in \mathcal{D}}} d_{\mathbf{x}}^2 d_{\mathbf{y}}^2 = \mathcal{D}_{\mathcal{C}} \mathcal{D}_{\mathcal{D}}. \quad (2.9)$$

2.2 MONOIDAL CATEGORIES

We treat all monoidal categories as strict, in that we do not pay attention to the bracketing of monoidal products, and do not make associators and unitors explicit. With the exception of the tensor product of vector spaces, we never use any symbol to denote monoidal products; instead

we simply write ab for the monoidal product of the objects a and b . Reversing the product of a monoidal category \mathcal{A} leads to another monoidal category, denoted \mathcal{A}^{rev} .

Most of the monoidal categories we consider are pivotal. In this case as well, we make use of the appropriate coherence theorem [NS07, Thm. 2.2] and treat the pivotal structure as strict. We will therefore not distinguish between left and right dualities, and denote by a^* the dual of an object a in a pivotal category. We occasionally make use of the fact that a pivotal structure on a category \mathcal{A} gives rise to a distinguished monoidal equivalence

$$\overline{\mathcal{A}} \cong \mathcal{A}. \quad (2.10)$$

We denote the evaluation and coevaluation maps by

$$\text{ev}^a : a \otimes a^* \rightarrow \mathbb{1} \quad \text{and} \quad {}_a\text{coev} : \mathbb{1} \rightarrow a^* \otimes a. \quad (2.11)$$

Instead of distinguishing between left and right evaluation and coevaluation, we stick to this convention and use

$$\text{ev}^{a^*} : a^* \otimes a \rightarrow \mathbb{1} \quad \text{and} \quad {}_{a^*}\text{coev} : \mathbb{1} \rightarrow a \otimes a^* \quad (2.12)$$

for the other duality. The position of the subscript and superscript a is intentional, as will be clarified in Section 2.6.

A pivotal fusion category \mathcal{A} is in two ways a Calabi-Yau category, as both the left and the right pivotal trace is a trace in the sense of Calabi-Yau categories. If the two traces agree, the category \mathcal{A} is called *spherical*, and it carries the structure of a Calabi-Yau category in a canonical way.

2.3 DIAGRAMMATIC NOTATIONS

In some situations, especially when working with pivotal categories, we allow ourselves to represent morphisms in the diagrammatic notation of string diagrams. These are always read bottom-to-top: for example, given morphisms $f : x \otimes y^* \rightarrow z$, $g : y \rightarrow w^*$ in a pivotal category \mathcal{A} , we might write

$$(z \otimes g) \circ (f \otimes y) \circ (x \otimes {}_y\text{coev}) = \begin{array}{c} \begin{array}{c} \downarrow z \\ \boxed{f} \\ \uparrow x \end{array} \quad \begin{array}{c} \downarrow w \\ \boxed{g} \\ \uparrow y \end{array} \end{array} . \quad (2.13)$$

For generalities on string diagrams, we refer to [TV17].

Remark 2.2. Given that the aim of this paper is to define a formalism that could be called a graphical calculus, which moreover is closely related to string diagram notations, all graphical calculations should be done with care. First of all, we emphasize that the extruded graphs, which are our main subjects, to be introduced in Section 3, are distinct from string diagrams and only specialize to the known graphical calculus in some cases, which are laid out in Section 5. Secondly, all diagrammatic notation in this work is meant to illustrate algebraic expressions for the convenience of the reader, and a direct translation into such algebraic expressions is possible

at all times. In stark contrast to extruded graphs that will be examined thoroughly, we do not treat string diagrams and related notation as mathematical objects, but solely as a means to improve the legibility of (sometimes lengthy) formulae.

String diagrams in which all strands are labeled by objects and all coupons are labeled by appropriate morphisms represent a morphism. However, if we leave a coupon empty, we can take the string diagram to represent a linear map from the hom-space associated with the empty coupon to the hom-space in which the fully labeled string diagram evaluate to a morphism. When taking on this perspective, we emphasize the emptiness of the empty coupon by drawing it as a doubly outlined rectangle, as in the following example, in which both sides of the equation describe a linear map $\langle x \otimes y^*, z \rangle \rightarrow \langle x, z \otimes w^* \rangle$:

$$\begin{array}{c}
 \begin{array}{c}
 \downarrow w \\
 \boxed{g} \\
 \downarrow y \\
 \boxed{} \\
 \uparrow x
 \end{array}
 \begin{array}{c}
 \uparrow z \\
 \uparrow y
 \end{array}
 \end{array}
 = (f \mapsto (z \otimes g) \circ (f \otimes y) \circ (x \otimes y \text{coev})). \tag{2.14}$$

For reasons that will become apparent in Section 2.9, we refer to such diagrams with an empty box as *functorial diagrams* (for the hom-functor). Functorial diagrams may seem very similar to string diagrams, but note that their composition operations are quite different: while string diagrams are composed by vertical concatenation, functorial diagrams are composed by inserting the pre-composed diagram into the empty box of the post-composed diagram, as illustrated below.

$$\begin{array}{c}
 \begin{array}{c}
 \downarrow w \\
 \boxed{g} \\
 \downarrow y \\
 \boxed{} \\
 \uparrow x
 \end{array}
 \begin{array}{c}
 \uparrow z \\
 \uparrow y
 \end{array}
 = \begin{array}{c}
 \downarrow w \\
 \boxed{} \\
 \downarrow y \\
 \boxed{} \\
 \uparrow x
 \end{array}
 \circ \begin{array}{c}
 \downarrow w \\
 \boxed{g} \\
 \downarrow y \\
 \boxed{} \\
 \uparrow x
 \end{array}
 \begin{array}{c}
 \uparrow z \\
 \uparrow y
 \end{array}
 \end{array}
 \tag{2.15}$$

Later, in Sections 2.8 and 2.9, we will see more general functorial diagrams, of which those presented here are only a particular case.

2.4 HOM-SPACE CONTRACTIONS

For a finite-dimensional vector space V , we denote the image of id_V under the identification $\langle V, V \rangle \cong V \otimes V^*$ by $\star \in V \otimes V^*$. We frequently use a form of Sweedler notation whenever we need to write \star in \otimes -factorized form: $\star = \star_{(V)} \otimes \star_{(V^*)} \in V \otimes V^*$. For computational purposes, it is useful to recall that an explicit \otimes -factorized form of \star is given as follows: Pick a basis (φ_α) of V and denote the dual basis of V^* by (φ_α^*) . Then $\star = \sum_\alpha \varphi_\alpha \otimes \varphi_\alpha^*$.

In most cases we will encounter, V will be some hom-space $V = {}_c\langle x, y \rangle$ of a Calabi-Yau category \mathcal{C} . It then makes sense to consider the image of \star under the isomorphism ${}_c\langle x, y \rangle \otimes {}_c\langle x, y \rangle^* \cong {}_c\langle x, y \rangle \otimes {}_c\langle y, x \rangle$. We denote this image by \star as well, and its Sweedler components by

$\star = \star_{\langle x, y \rangle} \otimes \star_{\langle y, x \rangle}$. When using graphical notation, we write

$$\star = \begin{array}{c} |y \\ \circlearrowleft \star \\ |x \end{array} \otimes \begin{array}{c} |x \\ \circlearrowleft \star \\ |y \end{array} . \quad (2.16)$$

A useful and well-known relation which is best expressed in this notation is the following equation, whose left-hand side is sometimes referred to as a *resolution of the identity* of an object x in a Calabi-Yau category \mathcal{C} :

$$\sum_{\mathbf{x}} d_{\mathbf{x}} \star_{\langle \mathbf{x}, x \rangle} \circ \star_{\langle x, \mathbf{x} \rangle} = \sum_{\mathbf{x}} d_{\mathbf{x}} \begin{array}{c} |x \\ \circlearrowleft \star \\ \mathbf{x} \\ \circlearrowleft \star \\ |x \end{array} = \text{id}_x. \quad (2.17)$$

The notation can also be used to conveniently express the multiplicity $\dim \langle x, \mathbf{x} \rangle$ of a simple object \mathbf{x} in an object x in a Calabi-Yau category \mathcal{C} :

$$\dim \langle x, \mathbf{x} \rangle = \text{Tr}_{\mathcal{C}}(\star_{\langle \mathbf{x}, x \rangle} \circ \star_{\langle x, \mathbf{x} \rangle}). \quad (2.18)$$

2.5 ENDS AND COENDS

Quantum dimensions are hard to keep track of and their appearance in equations can sometimes seem mysterious. In this section and the following, we aim to systematize our treatment with the following observation: Quantum dimensions appear whenever an isomorphism between an end and a coend is expressed in components. To make the meaning of this credo precise, we first establish in this section that we distinguish between ends and coends even in the semisimple case, and that a Calabi-Yau structure establishes an isomorphism between the two. Next, in Section 2.6, we develop a calculus of components of morphisms between ends and coends, which is a necessary tool later on.

In order to fix notation, we briefly recall the notions of an end and a coend. Let \mathcal{X} and \mathcal{Y} be arbitrary categories. An *end* of a functor $S : \overline{\mathcal{X}} \times \mathcal{X} \rightarrow \mathcal{Y}$ is an object $\int_x S(x, x) \in \mathcal{Y}$, together with *structure morphisms* ${}_x\tau : \int_x S(x, x) \rightarrow S(x', x')$ for all $x' \in \mathcal{X}$ that form a dinatural transformation (meaning that for every $f : x' \rightarrow x''$, $S(f, x'') \circ {}_{x''}\tau = S(x', f) \circ {}_{x'}\tau$), satisfying the universal property that morphisms $y \rightarrow \int_x S(x, x)$ are in bijection with dinatural transformations $y \Rightarrow S$ for any object $y \in \mathcal{Y}$. The notion of a *coend* $\int^x S(x, x)$ is dual, and we denote its structure morphisms by $\sigma^{x'} : S(x', x') \rightarrow \int^x S(x, x)$.

In case the category \mathcal{X} is a (finite and semisimple) Calabi-Yau category and \mathcal{Y} is abelian, ends and coends can be understood explicitly as products or coproducts over a complete set of representatives of simple objects \mathbf{x} of \mathcal{X} : There are canonical morphisms $\int_x S(x, x) \rightarrow \prod_{\mathbf{x}} S(\mathbf{x}, \mathbf{x})$ and $\int^x S(x, x) \rightarrow \coprod_{\mathbf{x}} S(\mathbf{x}, \mathbf{x})$, defined using the universal property of the product and the coproduct.

$$\begin{array}{ccc} \int_x S(x, x) & \dashrightarrow & \prod_{\mathbf{x}} S(\mathbf{x}, \mathbf{x}) \\ \searrow \scriptstyle {}_y\tau & & \downarrow \\ & & S(\mathbf{y}, \mathbf{y}) \end{array} \qquad \begin{array}{ccc} \int^x S(x, x) & \dashrightarrow & \coprod_{\mathbf{x}} S(\mathbf{x}, \mathbf{x}) \\ \uparrow \scriptstyle \sigma^{\mathbf{y}} & & \nearrow \\ & & S(\mathbf{y}, \mathbf{y}) \end{array} \quad (2.19)$$

These morphisms, which are the unique dashed arrows that make the diagrams (2.19) commute for all simple objects $\mathbf{y} \in \mathcal{X}$, are isomorphisms. In order to prove this, one shows that if \mathcal{X} is Calabi-Yau, then any dinatural transformation $\eta : y \rightarrow S$ can be reconstructed from its components ${}_{\mathbf{x}}\eta : y \rightarrow S(\mathbf{x}, \mathbf{x})$ on simple objects $\mathbf{x} \in \mathcal{X}$. This follows from the next lemma.

Lemma 2.3. *The components ${}_x\eta$ of a dinatural transformation $\eta : y \rightarrow S$ for general objects $x \in \mathcal{X}$ can be given in terms of the components ${}_{\mathbf{x}}\eta$ of η for simple objects $\mathbf{x} \in \mathcal{X}$:*

$${}_x\eta = \sum_{\mathbf{x}} d_{\mathbf{x}} S(\star_{\langle x, \mathbf{x} \rangle}, \star_{\langle \mathbf{x}, x \rangle}) \circ {}_{\mathbf{x}}\eta. \quad (2.20)$$

Dually, for a dinatural transformation $\epsilon : S \rightarrow y$, the following formula holds:

$$\epsilon^x = \sum_{\mathbf{x}} d_{\mathbf{x}} \epsilon^{\mathbf{x}} \circ S(\star_{\langle \mathbf{x}, x \rangle}, \star_{\langle x, \mathbf{x} \rangle}). \quad (2.21)$$

Proof. The computation is straightforward. In the first step, a resolution of the identity, see (2.17), is inserted:

$$\begin{aligned} {}_x\eta &\stackrel{(2.17)}{=} \sum_{\mathbf{x}} d_{\mathbf{x}} S(\star_{\langle \mathbf{x}, x \rangle} \circ \star_{\langle x, \mathbf{x} \rangle}, x) \circ {}_x\eta \\ &= \sum_{\mathbf{x}} d_{\mathbf{x}} S(\star_{\langle x, \mathbf{x} \rangle}, x) \circ S(\star_{\langle \mathbf{x}, x \rangle}, x) \circ {}_x\eta \\ &= \sum_{\mathbf{x}} d_{\mathbf{x}} S(\star_{\langle x, \mathbf{x} \rangle}, x) \circ S(x, \star_{\langle \mathbf{x}, x \rangle}) \circ {}_{\mathbf{x}}\eta \\ &= \sum_{\mathbf{x}} d_{\mathbf{x}} S(\star_{\langle x, \mathbf{x} \rangle}, \star_{\langle \mathbf{x}, x \rangle}) \circ {}_{\mathbf{x}}\eta. \end{aligned} \quad (2.22)$$

The second equality uses the (contravariant) functoriality of S , and the third equality follows from the dinaturality of η .

The equation (2.21) is proved similarly. \square

Of course, in any abelian category, the coproduct and the product can both be identified with the direct sum. In a Calabi-Yau category \mathcal{X} , the two isomorphisms in (2.19) can be thus be composed to produce an isomorphism $\int_x S(x, x) \cong \int^x S(x, x)$. However, it turns out that a modified version of this isomorphism is more natural to consider. We refer to this modified version $\Theta_{\mathcal{X}}$ as the isomorphism between the end and the coend *induced by the trace* on \mathcal{X} .

$$\Theta_{\mathcal{X}} : \int_{x \in \mathcal{X}} S(x, x) \xrightarrow{\cong} \int^{x \in \mathcal{X}} S(x, x). \quad (2.23)$$

Here and going forward, we talk about $\Theta_{\mathcal{X}}$ as *an* isomorphism – but really, it is a family of isomorphisms for each functor S . We suppress this in the notation.

Unlike the isomorphism obtained from (2.19), $\Theta_{\mathcal{X}}$ carries information about the trace structure on \mathcal{X} . It is defined as the composition

$$\Theta_{\mathcal{X}} := \sum_{\mathbf{y}} d_{\mathbf{y}} \sigma^{\mathbf{y}} \circ {}_{\mathbf{y}}\tau, \quad (2.24)$$

meaning that the following diagram commutes.

$$\begin{array}{ccc}
\int_x S(x, x) & \xrightarrow{\Theta_{\mathcal{X}}} & \int^x S(x, x) \\
\cong \uparrow & & \downarrow \cong \\
\prod_{\mathbf{x}} S(\mathbf{x}, \mathbf{x}) & & \coprod_{\mathbf{x}} S(\mathbf{x}, \mathbf{x}) \\
\downarrow \cong & & \cong \uparrow \\
\bigoplus_{\mathbf{x}} S(\mathbf{x}, \mathbf{x}) & \xrightarrow{\bigoplus_{\mathbf{x}} \text{d}_{\mathbf{x}} \text{id}_{S(\mathbf{x}, \mathbf{x})}} & \bigoplus_{\mathbf{x}} S(\mathbf{x}, \mathbf{x})
\end{array} \tag{2.25}$$

Later, in Lemma 2.21, we will see a conceptual reason for why the isomorphism $\Theta_{\mathcal{X}}$ as defined in (2.24) is more relevant than other choices of isomorphism.

2.6 COMPUTING WITH COMPONENTS

We continue by establishing some notational conventions for the components of morphisms between ends and coends. This will be necessary for some practical computations later on.

Let \mathcal{X} and \mathcal{Y} be abelian, and S be a functor as above. Due to the respective universal properties, it is natural to consider morphisms *into* ends and *out of* coends. Given a morphism

$$f : x \rightarrow \int_i S(i, i) \tag{2.26}$$

from any object x into an end, we call the family of morphisms

$${}_j f := {}_j \tau \circ f : x \rightarrow S(j, j) \tag{2.27}$$

obtained by post-composition with the structure map of the end the *components* of f . This family is dinatural.

Conversely, given a dinatural family

$${}_j f : x \rightarrow S(j, j), \tag{2.28}$$

we write for the unique morphism to end implied by the universal property

$$\int_i f_j : x \rightarrow \int_i S(i, i). \tag{2.29}$$

A dual definition holds for the coend: Given a morphism

$$g : \int^i S(i, i) \rightarrow y, \tag{2.30}$$

we call the morphisms

$$g^j := g \circ \sigma^j : S(j, j) \rightarrow y \tag{2.31}$$

the *components* of g , which form a dinatural family. Similarly, any dinatural family $g^j : S(j, j) \rightarrow y$ assembles into a unique morphism

$$\int_i g^i. \tag{2.32}$$

out of the coend. Let us now require the category \mathcal{X} to be equipped with a Calabi-Yau structure. Using the canonical isomorphism $\Theta_{\mathcal{X}}$ to identify the end and the coend, the morphisms f and g can be composed. We thus define

$$g \bullet f := g \circ \Theta_{\mathcal{X}} \circ f. \quad (2.33)$$

Moreover, we introduce rules for raising and lowering indices:

$${}^j f := d_j {}_j f \quad \text{and} \quad g_j := d_j g^j. \quad (2.34)$$

Using this notation, we find that

$$g \bullet f = \sum_{\mathbf{x}} d_{\mathbf{x}} g^{\mathbf{x}} \circ_{\mathbf{x}} f = \sum_{\mathbf{x}} g_{\mathbf{x}} \circ_{\mathbf{x}} f = \sum_{\mathbf{x}} g^{\mathbf{x}} \circ^{\mathbf{x}} f, \quad (2.35)$$

where the sum runs over representatives of simple objects of the finite semisimple category \mathcal{X} . A takeaway from equation (2.35) is that whenever we encounter an expression where a sum over simple objects \mathbf{x} is involved, we should expect both instances of \mathbf{x} in the expression to be raised, both to be lowered, or else for a dimension $d_{\mathbf{x}}$ to be involved.

Remark 2.4. For a non-simple object j , the dimension d_j might be zero. Thus, the raising and lowering operations from (2.34) do not, in general, have inverses. This is not a problem when the object j is simple.

Morphisms ${}^j f$ with raised indices and g_j with lowered indices are to be viewed as the components of maps *into* coends and *out of* ends, respectively. We sometimes refer to such morphisms as *atypical* morphisms. For instance, let there be maps

$$h : x \rightarrow \int^i S(i, i) \quad \text{and} \quad k : \int_i S(i, i) \rightarrow y. \quad (2.36)$$

By the (*atypical*) components of h and k , we mean the morphisms

$${}^j h := d_j {}_j \tau \circ \Theta_{\mathcal{X}}^{-1} \circ h : x \rightarrow S(j, j) \quad \text{and} \quad k_j := d_j k \circ \Theta_{\mathcal{X}}^{-1} \circ \sigma^j : S(j, j) \rightarrow y. \quad (2.37)$$

Since the morphisms h and k are determined by their components, we allow ourselves to write

$$h = \int^i {}^j h \quad \text{and} \quad k = \int_i k_j. \quad (2.38)$$

Remark 2.5 (Atypical dinaturality). The atypical components ${}^j h$ from (2.37) form a family of morphisms satisfying a property that is similar to a dinaturality condition: Given a morphism $\alpha : i \rightarrow j$ in \mathcal{X} , we find

$$d_i S(j, \alpha) \circ {}^j h = d_j S(\alpha, i) \circ {}^i h. \quad (2.39)$$

One can check that families ${}^j h$ of morphisms satisfying this atypical dinaturality condition are in canonical bijection with maps $h : x \rightarrow \int^i S(i, i)$.

While for our purposes, it would suffice to consider components of atypical morphisms (and even regular morphisms as in (2.30)) only for simple objects, this justifies why we do not need to make such a restriction.

The definitions (2.37) are chosen such that

$$g \circ h = \sum_{\mathbf{x}} g^{\mathbf{x}} \circ^{\mathbf{x}} h \quad \text{and} \quad k \circ f = \sum_{\mathbf{x}} k_{\mathbf{x}} \circ_{\mathbf{x}} f \quad (2.40)$$

hold.

An example for notation using raised and lowered indices are the evaluation and coevaluation morphisms ev^a and ${}_a\text{coev}$ for objects $a \in \mathcal{A}$ in a pivotal category. These morphism form dinatural transformations $- \otimes (-)^* \rightarrow \mathbb{1}$ and $\mathbb{1} \rightarrow (-)^* \otimes -$, respectively, and thus form the components of morphisms

$$\text{ev} := \int_a \text{ev}^a : \int_a a a^* \rightarrow \mathbb{1} \quad \text{and} \quad \text{coev} := \int_a {}_a\text{coev} : \mathbb{1} \rightarrow \int_a a^* a. \quad (2.41)$$

The identity morphism $\text{id} : \int_x S(x, x) \rightarrow \int_x S(x, x)$ of any end is typical in that it is a morphism *into* an end, and atypical in that it is also a morphism *out of* an end. Its components ${}_x\text{id}$ are the end's structure morphisms

$${}_x\text{id} = {}_x\tau. \quad (2.42)$$

Using the formula for atypical components (2.37), we get

$${}_x\text{id}_y = {}_x\tau_y = d_x {}_x\tau \circ \Theta_{\mathcal{X}}^{-1} \circ \sigma^y. \quad (2.43)$$

For simple objects \mathbf{x}, \mathbf{y} , it can be read from the diagram (2.25) that the formula (2.43) becomes

$${}_x\text{id}_y = {}_x\tau_y = \delta_{\mathbf{x}, \mathbf{y}} \text{id}_{S(\mathbf{x}, \mathbf{x})}. \quad (2.44)$$

The same result holds for the structure morphisms of a coend:

$${}^{\mathbf{x}}\sigma^{\mathbf{y}} = {}^{\mathbf{x}}\tau_{\mathbf{y}} = \delta_{\mathbf{x}, \mathbf{y}} \text{id}_{S(\mathbf{x}, \mathbf{x})}. \quad (2.45)$$

Of course, equation (2.43) also describes the components of the inverse to the isomorphism $\Theta_{\mathcal{X}}$, which was defined in Section 2.5:

$${}_{\mathbf{x}}(\Theta_{\mathcal{X}}^{-1})^{\mathbf{y}} = {}_{\mathbf{x}}\tau \circ \Theta_{\mathcal{X}}^{-1} \circ \sigma^{\mathbf{y}} = \frac{\delta_{\mathbf{x}, \mathbf{y}}}{d_{\mathbf{x}}} \text{id}_{S(\mathbf{x}, \mathbf{x})}. \quad (2.46)$$

We learned from Lemma 2.3 how structure maps for general objects are expressed in terms of structure maps for simple objects. Applying this to (2.46), it is easy to show that for general objects $x, y \in \mathcal{X}$, we the components of $\Theta_{\mathcal{X}}^{-1}$ take the form

$${}_x(\Theta_{\mathcal{X}}^{-1})^y = {}_x\tau \circ \Theta_{\mathcal{X}}^{-1} \circ \sigma^y = S(\star_{\langle x, y \rangle}, \star_{\langle y, x \rangle}). \quad (2.47)$$

The isomorphism $\Theta_{\mathcal{X}}$, which is used in the definition of atypical components, is itself an atypical morphism in two ways: It is a morphism out of an end and into a coend. Its components are given as follows, for simple objects $\mathbf{x}, \mathbf{y} \in \mathcal{X}$:

$$\begin{aligned} {}^{\mathbf{y}}(\Theta_{\mathcal{X}})_{\mathbf{x}} &= {}^{\mathbf{y}} \left(\sum_{\mathbf{z}} d_{\mathbf{z}} \sigma^{\mathbf{z}} \circ {}_{\mathbf{z}}\tau \right)_{\mathbf{x}} = \sum_{\mathbf{z}} d_{\mathbf{z}} {}^{\mathbf{y}}\sigma^{\mathbf{z}} \circ {}_{\mathbf{z}}\tau_{\mathbf{x}} = \sum_{\mathbf{z}} d_{\mathbf{z}} \delta_{\mathbf{y}, \mathbf{z}} \delta_{\mathbf{z}, \mathbf{x}} \text{id}_{S(\mathbf{x}, \mathbf{x})} \\ &= d_{\mathbf{x}} \delta_{\mathbf{y}, \mathbf{x}} \text{id}_{S(\mathbf{x}, \mathbf{x})}. \end{aligned} \quad (2.48)$$

2.7 TRACED BIMODULE CATEGORIES

Keeping in mind that a (linear) monoidal category is the categorification of a ring, it is natural to also consider the categorification of the notion of a module over a ring, which is called a *module category*. Given a monoidal category \mathcal{A} , one can consider *left \mathcal{A} -module categories* \mathcal{M} . This is a category equipped with an *action functor* $\mathcal{A} \times \mathcal{M} \rightarrow \mathcal{M}$, denoted $(a, m) \mapsto am$, together with coherence data and axioms. For details, we refer to [EGNO15].

We are interested only in so-called *exact* module categories over finite tensor categories: A finite left \mathcal{A} -module category \mathcal{M} is called exact iff the object $Pm \in \mathcal{M}$ is projective for any projective object $P \in \mathcal{A}$ and any object $m \in \mathcal{M}$. If \mathcal{A} is a fusion category – which is the setting throughout this work – then the exact module categories over \mathcal{A} are precisely the finite semisimple module categories. From here on, we assume all module categories to be exact by default.

There are the obvious related notions of right module categories and bimodule categories. A left \mathcal{A} -module category can be equivalently described as a right \mathcal{A}^{rev} -module category. An \mathcal{A} - \mathcal{B} -bimodule category is the same as a left $\mathcal{A} \boxtimes \mathcal{B}^{\text{rev}}$ -module category. Lastly, every linear category can be canonically equipped with the structure of a left or right vect-module category. Hence, a left \mathcal{A} -module category can also be seen as an \mathcal{A} -vect-bimodule category.

We will make tacit use of these identifications throughout the thesis. To keep in mind which type of module category a particular category is, we sometimes write, for instance ${}_{\mathcal{A}}\mathcal{M}_{\mathcal{B}} = \mathcal{M}$ for an \mathcal{A} - \mathcal{B} -bimodule category, and similar for left and right module categories.

For every fusion category \mathcal{A} , we can consider the *regular bimodule category* ${}_{\mathcal{A}}\mathcal{A}_{\mathcal{A}}$, whose action functors are given by the monoidal product.

The bimodule categories we consider have internal hom-objects with respect to each action. This means that given objects m, n in a bimodule category ${}_{\mathcal{A}}\mathcal{M}_{\mathcal{B}}$, there are objects ${}_{\mathcal{A}}[m, n] \in \mathcal{A}$ and ${}_{\mathcal{B}}[m, n] \in \mathcal{B}$ for which there are isomorphisms

$${}_{\mathcal{A}}\langle a, {}_{\mathcal{A}}[m, n] \rangle \cong {}_{\mathcal{M}}\langle am, n \rangle, \quad {}_{\mathcal{B}}\langle b, {}_{\mathcal{A}}[m, n] \rangle \cong {}_{\mathcal{M}}\langle bm, n \rangle. \quad (2.49)$$

Pivotal structures on monoidal categories are important to us, and one reason for this is that they lead to a unique module structure on the opposite of a module category: For a bimodule category ${}_{\mathcal{A}}\mathcal{M}_{\mathcal{B}}$ over pivotal categories \mathcal{A} and \mathcal{B} , the *opposite* category $\overline{\mathcal{M}}$ is canonically a \mathcal{B} - \mathcal{A} -bimodule category, with actions defined by $b\overline{m}a := \overline{a^* m b^*}$. Without the pivotal structures, different choices of dualities will lead to different action functors on $\overline{\mathcal{M}}$.

If a bimodule category ${}_{\mathcal{A}}\mathcal{M}_{\mathcal{B}}$ over pivotal categories \mathcal{A} and \mathcal{B} also carries the structure of a Calabi-Yau category, it is natural to impose the following consistency condition: Let $a \in \mathcal{A}$, $b \in \mathcal{B}$, and $m \in \mathcal{M}$ be objects, and let $f : amb \rightarrow amb$ be an endomorphism in \mathcal{M} . The morphism

$$\text{ptr}(f) := (\text{ev}^{a^*} m \text{ev}^b) \circ (a^* f b^*) \circ ({}_a \text{coev} m {}_b \text{coev}), \quad (2.50)$$

which is an endomorphism of m , is called the *partial trace* of f with respect to a and b . The consistency condition between the Calabi-Yau structure and the module actions on \mathcal{M} mentioned above is

$$\text{Tr}_{\mathcal{M}}(f) = \text{Tr}_{\mathcal{M}}(\text{ptr}(f)). \quad (2.51)$$

In order to illustrate equations such as (2.51), we can make use of a type of string diagram found in [Sch13b]. These diagrams represent morphisms in (bi-)module categories and are read from

bottom to top. In pictures, the trace compatibility condition (2.51) assumes the form

$$\mathrm{Tr}_{\mathcal{M}} \left(\begin{array}{c} \begin{array}{|c|c|c|} \hline \begin{array}{c} a \\ \uparrow \\ \hline \end{array} \\ \hline \end{array} \\ \begin{array}{|c|c|c|} \hline \begin{array}{c} m \\ \uparrow \\ \hline \end{array} \\ \hline \end{array} \\ \begin{array}{|c|c|c|} \hline \begin{array}{c} b \\ \uparrow \\ \hline \end{array} \\ \hline \end{array} \\ \hline \begin{array}{|c|} \hline \begin{array}{c} f \\ \hline \end{array} \\ \hline \end{array} \\ \hline \begin{array}{|c|c|c|} \hline \begin{array}{c} a \\ \uparrow \\ \hline \end{array} \\ \hline \end{array} \\ \begin{array}{|c|c|c|} \hline \begin{array}{c} m \\ \uparrow \\ \hline \end{array} \\ \hline \end{array} \\ \begin{array}{|c|c|c|} \hline \begin{array}{c} b \\ \uparrow \\ \hline \end{array} \\ \hline \end{array} \\ \hline \end{array} \right) = \mathrm{Tr}_{\mathcal{M}} \left(\underbrace{\begin{array}{c} \begin{array}{|c|} \hline \begin{array}{c} m \\ \uparrow \\ \hline \end{array} \\ \hline \end{array} \\ \begin{array}{|c|} \hline \begin{array}{c} a \\ \downarrow \\ \hline \end{array} \\ \hline \end{array} \\ \begin{array}{|c|} \hline \begin{array}{c} f \\ \hline \end{array} \\ \hline \end{array} \\ \begin{array}{|c|} \hline \begin{array}{c} b \\ \downarrow \\ \hline \end{array} \\ \hline \end{array} \\ \begin{array}{|c|} \hline \begin{array}{c} m \\ \downarrow \\ \hline \end{array} \\ \hline \end{array} \\ \hline \end{array} \right)_{\mathrm{ptr}(f)}. \quad (2.52)$$

Traces on module categories over pivotal fusion categories that satisfy (2.51) were first considered in [Sch13b] and are called *(bi-)module traces*. We refer to a bimodule category equipped with a bimodule trace as a *traced bimodule category*. The following lemma, which is easy to verify, shows how the property to admit a bimodule trace is related to the property of sphericity for pivotal fusion categories.

Lemma 2.6. *Let \mathcal{A} be a pivotal fusion category. The following statements are equivalent.*

1. \mathcal{A} is a spherical fusion category.
2. The regular bimodule category ${}_{\mathcal{A}}\mathcal{A}_{\mathcal{A}}$ admits a bimodule trace.

If either statement is true, then the bimodule trace on ${}_{\mathcal{A}}\mathcal{A}_{\mathcal{A}}$ is unique up to a normalization factor. If in addition, the bimodule trace is normalized such that the dimension of the monoidal unit is 1, then the bimodule trace is equal to the (left or right) pivotal trace.

Remark 2.7. In light of Lemma 2.6, the name "spherical bimodule category" would also seem to make sense for traced bimodule categories. We chose our terminology for the following reason.

As explained in [DSS20, Sec. 3.5], there are two notions of sphericity one can consider for pivotal tensor categories. A pivotal tensor category \mathcal{C} can be *spherical*, meaning that the pivotal structure squares to the Radford isomorphism – or it can be *trace spherical*, meaning that the left and right pivotal traces are equal. If \mathcal{C} is semi-simple, these notions of sphericity coincide, but otherwise, they are independent properties.

The concept of sphericity can be generalized to module categories [FGJS22] – there, too, the notion of a Radford isomorphism [FSS20a] and that of a pivotal structure [Sch15; Shi20] exist. On a semisimple bimodule category, pivotal structures and bimodule traces are equivalent structures. Sphericity is in this case an additional normalization condition on the bimodule trace, which we have no desire to impose.

Remark 2.8. Given two \mathcal{A} -module categories \mathcal{M} and \mathcal{N} , the product category $\mathcal{M} \times \mathcal{N}$ can be equipped with the structure of an \mathcal{A} -module category by simultaneous action on the components, which is denoted $\mathcal{M} \boxplus \mathcal{N}$. This module category is called the direct sum of \mathcal{M} and \mathcal{N} . A module category \mathcal{M} is called *indecomposable* if the existence of an equivalence of module categories $\mathcal{M} \cong \mathcal{N} \boxplus \mathcal{K}$ implies that either \mathcal{N} or \mathcal{K} is equivalent to \mathcal{M} , with the other being trivial. The structure of a bimodule trace on an indecomposable bimodule category is, if it exists, unique up to a scalar [Sch13b, Prop. 4.4]. The question whether or not a (bi-)module category admits a bimodule trace can be stated as an eigenvalue problem [Sch13b, Prop. 5.4, Prop. 5.7].

A module trace also provides a relation between the (pivotal) dimension of an internal hom object, and the dimensions of the objects in the module category:

Lemma 2.9. *Given a left \mathcal{A} -module category \mathcal{M} over a spherical fusion category \mathcal{A} with a module trace, the following equality holds for simple objects $\mathbf{m}, \mathbf{n} \in \mathcal{M}$:*

$$d_{\mathcal{A}[\mathbf{m}, \mathbf{n}]} = \frac{\mathcal{D}_{\mathcal{A}}}{\mathcal{D}_{\mathcal{M}}} d_{\mathbf{m}} d_{\mathbf{n}}. \quad (2.53)$$

Proof. Following [Sch13b, Sec. 5], we call the square matrix Q with entries

$$Q_{\mathbf{nm}} := d_{\mathcal{A}[\mathbf{m}, \mathbf{n}]} \quad (2.54)$$

for (representatives of isoclasses of) simple objects $\mathbf{m}, \mathbf{n} \in \mathcal{M}$ the *dimension matrix* of \mathcal{M} . From [Sch13b, Prop. 5.7], we know that Q is of rank 1 with only non-zero entries. This implies that Q is of the form $Q_{\mathbf{nm}} = \xi_{\mathbf{n}} \zeta_{\mathbf{m}}$ for non-zero scalars $\xi_{\mathbf{n}}, \zeta_{\mathbf{m}} \in \mathbb{K}$.

Moreover, the module trace on \mathcal{M} causes the dual of the internal hom to behave much like the dual of the hom-space:

$${}_{\mathcal{A}}[m, n]^* = {}_{\mathcal{A}}[n, m] \quad (2.55)$$

for all objects $m, n \in \mathcal{M}$. This is easy to check using the Yoneda lemma; for $a \in \mathcal{A}$, we have:

$$\begin{aligned} \langle a, {}_{\mathcal{A}}[n, m] \rangle &\cong \langle an, m \rangle \cong \langle m, an \rangle^* \cong \langle a^* m, n \rangle^* \\ &\cong \langle a^*, {}_{\mathcal{A}}[m, n] \rangle^* \cong \langle {}_{\mathcal{A}}[m, n], a^* \rangle \cong \langle a, {}_{\mathcal{A}}[m, n]^* \rangle. \end{aligned} \quad (2.56)$$

Due to (2.55), the dimension matrix Q is symmetric, which means that $\xi_{\mathbf{m}} = \zeta_{\mathbf{m}}$ for all simple representatives $\mathbf{m} \in \mathcal{M}$.

The dimension vector is an eigenvector of the dimension matrix Q with eigenvalue $\mathcal{D}_{\mathcal{A}}$, see [Sch13b, Prop. 5.4]:

$$\sum_{\mathbf{m}} Q_{\mathbf{nm}} d_{\mathbf{m}} = \sum_{\mathbf{m}} \xi_{\mathbf{n}} \xi_{\mathbf{m}} d_{\mathbf{m}} = \mathcal{D}_{\mathcal{A}} d_{\mathbf{n}}. \quad (2.57)$$

As $\xi_{\mathbf{n}}$ and $\mathcal{D}_{\mathcal{A}}$ are non-zero, this is equivalent to the following:

$$\frac{\sum_{\mathbf{m}} \xi_{\mathbf{m}} d_{\mathbf{m}}}{\mathcal{D}_{\mathcal{A}}} = \frac{d_{\mathbf{n}}}{\xi_{\mathbf{n}}} =: \lambda, \quad (2.58)$$

where we introduced a non-zero scalar λ that does not depend on \mathbf{n} . Substituting $\xi_{\mathbf{m}} = \frac{d_{\mathbf{m}}}{\lambda}$, we find

$$\frac{\sum_{\mathbf{m}} d_{\mathbf{m}} d_{\mathbf{m}}}{\lambda \mathcal{D}_{\mathcal{A}}} = \lambda, \quad \text{and hence} \quad \frac{\mathcal{D}_{\mathcal{M}}}{\mathcal{D}_{\mathcal{A}}} = \lambda^2. \quad (2.59)$$

Finally, we obtain the statement of the lemma:

$$d_{\mathcal{A}[\mathbf{m}, \mathbf{n}]} = Q_{\mathbf{nm}} = \xi_{\mathbf{n}} \xi_{\mathbf{m}} = \frac{d_{\mathbf{n}} d_{\mathbf{m}}}{\lambda^2} = \frac{\mathcal{D}_{\mathcal{A}}}{\mathcal{D}_{\mathcal{M}}} d_{\mathbf{m}} d_{\mathbf{n}}. \quad (2.60)$$

□

In Section 2.4, we reviewed how traces exhibit hom-spaces as the duals of other hom-spaces, and introduced \star -notation as a shorthand for working with elements of a pair of dual bases. The calculus of \star -notation in dual hom-spaces behaves nicely with respect to the module structure if the duality comes from a module trace. More, precisely, the following lemma holds.

Lemma 2.10. *Let \mathcal{M} be a left \mathcal{A} -module category over a spherical fusion category \mathcal{A} with a module trace. Let there be objects $m, n \in \mathcal{M}$ and $a \in \mathcal{A}$, and let (φ_α) denote a basis of the hom-space $\mathcal{M}\langle m, an \rangle$. As in Section 2.4, we denote the elements of the dual base by $\varphi_\alpha^* \in \langle an, m \rangle$. Then the α -indexed families of morphisms*

$$(\text{ev}^{a^*} n) \circ (a^* \varphi_\alpha) \quad \text{and} \quad (a^* \varphi_\alpha^*) \circ ({}_a \text{coev } n) \quad (2.61)$$

form dual bases of the hom-sets $\langle a^* m, n \rangle$ and $\langle n, a^* m \rangle$, respectively.

Using the \star -notation introduced in Section 2.4, this statement can be expressed as the equality

$$\star_{\langle a^* m, n \rangle} \otimes \star_{\langle n, a^* m \rangle} = \left((\text{ev}^{a^*} n) \circ (a^* \star_{\langle m, an \rangle}) \right) \otimes \left((a^* \star_{\langle an, m \rangle}) \circ ({}_a \text{coev } n) \right), \quad (2.62)$$

or graphically as

$$\begin{array}{c} \begin{array}{c} | \\ n \\ \circlearrowleft \\ | \\ m \\ \downarrow \\ a \end{array} \otimes \begin{array}{c} a \downarrow \\ | \\ m \\ \circlearrowright \\ | \\ n \end{array} = \begin{array}{c} | \\ m \\ \circlearrowleft \\ | \\ n \\ \downarrow \\ a \end{array} \otimes \begin{array}{c} a \downarrow \\ | \\ m \\ \circlearrowright \\ | \\ n \end{array}. \end{array} \quad (2.63)$$

Proof. We merely need to show that the duality relation

$$\text{Tr}_{\mathcal{M}} \left((\text{ev}^{a^*} n) \circ (a^* \varphi_\alpha) \circ (a^* \varphi_{\tilde{\alpha}}^*) \circ ({}_a \text{coev } n) \right) = \delta_{\alpha, \tilde{\alpha}} \quad (2.64)$$

holds. Using the compatibility (2.51) of the module trace with the partial trace, it is easy to see that the duality relation (2.64) is inherited from the duality relation of the original dual bases $\varphi_\alpha, \varphi_{\tilde{\alpha}}^*$:

$$\begin{aligned} & \text{Tr}_{\mathcal{M}} \left((\text{ev}^{a^*} n) \circ (a^* \varphi_\alpha) \circ (a^* \varphi_{\tilde{\alpha}}^*) \circ ({}_a \text{coev } n) \right) \\ & \stackrel{(2.50)}{=} \text{Tr}_{\mathcal{M}} (\text{ptr}(\varphi_\alpha \circ \varphi_{\tilde{\alpha}}^*)) \\ & \stackrel{(2.51)}{=} \text{Tr}_{\mathcal{M}} (\varphi_\alpha \circ \varphi_{\tilde{\alpha}}^*) \\ & = \delta_{\alpha, \tilde{\alpha}}. \end{aligned} \quad (2.65)$$

□

2.8 CENTERS OF BIMODULE CATEGORIES

Let ${}_A \mathcal{M}_A$ be an \mathcal{A} - \mathcal{A} -bimodule category. The linear category $Z_{\mathcal{A}}(\mathcal{M})$ is called the *center* of \mathcal{M} and has as objects pairs $z = (m, \text{br}^z)$, where $m \in \mathcal{M}$ is an object of \mathcal{M} and br^z , called the *balancing* of z , is a family of isomorphisms $\text{br}_a^z : am \rightarrow ma$ for each object $a \in \mathcal{A}$, satisfying the conditions $\text{br}_{ab}^z = (\text{br}_a^z b) \circ (a \text{br}_b^z)$ and $\text{br}_{\mathbb{1}}^z = \text{id}_m$. Morphisms $f : z \rightarrow z' = (m', \text{br}^{z'})$ are morphisms $f : m \rightarrow m'$ satisfying the condition that $\text{br}_a^{z'} \circ (a f) = (f a) \circ \text{br}_a^z$. We denote the

forgetful functor $z \mapsto m$, which forgets the balancing, by $U : Z_{\mathcal{A}}(\mathcal{M}) \rightarrow \mathcal{M}$. If \mathcal{M} is the regular bimodule category ${}_{\mathcal{A}}\mathcal{A}_{\mathcal{A}}$, the center $Z_{\mathcal{A}}(\mathcal{A})$ is the more widely known Drinfeld center of \mathcal{A} (as a linear category).

We frequently use a particular pair of morphisms (e.g. in Lemma 2.23 below)

$$\text{brev}_z^a : ama^* \rightarrow m \quad \text{and} \quad {}_a\text{cobrev}_z : m \rightarrow a^*ma, \quad (2.66)$$

called *braided evaluation* and *braided coevaluation* for objects $z = (m, \text{br}^z) \in Z_{\mathcal{A}}(\mathcal{M})$ and $a \in \mathcal{A}$. They can be defined in two equivalent ways, which are the left- and right-hand sides of the equations below.

$$\text{brev}_z^a := (m \text{ev}^a) \circ (\text{br}_a^z a^*) = (\text{ev}^a m) \circ (a (\text{br}_{a^*}^z)^{-1}), \quad (2.67)$$

$${}_a\text{cobrev}_z := ((\text{br}_{a^*}^z)^{-1} a) \circ (m {}_a\text{coev}) = (a^* \text{br}_a^z) \circ ({}_a\text{coev} m). \quad (2.68)$$

In diagrammatic notation, we represent the braided evaluation and coevaluation as

$$\text{brev}_z^a = \begin{array}{c} z \\ | \\ a \curvearrowright \end{array} \quad \text{and} \quad {}_a\text{cobrev}_z = \begin{array}{c} \cup \\ | \\ z \end{array}, \quad (2.69)$$

where we introduced the convention that objects of the center are drawn as red lines. We also use the label z as opposed to m , because we make use of the balancing as well. In practice, this means that black lines and red lines can cross in all diagrams we consider. Unlike for a braided monoidal category, there are no over- and undercrossings that need to be distinguished.

Remark 2.11. Any linear category \mathcal{X} can be seen as a vect-vect-bimodule category. With respect to these vect-actions, every object $x \in \mathcal{X}$ admits a balancing, and all balancings are isomorphic. Hence, there is an equivalence of categories $\mathcal{X} \cong Z_{\text{vect}}(\mathcal{X})$.

Remark 2.12. An alternative model for the center is given by the category of bimodule functors and bimodule natural transformations $\text{Fun}_{\mathcal{A}|\mathcal{A}}(\mathcal{A}, \mathcal{M})$: There is a canonical equivalence of categories

$$\text{Fun}_{\mathcal{A}|\mathcal{A}}(\mathcal{A}, \mathcal{M}) \cong Z_{\mathcal{A}}(\mathcal{M}). \quad (2.70)$$

The center of a module category can also be characterized by a universal property, which needs the notion of a balanced functor. A functor $F : \mathcal{M} \rightarrow \mathcal{X}$, equipped with a family of isomorphisms $\gamma_{a,m} : F(am) \rightarrow F(ma)$, natural in $a \in \mathcal{A}$ and $m \in \mathcal{M}$, which moreover satisfies $\gamma_{ab,m} = \gamma_{b,ma} \circ \gamma_{a,bm}$, is called a *balanced functor*. Balanced functors form a category $\text{Fun}^{\text{bal}}(\mathcal{M}, \mathcal{X})$, whose morphisms are balanced natural transformations, i.e. those natural transformations $\eta : F \Rightarrow G$ which are compatible with the balancings γ^F and γ^G of F and G in that $\gamma_{a,m}^G \circ \eta_{am} = \eta_{ma} \circ \gamma_{a,m}^F$. Up to equivalence, the center $Z_{\mathcal{A}}(\mathcal{M})$ is the unique category such that there is an equivalence of functor categories

$$\text{Fun}^{\text{bal}}(\mathcal{M}, \mathcal{X}) \cong \text{Fun}(Z_{\mathcal{A}}(\mathcal{M}), \mathcal{X}). \quad (2.71)$$

2.9 BALANCED FUNCTORS AND FUNCTORIAL DIAGRAMS

Let \mathcal{M} be a (left) module category over any monoidal category \mathcal{A} , and let \mathcal{N} be a right \mathcal{A} -module category. The category $\mathcal{N} \boxtimes \mathcal{M}$ is an \mathcal{A} - \mathcal{A} -bimodule category. The balanced functors out of categories of this form are of particular interest to us. We usually denote the balancing of a functor $F : \mathcal{N} \boxtimes \mathcal{M} \rightarrow \mathcal{X}$ into a category \mathcal{X} as $\text{bal}_{n,a,m} : F(na, m) \rightarrow F(n, am)$.

The prototypical example of such a balanced functor is the Hom-functor of a module category \mathcal{M} over a rigid monoidal category \mathcal{A} : Let $\mathcal{N} = \overline{\mathcal{M}}$, which is a right \mathcal{A} -module category with action $\overline{ma} := \overline{a^*m}$, where a^* here denotes the *right* dual. Then the evaluation morphism defines isomorphisms

$$\langle \overline{ma}, m' \rangle = \langle a^*m, m' \rangle \cong \langle m, am' \rangle, \quad (2.72)$$

which assemble into a balancing. The hom-functor of a bimodule category is even *bi-balanced*:

If \mathcal{N} is a \mathcal{B} - \mathcal{A} -bimodule category and \mathcal{M} is an \mathcal{A} - \mathcal{B} -bimodule category, then a functor

$$F : {}_{\mathcal{B}}\mathcal{N}_{\mathcal{A}} \boxtimes {}_{\mathcal{A}}\mathcal{M}_{\mathcal{B}} \rightarrow \mathcal{X} \quad (2.73)$$

as above, with one balancing for the \mathcal{A} -actions, and one balancing for the \mathcal{B} -actions, is called a *bi-balanced* functor iff the left and right balancings commute, meaning that

$$\begin{array}{ccc} & F(bna, m) & \\ \text{bal}_{na,b,m}^{\mathcal{B}} \swarrow & & \searrow \text{bal}_{bn,a,m}^{\mathcal{A}} \\ F(na, mb) & & F(bn, am) \\ \text{bal}_{n,a,mb}^{\mathcal{A}} \searrow & & \swarrow \text{bal}_{n,b,am}^{\mathcal{B}} \\ & F(n, amb) & \end{array} \quad (2.74)$$

commutes for all objects $a \in \mathcal{A}$, $b \in \mathcal{B}$, $n \in \mathcal{N}$ and $m \in \mathcal{M}$. This is equivalent to F being equipped with a single balancing between the right $\mathcal{A} \boxtimes \mathcal{B}^{\text{rev}}$ -action on \mathcal{N} and the left $\mathcal{A} \boxtimes \mathcal{B}^{\text{rev}}$ -action on \mathcal{M} .

Another notion of bi-balanced functor also plays a role for us. Consider a functor

$$G : {}_{\mathcal{A}}\mathcal{N}_{\mathcal{A}} \boxtimes {}_{\mathcal{B}}\mathcal{M}_{\mathcal{B}} \rightarrow \mathcal{X}, \quad (2.75)$$

where \mathcal{N} is an \mathcal{A} - \mathcal{A} -bimodule category, and \mathcal{M} is a \mathcal{B} - \mathcal{B} -bimodule category, which is equipped with two balancings, one for \mathcal{M} and one for \mathcal{N} , which are once more required to commute. If $\mathcal{A} = \mathcal{B}$, a functor can be bi-balanced either in the sense of (2.73), or in the sense of (2.75). The term "bi-balanced" functor is therefore ambiguous in this case. We say that a functor

$$F : {}_{\mathcal{A}}\mathcal{N}_{\mathcal{A}} \boxtimes {}_{\mathcal{A}}\mathcal{M}_{\mathcal{A}} \rightarrow \mathcal{X} \quad (2.76)$$

is *connected* bi-balanced if it is equipped with balancings between \mathcal{N} and \mathcal{M} as in (2.73), and *disconnected* bi-balanced if it is equipped with one balancing for \mathcal{N} and one balancing for \mathcal{M} as in (2.75).

Balanced functors, and especially bi-balanced functors, admit well-behaved functorial diagrams, which we will now discuss. We will see that these specialize to the functorial diagrams in Section 2.3 for the choice of the hom-functor as bi-balanced functor.

Given any functor $F : \mathcal{X} \rightarrow \mathcal{Z}$, and a string diagram

$$\begin{array}{c} | \\ \boxed{g} \\ | \\ \boxed{f} \\ | \end{array} = g \circ f, \quad (2.77)$$

we write the following for the morphism $F(g \circ f)$ in \mathcal{Z} :

$$\begin{array}{c} | \\ \boxed{g} \\ | \\ \boxed{f} \\ | \\ \hline F \end{array} := F \left(\begin{array}{c} | \\ \boxed{g} \\ | \\ \boxed{f} \\ | \end{array} \right). \quad (2.78)$$

Of course, the term $g \circ f$ may be replaced with any string diagram in \mathcal{X} . In the same spirit, let $S : \mathcal{Y} \times \mathcal{X} \rightarrow \mathcal{Z}$, and let h be a morphism in \mathcal{Y} . We then write

$$\begin{array}{c} | \\ \boxed{g} \\ | \\ \boxed{f} \\ | \\ \hline S \\ \hline \boxed{h} \\ | \end{array} := S \left(h, \begin{array}{c} | \\ \boxed{g} \\ | \\ \boxed{f} \\ | \end{array} \right) = S(h, g \circ f). \quad (2.79)$$

So far, this notation of functorial diagrams on the left-hand sides of (2.78) and (2.79) bears no advantage over what is written on the right-hand side of these equations. This changes when we consider balanced functors. Let ${}_{\mathcal{A}}\mathcal{M}$ and ${}_{\mathcal{A}}\mathcal{N}$ be left module categories over a pivotal category \mathcal{A} . Given objects $a \in \mathcal{A}$, $m \in \mathcal{M}$, and $n \in \mathcal{N}$, we draw the following functorial diagram to represent the balancing of a balanced functor $S : \overline{\mathcal{N}} \times \mathcal{M} \rightarrow \mathcal{X}$:

$$\begin{array}{c} | \\ a \curvearrowright \boxed{S} \\ | \\ n \end{array} \begin{array}{c} | \\ m \end{array} := \text{bal}_{n,a,m} : S(a^*n, m) \rightarrow S(n, am). \quad (2.80)$$

This notation allows us to represent morphisms in \mathcal{X} built from

- morphisms in the 2-image of S , that is, morphisms of the form $S(f, g)$ where f and g are morphisms in \mathcal{N} and \mathcal{M} , respectively; and
- the balancing isomorphisms of S , and their inverses.

For (connected) bi-balanced functors, bending around strands is allowed both on the left and on the right-hand side of functorial diagrams. To illustrate this, let \mathcal{M} and \mathcal{N} be \mathcal{A} - \mathcal{B} -bimodule categories, and as illustrated in the following picture, which represents a morphism $S(a^*n, mb^*) \rightarrow S(nb, m')$

$$= S(f, nb) \circ \text{bal}_{n,b,am}^{\text{right} -1} \circ \text{bal}_{n,a,mb}^{\text{left}}. \quad (2.81)$$

If we consider the special case where $\mathcal{N} = \mathcal{M} = \mathcal{B} = {}_{\mathcal{A}}\mathcal{A}_{\mathcal{A}}$ is the regular bimodule category, and $\mathcal{X} = \text{vect}$, we can choose S to be the hom-functor of \mathcal{A} , which is a bi-balanced functor. Functorial diagrams such as (2.81) then specialize to the functorial diagrams we encountered in Section 2.3, with the modification that the previously empty double-box is now labeled with the name of a functor, in this case Hom . The reason why functorial diagrams really specialize to the diagrams from Section 2.3 for the hom-functor is that "bending around strands" as in (2.80) encodes the hom-functor's balancing, which is defined using a coevaluation; on the other hand, the coevaluation is also represented by bending around a strand in the functorial diagrams from Section 2.3, which are derived from string diagrams. The hom-functor of a module category \mathcal{M} over \mathcal{A} also comes with a linear map $\langle m, m' \rangle \rightarrow \langle am, am' \rangle$ for each triple of objects $a \in \mathcal{A}$, $m, m' \in \mathcal{M}$, which is part of the data of module action functor. If \mathcal{A} is a rigid and pivotal, this linear map can be expressed using the balancing of the hom-functor, together with either an evaluation or a coevaluation. This is true of any balanced functor $S : \overline{\mathcal{N}} \times \mathcal{M} \rightarrow \mathcal{X}$ over a pivotal category \mathcal{A} : The two expressions

$$\text{bal}_{an,a,m} \circ S({}_{a\text{coev}} n, m) = a \left| \begin{array}{c} m \\ \boxed{S} \\ n \end{array} \right. = \text{bal}_{n,a^*,am}^{-1} \circ S(n, \text{ev}^{a^*} m). \quad (2.82)$$

are equal.

Of course, functorial diagrams can be composed, and the composition operation is the same we already encountered in (2.15): inserting the pre-composed diagram into the double-box of the post-composed diagram. In this way, functorial diagrams are similar to other approaches to graphical calculi, such as the "corollas" appearing, for example, in [FSY23, for the composition see Ex. 2.14].

We leave it to the reader to convince themselves that the evaluation of functorial diagrams is well-defined and that isotopic diagrams evaluate to equal morphisms. In any case, Remark 2.2

applies: Functorial diagrams throughout this work are meant as illustrations that can, at any point, be translated into standard notation. This is why we refrain from a more rigorous formalization of these diagrams.

2.10 (SPLIT) EQUALIZERS OF BI-BALANCED FUNCTORS

Let now ${}_{\mathcal{A}}\mathcal{N}_{\mathcal{A}}$ and ${}_{\mathcal{A}}\mathcal{M}_{\mathcal{A}}$ be \mathcal{A} - \mathcal{A} -bimodule categories. Recall from Section 2.9 that in this case we need to distinguish between *connected* and *disconnected* bi-balanced functors $S : \overline{\mathcal{N}} \times \mathcal{M} \rightarrow \mathcal{X}$. In this section, we will always mean connected bi-balanced functors. We will encounter situations in which a bi-balanced functor S is fed arguments from the centers $x \in Z_{\mathcal{A}}(\mathcal{N})$ and $y \in Z_{\mathcal{A}}(\mathcal{M})$: Expressions of the form $S(U(x), U(y))$ appear. These objects of \mathcal{X} have a distinguished subobject, namely the limit of the diagram

$$\begin{array}{ccc}
 & \begin{array}{c} \text{\scriptsize } a \uparrow \\ \boxed{S} \\ \text{\scriptsize } \downarrow x \\ \text{\scriptsize } y \end{array} & \longrightarrow \int_a S(aU(x), aU(y)) \\
 S(U(x), U(y)) & \searrow & \\
 & \begin{array}{c} \text{\scriptsize } y \downarrow \\ \boxed{S} \\ \text{\scriptsize } \uparrow x \\ \text{\scriptsize } a \end{array} & \longrightarrow \int_a S(U(x)a, U(y)a)
 \end{array} \quad . \quad (2.83)$$

The diagonal arrows in this diagram are to be understood as follows: Being morphisms into ends, they are determined by their components for objects $a \in \mathcal{A}$. These components are given by the functorial diagrams that label the arrows; they were discussed in (2.82). This limit of (2.83) can equivalently be expressed as the equalizer

$$\text{eq} \longleftarrow S(U(x), U(y)) \begin{array}{c} \xrightarrow{\begin{array}{c} \text{\scriptsize } f = \\ \text{\scriptsize } a \uparrow \\ \boxed{S} \\ \text{\scriptsize } \downarrow x \\ \text{\scriptsize } y \end{array}} \\ \xrightarrow{\begin{array}{c} \boxed{S} \\ \text{\scriptsize } \uparrow x \\ \text{\scriptsize } a \end{array}} \\ \xrightarrow{\begin{array}{c} \text{\scriptsize } y \downarrow \\ \boxed{S} \\ \text{\scriptsize } \uparrow x \\ \text{\scriptsize } a \end{array}} \end{array} \int_a S(aU(x), U(y)a) \quad , \quad (2.84)$$

which is why we refer to eq as the *equalizer* of the (connected) bi-balanced functor S on x and y , or just as the equalizer of S .

Example 2.13. If $\mathcal{M} = \mathcal{N}$ and $S : \overline{\mathcal{M}} \times \mathcal{M} \rightarrow \text{vect}$ is the hom-functor, then the equalizer of S on $x, y \in Z_{\mathcal{A}}(\mathcal{M})$ is the hom-space of the center $Z_{\mathcal{A}}(\mathcal{M})\langle x, y \rangle$.

Remark 2.14. A bi-balanced natural transformation $\eta : S \Rightarrow S'$ from S to another bi-balanced functor S' defines a morphism of diagrams between the (2.83) and the diagram obtained from (2.83) by replacing S with S' . Therefore, η defines a morphism from the equalizer of S to the equalizer of S' , for any given pair of objects $x \in Z_{\mathcal{A}}(\mathcal{N})$, $y \in Z_{\mathcal{A}}(\mathcal{M})$.

In the finite semisimple context which we are interested in, meaning that \mathcal{A} is a spherical fusion category and \mathcal{M} and \mathcal{N} are exact, hence semisimple, bimodule categories, and S is linear, hence exact in both arguments, equalizers of bi-balanced functors come with important additional structure: Let us recall the concept of a split equalizer.

Definition 2.15. Let u, v, w be objects of any category \mathcal{X} . A *split equalizer* is a diagram of the form

$$u \begin{array}{c} \xleftarrow{r} \\ \xrightarrow[e]{\quad} \\ \end{array} v \begin{array}{c} \xleftarrow[t]{\quad} \\ \xrightarrow[f]{\quad} \\ \xrightarrow[g]{\quad} \\ \end{array} w, \quad (2.85)$$

where $t \circ f = \text{id}_v$, $t \circ g = e \circ r$, $f \circ e = g \circ e$, and $r \circ e = \text{id}_u$. In particular, r and t are retracts of e and f , respectively.

A *contractible pair* is a pair of parallel morphisms $f, g : v \rightarrow w$, together with a morphism $t : w \rightarrow v$, such that an equalizer of f and g exists, $t \circ f = \text{id}_v$, and $f \circ t \circ g = g \circ t \circ g$.

The following result is well-known, see [Mac71, §VI.6, Exc. 2].

Lemma 2.16. *Split equalizers are in one-to-one correspondence to contractible pairs with a choice of equalizer.*

Proof. Given a split equalizer, e is automatically an equalizer of f and g : Take any morphism $h : q \rightarrow v$ such that $f \circ h = g \circ h$, and assume there is some $k : q \rightarrow u$ such that $h = e \circ k$. Then $r \circ h = r \circ e \circ k = k$, so if any morphism k exists, it must be equal to $r \circ h$. It remains to check that h factors through u via $r \circ h$, which is the case:

$$e \circ r \circ h = t \circ g \circ h = t \circ f \circ h = h. \quad (2.86)$$

Moreover, the condition

$$f \circ t \circ g = f \circ e \circ r = g \circ e \circ r = g \circ t \circ g \quad (2.87)$$

is satisfied. It follows that (f, g) , together with t , is a contractible pair.

Conversely, let (f, g) , together with t , be a contractible pair, and define (u, e) to be an equalizer of f and g . We denote by h the endomorphism $h = t \circ g : v \rightarrow v$. By the universal property of the equalizer, there is a unique morphism $r : v \rightarrow u$ such that $e \circ r = h$. We now have all morphisms that appear in the diagram (2.85). To conclude that they form a split equalizer, we need to check the rules of composition. The first condition, $t \circ f = \text{id}_v$, is also a condition for contractible pairs, and thus still holds. The second condition, $t \circ g = h = e \circ r$ was imposed when we defined r . The third condition, $f \circ e = g \circ e$, holds because e is an equalizer. For the last condition, we compute

$$e \circ r \circ e = t \circ g \circ e = t \circ f \circ e = e, \quad (2.88)$$

and deduce that $r \circ e = \text{id}_u$, because e , being an equalizer, is monic. \square

Notice that the endomorphism h is an idempotent, and its image is u . The next statement is the reason why we are interested in split equalizers.

Lemma 2.17. *Let \mathcal{A} be a spherical fusion category, and let \mathcal{M} and \mathcal{N} be exact \mathcal{A} - \mathcal{A} -bimodule categories. Let $S : \mathcal{N} \times \mathcal{M} \rightarrow \mathcal{X}$ be a bi-balanced functor into a linear category \mathcal{X} . Then the pivotal structure on \mathcal{A} determines a distinguished splitting of the equalizer of S from (2.83). Hence, the equalizer of S is exhibited not only as a subobject, but as a retract.*

Proof. We call the top and bottom arrows of the equalizer diagram (2.83) f and g , respectively. By Lemma 2.16, we only need to build a morphism $t : \int_a S(aU(x), U(y)a) \rightarrow S(U(x), U(y))$ using the pivotal structure of \mathcal{A} , such that (f, g, t) form a contractible pair. Notice that as a morphism out of an end, t is an atypical morphism in the sense of Section 2.6. We therefore first define a morphism $\tilde{t} : \int_a S(aU(x), U(y)a) \rightarrow S(U(x), U(y))$, given on components by

$$\tilde{t}^a := \begin{array}{c} y \\ | \\ \text{---} \\ | \\ \text{---} \\ | \\ \text{---} \\ | \\ \text{---} \\ | \\ x \end{array} \cdot \quad (2.89)$$

The map t is then obtained by precomposing \tilde{t} with the isomorphism $\Theta_{\mathcal{A}}$, which turns the end into a coend, and normalizing:

$$t := \frac{1}{\mathcal{D}_{\mathcal{A}}} \tilde{t} \circ \Theta_{\mathcal{A}}. \quad (2.90)$$

This is the point where the pivotality of \mathcal{A} enters, as $\Theta_{\mathcal{A}}$ depends on this structure.

We start proving that (f, g, t) is a contractible pair by showing that t is a retraction of f . We calculate

$$\begin{aligned} t \circ f &= \frac{1}{\mathcal{D}_{\mathcal{A}}} \tilde{t} \circ \Theta_{\mathcal{A}} \circ f \stackrel{(2.33)}{=} \frac{1}{\mathcal{D}_{\mathcal{A}}} \tilde{t} \bullet f \stackrel{(2.35)}{=} \frac{1}{\mathcal{D}_{\mathcal{A}}} \sum_{\mathbf{a}} d_{\mathbf{a}} \tilde{t}^{\mathbf{a}} \circ_{\mathbf{a}} f \\ &= \frac{1}{\mathcal{D}_{\mathcal{A}}} \sum_{\mathbf{a}} d_{\mathbf{a}} \mathbf{a} \cdot \begin{array}{c} y \\ | \\ \text{---} \\ | \\ \text{---} \\ | \\ \text{---} \\ | \\ \text{---} \\ | \\ x \end{array} = \text{id}_{S(U(x), U(y))}. \end{aligned} \quad (2.91)$$

To complete the proof, we need to check that the other condition, $f \circ t \circ g = g \circ t \circ g$, holds. To this end, we abbreviate $h := t \circ g$ and find, by a calculation similar to (2.91),

$$h = \frac{1}{\mathcal{D}_{\mathcal{A}}} \sum_{\mathbf{a}} d_{\mathbf{a}} \begin{array}{c} y \\ | \\ \text{---} \\ | \\ \text{---} \\ | \\ \text{---} \\ | \\ \text{---} \\ | \\ x \end{array}, \quad (2.92)$$

which is an endomorphism of $S(U(x), U(y))$. Since $\frac{1}{\mathcal{D}_A}$ is a global factor in the following computation, we omit it. On components, we obtain:

$$\begin{aligned}
{}_b f \circ h &= \sum_{\mathbf{a}} d_{\mathbf{a}} \text{ (diagram with } S \text{ box, } x \text{ and } y \text{ wires, } a \text{ and } b \text{ labels)} = \sum_{\mathbf{a}, \mathbf{c}} d_{\mathbf{a}} d_{\mathbf{c}} \text{ (diagram with } S \text{ box, } x \text{ and } y \text{ wires, } a, b, c \text{ labels)} \\
&= \sum_{\mathbf{a}, \mathbf{c}} d_{\mathbf{a}} d_{\mathbf{c}} \text{ (diagram with } S \text{ box, } x \text{ and } y \text{ wires, } a, b, c \text{ labels)} = \sum_{\mathbf{c}} d_{\mathbf{c}} \text{ (diagram with } S \text{ box, } x \text{ and } y \text{ wires, } c \text{ label)} = {}_b g \circ h.
\end{aligned} \tag{2.93}$$

Hence, $f \circ h = g \circ h$, and the proof is complete. \square

Remark 2.18. Lemma 2.17 is an example for how pivotal dimensions in equations such as (2.92) arise from the isomorphism Θ_A between an end and a coend – in this case, expressed by the operation \bullet . This conceptual source of quantum dimensions is a motivation for the introduction of Θ_A in the first place. In fact, throughout the remainder of this paper, quantum dimensions will never be introduced into equations ad hoc, but will always stem from an identification of end and coend via Θ_A .

The retract structure of the equalizer of a bi-balanced functor is preserved by bi-balanced natural transformations. In order to prove this, we need the following, elementary lemma.

Lemma 2.19. *Let \mathcal{X} be a category, and let*

$$x \begin{array}{c} \xleftarrow{\pi} \\ \xrightarrow{\iota} \end{array} y \quad \text{and} \quad x' \begin{array}{c} \xleftarrow{\pi'} \\ \xrightarrow{\iota'} \end{array} y' \tag{2.94}$$

be retracts in \mathcal{X} . Denote the corresponding idempotents by $h = \iota \circ \pi$ and $h' = \iota' \circ \pi'$. A morphism $\varphi : y \rightarrow y'$ which satisfies

$$\begin{array}{ccc}
y & \xrightarrow{h} & y \\
\downarrow \varphi & & \downarrow \varphi \\
y' & \xrightarrow{h'} & y'
\end{array} \tag{2.95}$$

is a morphism of retracts, meaning that

$$\begin{array}{ccc}
x & \xrightarrow{\iota} & y \\
\downarrow \psi & & \downarrow \varphi \\
x' & \xrightarrow{\iota'} & y'
\end{array} \quad \text{and} \quad \begin{array}{ccc}
y & \xrightarrow{\pi} & x \\
\downarrow \varphi & & \downarrow \psi \\
y' & \xrightarrow{\pi'} & x'
\end{array} \tag{2.96}$$

commute for $\psi = \pi' \circ \varphi \circ \iota$. Conversely, any pair of morphisms (φ, ψ) which satisfies (2.96) also satisfies (2.95), and $\psi = \pi' \circ \varphi \circ \iota$ holds.

We can now return to considering equalizers of bi-balanced functors.

Lemma 2.20. *Let $\eta : S \rightarrow S'$ be a bi-balanced natural transformation of bi-balanced functors $S, S' : \overline{\mathcal{N}} \times \mathcal{M} \rightarrow \mathcal{X}$, where \mathcal{M} and \mathcal{N} are \mathcal{A} - \mathcal{A} -bimodule categories for a spherical fusion category \mathcal{A} . Denote by $r : S(U(x), U(y)) \rightarrow \text{eq}$ and $r' : S'(U(x), U(y)) \rightarrow \text{eq}'$ the retractions into the equalizers of S and S' on $x \in Z_{\mathcal{A}}(\mathcal{N})$ and $y \in Z_{\mathcal{A}}(\mathcal{M})$ from Lemma 2.17. Then η defines a morphism of retracts in that*

$$\begin{array}{ccc} S(U(x), U(y)) & \xrightarrow{r} & \text{eq} \\ \downarrow \eta_{U(x), U(y)} & & \downarrow \psi \\ S'(U(x), U(y)) & \xrightarrow{r'} & \text{eq}' \end{array} \quad (2.97)$$

commutes for $\psi = \pi' \circ \eta_{U(x), U(y)} \circ \iota$.

Proof. It is straightforward to verify that

$$\begin{array}{ccc} S(U(x), U(y)) & \xrightarrow{h} & S(U(x), U(y)) \\ \downarrow \eta_{U(x), U(y)} & & \downarrow \eta_{U(x), U(y)} \\ S'(U(x), U(y)) & \xrightarrow{h'} & S'(U(x), U(y)) \end{array} \quad (2.98)$$

commutes if η is a bi-balanced natural transformation, using the idempotent h from (2.92). The claim then follows from Lemma 2.19. \square

2.11 SHIFTING ACTIONS UNDER (CO-)ENDS

Ends end coends of functors on module categories come with a structure that looks like, but is not quite, a balancing. Let \mathcal{M} be a left module category over a pivotal category \mathcal{A} , and let $S : \overline{\mathcal{M}} \times \mathcal{M} \rightarrow \mathcal{X}$ be a bilinear functor. We may define isomorphisms

$$\beta_a : \int_m S(m, am) \rightarrow \int_m S(a^*m, m) \quad \text{and} \quad \tilde{\beta}_a : \int^m S(m, am) \rightarrow \int^m S(a^*m, m) \quad (2.99)$$

for each $a \in \mathcal{A}$ via universal properties, such that the following squares commute:

$$\begin{array}{ccc} \int_m S(m, am) & \xrightarrow{\beta_a} & \int_m S(a^*m, m) \\ \downarrow a^*n\tau & & \downarrow n\tau \\ S(a^*n, aa^*n) & \xrightarrow{S(a^*n, \text{ev}^a n)} & S(a^*n, n) \end{array} \quad \begin{array}{ccc} \int^m S(m, am) & \xrightarrow{\tilde{\beta}_a} & \int^m S(a^*m, m) \\ \sigma^n \uparrow & & \sigma^{an} \uparrow \\ S(n, an) & \xrightarrow{S(\text{ev}^a n, an)} & S(a^*an, an) \end{array} \quad (2.100)$$

Lemma 2.21. *Assume that \mathcal{M} carries the structure of a module trace, such that a distinguished isomorphism $\Theta_{\mathcal{M}}$ exists. Then the maps β_a and $\tilde{\beta}_a$ are related in that the following diagram commutes:*

$$\begin{array}{ccc} \int_m S(m, am) & \xrightarrow{\beta_a} & \int_m S(a^*m, m) \\ \downarrow \Theta_{\mathcal{M}} & & \downarrow \Theta_{\mathcal{M}} \\ \int^m S(m, am) & \xrightarrow{\tilde{\beta}_a} & \int^m S(a^*m, m) \end{array} \quad (2.101)$$

Proof. The diagram (2.101) compares two morphisms from an end into a coend. To show that they are equal, we compare their (atypical) components, as introduced in Section 2.6. It suffices to check the simple components. Let therefore $\mathbf{n}, \mathbf{k} \in \mathcal{M}$ be simple objects. Our goal is to prove that

$$\mathbf{k}(\Theta_{\mathcal{M}} \circ \beta_a)_{\mathbf{n}} = \mathbf{k}(\tilde{\beta}_a \circ \Theta_{\mathcal{M}})_{\mathbf{n}}. \quad (2.102)$$

Using the definition of atypical components (2.37), we find that the respective terms are equal to

$$\begin{aligned} \mathbf{k}(\Theta_{\mathcal{M}} \circ \beta_a)_{\mathbf{n}} &= d_{\mathbf{n}} d_{\mathbf{k}} \mathbf{k}\tau \circ \Theta_{\mathcal{M}}^{-1} \circ \Theta_{\mathcal{M}} \circ \beta_a \circ \Theta_{\mathcal{M}}^{-1} \circ \sigma^{\mathbf{n}} \\ &= d_{\mathbf{n}} d_{\mathbf{k}} \mathbf{k}\tau \circ \beta_a \circ \Theta_{\mathcal{M}}^{-1} \circ \sigma^{\mathbf{n}} \\ \mathbf{k}(\tilde{\beta}_a \circ \Theta_{\mathcal{M}})_{\mathbf{n}} &= d_{\mathbf{n}} d_{\mathbf{k}} \mathbf{k}\tau \circ \Theta_{\mathcal{M}}^{-1} \circ \tilde{\beta}_a \circ \Theta_{\mathcal{M}} \circ \Theta_{\mathcal{M}}^{-1} \circ \sigma^{\mathbf{n}} \\ &= d_{\mathbf{n}} d_{\mathbf{k}} \mathbf{k}\tau \circ \Theta_{\mathcal{M}}^{-1} \circ \tilde{\beta}_a \circ \sigma^{\mathbf{n}}. \end{aligned} \quad (2.103)$$

If we raise and lower all indices involved according to the rules (2.34), we can drop the dimension factors from the equations. In the next step, we use the definition of β and $\tilde{\beta}$ as given in (2.100).

$$\begin{aligned} \mathbf{k}(\Theta_{\mathcal{M}} \circ \beta_a)^{\mathbf{n}} &= \mathbf{k}\tau \circ \beta_a \circ \Theta_{\mathcal{M}}^{-1} \circ \sigma^{\mathbf{n}} \\ &= S(a^* \mathbf{k}, \text{ev}^a \mathbf{k}) \circ a^* \mathbf{k}\tau \circ \Theta_{\mathcal{M}}^{-1} \circ \sigma^{\mathbf{n}} \\ \mathbf{k}(\tilde{\beta}_a \circ \Theta_{\mathcal{M}})^{\mathbf{n}} &= \mathbf{k}\tau \circ \Theta_{\mathcal{M}}^{-1} \circ \tilde{\beta}_a \circ \sigma^{\mathbf{n}} \\ &= \mathbf{k}\tau \circ \Theta_{\mathcal{M}}^{-1} \circ \sigma^{a\mathbf{n}} \circ S(\text{ev}^{a^*} \mathbf{n}, a\mathbf{n}). \end{aligned} \quad (2.104)$$

At this point, we make use of Lemma 2.3, which gives us explicit forms of the structure morphisms $a^* \mathbf{k}\tau$ and $\sigma^{a\mathbf{n}}$ in terms of structure morphisms for simple objects.

$$\begin{aligned} \mathbf{k}(\Theta_{\mathcal{M}} \circ \beta_a)^{\mathbf{n}} &= S(a^* \mathbf{k}, \text{ev}^a \mathbf{k}) \circ \left(\sum_{\mathbf{i}} d_{\mathbf{i}} S(\star_{\langle a^* \mathbf{k}, \mathbf{i} \rangle}, a \star_{\langle \mathbf{i}, a^* \mathbf{k} \rangle}) \circ \mathbf{i}\tau \right) \circ \Theta_{\mathcal{M}}^{-1} \circ \sigma^{\mathbf{n}} \\ &= \sum_{\mathbf{i}} d_{\mathbf{i}} S(\star_{\langle a^* \mathbf{k}, \mathbf{i} \rangle}, (\text{ev}^a \mathbf{k}) \circ (a \star_{\langle \mathbf{i}, a^* \mathbf{k} \rangle})) \circ \mathbf{i}\tau \circ \Theta_{\mathcal{M}}^{-1} \circ \sigma^{\mathbf{n}} \\ &\stackrel{(2.46)}{=} \sum_{\mathbf{i}} d_{\mathbf{i}} S(\star_{\langle a^* \mathbf{k}, \mathbf{i} \rangle}, (\text{ev}^a \mathbf{k}) \circ (a \star_{\langle \mathbf{i}, a^* \mathbf{k} \rangle})) \frac{\delta_{\mathbf{n}, \mathbf{i}}}{d_{\mathbf{i}}} \\ &= S(\star_{\langle a^* \mathbf{k}, \mathbf{n} \rangle}, (\text{ev}^a \mathbf{k}) \circ (a \star_{\langle \mathbf{n}, a^* \mathbf{k} \rangle})) \\ \mathbf{k}(\tilde{\beta}_a \circ \Theta_{\mathcal{M}})^{\mathbf{n}} &= \mathbf{k}\tau \circ \Theta_{\mathcal{M}}^{-1} \circ \left(\sum_{\mathbf{i}} d_{\mathbf{i}} \sigma^{\mathbf{i}} \circ S(a^* \star_{\langle \mathbf{i}, a\mathbf{n} \rangle}, \star_{\langle a\mathbf{n}, \mathbf{i} \rangle}) \right) \circ S(\text{ev}^{a^*} \mathbf{n}, a\mathbf{n}) \\ &= \sum_{\mathbf{i}} d_{\mathbf{i}} \mathbf{k}\tau \circ \Theta_{\mathcal{M}}^{-1} \circ \sigma^{\mathbf{i}} \circ S((\text{ev}^{a^*} \mathbf{n}) \circ (a^* \star_{\langle \mathbf{i}, a\mathbf{n} \rangle}), \star_{\langle a\mathbf{n}, \mathbf{i} \rangle}) \\ &\stackrel{(2.46)}{=} \sum_{\mathbf{i}} d_{\mathbf{i}} \frac{\delta_{\mathbf{k}, \mathbf{i}}}{d_{\mathbf{i}}} S((\text{ev}^{a^*} \mathbf{n}) \circ (a^* \star_{\langle \mathbf{i}, a\mathbf{n} \rangle}), \star_{\langle a\mathbf{n}, \mathbf{i} \rangle}) \\ &= S((\text{ev}^{a^*} \mathbf{n}) \circ (a^* \star_{\langle \mathbf{k}, a\mathbf{n} \rangle}), \star_{\langle a\mathbf{n}, \mathbf{k} \rangle}). \end{aligned} \quad (2.105)$$

It follows from Lemma 2.10 that these expressions are equal, as long as the trace on \mathcal{M} is a module trace. \square

By recognizing that $\mathbf{k}(\Theta_{\mathcal{M}} \circ \beta_a)^{\mathbf{n}} = \mathbf{k}(\beta_a)^{\mathbf{n}}$ and $\mathbf{k}(\tilde{\beta}_a \circ \Theta_{\mathcal{M}})^{\mathbf{n}} = \mathbf{k}(\tilde{\beta}_a)^{\mathbf{n}}$, we see that the proof of Lemma 2.21 provided us with the useful simple components of the morphism β :

$$\begin{aligned} \mathbf{k}(\beta_a)^{\mathbf{n}} &= S(a^* \mathbf{k}, \text{ev}^a \mathbf{k}) \circ \sum_{\mathbf{i}} d_{\mathbf{i}} S(\star_{\langle a^* \mathbf{k}, \mathbf{i} \rangle}, a \star_{\langle \mathbf{i}, a^* \mathbf{k} \rangle}) \frac{\delta_{\mathbf{i} \mathbf{n}}}{d_{\mathbf{n}}} \\ &= S(\star_{\langle a^* \mathbf{k}, \mathbf{n} \rangle}, (\text{ev}^a \mathbf{k}) \circ (a \star_{\langle \mathbf{n}, a^* \mathbf{k} \rangle})). \end{aligned} \quad (2.106)$$

Moreover, Lemma 2.21 showed that ${}_k(\beta_a)^n = {}_k(\tilde{\beta}_a)^n$, also for non-simple objects n and k . This justifies some abuse of notation: From here on, we denote both β_a and $\tilde{\beta}_a$ by β_a .

The morphisms β_a are of interest to us for some particular choices of S , which we now discuss. A calculation involving Lemma 2.3 reveals that the (2.106) holds also for non-simple objects n and k .

- For $S = - \boxtimes -$, the morphisms β_a are isomorphisms, and form balancings for the objects $\int_m \bar{m} \boxtimes m$ and $\int^m \bar{m} \boxtimes m$ of $\overline{\mathcal{M}} \boxtimes \mathcal{M}$. Their components are given by

$${}_k(\beta_a)^n = \star_{\langle a^* k, n \rangle} \boxtimes \left((\text{ev}^a k) \circ (a \star_{\langle n, a^* k \rangle}) \right) = \left((\text{ev}^{a^*} n) \circ (a^* \star_{\langle k, an \rangle}) \right) \boxtimes \star_{\langle an, k \rangle}. \quad (2.107)$$

- Let \mathcal{A} be a spherical fusion category, let ${}_{\mathcal{A}}\mathcal{N}_{\mathcal{A}}$ be an \mathcal{A} - \mathcal{A} -bimodule category, fix $m \in \mathcal{N}$ and set $S_m := -m(-)^*$ as a functor ${}_{\mathcal{A}}\mathcal{A} \times \overline{\mathcal{A}}_{\mathcal{A}} \rightarrow {}_{\mathcal{A}}\mathcal{N}_{\mathcal{A}}$. The morphisms β_a associated with S_m again assemble into balancings. We can thus define functors $\boxtimes, \boxdot : \mathcal{N} \rightarrow Z_{\mathcal{A}}(\mathcal{N})$, called (*left and right induction functors*) via

$$\boxtimes(m) := \left(\int^a ama^*, \beta \right) \quad \text{and} \quad \boxdot(m) := \left(\int_a ama^*, \beta \right). \quad (2.108)$$

The components of the balancings are given by

$${}_c(\beta_a)^b = \star_{\langle a^* c, b \rangle} m \left((\text{ev}^a c) \circ (a \star_{\langle b, a^* c \rangle}) \right) = \left((\text{ev}^{a^*} b) \circ (a^* \star_{\langle c, ab \rangle}) \right) m \star_{\langle ab, c \rangle}. \quad (2.109)$$

The left and right induction functors are left and right adjoint to the forgetful functor $U : Z_{\mathcal{A}}(\mathcal{N}) \rightarrow \mathcal{N}$:

$$\boxtimes \dashv U \dashv \boxdot. \quad (2.110)$$

In our setting, where the spherical structure on \mathcal{A} defines an isomorphism between the end and the coend, there is a natural isomorphism $\boxtimes \cong \boxdot$, and the adjunctions (2.110) become Frobenius.

The adjunctions (2.110) are witnessed by isomorphisms

$$\text{adj}_{m,x}^{\boxtimes} : \mathcal{N} \langle m, U(x) \rangle \rightarrow Z_{\mathcal{A}}(\mathcal{N}) \langle \boxtimes(m), x \rangle \quad (2.111)$$

and

$$\text{adj}_{m,x}^{\boxdot} : \mathcal{N} \langle U(x), m \rangle \rightarrow Z_{\mathcal{A}}(\mathcal{N}) \langle x, \boxdot(m) \rangle, \quad (2.112)$$

natural in $m \in \mathcal{N}$ and $x \in Z_{\mathcal{A}}(\mathcal{N})$. For morphisms $f : m \rightarrow U(x)$, $g : U(x) \rightarrow m$, $f' : \boxtimes(m) \rightarrow x$ and $g' : x \rightarrow \boxtimes(m)$, these adjunction isomorphisms are given explicitly by the following expressions.

$$\text{adj}_{m,x}^{\boxtimes}(f) = \int_a \text{brev}_x^a \circ (a f a^*) \quad \text{and} \quad (\text{adj}_{m,x}^{\boxtimes})^{-1}(f') = f' \circ \sigma^{\mathbb{1}}; \quad (2.113)$$

$$\text{adj}_{m,x}^{\boxtimes}(g) = \int_a (a g a^*) \circ a^* \text{cobrev}_x \quad \text{and} \quad (\text{adj}_{m,x}^{\boxtimes})^{-1}(g') = \mathbb{1}\tau \circ g'. \quad (2.114)$$

Remark 2.22. Via the chain of isomorphisms

$$\mathcal{N}\langle -a, U(x) \rangle \cong \mathcal{N}\langle -, aU(x) \rangle \cong \mathcal{N}\langle -, U(x)a \rangle \cong \mathcal{N}\langle -a, U(x) \rangle, \quad (2.115)$$

$\mathcal{N}\langle -a, U(x) \rangle$ is a balanced functor in the sense of Section 2.8. Similarly, the induction functor \boxtimes is balanced, with the balancing given by the morphism β . The adjunction (2.111) defines a balanced natural isomorphism

$$\mathcal{N}\langle -, U(x) \rangle \cong Z_{\mathcal{A}(\mathcal{N})}\langle \boxtimes(-), x \rangle. \quad (2.116)$$

By the universal property (2.71) of the center, the linear functor $Z_{\mathcal{A}(\mathcal{N})}\langle -, x \rangle$ is the essentially unique functor $F : \overline{Z_{\mathcal{A}}(\mathcal{N})} \rightarrow \text{vect}$ in that a balanced natural isomorphism $\mathcal{N}\langle -, U(x) \rangle \cong F \circ \boxtimes$ exists. A similar statement holds for the other adjunction.

Lemma 2.23. *Given an \mathcal{A} - \mathcal{A} -bimodule category \mathcal{M} , the inclusion of the hom-space*

$$Z_{\mathcal{A}(\mathcal{M})}\langle x, y \rangle \hookrightarrow \mathcal{M}\langle U(x), U(y) \rangle \quad (2.117)$$

has, for a given spherical structure on \mathcal{A} , a canonical retraction $r : \mathcal{M}\langle U(x), U(y) \rangle \rightarrow Z_{\mathcal{A}(\mathcal{M})}\langle x, y \rangle$, given by

$$r(f) = \frac{1}{\mathcal{D}_{\mathcal{A}}} \sum_{\mathbf{a}} d_{\mathbf{a}} \text{brev}_y^{\mathbf{a}} \circ (\mathbf{a} f \mathbf{a}^*) \circ \mathbf{a}^* \text{cobrev}_x = \frac{1}{\mathcal{D}_{\mathcal{A}}} \sum_{\mathbf{a}} d_{\mathbf{a}} \begin{array}{c} | y \\ \circlearrowleft \\ \boxed{f} \\ \circlearrowright \\ | x \end{array} \mathbf{a}, \quad (2.118)$$

or in different notation,

$$\begin{aligned} r(f) &= \frac{1}{\mathcal{D}_{\mathcal{A}}} \text{brev}_y \bullet \boxtimes(f) \circ (-)^* \text{cobrev}_x \\ &= \frac{1}{\mathcal{D}_{\mathcal{A}}} \text{brev}_y \circ \boxtimes(f) \bullet (-)^* \text{cobrev}_x, \end{aligned} \quad (2.119)$$

where by $(-)^ \text{cobrev}_x$, we mean the morphism $U(x) \rightarrow \int_a a U(x) a^*$ with components $a^* \text{cobrev}_x$.*

This generalizes [BK10, Lem. 2.2], and is a direct corollary of Lemma 2.17: The connected bi-balanced functor in this case is the hom-functor in \mathcal{M} , as discussed in Example 2.13. Given $f : m \rightarrow U(y)$ and $g : U(x) \rightarrow m$ for some $m \in \mathcal{M}$ as in (2.114), the retraction r from Lemma 2.23

of the composition $f \circ g$ can also be expressed in terms of the adjunction isomorphisms (2.112) and (2.111):

$$r(f \circ g) = \frac{1}{\mathcal{D}_{\mathcal{A}}} \text{adj}_{m,y}^{\boxtimes}(f) \bullet \text{adj}_{m,x}^{\boxtimes}(g). \quad (2.120)$$

Lemma 2.23 can be used to investigate the center of a *traced* bimodule category. Explicitly, we will see the following:

Lemma 2.24. *Let \mathcal{A} be a spherical fusion category, and let \mathcal{M} be a traced \mathcal{A} - \mathcal{A} -bimodule category. The center $Z_{\mathcal{A}}(\mathcal{M})$ can be equipped with the structure of a Calabi-Yau category, whose trace function is defined, for an endomorphism $f : x \rightarrow x$ in $Z_{\mathcal{A}}(\mathcal{M})$, by*

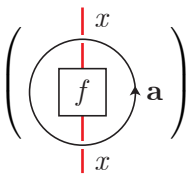
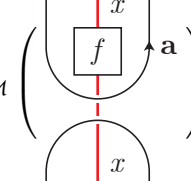
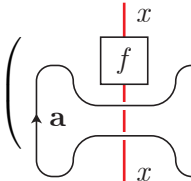
$$\text{Tr}_{Z_{\mathcal{A}}(\mathcal{M})}(f) := \frac{1}{\mathcal{D}_{\mathcal{A}}} \text{Tr}_{\mathcal{M}}(f). \quad (2.121)$$

Of course, the normalization factor $\frac{1}{\mathcal{D}_{\mathcal{A}}}$ in (2.121) is a convention. The reason for this particular choice will be made clear by Remark 2.29. Before we prove Lemma 2.24, we need some intermediate results. First, observe that the retraction r from Lemma 2.23, composed with the inclusion (2.117), defines an idempotent $h : \mathcal{M}\langle U(x), U(y) \rangle \rightarrow \mathcal{M}\langle U(x), U(y) \rangle$, which also appeared in Lemma 2.17. This idempotent leaves the trace invariant:

Lemma 2.25. *Let $x \in Z_{\mathcal{A}}(\mathcal{M})$ and let f be an endomorphism of $U(x)$ in \mathcal{M} . Then*

$$\text{Tr}_{\mathcal{M}}(f) = \text{Tr}_{\mathcal{M}}(h(f)). \quad (2.122)$$

Proof. The proof is a direct calculation:

$$\begin{aligned} \text{Tr}_{\mathcal{M}}(h(f)) &= \frac{1}{\mathcal{D}_{\mathcal{A}}} \sum_{\mathbf{a}} d_{\mathbf{a}} \text{Tr}_{\mathcal{M}} \left(\text{Diagram 1} \right) = \frac{1}{\mathcal{D}_{\mathcal{A}}} \sum_{\mathbf{a}} d_{\mathbf{a}} \text{Tr}_{\mathcal{M}} \left(\text{Diagram 2} \right) \\ &= \frac{1}{\mathcal{D}_{\mathcal{A}}} \sum_{\mathbf{a}} d_{\mathbf{a}} \text{Tr}_{\mathcal{M}} \left(\text{Diagram 3} \right) = \text{Tr}_{\mathcal{M}}(f). \end{aligned} \quad (2.123)$$




The first equality is (2.118), the second uses the symmetry of the trace, and the third uses the compatibility of the bimodule trace on \mathcal{M} with the pivotal structure on \mathcal{A} . \square

It is an even more straightforward observation that, for objects $x, y, z \in Z_{\mathcal{A}}(\mathcal{M})$, a morphism $f : y \rightarrow z$ in $Z_{\mathcal{A}}(\mathcal{M})$, and a morphism $g : U(x) \rightarrow U(y)$ in \mathcal{M} , the equality

$$f \circ r(g) = r(f \circ g) \quad (2.124)$$

holds. Now we are in a position to prove the lemma.

Proof of Lemma 2.24. It is clear that the candidate $\mathrm{Tr}_{Z_{\mathcal{A}}(\mathcal{M})}$ for the trace function defined in (2.121) inherits the symmetry property from the trace $\mathrm{Tr}_{\mathcal{M}}$ on \mathcal{M} . It remains to check whether it is also non-degenerate. To this end, let $f : y \rightarrow z$ be a morphism as before. We need to check that if for every $g \in Z_{\mathcal{A}}(\mathcal{M})\langle z, y \rangle$, we have $\mathrm{Tr}_{Z_{\mathcal{A}}(\mathcal{M})}(f \circ \tilde{g}) = 0$, then $f = 0$. As the normalization factor $\frac{1}{\mathcal{D}_{\mathcal{A}}}$ in the definition of $\mathrm{Tr}_{Z_{\mathcal{A}}(\mathcal{M})}$ is not relevant for the validity of the statement, the condition $\forall \tilde{g} \in \langle z, y \rangle, \mathrm{Tr}_{Z_{\mathcal{A}}(\mathcal{M})}(f \circ \tilde{g}) = 0$ is equivalent to:

$$\forall \tilde{g} \in \langle z, y \rangle, \mathrm{Tr}_{\mathcal{M}}(f \circ \tilde{g}) = 0 \quad (2.125)$$

Since r is surjective, there is some $g \in {}_{\mathcal{M}}\langle U(z), U(y) \rangle$ such that $\tilde{g} = r(g)$. Hence, (2.125) is equivalent to $\forall g \in \langle U(z), U(y) \rangle, \mathrm{Tr}_{\mathcal{M}}(f \circ r(g)) = 0$. Moreover, from (2.124) and Lemma 2.25, we know that

$$\mathrm{Tr}_{\mathcal{M}}(f \circ r(g)) = \mathrm{Tr}_{\mathcal{M}}(r(f \circ g)) = \mathrm{Tr}_{\mathcal{M}}(f \circ g). \quad (2.126)$$

Thus, the statement we want to prove is that $\forall g \in \langle U(z), U(y) \rangle, \mathrm{Tr}_{\mathcal{M}}(f \circ g) = 0$ implies $f = 0$. This is true by the non-degeneracy of the trace on \mathcal{M} . \square

2.12 RELATIVE DELIGNE PRODUCTS AND SCHAUMANN'S TRICATEGORY.

Traced bimodule categories over spherical fusion categories organize into a tricategory $\mathrm{BiMod}^{\mathrm{Tr}}$, as shown in [Sch13a, Thm. 4.10.3]. The objects of $\mathrm{BiMod}^{\mathrm{Tr}}$ are spherical fusion categories. 1-morphisms between objects \mathcal{A} and \mathcal{B} are traced \mathcal{A} - \mathcal{B} -bimodule categories. 2-morphisms are bimodule functors, and 3-morphisms are bimodule natural transformations. In order to define the composition of 1-morphisms, a way to combine a traced \mathcal{A} - \mathcal{B} -bimodule category ${}_{\mathcal{A}}\mathcal{M}_{\mathcal{B}}$ with a traced \mathcal{B} - \mathcal{C} -bimodule category ${}_{\mathcal{B}}\mathcal{N}_{\mathcal{C}}$ to obtain a traced \mathcal{A} - \mathcal{C} -bimodule category is needed. This is afforded by the *relative Deligne product*. For us, it is convenient to realize it as the center of the \mathcal{B} - \mathcal{B} -bimodule category $\mathcal{M}_{\mathcal{B}} \boxtimes_{\mathcal{B}} \mathcal{N}$:

$$\mathcal{M} \square_{\mathcal{B}} \mathcal{N} := Z_{\mathcal{B}}(\mathcal{M}_{\mathcal{B}} \boxtimes_{\mathcal{B}} \mathcal{N}). \quad (2.127)$$

In notation, we sometimes omit the spherical fusion category \mathcal{B} when there is no ambiguity, simply writing

$$\mathcal{M} \square \mathcal{N} := \mathcal{M} \square_{\mathcal{B}} \mathcal{N}. \quad (2.128)$$

Remark 2.26. Recall that balanced functors and balanced natural transformations form a category $\mathrm{Fun}^{\mathrm{bal}}(\mathcal{M} \boxtimes \mathcal{N}, \mathcal{Y})$. The universal property of the center (2.71) specializes to this case: There is an equivalence of categories

$$\mathrm{Fun}^{\mathrm{bal}}(\mathcal{M} \boxtimes \mathcal{N}, \mathcal{Y}) \cong \mathrm{Fun}(\mathcal{M} \square \mathcal{N}, \mathcal{Y}). \quad (2.129)$$

Indeed, one usually defines the relative Deligne product by the universal property that for each linear category \mathcal{Y} , an equivalence (2.129) exists.

The category $\mathcal{M} \square \mathcal{N}$ still carries a left \mathcal{A} -action inherited from \mathcal{M} and a right \mathcal{C} -action inherited from \mathcal{N} , and is indeed an \mathcal{A} - \mathcal{C} -bimodule category. This defines the composition of 1-morphisms in the tricategory $\mathrm{BiMod}^{\mathrm{Tr}}$.

Moreover, the tricategory BiMod^{Tr} admits a \mathcal{B} -trace in the sense of [FSS17, Defn. 5.1]. For us, the \mathcal{B} -trace is the assignment ${}_{\mathcal{A}}\mathcal{M}_{\mathcal{A}} \mapsto Z_{\mathcal{A}}(\mathcal{M})$ of a bimodule category to its center. Given bimodule categories ${}_{\mathcal{A}}\mathcal{M}_{\mathcal{B}}$ and ${}_{\mathcal{B}}\mathcal{N}_{\mathcal{A}}$, there is a canonical equivalence

$$Z_{\mathcal{A}}(\mathcal{M} \square_{\mathcal{B}} \mathcal{N}) \cong Z_{\mathcal{B}}(\mathcal{N} \square_{\mathcal{A}} \mathcal{M}). \quad (2.130)$$

We also use "dangling product" notation for this category, as in

$$\mathcal{M} \square \mathcal{N} \square := Z_{\mathcal{A}}(\mathcal{M} \square_{\mathcal{B}} \mathcal{N}). \quad (2.131)$$

Remark 2.27. By Remark 2.11, the relative Deligne product specializes to the ordinary Deligne product in the case that $\mathcal{B} = \text{vect}$, i.e.

$$\mathcal{M} \square_{\text{vect}} \mathcal{N} \cong \mathcal{M} \boxtimes \mathcal{N}. \quad (2.132)$$

Recall the induction functors \square and \boxtimes from (2.110). We denote

$$m \square n := \square(m \boxtimes n) \quad \text{and} \quad m \boxtimes n := \boxtimes(m \square n). \quad (2.133)$$

The dangling product notation from (2.131) can be used here as well: We may write $m \square n \square$ for an object in $\mathcal{M} \square \mathcal{N} \square$. As a composition, the relative Deligne product is associative (in the sense that it comes with an appropriately coherent set of equivalences witnessing associativity) and unital. We slightly abuse notation by treating the relative Deligne product as if it were strictly associative: we do not pay attention to bracketing and make no explicit use of associators.

We do, however, pay closer attention to the equivalences witnessing unitality. To understand them, first note that the identity 1-morphism $\mathcal{A} \rightarrow \mathcal{A}$ is the regular bimodule category ${}_{\mathcal{A}}\mathcal{A}_{\mathcal{A}}$. Unitality requires an equivalence of \mathcal{A} - \mathcal{B} -bimodule categories

$${}_{\mathcal{A}}\mathcal{A} \square \mathcal{M}_{\mathcal{B}} \cong {}_{\mathcal{A}}\mathcal{M}_{\mathcal{B}} \quad (2.134)$$

for every \mathcal{A} - \mathcal{B} -bimodule category \mathcal{M} . This equivalence is given, on objects of the form $a \boxtimes m \in \mathcal{A} \square \mathcal{M}$, by

$$a \boxtimes m \mapsto am \in \mathcal{M}, \quad (2.135)$$

with pseudo-inverse

$$n \mapsto \mathbf{1} \boxtimes n \in \mathcal{A} \square \mathcal{M}, \quad (2.136)$$

for $n \in \mathcal{N}$.

In order for the composition in the tricategory BiMod^{Tr} to be well-defined, there needs to be a canonical way to define a bimodule trace on $\mathcal{M} \square \mathcal{N}$, constructed from the bimodule traces on \mathcal{M} and \mathcal{N} . A construction of a trace on $\mathcal{M} \square \mathcal{N}$ is provided by Lemma 2.24, but we do not yet know whether this trace respects the bimodule structure. On the other hand, a bimodule trace for $\mathcal{M} \square \mathcal{N}$ is constructed in [Sch13a, Prop. 4.10.1]. The next lemma shows that these traces are indeed equal, making calculations involving the trace on the relative Deligne product easy to perform.

Lemma 2.28. *The bimodule trace on $\mathcal{M} \square_{\mathcal{B}} \mathcal{N}$ defined in [Sch13a, Prop. 4.10.1] is the trace for the center of a traced bimodule category defined in Lemma 2.24. In particular, it has the following property: For endomorphisms $f : m \rightarrow m$ in \mathcal{M} and $g : n \rightarrow n$ in \mathcal{N} ,*

$$\mathrm{Tr}_{\mathcal{M} \square_{\mathcal{B}} \mathcal{N}}(f \boxtimes g) = \mathrm{Tr}_{\mathcal{M} \square_{\mathcal{B}} \mathcal{N}}(f \boxtimes g) = \mathrm{Tr}_{\mathcal{M}}(f) \mathrm{Tr}_{\mathcal{N}}(g). \quad (2.137)$$

In particular,

$$d_{m \boxtimes n} = d_{m \boxtimes n} = d_m d_n. \quad (2.138)$$

Proof. The bimodule trace on $\mathcal{M} \square_{\mathcal{B}} \mathcal{N}$ is defined by a balanced natural isomorphism

$$\mathcal{M} \square_{\mathcal{B}} \langle x, y \rangle \cong \mathcal{M} \square_{\mathcal{B}} \langle y, x \rangle^*, \quad (2.139)$$

natural in the objects $x, y \in \mathcal{M} \square_{\mathcal{B}} \mathcal{N}$. As outlined in the proof of [Sch13a, Prop. 4.10.1], it suffices to specify this isomorphism for $y = m \boxtimes n$ for some objects $m \in \mathcal{M}$, $n \in \mathcal{N}$, in which case it is given by the following composition:

$$\begin{array}{ccc}
\langle x, m \boxtimes n \rangle & & h \\
\downarrow (\mathrm{adj}_{m \boxtimes n, x}^{\boxtimes})^{-1} & & \downarrow \\
\langle U(x), m \boxtimes n \rangle & & (\mathrm{adj}_{m \boxtimes n, x}^{\boxtimes})^{-1}(h) \\
\downarrow \text{Trace on } \mathcal{M} \boxtimes \mathcal{N} & & \downarrow \\
\langle m \boxtimes n, U(x) \rangle^* & & \mathrm{Tr}_{\mathcal{M} \boxtimes \mathcal{N}} \left((\mathrm{adj}_{m \boxtimes n, x}^{\boxtimes})^{-1}(h) \circ - \right) \\
\downarrow (\mathrm{adj}_{m \boxtimes n, x}^{\boxtimes})^{-1} & & \downarrow \\
\langle m \boxtimes n, x \rangle^* & & \mathrm{Tr}_{\mathcal{M} \boxtimes \mathcal{N}} \left((\mathrm{adj}_{m \boxtimes n, x}^{\boxtimes})^{-1}(h) \circ (\mathrm{adj}_{m \boxtimes n, x}^{\boxtimes})^{-1}(-) \right) \\
\downarrow \Theta_{\mathcal{B}} & & \downarrow \\
\langle m \boxtimes n, x \rangle^* & & \mathrm{Tr}_{\mathcal{M} \boxtimes \mathcal{N}} \left((\mathrm{adj}_{m \boxtimes n, x}^{\boxtimes})^{-1}(h) \circ (\mathrm{adj}_{m \boxtimes n, x}^{\boxtimes})^{-1}(- \circ \Theta_{\mathcal{B}}^{-1}) \right)
\end{array} \quad (2.140)$$

The isomorphism (2.140) defines a pairing $(-, -)$ between the vector spaces $\langle x, m \boxtimes n \rangle$ and $\langle m \boxtimes n, x \rangle$, which is related to the bimodule trace on $\mathcal{M} \square_{\mathcal{B}} \mathcal{N}$ by

$$\mathrm{Tr}_{\mathcal{M} \square_{\mathcal{B}} \mathcal{N}}(k \circ h) = (h, k) \quad (2.141)$$

for $h : x \rightarrow m \boxtimes n$ and $k : m \boxtimes n \rightarrow x$. Let $q : x \rightarrow x$ be an endomorphism of $x \in \mathcal{M} \square_{\mathcal{B}} \mathcal{N}$. Using the retraction r from Lemma 2.23, we know that

$$q = r(q) \stackrel{(2.120)}{=} \frac{1}{\mathcal{D}_{\mathcal{B}}} \mathrm{adj}_{U(x), x}^{\boxtimes}(q) \bullet \mathrm{adj}_{U(x), x}^{\boxtimes}(\mathrm{id}_{U(x)}). \quad (2.142)$$

This allows us to write q as the composition $q = k \circ h$ with

$$k = \frac{1}{\mathcal{D}_{\mathcal{B}}} \mathrm{adj}_{U(x), x}^{\boxtimes}(q) \circ \Theta_{\mathcal{B}} \quad \text{and} \quad h = \mathrm{adj}_{U(x), x}^{\boxtimes}. \quad (2.143)$$

In making these choices for k and h , we have set $m \boxtimes n = U(x)$. In general, $U(x)$ will not factorize so nicely, but instead be a direct sum $U(x) = \bigoplus_{i \in I} m_i \boxtimes n_i$ over a finite set I . Since all functors involved are linear, this does not cause a problem, and we ignore the subtlety.

We can now calculate

$$\begin{aligned} \mathrm{Tr}_{\mathcal{M} \square \mathcal{N}}(q) &= \mathrm{Tr}_{\mathcal{M} \square \mathcal{N}}(k \circ h) \\ &= \mathrm{Tr}_{\mathcal{M} \boxtimes \mathcal{N}} \left(\underbrace{(\mathrm{adj}_{m \boxtimes n, x}^{\boxtimes})^{-1}(h)}_{\mathrm{id}_{U(x)}} \circ \underbrace{(\mathrm{adj}_{m \boxtimes n, x}^{\boxtimes})^{-1}(k \circ \Theta_{\mathcal{B}}^{-1})}_{\frac{1}{\mathcal{D}_{\mathcal{B}}} q} \right) \\ &= \frac{1}{\mathcal{D}_{\mathcal{B}}} \mathrm{Tr}_{\mathcal{M} \boxtimes \mathcal{N}}(q). \end{aligned} \quad (2.144)$$

This is indeed the formula (2.121) for the trace of the center of a bimodule category. \square

Remark 2.29. The unitor equivalence

$$\mathcal{A} \square \mathcal{A} \cong \mathcal{A} \quad (2.145)$$

from (2.134) for a spherical fusion category \mathcal{A} is an equivalences between two traced bimodule categories. Lemma 2.28 implies that this equivalence preserves the trace. This compatibility is the reason for the normalization factor $\frac{1}{\mathcal{D}_{\mathcal{A}}}$ in the definition (2.121) of the Calabi-Yau structure for the center of a traced bimodule category.

Remark 2.30 (Sweedler notation for forgetful functors.). Due to its definition as a center (2.127), the relative Deligne product $\mathcal{M} \square_{\mathcal{B}} \mathcal{N}$ comes with a forgetful functor $U : \mathcal{M} \square_{\mathcal{B}} \mathcal{N} \rightarrow \mathcal{M} \boxtimes \mathcal{N}$. We will often use a form of Sweedler notation for this functor, writing

$$U(x) = x_{(\mathcal{M})} \boxtimes x_{(\mathcal{N})} \quad (2.146)$$

for $x \in \mathcal{M} \square \mathcal{N}$. Some care has to be applied when using this notation for more than two factors. Let $x \in \mathcal{M} \square_{\mathcal{B}} \mathcal{N} \square_{\mathcal{C}} \mathcal{K}$. There are now three forgetful functors: $U_{\mathcal{B}}$ forgets only the \mathcal{B} -balancing, $U_{\mathcal{C}}$ forgets only the \mathcal{C} -balancing, and U forgets both. We denote $U_{\mathcal{C}}(x) = x_{(\mathcal{M} \square \mathcal{N})} \boxtimes x_{(\mathcal{K})}$, but really, we mean by this a sum of \boxtimes -factorized terms

$$U_{\mathcal{C}}(x) = x_{(\mathcal{M} \square \mathcal{N})} \boxtimes x_{(\mathcal{K})} = \bigoplus_{i \in I} x_{(\mathcal{M} \square \mathcal{N}, i)} \boxtimes x_{(\mathcal{K}, i)}, \quad (2.147)$$

where I is a finite indexing set. If we encounter a term such as " $\mathcal{M} \square \mathcal{N} \langle y, x_{(\mathcal{M} \square \mathcal{N})} \rangle \otimes F(x_{(\mathcal{K})})$ ", with $x \in \mathcal{M} \square \mathcal{N}$ and $F : \mathcal{K} \rightarrow \mathcal{X}$ some linear functor, we should read it as

$$\mathcal{M} \square \mathcal{N} \langle y, x_{(\mathcal{M} \square \mathcal{N})} \rangle \otimes F(x_{(\mathcal{K})}) := \bigoplus_{i \in I} \mathcal{M} \square \mathcal{N} \langle y, x_{(\mathcal{M} \square \mathcal{N}, i)} \rangle \otimes F(x_{(\mathcal{K}, i)}). \quad (2.148)$$

More frequently, however, we are presented with a factorized expression for $U(x)$, rather than $U_{\mathcal{C}}(x)$:

$$U(x) = x_{(\mathcal{M})} \boxtimes x_{(\mathcal{N})} \boxtimes x_{(\mathcal{K})} = \bigoplus_{j \in J} x_{(\mathcal{M}, j)} \boxtimes x_{(\mathcal{N}, j)} \boxtimes x_{(\mathcal{K}, j)}. \quad (2.149)$$

It is tempting to replace $x_{(\mathcal{M}\square\mathcal{N})}$ with $(x_{(\mathcal{M})} \boxtimes x_{(\mathcal{N})}, \text{bal}^{\mathcal{B}})$ in (2.148), writing it as an object with a \mathcal{B} -balancing. However, we run into a problem: Inserting this expression into our running example leads to

$$\mathcal{M}\square\mathcal{N}\langle y, (x_{(\mathcal{M})} \boxtimes x_{(\mathcal{N})}, \text{bal}^{\mathcal{B}}) \rangle \otimes F(x_{(\mathcal{K})}) \stackrel{?}{=} \bigoplus_{j \in J} \mathcal{M}\square\mathcal{N}\langle y, (x_{(\mathcal{M},j)} \boxtimes x_{(\mathcal{N},j)}, \text{bal}_j^{\mathcal{B}}) \rangle \otimes F(x_{(\mathcal{K},j)}). \quad (2.150)$$

This is not a well-defined term because $(x_{(\mathcal{M},j)} \boxtimes x_{(\mathcal{N},j)}, \text{bal}_j^{\mathcal{B}})$ is not in general an object in $\mathcal{M}\square\mathcal{N}$ – while the components $\text{bal}_j^{\mathcal{B}}$ of the balancing $\text{bal}^{\mathcal{B}}$ exist, they are not balancings of the objects $x_{(\mathcal{M},j)} \boxtimes x_{(\mathcal{N},j)}$, since they may not be isomorphisms.

This type of Sweedler notation can be used, for example, in the following context: Let ${}_{\mathcal{A}}\mathcal{M}$ be a left module category over a spherical fusion category \mathcal{A} and let $x \in \overline{\mathcal{M}}\square\mathcal{M}$. The vector space ${}_{\mathcal{M}}\langle x_{(\overline{\mathcal{M}})}, x_{(\mathcal{M})} \rangle$ – by which we really mean the direct sum $\bigoplus_{i \in I} {}_{\mathcal{M}}\langle x_{(\overline{\mathcal{M},i})}, x_{(\mathcal{M},i)} \rangle$ for some decomposition $U(x) \cong \bigoplus_{i \in I} x_{(\overline{\mathcal{M},i})} \boxtimes x_{(\mathcal{M},i)}$ – has a distinguished subspace. To see this, note that the functor $\overline{\mathcal{A}} \boxtimes \mathcal{A} \rightarrow \text{vect}$ defined by ${}_{\mathcal{M}}\langle x_{(\overline{\mathcal{M}})} -, -x_{(\mathcal{M})} \rangle$ is connected bi-balanced: One balancing comes from the hom-functor, and one comes from the balancing of x . We can thus consider the equalizer of this connected bi-balanced functor at $\overline{\mathbb{1}}$ and $\mathbb{1}$ in the sense of Section 2.10, which is a subspace of ${}_{\mathcal{M}}\langle x_{(\overline{\mathcal{M}})}, x_{(\mathcal{M})} \rangle$ denoted as ${}_{\mathcal{M}}^{\mathcal{A}}\langle x \rangle$. If x has the property that its image $U(x) \in \overline{\mathcal{M}} \boxtimes \mathcal{M}$ factorizes, i.e. $U(x) = \overline{n} \boxtimes m$ for some objects $m, n \in \mathcal{M}$, we write

$${}_{\mathcal{M}}^{\mathcal{A}}\langle n, m \rangle := {}_{\mathcal{M}}^{\mathcal{A}}\langle x \rangle. \quad (2.151)$$

In this case, the balancing of x can be expressed as an $(a \in \mathcal{A})$ -indexed collection of isomorphisms

$$\text{bal}_{(\overline{\mathcal{M}},a)} \otimes \text{bal}_{(\mathcal{M},a)} : \overline{n}a \boxtimes m \rightarrow \overline{n} \boxtimes am. \quad (2.152)$$

The vector space ${}_{\mathcal{M}}^{\mathcal{A}}\langle n, m \rangle$ is then the subspace of ${}_{\mathcal{M}}\langle n, m \rangle$ which consists of those morphisms $f : n \rightarrow m$ that satisfy

$$af = \text{bal}_{(\mathcal{M},a)} \circ (\text{ev}^a f) \circ (a \text{bal}_{(\overline{\mathcal{M}},a)}). \quad (2.153)$$

We allow ourselves to write

$${}_{\mathcal{M}}^{\mathcal{A}}\langle x_{(\overline{\mathcal{M}})}, x_{(\mathcal{M})} \rangle := {}_{\mathcal{M}}^{\mathcal{A}}\langle x \rangle. \quad (2.154)$$

even if $U(x)$ does not \boxtimes -factorize. As an immediate corollary of Lemma 2.17, we obtain

Lemma 2.31. *The pivotal structure on \mathcal{A} defines a distinguished surjection*

$$r : {}_{\mathcal{M}}\langle x_{(\overline{\mathcal{M}})}, x_{(\mathcal{M})} \rangle \rightarrow {}_{\mathcal{M}}^{\mathcal{A}}\langle x_{(\overline{\mathcal{M}})}, x_{(\mathcal{M})} \rangle, \quad (2.155)$$

which exhibits the subspace as a retract.

2.13 EILENBERG-WATTS-EQUIVALENCES.

It is well-known [ENOM10, Prop. 3.5] that an alternative model for the relative Deligne product is given by a category of module functors:

$$\mathcal{M} \square \mathcal{N} \cong \text{Fun}_{\mathcal{B}}(\overline{\mathcal{M}}, \mathcal{N}). \quad (2.156)$$

Taking Remark 2.27 into account, we find that (2.156) specializes, for linear categories \mathcal{X} and \mathcal{Y} , to

$$\mathcal{X} \boxtimes \mathcal{Y} \cong \text{Fun}(\overline{\mathcal{X}}, \mathcal{Y}). \quad (2.157)$$

We continue by making explicit two distinct equivalences witnessing (2.157), in the form given in [FSS20a, Def. 3.1].

$$\begin{aligned} \text{EW} : x \boxtimes y &\mapsto \langle -, x \rangle^* \otimes y \\ \text{coEW} : x \boxtimes y &\mapsto \langle x, - \rangle \otimes y. \end{aligned} \quad (2.158)$$

Respective pseudo-inverses are given by

$$\begin{aligned} \widetilde{\text{EW}} : F &\mapsto \int_x x \boxtimes F(x) \\ \text{co}\widetilde{\text{EW}} : F &\mapsto \int^x x \boxtimes F(x). \end{aligned} \quad (2.159)$$

We call the functors defined in (2.158) and (2.159) the *Eilenberg-Watts equivalences*. The fact that they are indeed equivalences is proved in [FSS20a, Thm. 3.2].

Remark 2.32. Recall that there is a canonical equivalence of categories $\overline{\mathcal{X}} \boxtimes \overline{\mathcal{Y}} \cong \overline{\mathcal{Y}} \boxtimes \overline{\mathcal{X}}$. An object $x \boxtimes y \in \mathcal{X} \boxtimes \mathcal{Y}$ thus defines an object $\overline{x \boxtimes y} = \overline{y} \boxtimes \overline{x} \in \overline{\mathcal{Y}} \boxtimes \overline{\mathcal{X}}$, which the Eilenberg-Watts equivalences (2.158) turn into functors $\overline{\mathcal{X}} \rightarrow \overline{\mathcal{Y}}$ and functors $\overline{\mathcal{Y}} \rightarrow \overline{\mathcal{X}}$, respectively. These functors are related insofar as $\text{EW}(\overline{x \boxtimes y}) : \overline{\mathcal{Y}} \rightarrow \overline{\mathcal{X}}$ is left adjoint to $\text{coEW}(\overline{x \boxtimes y}) : \overline{\mathcal{X}} \rightarrow \overline{\mathcal{Y}}$.

Suppose now that we have a right \mathcal{B} -module category \mathcal{M} and a left \mathcal{B} -module category \mathcal{N} instead of linear categories \mathcal{X} and \mathcal{Y} . Then the balancings on an object $m \boxtimes n \in \mathcal{M} \boxtimes \mathcal{N}$ are in bijection with structures of module functors on the linear functor $\text{EW}(m \boxtimes n)$. This fact is the main insight needed to prove that there exist *module Eilenberg-Watts equivalences* $\text{EW}_{\mathfrak{m}}, \text{coEW}_{\mathfrak{m}} : \mathcal{M} \square \mathcal{N} \rightarrow \text{Fun}_{\mathcal{B}}(\overline{\mathcal{M}}, \mathcal{N})$ witnessing (2.156), together with pseudo-inverses $\widetilde{\text{EW}}_{\mathfrak{m}}, \text{co}\widetilde{\text{EW}}_{\mathfrak{m}}$, such that the following diagrams commute [FSS20b, Prop. 4.1]:

$$\begin{array}{ccc} \mathcal{M} \square \mathcal{N} & \xrightarrow{\text{EW}_{\mathfrak{m}}} & \text{Fun}_{\mathcal{B}}(\overline{\mathcal{M}}, \mathcal{N}) & & \text{Fun}_{\mathcal{B}}(\overline{\mathcal{M}}, \mathcal{N}) & \xrightarrow{\widetilde{\text{EW}}_{\mathfrak{m}}} & \mathcal{M} \square \mathcal{N} \\ \downarrow U & & \downarrow U & & \downarrow U & & \downarrow U \\ \mathcal{M} \boxtimes \mathcal{N} & \xrightarrow{\text{EW}} & \text{Fun}(\overline{\mathcal{M}}, \mathcal{N}) & & \text{Fun}(\overline{\mathcal{M}}, \mathcal{N}) & \xrightarrow{\widetilde{\text{EW}}} & \mathcal{M} \boxtimes \mathcal{N} \end{array} \quad (2.160)$$

$$\begin{array}{ccc} \mathcal{M} \square \mathcal{N} & \xrightarrow{\text{coEW}_{\mathfrak{m}}} & \text{Fun}_{\mathcal{B}}(\overline{\mathcal{M}}, \mathcal{N}) & & \text{Fun}_{\mathcal{B}}(\overline{\mathcal{M}}, \mathcal{N}) & \xrightarrow{\text{co}\widetilde{\text{EW}}_{\mathfrak{m}}} & \mathcal{M} \square \mathcal{N} \\ \downarrow U & & \downarrow U & & \downarrow U & & \downarrow U \\ \mathcal{M} \boxtimes \mathcal{N} & \xrightarrow{\text{coEW}} & \text{Fun}(\overline{\mathcal{M}}, \mathcal{N}) & & \text{Fun}(\overline{\mathcal{M}}, \mathcal{N}) & \xrightarrow{\text{co}\widetilde{\text{EW}}} & \mathcal{M} \boxtimes \mathcal{N} \end{array}$$

Here, U denotes both the forgetful functor from the relative Deligne product to the Deligne product and the functor which forgets a module functor's module structure.

2.14 SILENT AND COSILENT OBJECTS

In the above setting, let $\mathcal{M} = \overline{\mathcal{N}}$ and consider the identity functor $\text{id}_{\mathcal{N}}$, as well as the identity functor with the standard structure of a module functor, also denoted by $\text{id}_{\mathcal{N}}$. The images of $\text{id}_{\mathcal{N}}$ under the various Eilenberg-Watts equivalences are important enough to deserve their own names and notation. In accordance with [FSS22, Sec. 5.19], we call the objects

$$\begin{aligned} \mathbb{I}_{\mathcal{N}} &:= \widetilde{\text{EW}}(\text{id}_{\mathcal{N}}) = \int_n \bar{n} \boxtimes n \in \overline{\mathcal{N}} \boxtimes \mathcal{N}, \\ \mathbb{I}^{\mathcal{N}} &:= \text{co}\widetilde{\text{EW}}(\text{id}_{\mathcal{N}}) = \int^n \bar{n} \boxtimes n \in \overline{\mathcal{N}} \boxtimes \mathcal{N}, \\ \mathbb{F}_{\mathcal{N}} &:= \widetilde{\text{EW}}_{\text{m}}(\text{id}_{\mathcal{N}}) = \left(\int_n \bar{n} \boxtimes n, \beta \right) \in \overline{\mathcal{N}} \square \mathcal{N}, \\ \mathbb{F}^{\mathcal{N}} &:= \text{co}\widetilde{\text{EW}}_{\text{m}}(\text{id}_{\mathcal{N}}) = \left(\int^n \bar{n} \boxtimes n, \beta \right) \in \overline{\mathcal{N}} \square \mathcal{N} \end{aligned} \tag{2.161}$$

silent ($\mathbb{I}_{\mathcal{N}}$ and $\mathbb{F}_{\mathcal{N}}$) and *cosilent* ($\mathbb{I}^{\mathcal{N}}$ and $\mathbb{F}^{\mathcal{N}}$) objects. We remark that $U(\mathbb{F}_{\mathcal{N}}) = \mathbb{I}_{\mathcal{N}}$ and $U(\mathbb{F}^{\mathcal{N}}) = \mathbb{I}^{\mathcal{N}}$, and that we may consider $\mathbb{I}_{\mathcal{X}}$ and $\mathbb{I}^{\mathcal{X}}$ for arbitrary linear categories \mathcal{X} , not just module categories.

One can show that the balancings β appearing in the definition of $\mathbb{F}_{\mathcal{N}}$ and $\mathbb{F}^{\mathcal{N}}$ in (2.161) are indeed the ones we already considered in (2.107). We will later use the components of the morphisms $\text{brev}_{\mathbb{F}_{\mathcal{M}}}^a$ and ${}_a\text{cobrev}_{\mathbb{F}_{\mathcal{M}}}$, which can be easily calculated from (2.107) and (2.67) and are given by

$${}_k(\text{brev}_{\mathbb{F}_{\mathcal{M}}}^a)^n = \star_{\langle k, an \rangle} \boxtimes \star_{\langle an, k \rangle} : \bar{a}n \boxtimes an \rightarrow \bar{k} \boxtimes k, \tag{2.162}$$

$${}_k({}_a\text{cobrev}_{\mathbb{F}_{\mathcal{M}}})^n = \star_{\langle a^*k, n \rangle} \boxtimes \star_{\langle n, a^*k \rangle} : \bar{n} \boxtimes n \rightarrow \overline{a^*k} \boxtimes a^*k. \tag{2.163}$$

Lemma 2.33. *On a linear category \mathcal{X} , Calabi-Yau structures are in bijection with isomorphisms*

$$\mathbb{I}_{\mathcal{X}} \cong \mathbb{I}^{\mathcal{X}}. \tag{2.164}$$

On a module category ${}_{\mathcal{A}}\mathcal{M}$ over a pivotal fusion category \mathcal{A} , module traces are in bijection with isomorphisms

$$\mathbb{F}_{\mathcal{M}} \cong \mathbb{F}^{\mathcal{M}}. \tag{2.165}$$

Proof. We know from Section 2.5 how to construct an isomorphism $\Theta_{\mathcal{X}} : \mathbb{I}_{\mathcal{X}} \rightarrow \mathbb{I}^{\mathcal{X}}$ from a Calabi-Yau structure on \mathcal{X} . The assignment $d_{\mathcal{X}} := (\mathbf{x}(\Theta_{\mathcal{X}})^{\mathbf{x}})$ is the inverse to this construction.

That the module traces are those traces which lead to an isomorphism $\Theta_{\mathcal{M}}$ which is compatible with the balancing β on $\mathbb{F}_{\mathcal{M}}$ and $\mathbb{F}^{\mathcal{M}}$ was shown in Lemma 2.21. \square

Remark 2.34. Let \mathcal{X} be a Calabi-Yau category. It is easy to see that

$$d_{\mathbb{I}_{\mathcal{X}}} = d_{\mathbb{I}^{\mathcal{X}}} = \mathcal{D}_{\mathcal{X}}. \tag{2.166}$$

If \mathcal{M} is a traced left module category over a spherical fusion category \mathcal{A} , then by Lemma 2.28,

$$d_{\Phi_{\mathcal{M}}} = d_{\Phi^{\mathcal{M}}} = \frac{\mathcal{D}_{\mathcal{M}}}{\mathcal{D}_{\mathcal{A}}}. \quad (2.167)$$

Recall that under the module Eilenberg-Watts equivalences, the silent and cosilent objects $\Phi_{\mathcal{M}}$ and $\Phi^{\mathcal{M}}$ correspond to the identity module functor $\text{id}_{\mathcal{M}} \in \text{Fun}_{\mathcal{A}}(\mathcal{M}, \mathcal{M})$. If \mathcal{M} is irreducible, then $\text{Fun}_{\mathcal{A}}(\mathcal{M}, \mathcal{M})$ is a spherical fusion category with respect to a canonical pivotal structure that does not depend on the choice of trace on \mathcal{M} [Sch13b, Prop. 5.10]. Therefore, the monoidal unit $\text{id}_{\mathcal{M}}$ has pivotal dimension 1.

This shows that in general, the module Eilenberg-Watts equivalences do not preserve traces. At several points, categorical dimension factors will be present in our equations, whose appearance is rooted in this fact.

2.15 GENERALIZED YONEDA LEMMAS FOR BALANCED FUNCTORS

For a linear functor $F : \mathcal{X} \rightarrow \mathcal{Y}$ between linear categories, the following natural isomorphisms are known as *generalized Yoneda Lemmas*.

$$\int_x \langle -, x \rangle^* \otimes F(x) \cong F \quad (2.168)$$

$$\int^x \langle x, - \rangle \otimes F(x) \cong F. \quad (2.169)$$

A proof of these well-known identities is written up in [FSS20a, Prop. 2.7], see also [Rie14, Cor. 1.4.5 and Exc. 1.4.6]. Explicitly, the isomorphism (2.169) is given by the unique dashed morphism such that the following diagram commutes for all objects $x \in \mathcal{X}$.

$$\begin{array}{ccc} \int^x \langle x, x' \rangle \otimes F(x) & \dashrightarrow & F(x') \\ \sigma^x \uparrow & \nearrow & \\ \langle x, x' \rangle \otimes F(x) & & \end{array} \quad (2.170)$$

(The diagonal arrow is labeled $(f: x \rightarrow x') \mapsto F(f)$)

Here the diagonal arrow denotes the image of the map $\langle x, x' \rangle \rightarrow \langle F(x), F(x') \rangle$, $(f : x \rightarrow x') \mapsto F(f)$ under the isomorphism

$$\left\langle \langle x, x' \rangle, \langle F(x), F(x') \rangle \right\rangle \cong \left\langle \langle x, x' \rangle \otimes F(x), F(x') \right\rangle. \quad (2.171)$$

It is straightforward to check that the isomorphisms (2.168) and (2.169) are also natural in F .

We will now show that the isomorphisms (2.168) and (2.169) are well-behaved when F is a balanced functor. For this to make sense, let ${}_{\mathcal{A}}\mathcal{M}_{\mathcal{A}}$ be an \mathcal{A} - \mathcal{A} -bimodule category for a spherical fusion category \mathcal{A} . In the above situation, we replace \mathcal{X} with \mathcal{M} , and consider a balanced functor (see Section 2.8) $F : \mathcal{M} \rightarrow \mathcal{Y}$. The functor $\int^m \langle m, - \rangle \otimes F(m)$ has a balancing which is given, for

objects $n \in \mathcal{M}, a \in \mathcal{A}$, by the chain of isomorphisms

$$\begin{aligned} \int^m \langle m, an \rangle \otimes F(m) &\cong \int^m \langle a^*m, n \rangle \otimes F(m) \cong \int^m \langle m, n \rangle \otimes F(am) \cong \int^m \langle m, n \rangle \otimes F(ma) \\ &\cong \int^m \langle ma^*, n \rangle \otimes F(m) \cong \int^m \langle m, na \rangle \otimes F(m). \end{aligned} \quad (2.172)$$

Into this balancing, the (left and right) balancings of the hom-functor enters, as well as the isomorphisms β from (2.99) and the balancing of F .

Lemma 2.35. *For a balanced functor $F : \mathcal{M} \rightarrow \mathcal{Y}$, the isomorphisms*

$$\int^m \langle m, - \rangle \otimes F(m) \cong F \quad \text{and} \quad \int_m \langle -, m \rangle^* \otimes F(m) \quad (2.173)$$

from (2.169) and (2.168) form balanced natural isomorphisms.

Proof. We only prove the coend-version of the statement. We need to show that the outer paths around the following diagram commute:

$$\begin{array}{ccc} \int^m \langle m, an \rangle \otimes F(m) & \xrightarrow{\cong} & F(an) \\ \downarrow \cong & & \downarrow \text{id} \\ \int^m \langle a^*m, n \rangle \otimes F(m) & \text{(a)} & \\ \downarrow \cong & & \\ \int^m \langle m, n \rangle \otimes F(am) & \xrightarrow{\cong} & F(an) \\ \downarrow \cong & & \downarrow \cong \\ \int^m \langle m, n \rangle \otimes F(ma) & \xrightarrow{\cong} & F(na) \\ \downarrow \cong & & \downarrow \text{id} \\ \int^m \langle ma^*, n \rangle \otimes F(m) & & \\ \downarrow \cong & & \\ \int^m \langle m, na \rangle \otimes F(m) & \xrightarrow{\cong} & F(na) \end{array} \quad (2.174)$$

The middle square in (2.174) is a naturality diagram with respect to the isomorphism of functors $F(a-) \cong F(-a)$. The top and bottom cells are similar, so we only consider the top cell (a) in more detail. The cell (a) in (2.174) is also present in the next diagram. We can deduce that (a) commutes if the outer paths around (2.175) commute for all objects $k \in \mathcal{M}$.

$$\begin{array}{ccccc} & & & & (f:k \rightarrow an) \mapsto F(f) \\ & & & & \curvearrowright \\ & & & & (2.170) \\ \langle k, an \rangle \otimes F(k) & \xrightarrow{\sigma^k} & \int^m \langle m, an \rangle \otimes F(m) & \xrightarrow{\cong} & F(an) \\ \text{bal} \otimes F(k) \downarrow & & \downarrow \cong & & \downarrow \text{id} \\ \langle a^*k, n \rangle \otimes F(k) & \xrightarrow{\sigma^k} & \int^m \langle a^*m, n \rangle \otimes F(m) & \text{(a)} & \\ \langle a^*k, n \rangle \otimes F(a \text{coev } k) \downarrow & & \downarrow \cong & & \\ \langle a^*k, n \rangle \otimes F(aa^*k) & \xrightarrow{\sigma^{a^*k}} & \int^m \langle m, n \rangle \otimes F(am) & \xrightarrow{\cong} & F(an) \\ & & (2.170) & & \\ & & & & \curvearrowleft \\ & & & & (g:a^*k \rightarrow n) \mapsto F(ag) \end{array} \quad (2.175)$$

In (2.175), bal denotes the balancing of the hom-functor $\langle k, an \rangle \cong \langle a^*k, n \rangle$. In order to verify that the outer paths around (2.175) commute, we need to compose morphisms expressed in terms of the identification (2.171). Let us quickly observe how this is done in a decontextualization of our situation: let V, W be finite-dimensional vector spaces, and let x, y, z be objects in a linear category \mathcal{Y} . Let $f : V \rightarrow W$ be a linear map, $g : x \rightarrow y$ be a morphism, and denote by $(w \in W) \mapsto (h_w : y \rightarrow z)$ another morphism $W \otimes y \rightarrow z$ using the notational convention introduced in (2.171). Then the diagram

$$\begin{array}{ccc} V \otimes x & & \\ f \otimes g \downarrow & \searrow^{(v \in V) \mapsto (h_{f(v)} \circ g)} & \\ W \otimes y & \xrightarrow{(w \in W) \mapsto (h_w : y \rightarrow z)} & z \end{array} \quad (2.176)$$

commutes. Applied to our situation, the diagram reads

$$\begin{array}{ccc} \langle k, an \rangle \otimes F(k) & & \\ \text{bal} \otimes F({}_a \text{coev } k) \downarrow & \searrow^{(f : k \rightarrow an) \mapsto (F(a \text{ bal}(f)) \circ F({}_a \text{coev } k))} & \\ \langle a^*k, n \rangle \otimes F(aa^*k) & \xrightarrow{(g : a^*k \rightarrow n) \mapsto F(ag)} & F(an) \end{array} \quad (2.177)$$

If we can show that $F(a \text{ bal}(f)) \circ F({}_a \text{coev } k) = F(f)$, then the diagram (2.177) is equivalent to the boundary of (2.175), and the proof is done. Using the zig-zag identity $(a \text{ bal}(f)) \circ ({}_a \text{coev } k) = f$, we calculate

$$F(a \text{ bal}(f)) \circ F({}_a \text{coev } k) = F((a \text{ bal}(f)) \circ ({}_a \text{coev } k)) = F(f). \quad (2.178)$$

This shows that the cell (a) in (2.174) commutes. Commutativity of the bottom cell of (2.174) is proved in the same way. \square

Corollary 2.36. *For a left \mathcal{A} -module category \mathcal{M} , there is a balanced natural isomorphism*

$$\text{sil} : \mathcal{M}\langle -, - \rangle \cong \overline{\mathcal{M}} \boxtimes \mathcal{M} \langle - \boxtimes -, I^{\mathcal{M}} \rangle. \quad (2.179)$$

involving the cosilent object $I^{\mathcal{M}}$ from (2.161).

Proof. Apply Lemma 2.35 to the functor $F = \mathcal{M}\langle -, - \rangle$, which is balanced with respect to the bimodule structure on $\overline{\mathcal{M}} \boxtimes \mathcal{M}$, to obtain

$$\mathcal{M}\langle m, m' \rangle \cong \int^k \mathcal{M}\langle k, m' \rangle \otimes_{\mathcal{M}} \langle m, k \rangle \cong \int^k \overline{\mathcal{M}}\langle \overline{m'}, \overline{k} \rangle \otimes_{\mathcal{M}} \langle m, k \rangle \cong \int^k \overline{\mathcal{M}} \boxtimes \mathcal{M} \langle \overline{m'} \boxtimes m, \overline{k} \boxtimes k \rangle. \quad (2.180)$$

Then, use exactness to pull the coend inside the argument of the hom-functor. \square

Explicitly, sil is given on a morphism $f : m \rightarrow m'$ and in components for simple $\mathbf{n} \in \mathcal{M}$ by

$${}^{\mathbf{n}}\text{sil}(f) = d_{\mathbf{n}} \star_{\langle \mathbf{n}, m' \rangle} \boxtimes (\star_{\langle m', \mathbf{n} \rangle} \circ f) \quad (2.181)$$

with inverse

$$\text{sil}^{-1}(g) = \sum_{\mathbf{n}} ({}^{\mathbf{n}}g)_{(\overline{\mathcal{M}})} \circ ({}^{\mathbf{n}}g)_{(\mathcal{M})}. \quad (2.182)$$

For the special case $f = \text{id}_m$, combining (2.181) with (2.21) reveals that

$$\text{sil}(\text{id}_m) = \sigma^m : \overline{m} \boxtimes m \rightarrow \int^k \overline{k} \boxtimes k. \quad (2.183)$$

If \mathcal{M} is equipped with a module trace, then sil^{-1} can be applied to the isomorphism $\Theta_{\mathcal{M}} : \mathbb{I}_{\mathcal{M}} \rightarrow \mathbb{I}^{\mathcal{M}}$. More precisely, sil^{-1} is given, on simple components $(\Theta_{\mathcal{M}})_{\mathbf{k}}$ of $\Theta_{\mathcal{M}}$, by

$$\begin{aligned} \text{sil}^{-1}((\Theta_{\mathcal{M}})_{\mathbf{k}}) &\stackrel{(2.182)}{=} \sum_{\mathbf{n}} ({}^{\mathbf{n}}(\Theta_{\mathcal{M}})_{\mathbf{k}})_{(\overline{\mathcal{M}})} \circ ({}^{\mathbf{n}}(\Theta_{\mathcal{M}})_{\mathbf{k}})_{(\mathcal{M})} \\ &\stackrel{(2.48)}{=} \sum_{\mathbf{n}} \delta_{\mathbf{k}, \mathbf{n}} d_{\mathbf{n}} \text{id}_{\mathbf{n}} = d_{\mathbf{k}} \text{id}_{\mathbf{k}}. \end{aligned} \quad (2.184)$$

The image of $\Theta_{\mathcal{M}}$ under sil^{-1} is thus

$$\int^k \text{sil}^{-1}((\Theta_{\mathcal{M}})_k) = \int^k d_k \text{id}_k \in \int^k \langle k, k \rangle. \quad (2.185)$$

Remark 2.37. Suppose that $\overline{m}' \boxtimes m \in \overline{\mathcal{M}} \boxtimes \mathcal{M}$ is equipped with a balancing $\text{bal}_a : \overline{m}' a \boxtimes m \cong \overline{m}' \boxtimes am$ for $a \in \mathcal{A}$. Then the functor

$$\mathcal{M} \langle -m', -m \rangle : \overline{\mathcal{A}} \boxtimes \mathcal{A} \rightarrow \text{vect} \quad (2.186)$$

is even (connected) bi-balanced. The equalizer of this bi-balanced functor was already considered in (2.151) and is denoted ${}^{\mathcal{A}}\langle m', m \rangle$. The isomorphism sil defines a bi-balanced natural isomorphism

$$\mathcal{M} \langle -m', -m \rangle \cong \overline{\mathcal{M}} \boxtimes \mathcal{M} \langle \overline{m}' \boxtimes -m, \mathbb{I}^{\mathcal{M}} \rangle \cong \overline{\mathcal{M}} \boxtimes \mathcal{M} \langle \overline{m}' \boxtimes -m, -\mathbb{I}^{\mathcal{M}} \rangle. \quad (2.187)$$

The equalizer of the bi-balanced functor $\overline{\mathcal{M}} \boxtimes \mathcal{M} \langle \overline{m}' \boxtimes -m, -\mathbb{I}^{\mathcal{M}} \rangle$ is the hom-space of the relative Deligne product $\overline{\mathcal{M}} \square \mathcal{M} \langle (\overline{m}' \boxtimes m, \text{bal}), \mathbb{F}^{\mathcal{M}} \rangle$; we saw this already in Example 2.13. By Lemma 2.20, the bi-balanced natural isomorphism (2.187) defines a morphism of retracts, meaning that

$$\begin{array}{ccc} \mathcal{M} \langle m', m \rangle & \xrightarrow{\text{sil}} & \overline{\mathcal{M}} \boxtimes \mathcal{M} \langle \overline{m}' \boxtimes m, -\mathbb{I}^{\mathcal{M}} \rangle \\ \downarrow r & & \downarrow r \\ {}^{\mathcal{A}}\langle m', m \rangle & \longrightarrow & \overline{\mathcal{M}} \square \mathcal{M} \langle (\overline{m}' \boxtimes m, \text{bal}), \mathbb{F}^{\mathcal{M}} \rangle \end{array} \quad (2.188)$$

commutes, where the left vertical label is the retraction from Lemma 2.31, and the right vertical arrow is the retraction from Lemma 2.23.

2.16 CONTRACTION OPERATIONS

The identification of relative Deligne products with (bi)module functors via the Eilenberg-Watts endows relative Deligne products with composition operations, which we now aim to understand.

Consider two \mathcal{A} - \mathcal{B} -bimodule categories \mathcal{M} and \mathcal{N} , and a \mathcal{B} - \mathcal{A} -bimodule category \mathcal{K} . Let there be objects

$$x \in \mathcal{K} \boxtimes \mathcal{M} \boxtimes \quad \text{and} \quad y \in \overline{\mathcal{M}} \boxtimes \mathcal{N} \boxtimes. \quad (2.189)$$

Under the Eilenberg-Watts equivalences from Section 2.13, the objects x and y correspond to composable bimodule functors

$$\text{coEW}_m(x) : \overline{\mathcal{K}} \rightarrow \mathcal{M} \quad \text{and} \quad \text{coEW}_m(y) : \mathcal{M} \rightarrow \mathcal{N}. \quad (2.190)$$

By the *contraction* of x and y , we mean the object

$$x \bullet_{\mathcal{M}} y := \text{coEW}_m(\widetilde{\text{coEW}_m(y) \circ \text{coEW}_m(x)}) \in \mathcal{K} \boxtimes \mathcal{N} \boxtimes. \quad (2.191)$$

Making the definition of $x \bullet_{\mathcal{M}} y$ explicit in terms of an unbalanced object in $\mathcal{K} \boxtimes \mathcal{N}$ and balancings, we find that

$$U(x \bullet_{\mathcal{M}} y) = \mathcal{M} \langle y_{(\mathcal{M})}, x_{(\mathcal{M})} \rangle \otimes x_{(\mathcal{K})} \boxtimes y_{(\mathcal{N})}. \quad (2.192)$$

The balancings are obtained from the balancings of x and y , together with the balancing of the hom-functor.

In the case $\mathcal{M} = \mathcal{N}$, we can choose y to be the cosilent object $y = \Phi^{\mathcal{M}} \in \overline{\mathcal{M}} \boxtimes \mathcal{M} \boxtimes$. It follows directly from the definition (2.191) that there is a distinguished isomorphism

$$x \bullet_{\mathcal{M}} \Phi^{\mathcal{M}} \cong x. \quad (2.193)$$

In other words, the cosilent object $\Phi^{\mathcal{M}}$ acts as a unit for contraction. The contraction operation also inherits associativity and functoriality structures from the composition of bimodule functors.

Building on this contraction for objects, we introduce another notion of contraction, this time for morphisms. With x and y as above, consider objects $m \in \mathcal{M}$, $n \in \mathcal{N}$ and $k \in \mathcal{K}$, and morphisms

$$f : k \boxtimes m \rightarrow U(x) \quad \text{and} \quad g : \overline{m} \boxtimes n \rightarrow U(y). \quad (2.194)$$

The morphism

$$g \circ_m f : k \boxtimes n \rightarrow U(x \bullet_{\mathcal{M}} y) \quad (2.195)$$

into the contraction $U(x \bullet_{\mathcal{M}} y)$ from (2.192) is defined as follows. Note that the vector $f \otimes g$ inhabits the vector space

$$f \otimes g \in \langle k \boxtimes m \boxtimes \overline{m} \boxtimes n, x_{(\mathcal{K})} \boxtimes x_{(\mathcal{M})} \boxtimes \overline{y_{(\mathcal{M})}} \boxtimes y_{(\mathcal{N})} \rangle. \quad (2.196)$$

On this vector space, consider the linear map

$$\begin{aligned}
& \langle k \boxtimes m \boxtimes \bar{m} \boxtimes n, x_{(\mathcal{K})} \boxtimes x_{(\mathcal{M})} \boxtimes \overline{y_{(\mathcal{M})}} \boxtimes y_{(\mathcal{N})} \rangle \\
& \cong \langle k, x_{(\mathcal{K})} \rangle \otimes \langle m, x_{(\mathcal{M})} \rangle \otimes \langle \bar{m}, \overline{y_{(\mathcal{M})}} \rangle \otimes \langle n, y_{(\mathcal{N})} \rangle \\
& \cong \langle k, x_{(\mathcal{K})} \rangle \otimes \langle m, x_{(\mathcal{M})} \rangle \otimes \langle y_{(\mathcal{M})}, m \rangle \otimes \langle n, y_{(\mathcal{N})} \rangle \\
& \xrightarrow{\text{compose}} \langle k, x_{(\mathcal{K})} \rangle \otimes \langle y_{(\mathcal{M})}, x_{(\mathcal{M})} \rangle \otimes \langle n, y_{(\mathcal{N})} \rangle \\
& \cong \langle k \boxtimes n, \mathcal{M} \langle y_{(\mathcal{M})}, x_{(\mathcal{M})} \rangle \otimes x_{(\mathcal{K})} \boxtimes y_{(\mathcal{N})} \rangle \\
& = \langle k \boxtimes n, U(x \bullet_{\mathcal{M}} y) \rangle.
\end{aligned} \tag{2.197}$$

The contraction $g \circ_m f$ is obtained as the image of $f \otimes g$ under the map (2.197).

Remark 2.38. One can verify in a direct calculation using the explicit form (2.181) of the isomorphism sil that in the case $y = \Phi^{\mathcal{M}}$ and $g = \text{sil}(\tilde{g})$ for some morphism $\tilde{g} : n \rightarrow m$, the pushforward of the contraction $\text{sil}(\tilde{g}) \circ_m f$ under the isomorphism (2.193) is given by

$$f \circ (k \boxtimes \tilde{g}). \tag{2.198}$$

If in addition, $x = \Phi^{\mathcal{M}}$ is also cosilent, and $f = \text{sil}(\tilde{f})$ for some $\tilde{f} : m \rightarrow k$, then

$$g \circ_m f = \text{sil}(\tilde{f} \circ \tilde{g}) \tag{2.199}$$

Remark 2.39. Let $\bar{\mathcal{K}} = \mathcal{M} = \mathcal{N} = \mathcal{A}$ be the regular bimodule category. In this case, the objects x and y in the relative Deligne products become bimodule endofunctors of \mathcal{A} under the Eilenberg-Watts equivalence coEW_m . But the category of bimodule endofunctors of \mathcal{A} is isomorphic to the Drinfeld center $Z_{\mathcal{A}}(\mathcal{A})$ as a monoidal category. Thus, if we abuse notation and denote the corresponding objects in $Z_{\mathcal{A}}(\mathcal{A})$ also by x, y , the contraction $x \bullet_{\mathcal{A}} y$ is, as an object in $Z_{\mathcal{A}}(\mathcal{A})$, given by the monoidal product $x \otimes y$.

The morphisms (2.194) have as targets $U(x)$ and $U(y)$. Since the forgetful functor U has a left adjoint $\bar{\square}$, see (2.108), f and g can equivalently be expressed as living in the hom-spaces

$$f \in \bar{\mathcal{A}} \square_{\mathcal{A}} \square \langle \bar{a} \square b \square, x \rangle \quad \text{and} \quad g \in \bar{\mathcal{A}} \square_{\mathcal{A}} \square \langle \bar{b} \square c \square, x \rangle, \tag{2.200}$$

with $a, b, c \in \mathcal{A}$ taking on the roles of k, m and n in (2.194). Passing through the equivalence $\bar{\mathcal{A}} \square_{\mathcal{A}} \square \cong Z_{\mathcal{A}}(\mathcal{A})$, the objects $\bar{a} \square b \square$ and $\bar{b} \square c \square$ get mapped to $a^* b \square$ and $b^* c \square$, respectively. Passing back through the same adjunction, now only applied to one balancing, we find images of f and g in the hom-spaces ${}_{\mathcal{A}} \langle a^* b, U(x) \rangle$ and ${}_{\mathcal{A}} \langle b^* c, U(y) \rangle$. In the same way, the contraction $g \circ_b f$ can be seen as a morphism in the hom-space ${}_{\mathcal{A}} \langle a^* c, U(x \otimes y) \rangle$. A calculation reveals that this morphism, by abuse of notation also denoted $g \circ_b f$, is given by

$$g \circ_b f = (f \otimes g) \circ (a^* \text{} _b \text{coev } c). \tag{2.201}$$

Remark 2.40. It is natural to extend the contraction operation to the case where the bimodule category \mathcal{K} is not present, meaning a contraction operation of

$$x \in \mathcal{M} \square \quad \text{and} \quad y \in \bar{\mathcal{M}} \square \mathcal{N} \square. \tag{2.202}$$

Such a one-sided contraction operation is defined, again for objects and for morphisms, in the obvious way: We have

$$U(x \bullet_{\mathcal{M}} y) = \mathcal{M} \langle y_{(\mathcal{M})}, U(x) \rangle \otimes y_{(\mathcal{N})} \quad (2.203)$$

and

$$g \circ_m f = (f \circ g_{(\mathcal{M})}) \otimes g_{(\mathcal{N})} : n \rightarrow U(x \bullet_{\mathcal{M}} y) \quad (2.204)$$

for $f : m \rightarrow U(x)$ and $g : \bar{m} \boxtimes n \rightarrow U(y)$.

2.17 MODULE (CO-)ENDS

The notion of a module coend is important to us, because it is used in the definition of the modular functor from [FSS22], on which we build.

Let $F : \overline{\mathcal{M}} \boxtimes \mathcal{M} \rightarrow \mathcal{Y}$ be a balanced functor. There are two morphisms

$$\int^m F(m, am) \rightrightarrows \int^m F(a^*m, m) \quad (2.205)$$

we can consider: One is induced by the balancing of F , and the other is the morphism β defined in (2.99), using the coend, but not the balancing. It makes sense to compare these morphisms. Specifically, we would like to compare the two related morphisms $\underline{\rho}$ and $\underline{\beta}$, which we now introduce. $\underline{\beta}$ is defined using universal properties such that the following diagram commutes:

$$\begin{array}{ccc} \int^m F(m, m) & \xrightarrow{\quad \underline{\beta} \quad} & \int_a \int^m F(am, am) \\ \sigma^m \uparrow & \searrow & \downarrow a\tau \\ F(m, m) & & \\ F(\text{ev}^{a^*} m, a^* \text{coev } m) & \searrow & \int^m F(am, am) \\ & & \downarrow \sigma^{a^* m} \\ & & F(aa^* m, aa^* m) \end{array} \quad (2.206)$$

Similarly, $\underline{\rho}$ is unique in that the following diagram commutes.

$$\begin{array}{ccc} \int^m F(m, m) & \xrightarrow{\quad \underline{\rho} \quad} & \int_a \int^m F(am, am) \\ \sigma^m \uparrow & \searrow & \downarrow a\tau \\ F(m, m) & & \\ F(\text{ev}^{a^*} m, m) & \searrow \rho_{a,m,m} & \int^m F(am, am) \\ & & \downarrow \sigma^m \\ & & F(am, am) \\ & \xrightarrow{\text{bal}_{am,a,m}^F} & \int^m F(am, am) \end{array} \quad (2.207)$$

Here, the arrow $\rho_{a,m,m}$ is defined as the composition $\text{bal}_{am,a,m}^F \circ F(\text{ev}^{a^*} m, m)$.

We thus introduce a type of coend which does not see the difference between the two morphisms. The following notion is a minor modification of the module (co-)ends introduced in [BM21].

Definition 2.41. Let $(F, \text{bal}^F) : \overline{\mathcal{M}} \boxtimes \mathcal{M} \rightarrow \mathcal{Y}$ be a balanced functor. The *module coend* $\oint^m F(m, m)$ of F is the equalizer of the diagram

$$\oint^m F(m, m) \xleftarrow{\iota} \int^m F(m, m) \begin{array}{c} \xrightarrow{\underline{\rho}} \\ \xrightarrow{\underline{\beta}} \end{array} \int_a \int^m F(am, am), \quad (2.208)$$

where the arrows $\underline{\rho}$ and $\underline{\beta}$ are given by (2.207) and (2.206).

Remark 2.42. In the case that F is the hom-functor $\mathcal{M}\langle -, - \rangle$, the balancing coaction $\langle m, m \rangle \rightarrow \langle am, am \rangle$ is the linear map given by $f \mapsto \text{id}_a f$ for $f : m \rightarrow m$. This is an easy to check consequence of both the definition of the balancing of the hom-functor.

In some particular situations (3.26), we will need to consider module coends of disconnected bi-balanced, rather than balanced functors. This is also possible:

Definition 2.43. Let \mathcal{M} be an \mathcal{A} - \mathcal{A} -bimodule category, and let $F : \overline{\mathcal{M}} \boxtimes \mathcal{M} \rightarrow \mathcal{Y}$ be a disconnected bi-balanced functor. Consider the morphism $\underline{\lambda} : \int^m F(m, m) \rightarrow \int_a \int^m F(am, am)$, which is given by the following chain of compositions of morphisms, which are constructed using the disconnected bi-balanced structure and the morphism β as defined in (2.99).

$$\begin{aligned} \int^m F(m, m) &\rightarrow \int_a \int^m F(a^* am, m) \rightarrow \int_a \int^m F(ama^*, m) \\ &\rightarrow \int_a \int^m F(am, ma) \rightarrow \int_a \int^m F(am, am). \end{aligned} \quad (2.209)$$

The *module coend* of F is the equalizer of $\underline{\lambda}$ and the morphism $\underline{\beta}$ which was defined in (2.206).

Our goal is to show that in our setting, the module coend, which is by definition a subobject of the regular coend, is also canonically a quotient of the regular coend, meaning there is a morphism $\int^m F(m, m) \rightarrow \oint^m F(m, m)$. To this end, we formulate the problem in such a way that Lemma 2.17 can be applied. Observe that if F is either balanced or disconnected bi-balanced,

$$S := \int^m F(-m, -m) : \overline{\mathcal{A}} \times \mathcal{A} \rightarrow \mathcal{Y} \quad (2.210)$$

is a connected bi-balanced functor: The left balancing is inherited from the balancing (or disconnected bi-balancing) of F , while the right balancing comes from the coend over m . The equalizer (2.208) (or the one from Definition 2.43) is the equalizer of the connected bi-balanced functor S on the object $\mathbb{1} \in Z_{\mathcal{A}}(\mathcal{A})$ in both arguments, as defined in (2.83). Thus, Lemma 2.17 implies that the equalizer (2.208) splits, as long as \mathcal{A} is a spherical fusion category. Moreover, Lemma 2.17 provides us with the structural data of the split equalizer: Consider the map \tilde{t} , which is unique such that the following diagram commutes:

$$\begin{array}{ccc} \int_a \int^m F(am, am) & \xrightarrow{\tilde{t}} & \int^m F(m, m) \\ \sigma^a \sigma^m \uparrow & \nearrow \sigma^{am} & \\ F(am, am) & & \end{array} . \quad (2.211)$$

The following endomorphism of $\int^m F(m, m)$ – which was denoted by $h = t \circ g$ in the proof of Lemma 2.16 – will play a greater role later on and thus deserves a name.

Definition 2.44. The *balancing idempotent* $h^F : \int^m F(m, m) \rightarrow \int^m F(m, m)$ is defined as the composition

$$h^F := \frac{1}{\mathcal{D}_A} \tilde{t} \bullet \underline{\rho} \text{ if } F \text{ is balanced, and } h^F := \frac{1}{\mathcal{D}_A} \tilde{t} \bullet \underline{\lambda} \text{ if } F \text{ is disconnected bi-balanced,} \quad (2.212)$$

using the operation \bullet defined in (2.33) to mediate between the end and the coend over a :

$$h^F: \int^m F(m, m) \xrightarrow{\underline{\rho} \text{ or } \underline{\lambda}} \int_a \int^m F(am, am) \xrightarrow{\Theta_{\mathcal{A}/\mathcal{D}_A}} \int^a \int^m F(am, am) \xrightarrow{\tilde{t}} \int^m F(m, m). \quad (2.213)$$

That h^F is indeed an idempotent is evident from Definition 2.15. Hence we have proved:

Theorem 2.45. *Let $F : \overline{\mathcal{M}} \boxtimes \mathcal{M} \rightarrow \mathcal{Y}$ be a balanced or disconnected bi-balanced functor. The balancing idempotent h^F from Definition 2.44 factors through the module coend, i.e. there exists a unique dashed arrow π^F , called the balancing projector, such that the following diagram commutes.*

$$\begin{array}{ccc} \int^m F(m, m) & \xrightarrow{h^F} & \int^m F(m, m) \\ \downarrow \pi^F & \nearrow \iota & \\ \oint^m F(m, m) & & \end{array} \quad (2.214)$$

This balancing projector π^F is a retraction of the inclusion $\iota : \oint^m F(m, m) \rightarrow \int^m F(m, m)$. Moreover, the balancing idempotent h^F really is an idempotent, the balancing projector π^F really is an epimorphism, and hence the module coend $\oint^m F(m, m)$ is the image of the balancing idempotent h^F .

Remark 2.46 (Module ends and module natural transformations). In complete analogy, it is possible to define a *module end* $\oint_m F(m, m)$ as a subobject of the regular end $\int_m F(m, m)$. This notion of module end is the one which appears in [BM21]. (Note, however, that the module coend from Definition 2.41 is different from the module coend in [BM21] in that it is a subobject, not a quotient, of the regular coend.)

Given \mathcal{A} -module categories \mathcal{M}, \mathcal{N} , and module functors $F, G : \mathcal{M} \rightarrow \mathcal{N}$, the space of natural transformations can be written as an end:

$$\text{Nat}(F, G) \cong \int_m \langle F(m), G(m) \rangle. \quad (2.215)$$

Similarly, the subspace of *module* natural transformations is isomorphic to a module end [BM21, Prop. 4.1]:

$$\text{Nat}_{\mathcal{A}}(F, G) \cong \oint_m \langle F(m), G(m) \rangle. \quad (2.216)$$

The end-version of Theorem 2.45 provides an explicit retraction

$$\text{Nat}(F, G) \twoheadrightarrow \text{Nat}_{\mathcal{A}}(F, G), \quad (2.217)$$

determined by the pivotal structure on \mathcal{A} .

We will encounter functors defined on a Deligne product with many factors, and with several independent balancings. This notion deserves a formalization. To this end, let ${}_{\mathcal{B}}\mathcal{N}$ be another module category over a spherical fusion category \mathcal{B} . Recall that $\mathcal{A} \boxtimes \mathcal{B}$ is again a spherical fusion category, and that $\mathcal{M} \boxtimes \mathcal{N}$ can be considered as a module category over $\mathcal{A} \boxtimes \mathcal{B}$.

Definition 2.47. We say that $F : \overline{\mathcal{M}} \boxtimes \mathcal{M} \boxtimes \overline{\mathcal{N}} \boxtimes \mathcal{N} \rightarrow \mathcal{Y}$ is a *piecewise balanced functor* if it is equipped with

- a balancing or disconnected bi-balancing for the functor $F(- \boxtimes - \boxtimes I_{\mathcal{N}}) : \overline{\mathcal{M}} \boxtimes \mathcal{M} \rightarrow \mathcal{Y}$, and
- a balancing or a disconnected bi-balancing for the functor $F(I_{\mathcal{M}} \boxtimes - \boxtimes -) : \overline{\mathcal{N}} \boxtimes \mathcal{N} \rightarrow \mathcal{Y}$,

such that balancing idempotents $h_{\mathcal{A}}$ and $h_{\mathcal{B}}$ for the functors $F(- \boxtimes - \boxtimes I_{\mathcal{N}})$ and $F(I_{\mathcal{M}} \boxtimes - \boxtimes -)$, which are both endomorphisms of $\int^m \int^n F(m, m, n, n)$, commute. Their composition

$$h := h_{\mathcal{A}} \circ h_{\mathcal{B}} = h_{\mathcal{B}} \circ h_{\mathcal{A}} \quad (2.218)$$

is called the *balancing idempotent* of F . The *piecewise module coend* $\oint^{\mathcal{M}, \mathcal{N}} F$ is the unique object such that the following diagram is a pullback square:

$$\begin{array}{ccc} \oint^{\mathcal{M}, \mathcal{N}} F & \longleftarrow & \oint^{m \in \mathcal{M}} \int^{n \in \mathcal{N}} F(m, m, n, n) \\ \downarrow & & \downarrow \\ \int^{n \in \mathcal{N}} \int^{m \in \mathcal{M}} F(m, m, n, n) & \longleftarrow & \int^{m \in \mathcal{M}} \int^{n \in \mathcal{N}} F(m, m, n, n) \end{array} \quad (2.219)$$

Remark 2.48. Recall that $\mathcal{A} \boxtimes \mathcal{B}$ is again a spherical fusion category, and that $\mathcal{M} \boxtimes \mathcal{N}$ can be considered as a module category over $\mathcal{A} \boxtimes \mathcal{B}$. There is a notion of *multi-balanced functor* $F : \overline{\mathcal{M}} \boxtimes \mathcal{M} \boxtimes \overline{\mathcal{N}} \boxtimes \mathcal{N} \rightarrow \mathcal{Y}$, which is a balanced functor with respect to the $\mathcal{A} \boxtimes \mathcal{B}$ -module structure. Every multi-balanced functor is a piecewise balanced functor, but the converse does not hold true. A functor which is piecewise balanced, but not multi-balanced, is given in Section 3.2, see Remark 3.8.

Proposition 2.49. *For a multi-balanced functor, the module coend (with respect to the $\mathcal{A} \boxtimes \mathcal{B}$ -action) agrees with the piecewise module coend.*

Sketch of Proof. We need to construct dashed arrows and show that the diagram

$$\begin{array}{ccc} \oint^{\mu \in \mathcal{M} \boxtimes \mathcal{N}} F(\mu, \mu) & \dashrightarrow & \oint^{m \in \mathcal{M}} \int^{n \in \mathcal{N}} F(m, m, n, n) \\ \vdots & & \downarrow \\ \int^{n \in \mathcal{N}} \int^{m \in \mathcal{M}} F(m, m, n, n) & \longleftarrow & \int^{m \in \mathcal{M}} \int^{n \in \mathcal{N}} F(m, m, n, n) \end{array} \quad (2.220)$$

is a pullback square. In order to construct the dashed arrows, note that a morphism $\oint^{\mu \in \mathcal{M} \boxtimes \mathcal{N}} F(\mu, \mu) \rightarrow \oint^{m \in \mathcal{M}} \int^{n \in \mathcal{N}} F(m, m, n, n)$ is, by the universal property of the equalizer from Definition 2.41, in bijection with morphisms $\oint^{\mu \in \mathcal{M} \boxtimes \mathcal{N}} F(\mu, \mu) \rightarrow \int^{m \in \mathcal{M}} \int^{n \in \mathcal{N}} F(m, m, n, n)$ satisfying the equalizing

property. Such a morphism is obtained the structure of $\oint^{\mu \in \mathcal{M} \boxtimes \mathcal{N}}$ as an equalizer. In this way, the horizontal dashed arrow (and similarly the vertical dashed arrow) in (2.220) are defined.

To see that (2.220) is indeed a pullback square, we first note that a cone over the solid part of the diagram (2.220) is a morphism $f : y \rightarrow \int^{m \in \mathcal{M}} \int^{n \in \mathcal{N}} F(m, m, n, n)$ which factors over both $\oint^{m \in \mathcal{M}} \int^{n \in \mathcal{N}} F(m, m, n, n)$ and $\oint^{n \in \mathcal{N}} \int^{m \in \mathcal{M}} F(m, m, n, n)$. This means that f satisfies two equalizing conditions. It can be shown that these two equalizing conditions (for the \mathcal{A} -action on \mathcal{M} and the \mathcal{B} -action on \mathcal{N} , respectively) are equivalent to the single equalizing condition for the $\mathcal{A} \boxtimes \mathcal{B}$ -action on $\mathcal{M} \boxtimes \mathcal{N}$. Thus, a cone over the solid part of (2.220) is the same as a cone over the equalizer diagram

$$\int^{\mu \in \mathcal{M} \boxtimes \mathcal{N}} F(\mu, \mu) \rightrightarrows \int_{\alpha \in \mathcal{A} \boxtimes \mathcal{B}} \int^{\mu \in \mathcal{M} \boxtimes \mathcal{N}} F(\alpha \mu, \alpha \mu). \quad (2.221)$$

Hence, the pullback of the former diagram is isomorphic to the equalizer of the latter, which by definition is the module coend of F with respect to the $\mathcal{A} \boxtimes \mathcal{B}$ -action. \square

Proposition 2.50. *The balancing idempotent*

$$h := h_{\mathcal{A}} \circ h_{\mathcal{B}} = h_{\mathcal{B}} \circ h_{\mathcal{A}} \quad (2.222)$$

is again an idempotent whose image is the piecewise module coend $\oint^{\mathcal{M}, \mathcal{N}} F$.

Proof. Proving that h is an idempotent is easy:

$$h \circ h = (h_{\mathcal{A}} \circ h_{\mathcal{B}}) \circ (h_{\mathcal{B}} \circ h_{\mathcal{A}}) = h_{\mathcal{A}} \circ h_{\mathcal{B}} \circ h_{\mathcal{A}} = h_{\mathcal{A}} \circ h_{\mathcal{A}} \circ h_{\mathcal{B}} = h_{\mathcal{A}} \circ h_{\mathcal{B}} = h. \quad (2.223)$$

It remains to show that the image of h is the piecewise module coend. We can use the universal property of the pullback to see that h factors over the piecewise module coend. For a unique dashed arrow π in the diagram below to exist, the outer paths of the diagram (2.224) have to commute. They do, due to the commutativity of $h_{\mathcal{A}}$ and $h_{\mathcal{B}}$.

$$\begin{array}{ccc} \int^m \int^n F(m, m, n, n) & \xrightarrow{\pi_{\mathcal{A}} \circ h_{\mathcal{B}}} & \oint^{m \in \mathcal{M}} \int^{n \in \mathcal{N}} F(m, m, n, n) \\ \downarrow \pi & \searrow \tilde{\iota}_{\mathcal{B}} & \downarrow \tilde{\iota}_{\mathcal{A}} \\ \int^m \int^n F(m, m, n, n) & \xrightarrow{\pi_{\mathcal{B}} \circ h_{\mathcal{A}}} & \oint^{m \in \mathcal{M}} \int^{n \in \mathcal{N}} F(m, m, n, n) \\ \downarrow \tilde{\iota}_{\mathcal{A}} & \swarrow \iota_{\mathcal{B}} & \downarrow \iota_{\mathcal{A}} \\ \oint^{n \in \mathcal{N}} \int^{m \in \mathcal{M}} F(m, m, n, n) & \xrightarrow{\iota_{\mathcal{B}}} & \int^{m \in \mathcal{M}} \int^{n \in \mathcal{N}} F(m, m, n, n) \end{array} \quad (2.224)$$

We show that π is surjective by proving that $\pi \circ \iota = \text{id}$, where $\iota = \iota_{\mathcal{B}} \circ \tilde{\iota}_{\mathcal{A}} = \iota_{\mathcal{A}} \circ \tilde{\iota}_{\mathcal{B}}$. Consider the diagram

$$\begin{array}{ccc} \oint^{\mathcal{M}, \mathcal{N}} F & \xrightarrow{f} & \oint^{m \in \mathcal{M}} \int^{n \in \mathcal{N}} F(m, m, n, n) \\ \downarrow h & \searrow \tilde{\iota}_{\mathcal{B}} & \downarrow \tilde{\iota}_{\mathcal{A}} \\ \oint^{\mathcal{M}, \mathcal{N}} F & \xrightarrow{\tilde{\iota}_{\mathcal{B}}} & \oint^{m \in \mathcal{M}} \int^{n \in \mathcal{N}} F(m, m, n, n) \\ \downarrow \tilde{\iota}_{\mathcal{A}} & \swarrow \iota_{\mathcal{B}} & \downarrow \iota_{\mathcal{A}} \\ \oint^{n \in \mathcal{N}} \int^{m \in \mathcal{M}} F(m, m, n, n) & \xrightarrow{\iota_{\mathcal{B}}} & \int^{m \in \mathcal{M}} \int^{n \in \mathcal{N}} F(m, m, n, n) \end{array} \quad (2.225)$$

If we can find morphisms f and g , such that $\iota_{\mathcal{A}} \circ f = \iota_{\mathcal{B}} \circ g$, then there exists a unique dashed arrow h such that $\tilde{\iota}_{\mathcal{B}} \circ h = f$ and $\tilde{\iota}_{\mathcal{A}} \circ h = g$. The choices $f = \tilde{\iota}_{\mathcal{B}}$ and $g = \tilde{\iota}_{\mathcal{A}}$ are valid, and in this case, $h = \text{id}$. Our aim is to show

$$\tilde{\iota}_{\mathcal{B}} \circ \pi \circ \iota = \tilde{\iota}_{\mathcal{B}} \quad \text{and} \quad \tilde{\iota}_{\mathcal{A}} \circ \pi \circ \iota = \tilde{\iota}_{\mathcal{A}}, \quad (2.226)$$

and to deduce by uniqueness of h that $\text{id} = h = \pi \circ \iota$. We proceed to check this by a direct calculation, in which we underline those terms that will be modified in the next step.

$$\begin{aligned} \tilde{\iota}_{\mathcal{B}} \circ \pi \circ \iota &= \pi_{\mathcal{A}} \circ \underline{h_{\mathcal{B}}} \circ \iota = \pi_{\mathcal{A}} \circ \iota_{\mathcal{B}} \circ \pi_{\mathcal{B}} \circ \underline{\iota} = \pi_{\mathcal{A}} \circ \iota_{\mathcal{B}} \circ \underline{\pi_{\mathcal{B}}} \circ \iota_{\mathcal{B}} \circ \tilde{\iota}_{\mathcal{A}} \\ &= \pi_{\mathcal{A}} \circ \underline{\iota_{\mathcal{B}}} \circ \tilde{\iota}_{\mathcal{A}} = \underline{\pi_{\mathcal{A}}} \circ \iota_{\mathcal{A}} \circ \tilde{\iota}_{\mathcal{B}} = \tilde{\iota}_{\mathcal{B}}. \end{aligned} \quad (2.227)$$

The other equation in (2.226) is proved in the same way. \square

Definition 2.51. The corestriction of the idempotent h from Proposition 2.50 onto its image is denoted

$$\pi : \int^m \int^n F(m, m, n, n) \rightarrow \oint^{\mathcal{M}, \mathcal{N}} F, \quad (2.228)$$

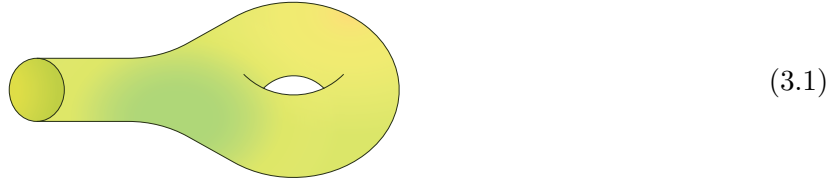
and is called the *piecewise balancing projector* of F .

3 EXTRUDED GRAPHS AND THEIR EVALUATION

3.1 DEFECT MANIFOLDS AND EXTRUDED GRAPHS

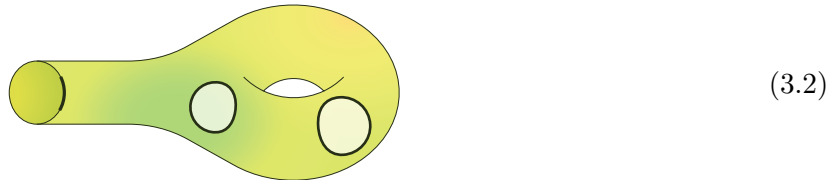
The evaluation procedure that will be constructed in Section 3.3 is defined on a particular class of cylinders over decorated surfaces called *extruded graphs*, that we now introduce. They are similar to the labeled defect surfaces considered in [FSS22]. We distinguish between the following types of surfaces with additional structure.

Surface.



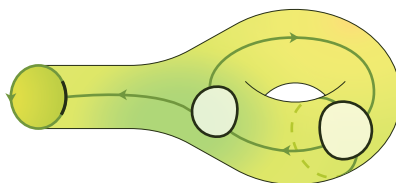
By a surface, we always mean a smooth, oriented, compact 2-manifold, possibly with boundary.

Node Surface.



A surface Σ with a finite number of embedded disks in its interior $\text{Int}(\Sigma)$ and a finite number of embedded intervals on its boundary $\partial\Sigma$ is called a *node surface*, and the embedded disks and intervals are called *nodes*. The node surface (3.2) has three nodes: two disks, and one interval.

(Fine) Unlabeled Defect Surface.



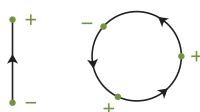
(3.3)

A node surface Σ is called an unlabeled defect surface if it is endowed with finitely many embedded disjoint intervals, called *defect lines*, that must meet the following criteria:

- The end points of each defect line must lie on the boundary of a disk-shaped node or in an interval node.
- The interior of the defect lines must be disjoint from the disk and interval nodes.
- Each disk node must be adjacent to at least one defect line.
- The boundary $\partial\Sigma$ of Σ is covered entirely by interval nodes and defect lines.

The connected components of the complement of defect lines and disk and interval nodes in σ are called *domains*. In addition to these requirements, we only consider *fine* unlabeled defect surfaces, which means that all domains are disks.

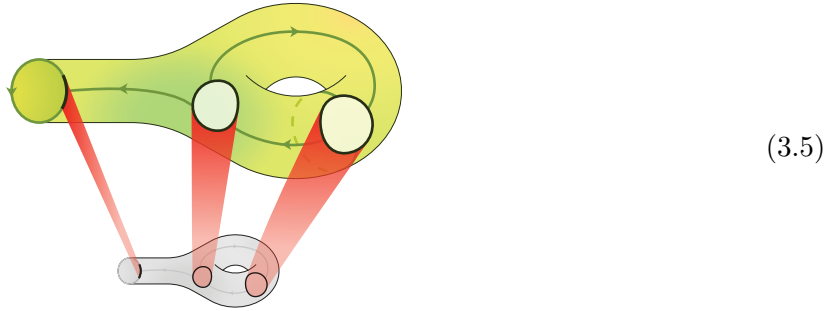
Defect 1-Manifold.



(3.4)

The interval nodes and the boundary of the disk nodes of an unlabeled defect surface are examples of *defect 1-manifolds*: These are compact, smooth, oriented 1-manifolds, possibly with boundary (i.e. a disjoint union of finitely many closed intervals and circles), with finitely many *marked points*, meaning a set of distinguished points on the 1-manifold, each equipped with a sign. The boundary of any defect 1-manifold must consist of marked points. In case the defect 1-manifold is obtained from an unlabeled defect surface, the marked points are given by the end points of defect lines, with signs depending on whether the defect line starts (−) or ends (+) at a point.

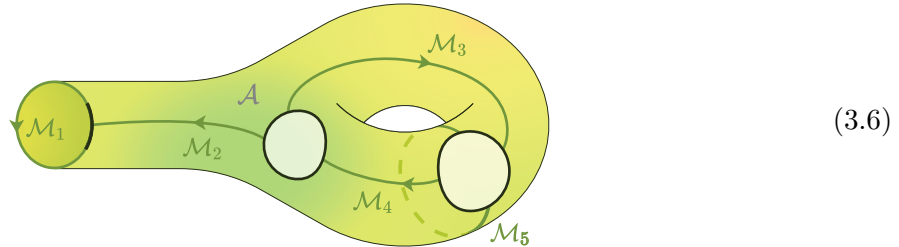
Extruded Defect Surface.



To each defect surface Σ , we assign an *extruded defect surface*, which topologically is given by the cylinder $\Sigma \times [0, 1]$. We identify the original defect surface with one of the boundary components, called the *coat*: $\Sigma \cong \Sigma \times \{0\}$. The other boundary component $\Sigma \times \{1\}$ is called the *core*. If i is a disk or interval node in Σ , then the cylinder $i \times [0, 1] \subset \Sigma \times [0, 1]$ stretching from the coat to the core is called a *ray*. In pictures such as (3.5), the coat is always drawn in green, and the core is always gray, while the rays are red. We usually only draw the coat and the core, and not the entire 3-manifold $\Sigma \times [0, 1]$.

This structure is only mildly 3-dimensional, as the topology is entirely determined by the defect surface Σ . This justifies the name *extruded* defect surface.

Labeled Defect Surface.



We consider the following labeling of defect surfaces by algebraic data:

- Level 1 To each of the (two-dimensional) domains, we assign a spherical fusion category $\mathcal{A}, \mathcal{B}, \dots$
- Level 2 To each defect line adjacent to a domain labeled by \mathcal{A} on the left and a domain labeled by \mathcal{B} on the right, we assign a traced \mathcal{A} - \mathcal{B} -bimodule category \mathcal{M} . In case the defect line lies on the boundary of the surface, there is only one adjacent domain, and the algebraic label is a one-sided (left or right) module category, depending on the orientation.

In the example (3.6), there is only one domain, labeled by \mathcal{A} . Hence, all bimodule categories are \mathcal{A} - \mathcal{A} -bimodule categories, with the exception of \mathcal{M}_1 , which labels a defect line on the boundary and is thus merely a right traced \mathcal{A} -module category.

Labeled Defect 1-Manifold.

$$(3.7)$$

Defect 1-Manifolds can also be labeled by the same algebraic data: Each segment between marked points is assigned a spherical fusion category, and the marked points themselves are labeled by spherical bimodule categories. The interval nodes and the boundaries of the disk nodes of a labeled defect surface naturally carry the structure of labeled defect 1-manifolds. Then the orientation of a connected labeled defect 1-manifold L defines a (cyclic or linear) order of marked points, and hence a (cyclically or linearly) composable string $(\mathcal{M}_1, \mathcal{M}_2, \dots)$ of bimodule categories. If the sign of the marked point is negative, we use the opposite bimodule category $\overline{\mathcal{M}}_i$ instead. We call the relative Deligne product

$$\mathbb{T}^R(L) := \mathcal{M}_1 \square \mathcal{M}_2 \square \dots \tag{3.8}$$

the *ray category* of L . Similarly, the regular Deligne product

$$\mathbb{T}^N(L) := \mathcal{M}_1 \boxtimes \mathcal{M}_2 \boxtimes \dots \tag{3.9}$$

is called the *node category* of L . Recall from Section 2.12 that there is a forgetful functor $U : \mathbb{T}^R(L) \rightarrow \mathbb{T}^N(L)$ with adjoints $\boxleftarrow{\square}, \boxrightarrow{\square} : \mathbb{T}^N(L) \rightarrow \mathbb{T}^R(L)$ between ray and node categories.

Extruded Graph.

$$(3.10)$$

The complete labeling of an extruded defect surface requires two more layers of algebraic data.

Level 3 To each defect line labeled by a bimodule category \mathcal{M} on the coat, we assign in addition an object $m \in \mathcal{M}$.

To each ray, which is the cylinder over a (disk or interval) node L , we assign an object in the ray category $x \in \mathbb{T}^R(L)$.

Level 4 The choices of objects from the third level of labels permit us to associate a vector space to each node L . Let $(m_1 \in \mathcal{M}_1, m_2 \in \mathcal{M}_2, \dots)$ be the list of objects that label the defect lines adjacent to L , and let $x \in \mathbb{T}^{\mathbb{R}}(L)$ denote the ray label. We call the vector space

$$N_x(m_1, m_2, \dots) := {}_{\mathbb{T}^{\mathbb{N}}(L)}\langle m_1 \boxtimes m_2 \boxtimes \dots, U(x) \rangle \quad (3.11)$$

the *node space* for the node L . Here, U denotes the forgetful functor $\mathbb{T}^{\mathbb{R}}(L) \rightarrow \mathbb{T}^{\mathbb{N}}(L)$, which forgets the balancings that come with the relative Deligne product. The notion of node spaces allows us to define the first part of the fourth level of labels:

To each node, we assign a vector f in the node space, called a *node label*.

Finally, it is possible to construct, for each labeled defect surface Σ , a functor which assigns a vector space to a choice of ray labels for Σ . This functor is called the *block functor*, and its value for a specific choice of ray labels is called a *block space* T . The construction of the block functor has been the subject of [FSS22], and it will be briefly summarized in Section 3.2. We can now state the last part of the fourth level of labels:

To the core, we assign a vector φ in the linear dual of the block space T^* .

An extruded defect surface with all four layers of labels is called an *extruded graph*.

Remark 3.1. There are some differences between the definitions, the conventions, and the terminology in this paper and those in [FSS22]. First and foremost, all manifolds we consider carry less structure: they are only oriented, as opposed to 2-framed. The counterpart to this loss in topological structure is additional algebraic structure: The tensor categories considered in [FSS22] are only rigid, whereas we here require them to be equipped with a spherical structure. We also need a spherical structure on the bimodule categories.

Furthermore, all categories we consider are semisimple. While it is open whether non-semisimply labeled extruded graphs can be evaluated in a way similar to the one we will define in Section 3.3, we cannot expect to construct a 3-dimensional state-sum model with defects from non-semisimple data [BDSPV15, Appendix], which is our motivation for considering extruded graphs.

As a matter of perspective, we here chose to consider disk nodes and not circular boundary components. The reason for this is that we sometimes wish to consider the *underlying surface* of a defect surface, a concept which does not appear in [FSS22]. Another minor point is that we disallow circular defect lines: all defect lines must start and end at a node.

Taking these points into account, a labeled defect surface corresponds to a labeled defect surface in the terminology of [FSS22], and similarly for a labeled defect 1-manifold.

Remark 3.2 (The 2-dimensional Character of Extruded Graphs). We have introduced extruded graphs as a 3-dimensional structure. However, the third dimension is distinguished and carries no real information: being the cylinder over a defect surface, it is topologically completely determined by the defect surface. The ray labels could equivalently be associated with the nodes, and there is also no necessity to assign the datum of the core label to the core geometrically, and not just to the extruded graph as a whole.

From this perspective, extruded graphs can be viewed as 2-dimensional objects: labeled defect surfaces in the sense of (3.6) with an additional choice of object in the appropriate bimodule

category for each defect line, two labels for each node: an object in the associated ray category and a node label, and an additional choice of core label, which is part of the datum of an extruded graph, but not associated with a particular topological component.

Remark 3.3 (The 3-dimensional Character of Extruded Graphs). Despite the 2-dimensional picture from Remark 3.2 being sufficient to develop the theory of extruded graphs, let us now highlight why it is natural to view them as inherently 3-dimensional objects. Extruded graphs are related a class of diagrams that are associated with a tricategory, as described by [Hum12] and [BMS12], and several others. These diagrams, which we call *3-diagrams*, generalize the graphical calculus of string diagrams to tricategories. A 3-diagram in a given tricategory \mathcal{T} is a stratification of the standard cube $[0, 1]^3$, in which the 3-strata are labeled by objects of \mathcal{T} , the 2-strata (surfaces) are labeled by 1-morphisms, 1-strata (lines) by 2-morphisms, and 0-strata (vertices) by 3-morphisms of \mathcal{T} . 3-diagrams evaluate to 3-morphisms of \mathcal{T} . If we choose for \mathcal{T} the tricategory BiMod^{Tr} from Section 2.12, we find that 3-diagrams have 3-strata labeled by spherical fusion categories, surfaces labeled by traced bimodule categories, lines labeled by bimodule functors, and vertices labeled by bimodule natural transformations.

For comparison, consider now the following alternative description of an extruded graph on the sphere \mathbb{S}^2 . An extruded graph Σ on \mathbb{S}^2 consists of the standard closed 3-ball $B \subset \mathbb{R}^3$ of radius 1 with a stratification obtained as follows: There exists an oriented graph Γ on the surface of B such that the 2-strata of B are given by

- connected components of $\partial B \setminus \Gamma$; these 2-strata lie on the surface of B ; or
- for a given edge e of Γ , the radial sweep of e , meaning the surface $\{\lambda p \in B \subset \mathbb{R}^3 : p \in e, \lambda \in (0, 1)\}$.

Moreover, the 1-strata are

- edges of Γ , and
- for a given vertex v of Γ , the oriented straight line from v to the center $0 \in B$ of B .

The 0-strata are

- vertices of Γ , and
- the point $0 \in B$.

Let us view the "outside region" $\mathbb{R}^3 \setminus B$ as a 3-stratum of B . In addition, B has one 3-stratum per connected component of $\partial B \setminus \Gamma$.

Inspired by the labeling prescription for 3-diagrams in BiMod^{Tr} , we define how the different strata of B are to be labeled. We will label n -dimensional strata with $(3-n)$ -morphisms BiMod^{Tr} . Hence, for each 3-stratum, we pick a spherical fusion category. We only restrict the label of the outside region: Here, we pick the spherical fusion category vect . The 2-strata are labeled, according to their orientation, by a traced bimodule category, with actions from the spherical fusion categories that label the adjacent 3-strata. We leave this choice arbitrary for the 2-strata in the interior of B , but for the connected components of $\partial B \setminus \Gamma$, i.e. the 2-strata on the boundary

of B , we fix the \mathcal{A} -vect-bimodule category ${}_{\mathcal{A}}\mathcal{A}_{\text{vect}}$, where \mathcal{A} is the spherical fusion category that labels the 3-stratum in the interior of B which is adjacent to the 2-stratum in question. Each 1-stratum has a cyclically ordered set of composable bimodule categories associated with it, that label the adjacent 2-strata. The relative Deligne product over this cyclic string of bimodule categories is a linear category, from which we pick an object that labels the 1-stratum. The relative Deligne product can be realized as a category of bimodule functors, but we do not make this explicit here. For 1-strata in the interior of B – recall that these are radial lines – the associated category is just the ray category for the corresponding ray, after making the obvious identification of 3-strata with domains and interior 1-strata with rays. Let us now consider 1-strata on the boundary of B . These are the edges of Γ . They each have three adjacent 2-strata and three adjacent 3-strata. One of these 3-strata is the outside region labeled by vect , and the other two are labeled by spherical fusion categories \mathcal{A} and \mathcal{B} . Out of the adjacent 2-strata, one lies in the interior of B and is labeled by a traced bimodule category ${}_{\mathcal{A}}\mathcal{M}_{\mathcal{B}}$, while the other two lie on the boundary ∂B . We know that their labels are ${}_{\mathcal{A}}\mathcal{A}_{\text{vect}}$ and ${}_{\mathcal{B}}\mathcal{B}_{\text{vect}}$. The category associated with the 1-stratum is therefore $\overline{\mathcal{A}} \square_{\mathcal{A}} \mathcal{M} \square_{\mathcal{B}} \mathcal{B} \square_{\text{vect}}$, where the opposite of \mathcal{A} appears when taking orientations into account. Using that the center of a vect-vect-bimodule category is just the category itself, and that \mathcal{A} and \mathcal{B} are units for the relative Deligne product, as seen in (2.134), the associated category simplifies to

$$\overline{\mathcal{A}} \square_{\mathcal{A}} \mathcal{M} \square_{\mathcal{B}} \mathcal{B} \square_{\text{vect}} \cong \overline{\mathcal{A}} \square_{\mathcal{A}} \mathcal{M} \square_{\mathcal{B}} \mathcal{B} \cong \mathcal{M}. \quad (3.12)$$

Hence, a 1-stratum on the boundary of B , whose adjacent internal 2-stratum is labeled by a bimodule category \mathcal{M} , is labeled by an object $m \in \mathcal{M}$. Recall that this is also the appropriate choice of label for a defect line in an extruded graph.

So far, we have recovered the labeling prescription for domains, defect lines and rays of an extruded graph from another perspective. But crucially, while we previously treated defect lines and rays as entirely different things, we now saw that they can both be viewed as objects of the same type (1-strata), and that their respective labeling stems from a single, generalizing prescription. To arrive at this perspective, it was necessary to treat the extruded graph (or the stratified ball B) as a 3-dimensional object, and to source the labels of n -dimensional strata from the set of $(3 - n)$ -morphisms of the labeling tricategory BiMod^{Tr} . The labeling prescription can be extended to 0-strata, unifying both nodes and the core of an extruded graph on \mathbb{S}^2 . One can then see that the vector spaces of node labels and the vector space of core labels can be described in a consistent way using a small neighborhood of the respective 0-strata. We will not continue to make this explicit.

Instead, let us briefly make the connection to 3-diagrams for tricategories. If the tricategory \mathcal{T} has sufficiently well-behaved dualities, one can consider and evaluate non-progressive 3-diagrams [BMS12, Sec. 6.1]. In particular, a choice of embedding $B \hookrightarrow [0, 1]^3$ into the standard cube defines a non-progressive 3-diagram, which evaluates to a particular 3-morphism in BiMod^{Tr} : A bimodule natural endomorphism of the identity functor of the vect-vect-bimodule category vect – or in other words, a scalar in \mathbb{K} . It is expected, though at this time unproven, that the evaluation of non-progressive 3-diagrams is invariant under isotopies. For us, this would mean that the scalar associated to B is independent of the choice of embedding $B \hookrightarrow [0, 1]^3$. Currently, isotopy invariance is only known for a subclass of non-progressive 3-diagrams called surface

diagrams, in which the 2-skeleton of the stratification is a manifold [BMS12, Thm. 6.8]. A 3-diagram obtained from B is not a surface diagram. Part of the difficulty in proving a more general invariance theorem lies in how 0-strata of 3-diagrams are labeled by 3-morphisms in a tricategory. A 3-morphism has as source and target 2-morphisms, or more generally, linearly ordered compositions of 2-morphisms. The 1-strata adjacent to a 0-stratum, which are labeled by 2-morphisms, do not, in general, come with a linear order or a grouping into source and target 1-strata. In order to label the 0-stratum by a 3-morphism, choices for these orderings have to be made. Working with the combinatorics of how a 3-morphism should transform when a different choice of ordering is made appears difficult. Note that in the special case of surface diagrams, there is at least a cyclic order on the adjacent 1-strata of a 0-stratum, as they all embed into a surface.

For extruded graphs, this problem is resolved by the use of block spaces (to be defined in Section 3.2) for the core labels – they can be thought of as symmetric versions of hom-spaces for 3-morphisms. The technicalities of labels for 0-strata aside, we expect a close relationship between the scalar obtained from the evaluation of the 3-diagram $B \leftrightarrow [0, 1]^3$ and the evaluation of the corresponding extruded graph – the latter will be defined in Section 3.3 in a manifestly isotopy invariant way. As discussed in Remark 5.18, we also expect that extruded graphs can be used to define the evaluation of 3-diagrams in BiMod^{Tr} in a manifestly isotopy invariant way.

These considerations justify why we introduced extruded graphs as 3-dimensional entities. Even if the third dimension is superfluous in defining extruded graphs, it is helpful in understanding them.

Remark 3.4 (The $(2+\epsilon)$ -dimensional Character of Extruded Graphs). The definition of extruded graphs that we gave can be thought of as a compromise between the strictly 2-dimensional description proposed in Remark 3.2 and the fully 3-dimensional description outlined in Remark 3.3. Indeed, there is a very concrete reason why extruded graphs are not quite 2-dimensional and not quite 3-dimensional. Our main motivation for considering extruded graphs is a state-sum model with surface defects, which is outlined in Section 5.4. In this model, 3-manifolds are considered which are stratified and labeled by algebraic data in a way very similar to how the cube $[0, 1]^3$ is stratified and labeled to become a 3-diagram in BiMod^{Tr} , as just discussed in Remark 3.3. Ball neighborhoods of the 0-strata carry the structure of extruded graphs – but not all neighborhoods, only *infinitesimal* neighborhoods. "Infinitesimal" is here to be understood in a topological sense and means "regular in that all adjacent 1- and 2-strata intersect the boundary of the neighborhood transversally, and small enough in that it is homeomorphic to all of its regular ball sub-neighborhoods". When viewing this state-sum model as a source of extruded graphs, it is clear why they can be described in a purely 2-dimensional manner, despite being naturally 3-dimensional objects: The third dimension is purposefully chosen so small that nothing interesting happens in it.

3.2 THE MODULAR STATE-SUM FUNCTOR

The state-sum modular functor described in [FSS22] is crucial to the understanding of extruded graphs, and the labels of the core in particular. We briefly review an alteration of the modular functor, namely the oriented/spherical version as opposed to the framed/rigid version. Being a

symmetric monoidal functor between bicategories, the modular functor consists of several pieces of data. One of these pieces of data is the *block space* \mathbb{T} mentioned in the definition of extruded graphs, which is a vector space assigned to a labeled defect surface Σ together with a choice of ray labels.

Remark 3.5. We do not need to explicitly construct an oriented/spherical version of the modular functor from [FSS22], since we only need block spaces. Moreover, we only consider fine defect surfaces, for which block spaces are easier to define. In fact, moving to an oriented/spherical setting *simplifies* the construction in [FSS22] where the role of the framing was to control powers of the double dual (which in our situation is trivialized by the pivotal structure). Nevertheless, it is useful to think of the block space as a component of a larger structure, the modular functor, cf. [FSS22, Rem. 5.28].

We now fix a labeled defect surface Σ , a choice of ray labelings $x \boxtimes y \boxtimes \cdots \in \mathbb{T}^{\text{R}}(\Sigma)$, and proceed to recall the definition of the associated block space $\mathbb{T} = \mathbb{T}(x \boxtimes y \boxtimes \cdots)$. $\mathbb{T}^{\text{R}}(\Sigma)$ here denotes the Deligne product over the ray categories for all nodes L (intervals and disks) in Σ :

$$\mathbb{T}^{\text{R}}(\Sigma) := \boxtimes_L \mathbb{T}^{\text{R}}(L). \quad (3.13)$$

To this end, we first introduce the *node space functor* for a node L of Σ :

$$N_x(L) := {}_{\mathbb{T}^{\text{N}}(L)}\langle -, U(x) \rangle : \overline{\mathbb{T}^{\text{N}}(L)} \rightarrow \text{vect}. \quad (3.14)$$

Note that the values of this functor are the node spaces mentioned above. There is a (*total*) node space functor associated to the surface Σ :

$$N_{x,y,\dots} := \bigotimes_L N_x(L) : \boxtimes_L \overline{\mathbb{T}^{\text{N}}(L)} = \overline{\mathbb{T}^{\text{N}}} \rightarrow \text{vect}. \quad (3.15)$$

The Deligne product $\boxtimes_L \overline{\mathbb{T}^{\text{N}}(L)} = \overline{\mathbb{T}^{\text{N}}}$ denotes the (total) node category for the surface Σ . As each defect line starts and ends at a node, the associated bimodule category \mathcal{M} appears precisely twice in the total node category, once as \mathcal{M} and once as $\overline{\mathcal{M}}$. Thus the terms of the node category $\overline{\mathbb{T}^{\text{N}}}$ can be rearranged as follows:

$$\boxtimes_L \overline{\mathbb{T}^{\text{N}}(L)} = \mathbb{T}^{\text{N}} = \boxtimes_{\mathcal{M}} \mathcal{M} \boxtimes \overline{\mathcal{M}}, \quad (3.16)$$

where now \mathcal{M} runs over defect lines of Σ . Recall from (2.161) that there is a silent object

$$I_{\mathcal{M}} = \int_m m \boxtimes \overline{m} \in \mathcal{M} \boxtimes \overline{\mathcal{M}}. \quad (3.17)$$

The Deligne product over all of these objects $I_{\mathcal{M}}$ provides us with a distinguished object in the total node category:

$$\boxtimes_{\mathcal{M}} I_{\mathcal{M}} \cong I_{(\boxtimes_{\mathcal{M}} \mathcal{M})} \in \mathbb{T}^{\text{N}}. \quad (3.18)$$

Following [FSS22], we define the *pre-block space* as the value of the total node functor on this object (using the Sweedler-like notation for the forgetful functor U from (2.146)):

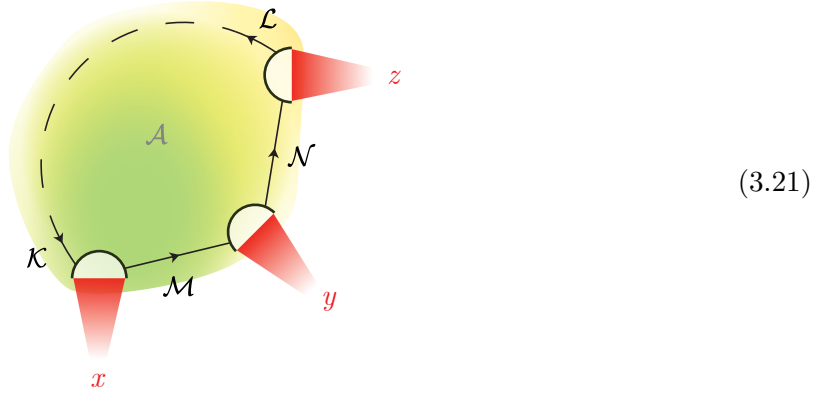
$$\mathbb{T}^{\text{P}} := N_{x,y,\dots}(I_{(\boxtimes_{\mathcal{M}} \mathcal{M})}) = {}_{\mathbb{T}^{\text{N}}}\left\langle \int_m \int_n m \boxtimes \overline{m} \boxtimes n \boxtimes \overline{n} \boxtimes \cdots, x_{(\mathcal{M})} \boxtimes \overline{y_{(\mathcal{M})}} \boxtimes z_{(\mathcal{N})} \boxtimes \overline{x_{(\mathcal{N})}} \boxtimes \cdots \right\rangle. \quad (3.19)$$

Remark 3.6. By Corollary 2.36, the pre-block space is isomorphic to the tensor product of hom-spaces

$$\mathrm{T}^{\mathrm{P}} \cong \langle y_{(\mathcal{M})}, x_{(\mathcal{M})} \rangle \otimes \langle x_{(\mathcal{N})}, z_{(\mathcal{N})} \rangle \otimes \cdots. \quad (3.20)$$

The block space T from [FSS22], which we work towards defining, is obtained as a subspace of the pre-block space T^{P} . It consists of those vectors satisfying a condition that we will now describe. It can be thought of as a *flatness condition*, see [FSS22, p. 5].

We pick a domain labeled by a spherical fusion category \mathcal{A} . Assume that one of the defect lines adjacent to \mathcal{A} is labeled by a spherical bimodule category \mathcal{M} , and *only one* of the two domains adjacent to the defect line is \mathcal{A} . Without loss of generality, we take \mathcal{M} to be a *left* \mathcal{A} -module. We denote the labels of the other defect lines adjacent to \mathcal{A} by $\mathcal{N}, \mathcal{K}, \mathcal{L}, \dots$, and rays by x, y, z, \dots



$$(3.21)$$

Consider the functor $S_{\mathcal{M}} : \mathcal{M} \boxtimes \overline{\mathcal{M}} \rightarrow \text{vect}$, given by

$$S_{\mathcal{M}}(m, \overline{m'}) := N_{x,y,\dots}(m \boxtimes \overline{m'} \boxtimes I_{\mathcal{N}} \boxtimes I_{\mathcal{K}} \boxtimes I_{\mathcal{L}} \boxtimes \cdots). \quad (3.22)$$

A comparison of (3.19) and (3.22) reveals that the pre-block space T^{P} is obtained from $S_{\mathcal{M}}$ as

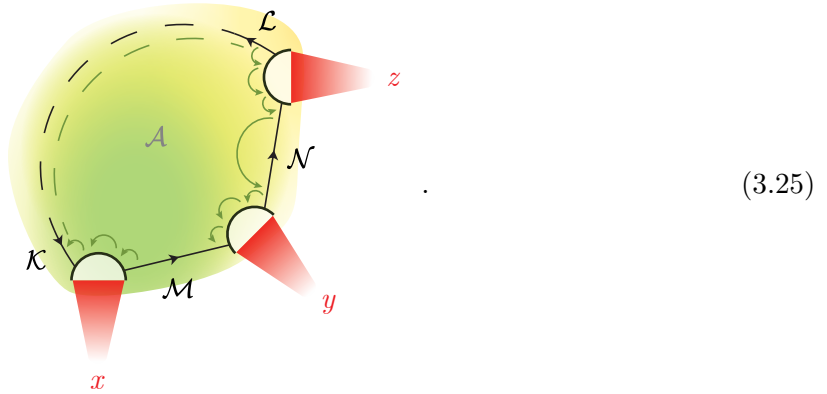
$$\mathrm{T}^{\mathrm{P}} = S_{\mathcal{M}}(I_{\mathcal{M}}). \quad (3.23)$$

We now equip $S_{\mathcal{M}}$ with the structure of a balanced functor, using the explicit form of the pre-block space given in (3.19). The balancing on $S_{\mathcal{M}}$ is obtained as a composition of the balancings for the silent objects $I_{\mathcal{N}}, I_{\mathcal{K}}, I_{\mathcal{L}}, \dots$, the \mathcal{A} -balancings of the ray labels x, y, z, \dots ,

and the balancings of the hom-functors which appear in the definition of $S_{\mathcal{M}}$ (3.22).

$$\begin{aligned}
S_{\mathcal{M}}(am, \overline{m'}) &= \int^{nkl} \langle k \boxtimes \overline{am} \boxtimes \dots, U(x) \rangle \otimes \langle m' \boxtimes \overline{n} \boxtimes \dots, U(y) \rangle \otimes \langle n \boxtimes \overline{l} \boxtimes \dots, U(z) \rangle \otimes \dots \\
&\quad \downarrow \text{Hom-balancing} \\
&\int^{nkl} \langle k \boxtimes \overline{m} \boxtimes \dots, U(x) a \rangle \otimes \langle m' \boxtimes \overline{n} \boxtimes \dots, U(y) \rangle \otimes \langle n \boxtimes \overline{l} \boxtimes \dots, U(z) \rangle \otimes \dots \\
&\quad \downarrow \text{balancing of } x \\
&\int^{nkl} \langle k \boxtimes \overline{m} \boxtimes \dots, a U(x) \rangle \otimes \langle m' \boxtimes \overline{n} \boxtimes \dots, U(y) \rangle \otimes \langle n \boxtimes \overline{l} \boxtimes \dots, U(z) \rangle \otimes \dots \\
&\quad \downarrow \text{Hom-balancing} \\
&\int^{nkl} \langle a^* k \boxtimes \overline{m} \boxtimes \dots, U(x) \rangle \otimes \langle m' \boxtimes \overline{n} \boxtimes \dots, U(y) \rangle \otimes \langle n \boxtimes \overline{l} \boxtimes \dots, U(z) \rangle \otimes \dots \\
&\quad \text{several balancings} \downarrow \\
&\int^{nkl} \langle k \boxtimes \overline{m} \boxtimes \dots, U(x) \rangle \otimes \langle m' \boxtimes \overline{n} \boxtimes \dots, U(y) \rangle \otimes \langle n \boxtimes \overline{al} \boxtimes \dots, U(z) \rangle \otimes \dots \\
&\quad \text{several balancings} \downarrow \\
&\int^{nkl} \langle k \boxtimes \overline{m} \boxtimes \dots, U(x) \rangle \otimes \langle m' \boxtimes \overline{n} \boxtimes \dots, U(y) \rangle \otimes \langle a^* n \boxtimes \overline{l} \boxtimes \dots, U(z) \rangle \otimes \dots \\
&\quad \text{several balancings} \downarrow \\
&\int^{nkl} \langle k \boxtimes \overline{m} \boxtimes \dots, U(x) \rangle \otimes \langle m' \boxtimes \overline{n} \boxtimes \dots, a U(y) \rangle \otimes \langle n \boxtimes \overline{l} \boxtimes \dots, U(z) \rangle \otimes \dots \\
&\quad \downarrow \text{Hom-balancing} \\
&\int^{nkl} \langle k \boxtimes \overline{m} \boxtimes \dots, U(x) \rangle \otimes \langle a^* m' \boxtimes \overline{n} \boxtimes \dots, U(y) \rangle \otimes \langle n \boxtimes \overline{l} \boxtimes \dots, U(z) \rangle \otimes \dots = S_{\mathcal{M}}(m, \overline{a^* m'}).
\end{aligned} \tag{3.24}$$

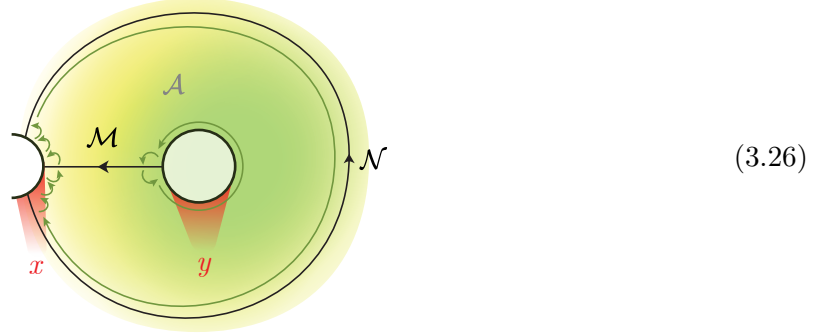
The balancing for $S_{\mathcal{M}}$ defined in (3.24) is called "holonomy" in [FSS22, Sec. 4.11]. As we will here consider several morphisms related to the idea of a holonomy operation, we refer to the balancing of $S_{\mathcal{M}}$ as the *holonomy balancing* $\text{hol}_{m,a,m'}$. It can be pictured as "walking around the boundary" of the domain \mathcal{A} with an object $a \in \mathcal{A}$:



(3.25)

Balanced functors $S_{\mathcal{M}}$, $S_{\mathcal{N}}$, and similar can be constructed for each defect line adjacent to \mathcal{A} , as long as those defect lines separate \mathcal{A} from a different domain, or lie on the boundary of the defect surface. It may be the case, however, that a defect line has the domain \mathcal{A} as its left- and

right-adjacent domain, as in the example (3.26).



\mathcal{M} is then an \mathcal{A} - \mathcal{A} -bimodule category. In this case, $S_{\mathcal{M}}$ is a disconnected bi-balanced functor (see Section 2.8), whose balancings are defined in a way that is very similar to the holonomy balancing from (3.24), by walking an element $a \in \mathcal{A}$ along the two paths pictured in (3.26).

The module coend is defined for both balanced (Definition 2.41) and disconnected bi-balanced functors (Definition 2.43), and we use it to define the block spaces. For this to be consistent, we need the result [FSS22, Lem. 4.22], which in our language assumes the following form:

Proposition 3.7. *There are canonical isomorphisms*

$$\oint^{m \in \mathcal{M}} S_{\mathcal{M}}(m, m) \cong \oint^{n \in \mathcal{N}} S_{\mathcal{N}}(n, n) \quad (3.27)$$

between module coends for each pair of defect lines $(\mathcal{M}, \mathcal{N})$ adjacent to \mathcal{A} .

In order to define block spaces, we need to consider all domains simultaneously. For each domain $\mathcal{A}, \mathcal{B}, \mathcal{C}, \dots$, choose a defect line \mathcal{M} adjacent to \mathcal{A} , \mathcal{N} adjacent to \mathcal{B} , \mathcal{K} adjacent to \mathcal{C} , and so on. Similar to the functor $S_{\mathcal{M}}$ for the single domain \mathcal{A} , we can construct a *piecewise* balanced functor (see Definition 2.47)

$$S_{\mathcal{M}, \mathcal{N}, \mathcal{K}, \dots} : \mathcal{M} \boxtimes \overline{\mathcal{M}} \boxtimes \mathcal{N} \boxtimes \overline{\mathcal{N}} \boxtimes \mathcal{K} \boxtimes \overline{\mathcal{K}} \boxtimes \dots \rightarrow \text{vect} \quad (3.28)$$

such that

$$S_{\mathcal{M}, \mathcal{N}, \mathcal{K}, \dots}(\mathbb{I}_{\mathcal{M}} \boxtimes \mathbb{I}_{\mathcal{N}} \boxtimes \mathbb{I}_{\mathcal{K}} \boxtimes \dots) = \mathbb{T}^{\mathbb{P}}. \quad (3.29)$$

Remark 3.8. $S_{\mathcal{M}, \mathcal{N}, \mathcal{K}, \dots}$ is a piecewise balanced functor, but not, in general, a multi-balanced functor. This motivates Definition 2.47.

Definition 3.9. For a labeled defect surface with a fixed choice of ray labels, the associated *block space* is the vector space given by the piecewise module coend

$$\mathbb{T} := \lim_{\mathcal{M}, \mathcal{N}, \mathcal{K}, \dots} \oint^{\mathcal{M}, \mathcal{N}, \mathcal{K}, \dots} S_{\mathcal{M}, \mathcal{N}, \mathcal{K}, \dots} \quad (3.30)$$

The limit is to be understood in terms of Proposition 3.7, which ensures that between every two module coends we consider, there is a canonical isomorphism.

When unraveling Definition 3.9, one can see that it agrees with the original definition of the block functor [FSS22, Def. 4.21]. Note that the block space \mathbb{T} is by definition a sub-vector space of the pre-block space \mathbb{T}^{p} .

Example 3.10. This example is a special case of [FSS22, Ex. 4.35]. Let \mathcal{A} and \mathcal{B} be spherical fusion categories, and let \mathcal{M} be an \mathcal{A} - \mathcal{B} -bimodule category and \mathcal{N} be a \mathcal{B} - \mathcal{A} -bimodule category. Consider as a labeled defect surface the sphere with two nodes and two defect lines connecting the nodes, such that each node has an incoming and an outgoing defect line attached. We label the domains by \mathcal{A} and \mathcal{B} , and the defect lines by \mathcal{M} and \mathcal{N} , accordingly. We pick ray labels $x \in \overline{\mathcal{M}} \square \mathcal{N} \square$ and $y \in \overline{\mathcal{N}} \square \mathcal{M} \square$ in the ray categories associated to the nodes. The pre-block space for this defect surface is the space of natural transformations

$$\mathbb{T}^{\text{p}} \cong \overline{\mathcal{N}} \square_{\mathcal{M}} \langle U(\bar{x}), U(y) \rangle \cong \text{Fun}(\mathcal{M}, \mathcal{N}) \langle \text{EW}(U\bar{x}), \text{EW}(U(y)) \rangle = \text{Nat}(\text{EW}(U(\bar{x})), \text{EW}(U(y))). \quad (3.31)$$

Note that the functor $\text{EW}(U(\bar{x}))$ can be expressed, according to Remark 2.32, as the left adjoint of $\text{coEW}(U(x))$. Furthermore, the block space is given by the subspace of bimodule natural transformations

$$\mathbb{T} \cong \overline{\mathcal{N}} \square_{\mathcal{M}} \square \langle \bar{x}, y \rangle \cong \text{Fun}_{\mathcal{A}|\mathcal{B}}(\mathcal{M}, \mathcal{N}) \langle \text{EW}_{\text{m}}(\bar{x}), \text{EW}_{\text{m}}(y) \rangle = \text{Nat}_{\text{m}}(\text{EW}_{\text{m}}(U(\bar{x})), \text{EW}_{\text{m}}(U(y))). \quad (3.32)$$

Remark 3.11. It is sometimes (e.g. in the formulation of the move of invariance \mathbf{G} that will be introduced in Section 4) convenient to consider formal linear combinations of extruded graphs, that is, objects of the form $\sum_{i=0}^N \lambda_i \Sigma_i$, where Σ_i are extruded graphs and $\lambda_i \in \mathbb{K}$.

In the same spirit, we allow ourselves to consider extruded graphs in which not every node is labeled by a vector in the respective node-space, but which rather comes with a choice of vector f in the total node space $\mathbb{N}_{x,y,\dots}$ from (3.15). The ordinary node-by-node labeling can be recovered if this vector is a pure tensor $f = f_x \otimes f_y \otimes \dots$. Then f_x, f_y, \dots are the labels for the individual nodes.

Remark 3.12. The concepts of (pre-)block spaces, node spaces and similar, which were reviewed in this section, apply to labeled defect surfaces. In the following, we will also use them for extruded graphs, where "the pre-block space of an extruded graph" strictly means "the pre-block space of the coat of an extruded graph", and analogously for other concepts.

Remark 3.13. The block space of a framed defect surface that is not fine has been expressed, in the case of the framed modular functor, as a limit over all framed fine refinements in [FSS22, Def. 5.24]. A fine refinement of a non-fine framed defect surface Σ is a fine defect surface, whose defect structure (nodes and defect lines) can be thought of as a subdivision of the framed defect structure of Σ . A similar construction can be expected to exist for the oriented state-sum modular functor on surfaces that are not fine, but has not been worked out to our knowledge.

3.3 DEFINITION OF THE EVALUATION

We are now in a position to introduce the main concept of this article: The definition of an evaluation procedure $|\cdot|$, which associates a scalar $|\Sigma| \in \mathbb{K}$ to an extruded graph Σ .

The idea for how the evaluation procedure will be defined in Definition 3.17 is as follows. While the block space is naturally a subspace of the pre-block space, the evaluation procedure requires more structure, namely, a retraction

$$\pi : T^{\mathbb{P}} \rightarrow T, \tag{3.33}$$

which exhibits the block space as a direct summand of the pre-block space. From the fourth-level labeling on the coat of Σ , that is, from the node labels, we can construct a vector $\nu \in T^{\mathbb{P}}$ in the pre-block space. On the other hand, the fourth-level labeling on the core, that is, the core label φ , is by definition a vector in the dual of the block space $\varphi \in T^*$. Using the pairing of T and T^* , the retraction π allows us to obtain a scalar from ν and φ :

$$|\Sigma| := (\pi(\nu), \varphi) = \varphi(\pi(\nu)). \tag{3.34}$$

Another perspective would be to use the pairing of $T^{\mathbb{P}}$ and $T^{\mathbb{P}*}$, and the dual $\pi^* : T^* \rightarrow T^{\mathbb{P}*}$ of the retraction π :

$$|\Sigma| := (\nu, \pi^*(\varphi)). \tag{3.35}$$

Of course, these two definitions agree.

We proceed to define the retraction π mentioned in (3.33). The fact that our fusion categories carry a pivotal structure (in contrast to [FSS22]) enters crucially into the definition of π .

Definition 3.14. Let Σ be a fine labeled defect surface, and let \mathcal{A} be a spherical fusion category which labels a domain of Σ . Let \mathcal{M} be a module category which labels a defect line adjacent to \mathcal{A} . Without loss of generality, assume that \mathcal{M} is a *left* \mathcal{A} -module category. The *holonomy idempotent for \mathcal{A} starting at \mathcal{M}* is the balancing idempotent for the functor $S_{\mathcal{M}}$ from (3.22) defined in Definition 2.44. Explicitly, for a domain \mathcal{A} as in the picture (3.21), it is the linear map

$$h_{\mathcal{A}} : T^{\mathbb{P}} \rightarrow T^{\mathbb{P}} \tag{3.36}$$

given by the following composition:

$$\begin{aligned}
\mathrm{TP} &= \int^{mnkl} \langle k \boxtimes \bar{m} \boxtimes \dots, U(x) \rangle \otimes \langle m \boxtimes \bar{n} \boxtimes \dots, U(y) \rangle \otimes \langle n \boxtimes \bar{l} \boxtimes \dots, U(z) \rangle \otimes \dots \\
&\quad \downarrow \mathcal{D}_{\mathcal{A}}^{-1} \text{ ev} \\
\int_a \int^{mnkl} \langle k \boxtimes \bar{m} \boxtimes \dots, U(x) \rangle \otimes \langle aa^* m \boxtimes \bar{n} \boxtimes \dots, U(y) \rangle \otimes \langle n \boxtimes \bar{l} \boxtimes \dots, U(z) \rangle \otimes \dots \\
&\quad \downarrow \Theta_{\mathcal{A}} \\
\int^a \int^{mnkl} \langle k \boxtimes \bar{m} \boxtimes \dots, U(x) \rangle \otimes \langle aa^* m \boxtimes \bar{n} \boxtimes \dots, U(y) \rangle \otimes \langle n \boxtimes \bar{l} \boxtimes \dots, U(z) \rangle \otimes \dots \\
&\quad \downarrow \text{balancing of } \Phi_{\mathcal{M}} \\
\int^a \int^{mnkl} \langle k \boxtimes \bar{a}m \boxtimes \dots, U(x) \rangle \otimes \langle a m \boxtimes \bar{n} \boxtimes \dots, U(y) \rangle \otimes \langle n \boxtimes \bar{l} \boxtimes \dots, U(z) \rangle \otimes \dots \\
&\quad \downarrow \text{Hom-balancing} \\
\int^a \int^{mnkl} \langle k \boxtimes \bar{m} \boxtimes \dots, U(x) a \rangle \otimes \langle a m \boxtimes \bar{n} \boxtimes \dots, U(y) \rangle \otimes \langle n \boxtimes \bar{l} \boxtimes \dots, U(z) \rangle \otimes \dots \\
&\quad \downarrow \text{balancing of } x \\
\int^a \int^{mnkl} \langle k \boxtimes \bar{m} \boxtimes \dots, a U(x) \rangle \otimes \langle a m \boxtimes \bar{n} \boxtimes \dots, U(y) \rangle \otimes \langle n \boxtimes \bar{l} \boxtimes \dots, U(z) \rangle \otimes \dots \\
&\quad \downarrow \text{Hom-balancing} \\
\int^a \int^{mnkl} \langle a^* k \boxtimes \bar{m} \boxtimes \dots, U(x) \rangle \otimes \langle a m \boxtimes \bar{n} \boxtimes \dots, U(y) \rangle \otimes \langle n \boxtimes \bar{l} \boxtimes \dots, U(z) \rangle \otimes \dots \\
&\quad \text{several balancings} \downarrow \\
\int^a \int^{mnkl} \langle k \boxtimes \bar{m} \boxtimes \dots, U(x) \rangle \otimes \langle a m \boxtimes \bar{n} \boxtimes \dots, U(y) \rangle \otimes \langle n \boxtimes \bar{a}l \boxtimes \dots, U(z) \rangle \otimes \dots \\
&\quad \text{several balancings} \downarrow \\
\int^a \int^{mnkl} \langle k \boxtimes \bar{m} \boxtimes \dots, U(x) \rangle \otimes \langle a m \boxtimes \bar{n} \boxtimes \dots, U(y) \rangle \otimes \langle a^* n \boxtimes \bar{l} \boxtimes \dots, U(z) \rangle \otimes \dots \\
&\quad \text{several balancings} \downarrow \\
\int^a \int^{mnkl} \langle k \boxtimes \bar{m} \boxtimes \dots, U(x) \rangle \otimes \langle a m \boxtimes \bar{n} \boxtimes \dots, a U(y) \rangle \otimes \langle n \boxtimes \bar{l} \boxtimes \dots, U(z) \rangle \otimes \dots \\
&\quad \downarrow \text{Hom-balancing} \\
\int^a \int^{mnkl} \langle k \boxtimes \bar{m} \boxtimes \dots, U(x) \rangle \otimes \langle a^* a m \boxtimes \bar{n} \boxtimes \dots, U(y) \rangle \otimes \langle n \boxtimes \bar{l} \boxtimes \dots, U(z) \rangle \otimes \dots \\
&\quad \downarrow \text{coev} \\
\int^{mnkl} \langle k \boxtimes \bar{m} \boxtimes \dots, U(x) \rangle \otimes \langle m \boxtimes \bar{n} \boxtimes \dots, U(y) \rangle \otimes \langle n \boxtimes \bar{l} \boxtimes \dots, U(z) \rangle \otimes \dots = \mathrm{TP}.
\end{aligned} \tag{3.37}$$

Proposition 3.15. *For any two defect lines \mathcal{M}, \mathcal{N} adjacent to \mathcal{A} , the holonomy idempotents for \mathcal{A} starting at \mathcal{M} and \mathcal{N} respectively are equal.*

The proof of Proposition 3.15 is similar to the proof of [FSS22, Lem. 4.22]. In fact, one can also define holonomy idempotents starting next to the ray labels $U(x), U(y), \dots$. All of these choices lead to the same morphism.

In accordance with Proposition 3.15, we call $h_{\mathcal{A}}$ simply the *holonomy idempotent for \mathcal{A}* , and no longer mention a starting point.

Definition 3.16. The *holonomy idempotent* of a labeled defect surface Σ is given by the composition

$$h := h_{\mathcal{A}} \circ h_{\mathcal{B}} \circ \cdots \quad (3.38)$$

of holonomy idempotents for each domain of Σ . Proposition 2.50 ensures that the order of terms in this composition does not matter.

By Proposition 2.50, the image of h is the block space

$$\text{im}(h) = \mathbb{T}. \quad (3.39)$$

We denote the corestriction of the holonomy idempotent h onto its image by π :

$$\begin{array}{ccc} \mathbb{T}^{\mathbb{P}} & \xrightarrow{h} & \mathbb{T}^{\mathbb{P}} \\ & \searrow \pi & \updownarrow \\ & & \mathbb{T} \end{array} \quad (3.40)$$

Definition 3.17 (Evaluation). Let Σ be an extruded graph with defect labels $m \in \mathcal{M}, n \in \mathcal{N}, \dots$, ray labels x, y, \dots , node labels f, g, \dots , and core label φ . Consider the following composition.

$$\begin{array}{ccc} \mathbb{N}_{x,y,\dots}(m \boxtimes \bar{m}, n \boxtimes \bar{n}, \dots) & & f \otimes g \otimes \cdots \\ \downarrow \mathbb{N}_{x,y,\dots}(m,n,\dots\tau) & \text{structure map of the end} & \downarrow \\ \mathbb{T}^{\mathbb{P}} = \mathbb{N}_{x,y,\dots}(\mathbb{I}_{\mathcal{M}}, \mathbb{I}_{\mathcal{N}}, \dots) & & \mathbb{N}_{x,y,\dots}(m,n,\dots\tau)(f \otimes g \otimes \cdots) \\ \downarrow \pi & & \downarrow \\ \mathbb{T} & & \pi(\mathbb{N}_{x,y,\dots}(m,n,\dots\tau)(f \otimes g \otimes \cdots)) \\ \downarrow \varphi & \text{core label} & \downarrow \\ \mathbb{K} & & (\varphi \circ \pi)(\mathbb{N}_{x,y,\dots}(m,n,\dots\tau)(f \otimes g \otimes \cdots)) \end{array} \quad (3.41)$$

We define the evaluation $|\Sigma|$ of Σ to be the image of the node labels f, g, \dots under the composition (3.41), i.e.

$$|\Sigma| := (\varphi \circ \pi)(\mathbb{N}_{x,y,\dots}(m,n,\dots\tau)(f \otimes g \otimes \cdots)). \quad (3.42)$$

Remark 3.18. It is sometimes convenient to consider extruded graphs either without node labels or without a core label. In the former case, it is clear that the evaluation of extruded graphs still yields a linear form on the total node space. To an extruded graph without core label we can still assign a vector in its block space, by simply not performing the last step in the evaluation procedure, for which a core label would be needed.

Remark 3.19. Definition 3.17 extends to linear combinations of extruded graphs as mentioned in Remark 3.11 in the obvious way:

$$\left| \sum_{i=0}^N \lambda_i \Sigma_i \right| := \sum_{i=0}^N \lambda_i |\Sigma_i|. \quad (3.43)$$

Moreover, it is immediate from Definition 3.17 that extruded graphs with not individual node labels, but a total node label, as discussed in Remark 3.11, can also be evaluated.

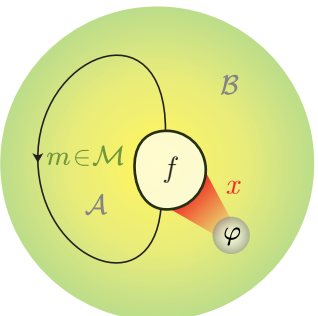
Remark 3.20. Our construction supposes that all (bi-)module categories are equipped with a trace. However, the trace structure is never used in the definition of the evaluation procedure. We will see in Remark 3.26 that the evaluation of extruded graphs becomes zero when module categories are involved that do not admit a module trace, and that traces provide distinguished choices for core labels.

Example 3.21 (Generalized 6j symbols). A homeomorphism between the surface of a tetrahedron and the sphere \mathbb{S}^2 defines a graph with 4 vertices and 6 edges on the sphere. Let us consider an extruded graph Σ on \mathbb{S}^2 , whose nodes and defect lines are obtained from the vertices and edges of the tetrahedron (after picking an orientation for each edge). The domains of Σ are labeled by arbitrary spherical fusion categories, and the defect lines by arbitrary traced bimodule categories. The object labels for the defect lines, as well as the ray labels, are all simple objects in the respective categories, and the core label is chosen arbitrarily. The evaluation of extruded graphs from Definition 3.17 defines a linear form on the total nodespace of Σ . This linear form is called a *generalized 6j-symbol*, a terminology which will be justified by Corollary 5.11, and, in a different sense, in Section 5.3.

Remark 3.22. A state-sum modular functor defined on non-fine defect surfaces as mentioned in Remark 3.13 would allow to evaluate also non-fine extruded graphs. Such a construction is beyond the scope of this work.

3.4 LASSO GRAPHS

As a first exercise, we explicitly compute the invariant for one of the simplest possible types of extruded graphs: A *lasso graph* Q , whose underlying surface is the sphere \mathbb{S}^2 . We will later see (Theorem 4.5) that any extruded graph on the sphere can be transformed – using the moves from Section 4 – into this lasso graph. A lasso graph is an extended graph Q : Its coat is a sphere with a single node and a single circular defect line starting and ending at the node.



(3.44)

There are four levels of algebraic labels to be specified:

- On the coat, the two hemispheres forming the connected components of the complement of the defect line are labeled by spherical fusion categories \mathcal{A} and \mathcal{B} .
- The defect line is labeled by a spherical bimodule category ${}_{\mathcal{A}}\mathcal{M}_{\mathcal{B}}$. Note that this implies that the ray category associated to the single node is the balanced category $\mathbb{T}^{\mathbb{R}} = \mathcal{M} \square_{\mathcal{B}} \overline{\mathcal{M}} \square_{\mathcal{A}}$, which contains a silent object $\Phi_{\mathcal{M}}$, as described in Section 2.14. In contrast, the node category is given by the (unbalanced) category $\mathbb{T}^{\mathbb{N}} = \mathcal{M} \boxtimes \overline{\mathcal{M}}$.
- The defect line carries an additional subordinate label: A choice of an object $m \in \mathcal{M}$. Moreover, we label the ray attached to the node by an object $x \in \mathbb{T}^{\mathbb{R}}$. These choices determine the node space to be the hom-space $N_x(m \boxtimes \overline{m}) = {}_{\mathbb{T}^{\mathbb{N}}}\langle m \boxtimes \overline{m}, U(x) \rangle$.
- We label the node by a vector $f \in N_x(m \boxtimes \overline{m})$. Moreover, we will see in (3.51) below that the block space for this defect surface is given by the vector space ${}_{\mathbb{T}^{\mathbb{R}}}\langle \Phi_{\mathcal{M}}, x \rangle$. Hence, the core label φ is a linear form $\varphi : \langle \Phi_{\mathcal{M}}, x \rangle \rightarrow \mathbb{K}$.

This completes the four levels of labels that determine the extruded graph Q . Our goal is to compute the scalar $|Q|$ using Definition 3.17.

To this end, we remark that the pre-block space of Q is given by

$$\mathbb{T}^{\mathbb{P}} = N_x(\mathbb{I}_{\mathcal{M}}) = {}_{\mathbb{T}^{\mathbb{N}}}\langle \mathbb{I}_{\mathcal{M}}, U(x) \rangle.$$

Recall the retraction $r : {}_{\mathbb{T}^{\mathbb{N}}}\langle \mathbb{I}_{\mathcal{M}}, U(x) \rangle \rightarrow {}_{\mathbb{T}^{\mathbb{R}}}\langle \Phi_{\mathcal{M}}, x \rangle$ between the hom-spaces, which we constructed algebraically in Lemma 2.23. We will show that the holonomy idempotent h is equal to the idempotent from which r is constructed; this is the crucial ingredient to the proof of Lemma 3.23 below. Then, we can deduce that the block space is the image of r , namely the hom-space ${}_{\mathbb{T}^{\mathbb{R}}}\langle \Phi_{\mathcal{M}}, x \rangle$ of the ray category. The retraction r will, in this case, be equal to the projection π from the pre-block space into the block space. To simplify the presentation, we here specialize to $\mathcal{B} = \text{vect}$. In essence, \mathcal{M} is now just a left \mathcal{A} -module category. On the topological level, vect -labeled domains can be removed entirely, so we are left with a disk with a single boundary node as our defect surface.

The computation for the more general case where \mathcal{B} is not necessarily vect does not provide additional insight. With this in mind, we can state the following:

Lemma 3.23. *With Q a lasso graph with the labeling described above, the evaluation $|Q| \in \mathbb{K}$ as defined in Definition 3.17 is given by*

$$|Q| = (\varphi \circ r)(f \circ_m \tau). \quad (3.45)$$

Moreover, we provide the following explicit description of the (atypical) components $r(f \circ_m \tau)_n : n \boxtimes \overline{n} \rightarrow U(x)$ in the sense of Section 2.6 for later use. They are given by the sum with respect to simple objects $\mathbf{a} \in \mathcal{A}$ over the compositions

$$n \boxtimes \overline{n} \xrightarrow{*\langle n, \mathbf{a}^* m \rangle \boxtimes *\langle \mathbf{a}^* m, n \rangle} \mathbf{a}^* m \boxtimes \overline{\mathbf{a}^* m} = \mathbf{a}^* m \boxtimes \overline{m} \mathbf{a} \xrightarrow{\mathbf{a}^* f \mathbf{a}} \mathbf{a}^* U(x) \mathbf{a} \xrightarrow{\frac{d_{\mathbf{a}} d_n}{\mathcal{D}_{\mathcal{A}}} \text{brev}_x \mathbf{a}^*} U(x), \quad (3.46)$$

or equivalently as:

$$r(f \circ_m \tau)_n = \sum_{\mathbf{a}} \frac{d_{\mathbf{a}} d_n}{D_{\mathcal{A}}} \text{brev}_x^{\mathbf{a}^*} \circ (\mathbf{a}^* f \mathbf{a}) \circ (\star_{\langle n, \mathbf{a}^* m \rangle} \boxtimes \star_{\langle \mathbf{a}^* m, n \rangle}). \quad (3.47)$$

Proof. Using that $N_x(m\tau)(f) = f \circ_m \tau$, the general formula (3.42) for the evaluation procedure simplifies to

$$|Q| = (\varphi \circ \pi)(f \circ_m \tau). \quad (3.48)$$

Comparison between (3.45) and (3.48) makes clear that if the projector π coincides with the retraction r from Lemma 2.23, (3.45) follows. Thus, the projector π , and to this end, the holonomy idempotent h , is to be computed.

Starting with an element $g \in \mathbb{T}^{\mathbb{P}} = \mathbb{T}^{\mathbb{N}} \langle I_{\mathcal{M}}, U(x) \rangle$, we calculate its image $h(g)$ under the holonomy idempotent h . Since h is a composition of several maps, the calculation is broken down into intermediate steps. The morphisms composing to h are given vertically in the leftmost column of (3.49). The middle column contains the images of g under the partial compositions of the morphisms. In particular, the bottom-most entry is equal to $h(g)$. The entries of the right column give the entries of the middle column in graphical notation. Moreover, in the middle and

right columns, we use the notation for maps between ends and coends from Section 2.6.

$$\begin{array}{ccc}
\langle \mathbf{I}_{\mathcal{M}}, U(x) \rangle & & \\
\downarrow \frac{1}{\mathcal{D}_{\mathcal{A}}} \text{ evaluation} & & \\
\int_a \langle a a^* \mathbf{I}_{\mathcal{M}}, U(x) \rangle & \int_a \frac{1}{\mathcal{D}_{\mathcal{A}}} \text{ev}^a g & = \int_a \frac{1}{\mathcal{D}_{\mathcal{A}}} \text{diagram} \\
\downarrow \Theta_{\mathcal{A}} & \downarrow & \\
\int_a \langle a a^* \mathbf{I}_{\mathcal{M}}, U(x) \rangle & \int_a \frac{d_a}{\mathcal{D}_{\mathcal{A}}} \text{ev}^a g & = \int_a \frac{d_a}{\mathcal{D}_{\mathcal{A}}} \text{diagram} \\
\downarrow \text{balancing of } \Phi_{\mathcal{M}} & \downarrow & \\
\int_a \langle a \mathbf{I}_{\mathcal{M}} a^*, U(x) \rangle & \int_a \frac{d_a}{\mathcal{D}_{\mathcal{A}}} (\text{ev}^a g) \circ (a \beta_{a^*}^{-1}) & = \int_a \frac{d_a}{\mathcal{D}_{\mathcal{A}}} \text{diagram} \\
& = \int_a \frac{d_a}{\mathcal{D}_{\mathcal{A}}} g \circ \text{brev}_{\Phi_{\mathcal{M}}}^a & \\
\downarrow \text{Hom-balancing} & \downarrow & \\
\int_a \langle a \mathbf{I}_{\mathcal{M}}, U(x) a \rangle & \int_a \frac{d_a}{\mathcal{D}_{\mathcal{A}}} (ga) \circ (\text{brev}_{\Phi_{\mathcal{M}}}^a a) \circ (a \mathbf{I}_{\mathcal{M}} a \text{coev}) & = \int_a \frac{d_a}{\mathcal{D}_{\mathcal{A}}} \text{diagram} \\
& \stackrel{\text{zig-zag}}{=} \int_a \frac{d_a}{\mathcal{D}_{\mathcal{A}}} (ga) \circ \beta_a & \\
\downarrow \text{balancing of } x & \downarrow & \\
\int_a \langle a \mathbf{I}_{\mathcal{M}}, a U(x) \rangle & \int_a \frac{d_a}{\mathcal{D}_{\mathcal{A}}} (\text{br}_a^x)^{-1} \circ (ga) \circ \beta_a & = \int_a \frac{d_a}{\mathcal{D}_{\mathcal{A}}} \text{diagram} \\
\downarrow \text{Hom-balancing} & \downarrow & \\
\int_a \langle a^* a \mathbf{I}_{\mathcal{M}}, U(x) \rangle & \int_a \frac{d_a}{\mathcal{D}_{\mathcal{A}}} (\text{ev}^{a^*} U(x)) \circ (a^* (\text{br}_a^x)^{-1}) \circ (a^* ga) \circ (a^* \beta_a) & = \int_a \frac{d_a}{\mathcal{D}_{\mathcal{A}}} \text{diagram} \\
& = \int_a \frac{d_a}{\mathcal{D}_{\mathcal{A}}} \text{brev}_x^{a^*} \circ (a^* ga) \circ (a^* \beta_a) & \\
\downarrow \text{coevaluation} & \downarrow & \\
\langle \mathbf{I}_{\mathcal{M}}, U(x) \rangle & \sum_{\mathbf{a}} \frac{d_{\mathbf{a}}}{\mathcal{D}_{\mathcal{A}}} \text{brev}_x^{\mathbf{a}^*} \circ (\mathbf{a}^* g \mathbf{a}) \circ (\mathbf{a}^* \beta_{\mathbf{a}}) \circ (\mathbf{a} \text{coev } \mathbf{I}_{\mathcal{M}}) & = \sum_{\mathbf{a}} \frac{d_{\mathbf{a}}}{\mathcal{D}_{\mathcal{A}}} \text{diagram} \\
& = \sum_{\mathbf{a}} \frac{d_{\mathbf{a}}}{\mathcal{D}_{\mathcal{A}}} \text{brev}_x^{\mathbf{a}^*} \circ (\mathbf{a}^* g \mathbf{a}) \circ \mathbf{a} \text{cobrev}_{\Phi_{\mathcal{M}}} & \\
\end{array}$$

(3.49)

From the bottom-most row, we can read off the expression for h , and conclude, using the graphical notation of functorial diagrams from Section 2.3,

$$h = \sum_{\mathbf{a}} \frac{d_{\mathbf{a}}}{\mathcal{D}_{\mathcal{A}}} \text{brev}_x^{\mathbf{a}^*} \circ (\mathbf{a}^* - \mathbf{a}) \circ {}_{\mathbf{a}}\text{cobrev}_{\Phi_{\mathcal{M}}} = \sum_{\mathbf{a}} \frac{d_{\mathbf{a}}}{\mathcal{D}_{\mathcal{A}}} \left(\begin{array}{c} x \\ \circlearrowleft \\ \square \\ \circlearrowright \\ I_{\mathcal{M}} \end{array} \right) \cdot \mathbf{a}. \quad (3.50)$$

Comparing with Lemma 2.23, we recognize that the expression (3.50) for h coincides with the retraction r , which projects onto the subspace

$$\text{im}(h) = \begin{array}{ccc} \mathbb{T}^{\text{R}}\langle \Phi_{\mathcal{M}}, x \rangle & \longleftrightarrow & \mathbb{T}^{\text{N}}\langle I_{\mathcal{M}}, U(x) \rangle \\ & \nwarrow \pi=r & \nearrow \\ & & \end{array} h.$$

This confirms that the block space is given by

$$\mathbb{T} = \mathbb{T}^{\text{R}}\langle \Phi_{\mathcal{M}}, x \rangle, \quad (3.51)$$

in agreement with [FSS22, Example 4.33], and consequently shows that the projector π is equal to the retraction r from Lemma 2.23. We have thus proven (3.45).

Turning to the second part of the lemma, we continue our calculation in order to obtain the explicit components (3.47), we recall from (2.163) that the components of ${}_{\mathbf{a}}\text{cobrev}_{\Phi_{\mathcal{M}}}$ for $n, k \in \mathcal{M}$ take the form

$$k({}_{\mathbf{a}}\text{cobrev}_{\Phi_{\mathcal{M}}})^n = \star_{\langle n, \mathbf{a}^* k \rangle} \boxtimes \star_{\langle \mathbf{a}^* k, n \rangle} \quad : \quad n \boxtimes \bar{n} \rightarrow \mathbf{a}^* k \boxtimes \bar{k} \mathbf{a}. \quad (3.52)$$

This allows us to give an explicit description of the components $\pi(g)_n$ of $\pi(g) = h(g) = r(g)$.

$$\begin{aligned} \pi(g)_n &= \sum_{\mathbf{a}} \frac{d_{\mathbf{a}}}{\mathcal{D}_{\mathcal{A}}} \text{brev}_x^{\mathbf{a}^*} \circ (\mathbf{a}^* g \mathbf{a}) \circ ({}_{\mathbf{a}}\text{cobrev}_{\Phi_{\mathcal{M}}})_n \\ &= \sum_{\mathbf{a}, \mathbf{k}} \frac{d_{\mathbf{a}}}{\mathcal{D}_{\mathcal{A}}} \text{brev}_x^{\mathbf{a}^*} \circ (\mathbf{a}^* g_{\mathbf{k}} \mathbf{a}) \circ {}_{\mathbf{k}}({}_{\mathbf{a}}\text{cobrev}_{\Phi_{\mathcal{M}}})_n \\ &= \sum_{\mathbf{a}, \mathbf{k}} \frac{d_{\mathbf{a}} d_n}{\mathcal{D}_{\mathcal{A}}} \text{brev}_x^{\mathbf{a}^*} \circ (\mathbf{a}^* g_{\mathbf{k}} \mathbf{a}) \circ {}_{\mathbf{k}}({}_{\mathbf{a}}\text{cobrev}_{\Phi_{\mathcal{M}}})^n \\ &\stackrel{(3.52)}{=} \sum_{\mathbf{a}, \mathbf{k}} \frac{d_{\mathbf{a}} d_n}{\mathcal{D}_{\mathcal{A}}} \text{brev}_x^{\mathbf{a}^*} \circ (\mathbf{a}^* g_{\mathbf{k}} \mathbf{a}) \circ (\star_{\langle n, \mathbf{a}^* \mathbf{k} \rangle} \boxtimes \star_{\langle \mathbf{a}^* \mathbf{k}, n \rangle}). \end{aligned} \quad (3.53)$$

Working towards (3.47), we are interested in substituting $f \circ {}_m \tau$ for g in the above expressions. To get started, we rewrite the term $f \circ {}_m \tau$:

$$\begin{aligned} f \circ {}_m \tau &\stackrel{(2.20)}{=} \sum_{\mathbf{k}} d_{\mathbf{k}} f \circ (\star_{\langle \mathbf{k}, m \rangle} \boxtimes \bar{m}) \circ (\star_{\langle m, \mathbf{k} \rangle} \boxtimes \bar{m}) \circ {}_{\mathbf{k}} \tau \\ &= \sum_{\mathbf{k}} d_{\mathbf{k}} f \circ (\star_{\langle \mathbf{k}, m \rangle} \boxtimes \star_{\langle m, \mathbf{k} \rangle}) \circ {}_{\mathbf{k}} \tau. \end{aligned} \quad (3.54)$$

From the last line, we can tell that the simple components $(f \circ_m \tau)_{\mathbf{k}}$ involve the term $\mathbf{k}'\tau_{\mathbf{k}}$, for which we have found an explicit formula in (2.45). Hence, the simple component $(f \circ_m \tau)_{\mathbf{k}}$ is given by

$$(f \circ_m \tau)_{\mathbf{k}} = d_{\mathbf{k}} f \circ (\star_{\langle \mathbf{k}, m \rangle} \boxtimes \star_{\langle m, \mathbf{k} \rangle}). \quad (3.55)$$

Combining (3.55) with (3.53), we obtain

$$\begin{aligned} \pi (f \circ_m \tau)_n &= \sum_{\mathbf{a}, \mathbf{k}} \frac{d_{\mathbf{a}} d_n d_{\mathbf{k}}}{\mathcal{D}_{\mathcal{A}}} \text{brev}_x^{\mathbf{a}^*} \circ \left(\mathbf{a}^* \left(f \circ (\star_{\langle \mathbf{k}, m \rangle} \boxtimes \star_{\langle m, \mathbf{k} \rangle}) \right) \mathbf{a} \right) \circ (\star_{\langle \mathbf{k}, \mathbf{a}^* n \rangle} \boxtimes \star_{\langle \mathbf{a}^* n, \mathbf{k} \rangle}) \\ &= \sum_{\mathbf{a}} \frac{d_{\mathbf{a}} d_n}{\mathcal{D}_{\mathcal{A}}} \text{brev}_x^{\mathbf{a}^*} \circ (\mathbf{a}^* f \mathbf{a}) \circ (\star_{\langle n, \mathbf{a}^* m \rangle} \boxtimes \star_{\langle \mathbf{a}^* m, n \rangle}). \end{aligned} \quad (3.56)$$

Using that $\pi = r$, we have obtained (3.47). \square

Remark 3.24. These calculations, involving dimension factors such as $d_{\mathbf{k}}$ look like they make use of the bimodule trace on \mathcal{M} . However, recall from Remark 3.20 that the trace structure does not enter into the definition of the evaluation procedure. In fact, the computation is independent of the choice of trace, and the same result can be obtained by equipping \mathcal{M} with an auxiliary Calabi-Yau structure.

Remark 3.25. The contents of Lemma 3.23 generalize to the case where \mathcal{B} is not necessarily vect. In particular, the general formula for the holonomy idempotent h is given by

$$h(g) = \sum_{\mathbf{a}, \mathbf{b}} \frac{d_{\mathbf{a}} d_{\mathbf{b}}}{\mathcal{D}_{\mathcal{A}} \mathcal{D}_{\mathcal{B}}} \text{brev}_x^{\mathbf{a}^* \boxtimes \mathbf{b}^*} \circ ((\mathbf{a}^* \boxtimes \mathbf{b}^*) g (\mathbf{a} \boxtimes \mathbf{b})) \circ_{\mathbf{a} \boxtimes \mathbf{b}} \text{cobrev}_{\Phi_{\mathcal{M}}}. \quad (3.57)$$

To continue the discussion of the evaluation of lasso graphs, we first restrict ourselves to a subset of lasso graphs called loop graphs. This is the content of the next section. We will later see (in Section 4, using the move **SV**) that understanding the evaluation of loop graphs is sufficient to understand the evaluation of all lasso graphs. Indeed, we give a concrete formula for the evaluation of lasso graphs in Proposition 5.13.

3.5 LOOP GRAPHS

Loop graphs form a subset of lasso graphs: they are characterized by special ray- and core labels. Let us use that the ray category $\mathcal{M} \square \overline{\mathcal{M}} \square$ of a lasso graph O has a cosilent object $\Phi^{\mathcal{M}}$, and specialize to the particular case $x = \Phi^{\mathcal{M}}$ when the ray label is cosilent. For this ray label, the block space for lasso graphs from (3.51) becomes the vector space

$$\mathbb{T} = \langle \Phi_{\mathcal{M}}, \Phi^{\mathcal{M}} \rangle. \quad (3.58)$$

An invertible map in this homomorphism space is given by the canonical isomorphism $\Theta_{\mathcal{M}}$ between the end and the coend induced by the module trace on \mathcal{M} , see Lemma 2.33. For the core label, we choose

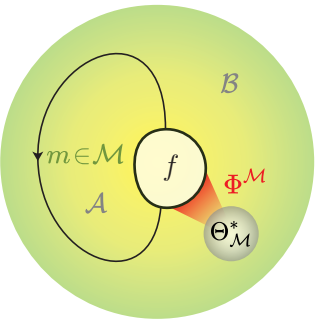
$$\varphi = \Theta_{\mathcal{M}}^* := \mathcal{D}_{\mathcal{A}} \mathcal{D}_{\mathcal{B}} \text{Tr}_{\mathcal{M} \square \overline{\mathcal{M}}} (\Theta_{\mathcal{M}}^{-1} \circ -), \quad (3.59)$$

which is a linear form on \mathbb{T} . For us, it is important that the value of $\Theta_{\mathcal{M}}^*$ on $\Theta_{\mathcal{M}}$ is

$$\Theta_{\mathcal{M}}^*(\Theta_{\mathcal{M}}) = \mathcal{D}_{\mathcal{A}}\mathcal{D}_{\mathcal{B}} \operatorname{Tr}_{\mathcal{M} \square \overline{\mathcal{M}} \square}(\Theta_{\mathcal{M}}^{-1} \circ \Theta_{\mathcal{M}}) = \mathcal{D}_{\mathcal{A}}\mathcal{D}_{\mathcal{B}} d_{\mathbb{F}_{\mathcal{M}}}^{(2.167)} \stackrel{\text{def}}{=} \mathcal{D}_{\mathcal{M}}. \quad (3.60)$$

A lasso graph with these choices for x and φ is called a *loop graph*.

Remark 3.26. In this example, we see clearly: If the category \mathcal{M} does not admit a bimodule trace, then the block space \mathbb{T} is trivial, and consequently, the evaluation is zero. On the other hand, once a bimodule trace is chosen, we have a canonical choice for a non-zero core label. This is why we require all bimodule categories to be equipped with a bimodule trace, even though this is not strictly necessary in order to define the evaluation, see Remark 3.20.



$$O = \text{Diagram} \quad (3.61)$$

Note that due to this choice, the node space takes the form $N_x(m) = \langle m \boxtimes \overline{m}, I^{\mathcal{M}} \rangle$, which by Corollary 2.36 is canonically isomorphic to the endomorphism space $\langle m, m \rangle$. We can thus identify the node label f with an endomorphism $f' = \operatorname{sil}^{-1}(f)$ of the object $m \in \mathcal{M}$:

$$f \in \langle m \boxtimes \overline{m}, I^{\mathcal{M}} \rangle \cong \langle m, m \rangle \ni f'. \quad (3.62)$$

Remark 3.27. The idea here is that $\mathbb{F}^{\mathcal{M}}$ and our choice of φ can be interpreted as *transparent* labels for the ray and the core, respectively. Without a core and a ray, the graph now only consists of an m -labeled loop drawn on a sphere, with a vertex labeled by a morphism $f' : m \rightarrow m$. This illustrates, in a special case, how specific extruded graphs can be identified with string diagrams on the sphere, which are ubiquitous in descriptions of Turaev-Viro state-sum models [TV17]. Since our construction should in this sense specialize to the ordinary graphical calculus for spherical categories (we will prove this in Theorem 5.12), we expect to obtain the scalar $\operatorname{Tr}_{\mathcal{M}}(f')$ from the evaluation. As we will see in Theorem 3.28, this is true.

The following result, stating that the evaluation of loop graphs gives, up to normalization, a trace, will be central as the last step of any practical application of the evaluation procedure.

Theorem 3.28. *Let O be a loop graph as in (3.61), that is, an extruded graph whose coat is a sphere with a single node and a single defect line, labeled by some object $m \in {}_{\mathcal{A}}\mathcal{M}_{\mathcal{B}}$ starting and ending at the node, whose ray is labeled by the cosilent object $\mathbb{F}^{\mathcal{M}}$ and whose core label is $\varphi = \Theta_{\mathcal{M}}^*$. Let the node of O be labeled by a vector $f = \operatorname{sil}(f')$, for a given endomorphism $f' : m \rightarrow m$.*

Then the evaluation of O as introduced in Definition 3.17 reduces essentially to the trace of f' :

$$|O| = \text{Tr}_{\mathcal{M}}(f'), \quad (3.63)$$

an expression involving the trace on \mathcal{M} provided by the spherical structure on \mathcal{M} .

Proof. We again restrict ourselves, without loss of generality, to the case $\mathcal{B} = \text{vect}$. The vector $\pi(f \circ_m \tau)$ we computed in Lemma 3.23 is now a map $\Phi_{\mathcal{M}} \rightarrow \Phi^{\mathcal{M}}$. As such, it has components

$${}^k(\pi(f \circ_m \tau))_n : n \boxtimes \bar{n} \rightarrow k \boxtimes \bar{k}. \quad (3.64)$$

We proceed to calculate these components, starting from the expression we obtained in (3.56).

$$\begin{aligned} {}^k(\pi(f \circ_m \tau))_n &\stackrel{(3.56)}{=} \sum_{\mathbf{a}} \frac{d_{\mathbf{a}} d_n}{\mathcal{D}_{\mathcal{A}}} k \left(\text{brev}_{\Phi^{\mathcal{M}}} \mathbf{a}^* \right) \circ (\mathbf{a}^* f \mathbf{a}) \circ (\star_{\langle n, \mathbf{a}^* m \rangle} \boxtimes \star_{\langle \mathbf{a}^* m, n \rangle}) \\ &= \sum_{\mathbf{a}} \frac{d_{\mathbf{a}} d_n}{\mathcal{D}_{\mathcal{A}}} (k \boxtimes \bar{k} \text{ ev}^{\mathbf{a}^*}) \circ \left({}^k(\beta_{\mathbf{a}^*}) \mathbf{a} \right) \circ (\mathbf{a}^* f \mathbf{a}) \circ (\star_{\langle n, \mathbf{a}^* m \rangle} \boxtimes \star_{\langle \mathbf{a}^* m, n \rangle}) \\ &= \sum_{\mathbf{a}, \mathbf{l}} \frac{d_{\mathbf{a}} d_n}{\mathcal{D}_{\mathcal{A}}} (k \boxtimes \bar{k} \text{ ev}^{\mathbf{a}^*}) \circ \left({}^k(\beta_{\mathbf{a}^*})^{\mathbf{l}} \mathbf{a} \right) \circ (\mathbf{a}^* ({}^{\mathbf{l}} f) \mathbf{a}) \circ (\star_{\langle n, \mathbf{a}^* m \rangle} \boxtimes \star_{\langle \mathbf{a}^* m, n \rangle}) \\ &= \sum_{\mathbf{a}, \mathbf{l}} \frac{d_{\mathbf{a}} d_n d_k}{\mathcal{D}_{\mathcal{A}}} (k \boxtimes \bar{k} \text{ ev}^{\mathbf{a}^*}) \circ \left({}^k(\beta_{\mathbf{a}^*})^{\mathbf{l}} \mathbf{a} \right) \circ (\mathbf{a}^* ({}^{\mathbf{l}} f) \mathbf{a}) \circ (\star_{\langle n, \mathbf{a}^* m \rangle} \boxtimes \star_{\langle \mathbf{a}^* m, n \rangle}) \\ &\stackrel{(2.107)}{=} \sum_{\mathbf{a}, \mathbf{l}} \frac{d_{\mathbf{a}} d_n d_k}{\mathcal{D}_{\mathcal{A}}} (k \boxtimes \bar{k} \text{ ev}^{\mathbf{a}^*}) \circ \left(\star_{\langle \mathbf{a}^* \mathbf{l}, k \rangle} \boxtimes \left((\star_{\langle k, \mathbf{a}^* \mathbf{l} \rangle} \mathbf{a}^*) \circ \mathbf{a}^* \text{ coev} \right) \mathbf{a} \right) \\ &\quad \circ (\mathbf{a}^* ({}^{\mathbf{l}} f) \mathbf{a}) \circ (\star_{\langle n, \mathbf{a}^* m \rangle} \boxtimes \star_{\langle \mathbf{a}^* m, n \rangle}) \\ &\stackrel{\text{zig-zag}}{=} \sum_{\mathbf{a}, \mathbf{l}} \frac{d_{\mathbf{a}} d_n d_k}{\mathcal{D}_{\mathcal{A}}} \left(\star_{\langle \mathbf{a}^* \mathbf{l}, k \rangle} \boxtimes \star_{\langle k, \mathbf{a}^* \mathbf{l} \rangle} \right) \circ (\mathbf{a}^* ({}^{\mathbf{l}} f) \mathbf{a}) \circ (\star_{\langle n, \mathbf{a}^* m \rangle} \boxtimes \star_{\langle \mathbf{a}^* m, n \rangle}). \end{aligned} \quad (3.65)$$

Writing $f : m \boxtimes \bar{m} \rightarrow \mathbb{I}^{\mathcal{M}}$ in (3.65) in \boxtimes -factorized form, we obtain

$${}^k(\pi(f \circ_m \tau))_n = \sum_{\mathbf{a}, \mathbf{l}} \frac{d_{\mathbf{a}} d_n d_k}{\mathcal{D}_{\mathcal{A}}} \left(\star_{\langle \mathbf{a}^* \mathbf{l}, k \rangle} \circ \left(\mathbf{a}^* ({}^{\mathbf{l}} f)_{(1)} \right) \circ \star_{\langle n, \mathbf{a}^* m \rangle} \right) \boxtimes \left(\star_{\langle k, \mathbf{a}^* \mathbf{l} \rangle} \circ \left(\overline{({}^{\mathbf{l}} f)}_{(2)} \mathbf{a} \right) \circ \star_{\langle \mathbf{a}^* m, n \rangle} \right). \quad (3.66)$$

The next step is to pass this expression through the isomorphism sil , defined in (2.179), which here takes the form

$$\langle \mathbb{I}_{\mathcal{M}}, \mathbb{I}^{\mathcal{M}} \rangle = \left\langle \int_n n \boxtimes \bar{n}, \int^k k \boxtimes \bar{k} \right\rangle \stackrel{\text{sil}}{\cong} \int^k \langle k, k \rangle. \quad (3.67)$$

We denote the image of $\pi(f \circ_m \tau)$ in $\int^k \langle k, k \rangle$ under the isomorphism (3.67) by θ . It is, according to (2.182), given by the composition of the two Deligne factors in (3.66), leading to

$$\theta = \int^k \sum_{\mathbf{a}, \mathbf{l}, \mathbf{n}} \frac{d_{\mathbf{a}} d_n d_k}{\mathcal{D}_{\mathcal{A}}} \star_{\langle \mathbf{a}^* \mathbf{l}, k \rangle} \circ \left(\mathbf{a}^* ({}^{\mathbf{l}} f)_{(1)} \right) \circ \star_{\langle n, \mathbf{a}^* m \rangle} \circ \star_{\langle \mathbf{a}^* m, n \rangle} \circ \left(\mathbf{a}^* ({}^{\mathbf{l}} f)_{(2)} \right) \circ \star_{\langle k, \mathbf{a}^* \mathbf{l} \rangle}. \quad (3.68)$$

We here used notation from Section 2.6: the integral symbol stands for the assembly of components into a single morphism. By (2.17), the composition factor $\sum_{\mathbf{n}} d_{\mathbf{n}} \star_{\langle \mathbf{n}, \mathbf{a}^* m \rangle} \circ \star_{\langle \mathbf{a}^* m, \mathbf{n} \rangle}$ is a resolution of the identity, hence equal to the identity on $\mathbf{a}^* m$, so the expression (3.68) simplifies to

$$\theta = \int^k \sum_{\mathbf{a}, \mathbf{l}} \frac{d_{\mathbf{a}} d_k}{\mathcal{D}_{\mathcal{A}}} \star_{\langle \mathbf{a}^* \mathbf{l}, k \rangle} \circ \left(\mathbf{a}^* ({}^{\mathbf{l}}f)_{(1)} \right) \circ \left(\mathbf{a}^* ({}^{\mathbf{l}}f)_{(2)} \right) \circ \star_{\langle k, \mathbf{a}^* \mathbf{l} \rangle}. \quad (3.69)$$

Let us introduce a set of scalars we call the *\mathbf{l} -isotypical traces* of $f' = \text{sil}^{-1}(f) : m \rightarrow m$, for simple objects $\mathbf{l} \in \mathcal{M}$:

$$f'_{(\mathbf{l})} := \text{Tr}_{\mathcal{M}} \left(({}^{\mathbf{l}}f)_{(1)} \circ ({}^{\mathbf{l}}f)_{(2)} \right) \in \mathbb{K}. \quad (3.70)$$

Clearly, the following relation holds, due to the endomorphism space of \mathbf{l} being one-dimensional:

$$\frac{f'_{(\mathbf{l})}}{d_{\mathbf{l}}} \text{id}_{\mathbf{l}} = ({}^{\mathbf{l}}f)_{(1)} \circ ({}^{\mathbf{l}}f)_{(2)}. \quad (3.71)$$

On the other hand, we can compute the trace of f' from the scalars $f'_{(\mathbf{l})}$ as follows, using first the explicit form for sil^{-1} from (2.182).

$$\text{Tr}_{\mathcal{M}}(f') = \sum_{\mathbf{l}} \text{Tr}_{\mathcal{M}} \left(({}^{\mathbf{l}}f)_{(2)} \circ ({}^{\mathbf{l}}f)_{(1)} \right) = \sum_{\mathbf{l}} \text{Tr}_{\mathcal{M}} \left(({}^{\mathbf{l}}f)_{(1)} \circ ({}^{\mathbf{l}}f)_{(2)} \right) \stackrel{(3.70)}{=} \sum_{\mathbf{l}} f'_{(\mathbf{l})}. \quad (3.72)$$

Keeping these results in mind, we make another auxiliary calculation. We will show that the following equality holds.

$$\sum_{\mathbf{a}} d_{\mathbf{a}} \star_{\langle \mathbf{a}^* \mathbf{l}, k \rangle} \circ \star_{\langle k, \mathbf{a}^* \mathbf{l} \rangle} = \frac{\mathcal{D}_{\mathcal{A}}}{\mathcal{D}_{\mathcal{M}}} d_{\mathbf{l}} \text{id}_k. \quad (3.73)$$

This is seen as follows. First, note that we may assume k to be simple. By Schur's lemma, it suffices to take the trace on both sides of (3.73), and prove that equation. We then calculate:

$$\begin{aligned} & \sum_{\mathbf{a}} d_{\mathbf{a}} \text{Tr}_{\mathcal{M}} \left(\star_{\langle \mathbf{a}^* \mathbf{l}, k \rangle} \circ \star_{\langle k, \mathbf{a}^* \mathbf{l} \rangle} \right) \\ & \stackrel{(2.18)}{=} \sum_{\mathbf{a}} d_{\mathbf{a}} \dim \langle \mathbf{k}, \mathbf{a}^* \mathbf{l} \rangle \\ & \stackrel{[\text{Sch13b, Prop. 5.6(i)}]}{=} d_{\mathcal{A}[\mathbf{k}, \mathbf{l}]} \\ & \stackrel{\text{Lemma 2.9}}{=} \frac{\mathcal{D}_{\mathcal{A}}}{\mathcal{D}_{\mathcal{M}}} d_{\mathbf{l}} d_k. \end{aligned} \quad (3.74)$$

Returning to the main calculation, we simplify the morphism (3.69) to:

$$\begin{aligned} \theta & \stackrel{(3.71)}{=} \int^k \sum_{\mathbf{a}, \mathbf{l}} \frac{1}{\mathcal{D}_{\mathcal{A}}} \frac{d_{\mathbf{a}} d_k}{d_{\mathbf{l}}} f'_{(\mathbf{l})} \star_{\langle \mathbf{a}^* \mathbf{l}, k \rangle} \circ \star_{\langle k, \mathbf{a}^* \mathbf{l} \rangle} \\ & \stackrel{(3.73)}{=} \int^k \sum_{\mathbf{l}} \frac{1}{\mathcal{D}_{\mathcal{M}}} d_k f'_{(\mathbf{l})} \text{id}_k \\ & \stackrel{(3.72)}{=} \frac{\text{Tr}_{\mathcal{M}}(f')}{\mathcal{D}_{\mathcal{M}}} \int^k d_k \text{id}_k. \end{aligned} \quad (3.75)$$

Since by (2.185) the image of $\Theta_{\mathcal{M}} : I_{\mathcal{M}} \rightarrow I^{\mathcal{M}}$ under the isomorphism (3.67) is $\int^k d_k \text{id}_k$, and using that the core label $\varphi = \Theta_{\mathcal{M}}^*$ maps $\Theta_{\mathcal{M}}$ to $\mathcal{D}_{\mathcal{M}}$, as was observed in (3.60), we obtain

$$|O| = \varphi(\pi(f \circ_m \tau)) = \text{Tr}_{\mathcal{M}}(f'). \quad (3.76)$$

The result (3.76) also holds true in the case where \mathcal{B} is not necessarily vect . \square

Remark 3.29. The normalization of the core label $\Theta_{\mathcal{M}}^*$ of a loop graph is chosen so that the evaluation of loop graphs can be expressed as a trace. Recall from Remark 2.34 that we expect categorical dimensions to appear especially when working with silent and cosilent objects.

Example 3.30. As an explicit example, we consider the fusion categories $\mathcal{A} = \text{vect}_G$ of vector spaces graded by a finite group G , and $\mathcal{B} = \text{vect}$. Recall that vect_G has one simple object \underline{g} for every group element $g \in G$. As explained in [EGNO15, Ex. 7.4.10], the indecomposable semisimple module categories over vect_G are classified by conjugacy classes of pairs (H, Ψ) , where $H \subset G$ is a subgroup and $\Psi \in H^2(H, \mathbb{K}^\times)$ is a cohomology class. The module category corresponding to such a pair is the linear category $\text{vect}_{H \setminus G}$, equipped with a left vect_G -action. The pivotal structures on vect_G are in bijection with characters $\kappa \in \text{Grp}\langle G, \mathbb{K}^\times \rangle$, and a module trace on $\text{vect}_{H \setminus G}$ exists iff $\kappa|_H = 1$ [Sch13b, Ex. 3.13]. Moreover, such a module trace is unique up to rescaling, and can be normalized by setting $d_{\underline{e}} = 1$. Using Theorem 3.28, we can evaluate a loop graph as in (3.61) with labels $\mathcal{A} = \text{vect}_G$, $\mathcal{B} = \text{vect}$, and $\mathcal{M} = \text{vect}_{H \setminus G}$, with a suitable choice of pivotal structure κ and any endomorphism f in $\text{vect}_{H \setminus G}$.

To get even more specific, let us work over $\mathbb{K} = \mathbb{C}$, choose $G = \mathbb{Z}_4$ and $H = 2\mathbb{Z}_2$, such that $\mathcal{M} = \text{vect}_{\mathbb{Z}_4/2\mathbb{Z}_2} = \text{vect}_{\mathbb{Z}_2}$ as a linear category, and fix the trivial cocycle $\Psi = 1$ for the module category structure. There are four characters of \mathbb{Z}_4 , which map $1 \in \mathbb{Z}_4$ to the four roots of unity, and hence define four pivotal structures on $\text{vect}_{\mathbb{Z}_4}$. Out of these four characters, only two survive the condition $\kappa|_H = 1$; these are defined by $\kappa_+ = 1$ and $\kappa_-(1) = -1$. Each of these two pivotal structures on $\text{vect}_{\mathbb{Z}_4}$ induces a normalized module trace on $\text{vect}_{\mathbb{Z}_2}$: the usual trace, where $d_{\underline{0}} = 1$ and $d_{\underline{1}} = 1$, and the super trace, for which we have $d_{\underline{0}} = 1$ and $d_{\underline{1}} = -1$.

Let now V_0, V_1 be finite-dimensional vector spaces, and pick endomorphisms f_0 and f_1 , respectively. The loop graph

$$O = \bigoplus_{V_0 \oplus V_1 \in \text{vect}_{\mathbb{Z}_2}} \text{vect}_{\mathbb{Z}_4} \text{ with endomorphism } f_0 \oplus f_1 \quad (3.77)$$

is evaluated, depending on the choice of character κ_+ or κ_- , to $|O| = \text{Tr}(f_0) + \text{Tr}(f_1)$, or to $|O| = \text{Tr}(f_0) - \text{Tr}(f_1)$, using the ordinary trace for endomorphisms of vector spaces.

4 MOVES OF INVARIANCE

Whereas Section 3 was concerned with defining an evaluation procedure for extruded graphs, we will now justify that our construction can actually be seen as a *graphical calculus*. This term

here means that the evaluation behaves nicely under certain transformations of topological and algebraic data, which we call *moves*. Moreover, we will see that our construction contains as a special case the usual graphical calculus for spherical fusion categories. In addition, the moves presented in this section form a toolset that makes the abstractly defined evaluation procedure easily computable.

4.1 OVERVIEW OF MOVES

By a move, we mean:

- A pair of extruded graphs $(\Sigma_T, \Sigma_{T'})$. We view Σ_T as the extruded graph *before* the move is performed, and $\Sigma_{T'}$ as the extruded graph *after* the move, even though all moves can be reversed.
- Within Σ_T and $\Sigma_{T'}$, there are regions $\Sigma \subset \Sigma_T$ and $\Sigma' \subset \Sigma_{T'}$ such that $\Sigma_T \setminus \Sigma = \Sigma_{T'} \setminus \Sigma'$. The boundaries of these regions cross defect lines of Σ_T and $\Sigma_{T'}$ only perpendicularly.
- We call a move an *invariance* or a *move of invariance* iff $|\Sigma_T| = |\Sigma_{T'}|$.

When discussing moves throughout this section, we only ever make the regions Σ and Σ' explicit, and do not put assumptions on the total defect surfaces Σ_T and $\Sigma_{T'}$. The so-obtained moves are highly local.

We now aim to define the set of moves that we consider. Foundational to any move is a local change the topology of an extruded graph. In the first step, we show that the topological changes prompt canonical choices of post-move labels of all four levels of algebraic data, with the single exception being the core label. The transformation of the core label is postponed. On the lowest level of labelings (node labels), the relabeling amounts to a linear map between node spaces

$$\psi : N_x(m) \rightarrow N_{x'}(m').$$

Here, m and x stand for a collection of pre-move defect and ray labels, and m' and x' stand for their counterparts after the move.

We distinguish between *elementary moves* and *composite moves*. They differ by the way in which we prove that they are invariances: For the former, we must show the invariance property using the definition of the evaluation procedure $|-|$, while for the latter, the invariance property is obvious once we show that they are combinations of elementary moves.

We will consider the following elementary moves:

OR – ORIENTATION REVERSAL One of the most basic changes one can make to an extruded graph is the flipping of a defect line’s orientation.

$$(4.1)$$

In the **OR**-move, a defect line labeled by an object m in an \mathcal{A} - \mathcal{B} -bimodule category \mathcal{M} is replaced by a defect line with opposite orientation. This new defect line needs a \mathcal{B} - \mathcal{A} -bimodule category for a label. For this we choose $\overline{\mathcal{M}}$, and as the post-move object label we take $\overline{m} \in \overline{\mathcal{M}}$. Note that $\overline{\mathcal{M}}$ is unambiguously defined only because \mathcal{A} and \mathcal{B} are equipped with pivotal structures.

We denote the node labels of the nodes adjacent to the \mathcal{M} -labeled defect line by f and g , and the adjacent ray labels by x and y . In the definition of ray categories, a distinction is made between incoming and outgoing defect lines at a certain node. This determines whether the bimodule category that labels the defect line is used, or its opposite. Due to this, the ray categories (and the node categories) before and after the move are identical – up to the identification $\overline{\mathcal{M}} \cong \mathcal{M}$, which becomes an equality for strict pivotal structures on \mathcal{A} and \mathcal{B} . Hence, there is a canonical identification of the node spaces before and after the move, defining the map

$$\psi : N_{x,y}(m) \rightarrow N'_{x,y}(\overline{m}).$$

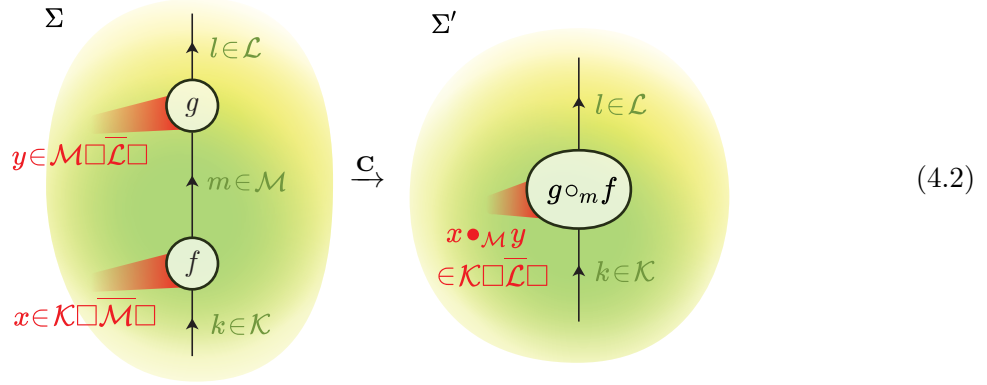
Remark 4.1. When comparing the **OR**-move to the corresponding move in the ordinary graphical calculus for tensor categories, one notices that a pivotal structure is required to flip the direction of a strand. This is because the dual of an object provides the correct label for the reversed strand. While we do work with pivotal bimodule categories (due to the trace), the pivotal structure is not used at this point.

The requirement of a pivotal structure in the oriented graphical calculus of tensor categories comes from the fact that all strands are labeled by the objects of a single tensor category \mathcal{C} . Strands labeled by objects of the opposite $\overline{\mathcal{C}}$, which would result from the **OR**-move as presented here, are not allowed. In order to obtain the analogous move of string diagrams for tensor categories, our **OR**-move needs to be combined with an equivalence $\overline{\mathcal{C}} \cong \mathcal{C}$; and a distinguished equivalence of this type is provided precisely by a pivotal structure on \mathcal{C} . This is described in more detail in Lemma 5.5.

The proof that the move **OR** is a move of invariance is the content of Section 4.2.2.

C – CONTRACTION The contraction move allows us to transform two nodes, connected by a defect line, into a single node, thereby dissolving the defect line. It specializes to the composition

of morphisms.



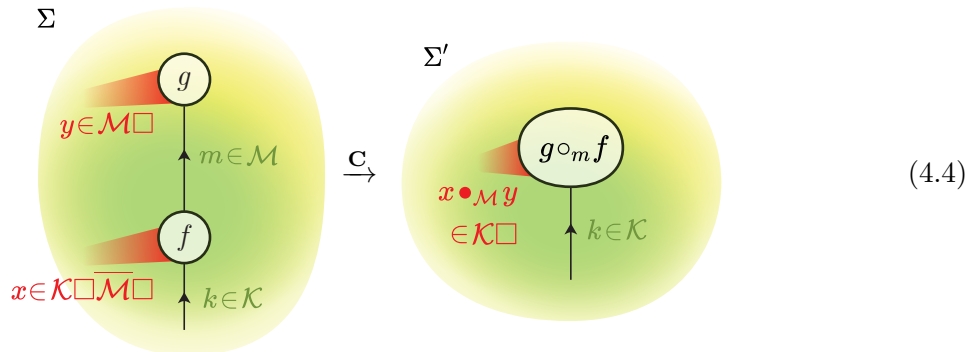
The step **C** takes place inside a disk-shaped region Σ with two nodes on a defect surface. We refer to the nodes by their labels f and g . There are three defect lines inside Σ : The first one enters the region and ends at f , the second connects f to g (in this direction), and the third starts at g and leaves the region. The defect lines split Σ into two domains, labeled by spherical fusion categories \mathcal{A} and \mathcal{B} , respectively. Accordingly, the three defect lines are labeled by objects k , m and l in spherical \mathcal{A} - \mathcal{B} -bimodule categories \mathcal{K} , \mathcal{M} and \mathcal{L} . These categories determine the node categories at the nodes f and g , namely $\mathbb{T}^{\mathbb{R}}(f) = \mathcal{K} \boxtimes \overline{\mathcal{M}}$ and $\mathbb{T}^{\mathbb{R}}(g) = \mathcal{M} \boxtimes \overline{\mathcal{L}}$. We choose objects $x \in \mathbb{T}^{\mathbb{R}}(f)$ and $y \in \mathbb{T}^{\mathbb{R}}(g)$ to label the rays. This finally pins down the relevant hom-spaces for f and g : $f \in \langle k \boxtimes \bar{m}, U(x) \rangle$ and $g \in \langle m \boxtimes \bar{l}, U(y) \rangle$.

After the move, Σ is replaced by the similar region Σ' which only has one node labeled by $g \circ_m f$, with two attached defect lines, one coming into the region labeled by $k \in \mathcal{K}$, and one leaving the region, labeled by $l \in \mathcal{L}$. The single ray is labeled by the object $x \bullet_{\mathcal{M}} y$ in the ray category $\mathbb{T}^{\mathbb{R}'} = \mathcal{K} \boxtimes \overline{\mathcal{L}}$. This justifies the label for the node, since $g \circ_m f \in \langle k \boxtimes \bar{l}, x \bullet_{\mathcal{M}} y \rangle$.

The linear map between node spaces is thus given by

$$\psi : g \otimes f \mapsto g \circ_m f. \tag{4.3}$$

There is also a "one-sided" version of the **C**-move, where the \mathcal{L} -labeled defect line (or alternatively, the \mathcal{K} -labeled defect line) is not present:



As was mentioned in Remark 2.40, the contraction operations for objects and morphisms are well-defined even in this case, so that we get ray and node labels. Note however that a move without \mathcal{K} and \mathcal{L} does not exist, as this would result in a node without any defect lines, which is not allowed.

The proof that the move **C** is a move of invariance is the content of Section 4.2.3.

Remark 4.2. A special case we are interested in is that where $\mathcal{M} = \mathcal{L} = \mathcal{K}$ and $x = y = \Phi^{\mathcal{M}}$. Recall from (2.193) that the cosilent object behaves as a unit for the contraction operation: $\Phi^{\mathcal{M}} \bullet_{\mathcal{M}} \Phi^{\mathcal{M}} \cong \Phi^{\mathcal{M}}$. The node space

$$N_{\Phi^{\mathcal{M}}, \Phi^{\mathcal{M}}}(k, m, l\tau) = \int^{ij} \langle m \boxtimes \bar{l}, i \boxtimes \bar{i} \rangle \otimes \langle k \boxtimes \bar{m}, j \boxtimes \bar{j} \rangle$$

is now canonically isomorphic, via the isomorphism sil from Corollary 2.36, to

$$N_{\Phi^{\mathcal{M}}, \Phi^{\mathcal{M}}}(k, m, l\tau) \cong \langle m, l \rangle \otimes \langle k, m \rangle.$$

Similarly, for the post-move node space, we have

$$N_{\Phi^{\mathcal{M}}}(k, l) = \int^n \langle k \boxtimes \bar{l}, n \boxtimes \bar{n} \rangle \cong \langle k, l \rangle.$$

In Remark 2.38, we have seen that under these isomorphisms, the map $g \otimes f \mapsto g \circ_m f$ becomes $\tilde{g} \otimes \tilde{f} \mapsto \tilde{g} \circ \tilde{f}$. Hence, the **C**-move specializes to the composition of morphisms when the rays are transparent (that is, labeled by $\Phi^{\mathcal{M}}$).

EF – EDGE FUSION The edge fusion move allows us to merge parallel defect lines which share start and end nodes. In the ordinary graphical calculus for spherical fusion categories, this move conveys the statement that drawing parallel lines amounts to taking monoidal products.

The region Σ is disk-shaped and contains two defect lines, running in parallel between the only two nodes that lie partially in Σ . In contrast, the post-move region Σ' features just a single defect line connecting the node segments. The three domains of Σ are labeled by spherical fusion categories \mathcal{A} , \mathcal{B} and \mathcal{C} , and the defect lines are labeled by objects in bimodule categories $m \in {}_{\mathcal{A}}\mathcal{M}_{\mathcal{B}}$ and $n \in {}_{\mathcal{B}}\mathcal{N}_{\mathcal{C}}$, respectively. This means the node f attached to the start of the defect lines is assigned a ray category of the form $\mathbb{T}^{\text{R}}(f) = \dots \square \bar{\mathcal{N}} \square \bar{\mathcal{M}} \square \dots$, while the other node g is

assigned $\mathbb{T}^{\mathbb{R}}(g) = \dots \square \mathcal{M} \square \mathcal{N} \square \dots$. We pick corresponding labels for the rays $x \in \mathbb{T}^{\mathbb{R}}(f)$ and $y \in \mathbb{T}^{\mathbb{R}}(g)$.

The single defect line in the region Σ' is labeled by the \mathcal{A} - \mathcal{C} -bimodule category $\mathcal{M} \square \mathcal{N}$. As the object label for the single defect line, we choose the relative Deligne product $m \boxtimes n$. The ray categories associated with the nodes are canonically equivalent to those of the pre-move surface Σ , allowing us to use the same objects x and y for the rays of Σ' . Note, however, that the forgetful functor $U' : \mathbb{T}^{\mathbb{R}'} \rightarrow \mathbb{T}^{\mathbb{N}'}$ is not identified with $U : \mathbb{T}^{\mathbb{R}} \rightarrow \mathbb{T}^{\mathbb{N}}$ under these equivalences: U' does not forget the \mathcal{B} -balancing, while U does.

Hence, there are adjunctions

$$\langle \bar{n} \boxtimes \bar{m} \boxtimes \dots, U(x) \rangle \cong \langle \overline{m \boxtimes n} \boxtimes \dots, U'(x) \rangle$$

and

$$\langle m \boxtimes n \boxtimes \dots, U(y) \rangle \cong \langle m \boxtimes n \boxtimes \dots, U'(y) \rangle.$$

We saw in Section 2 below (2.110) that the spherical structure on \mathcal{B} defines an isomorphism $\Theta_{\mathcal{B}} : m \boxtimes n \cong m \square n$. The map $\psi : N_{x,y}(m, n) \rightarrow N'_{x,y}(m \square n)$ between node spaces is given by the composition

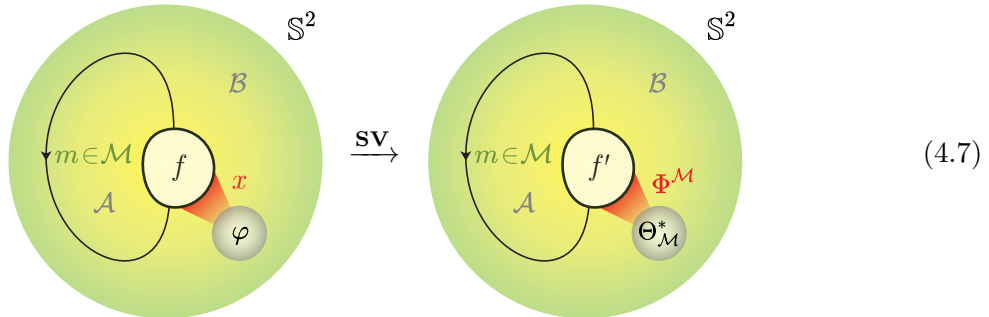
$$\begin{aligned} N_{x,y}(m, n) &= \langle \bar{n} \boxtimes \bar{m} \boxtimes \dots, U(x) \rangle \otimes \langle m \boxtimes n \boxtimes \dots, U(y) \rangle \\ &\cong \langle \overline{m \boxtimes n} \boxtimes \dots, U'(x) \rangle \otimes \langle m \boxtimes n \boxtimes \dots, U'(y) \rangle \\ &\xrightarrow{\frac{1}{\mathcal{D}_{\mathcal{B}}} \Theta_{\mathcal{B}}} \langle \overline{m \square n} \boxtimes \dots, U'(x) \rangle \otimes \langle m \square n \boxtimes \dots, U'(y) \rangle = N'_{x,y}(m \square n). \end{aligned} \quad (4.6)$$

With this, we know the complete set of labels after the move.

The proof that the move **EF** is a move of invariance is the content of Section 4.2.4.

SV – SUBSIDE VERTEX The **SV**-move allows us to transform a lasso graph into a loop graph. These types of extruded graphs on the sphere were discussed in Sections 3.4 and 3.5, but until now, we only fully understand the evaluation of loop graphs (see Theorem 3.28). Combining this result with the **SV**-move, we will also be able to evaluate arbitrary lasso graphs.

To a given lasso graph with labels as in (4.7), we need to assign a loop graph with a node label f' depending on f and φ .



Recall from Section 3.4 that the block space of a lasso graph with labels as in (4.7) is given by the hom-space $\mathbb{T} = \langle \Phi_{\mathcal{M}}, x \rangle$ in the ray category $\mathbb{T}^{\mathbb{R}}$. Consequently, the core label φ is a vector in the dual space

$$\varphi \in \langle \Phi_{\mathcal{M}}, x \rangle^*. \quad (4.8)$$

As discussed in Section 2.12, the ray category $\mathbb{T}^{\mathbb{R}} = \mathcal{M} \square \overline{\mathcal{M}} \square$ inherits the structure of a Calabi-Yau category from the spherical bimodule category \mathcal{M} . This means (see Section 2.1) there is an isomorphism

$$\langle x, \Phi_{\mathcal{M}} \rangle \cong \langle \Phi_{\mathcal{M}}, x \rangle^*, \quad (4.9)$$

given by $\rho \mapsto \text{Tr}_{\mathbb{T}^{\mathbb{R}}}(\rho \circ -)$. We use this to translate the core label into a morphism $\tilde{\varphi} : x \rightarrow \Phi_{\mathcal{M}}$ such that

$$\varphi(\rho) = \text{Tr}_{\mathbb{T}^{\mathbb{R}}}(\tilde{\varphi} \circ \rho). \quad (4.10)$$

Recall that the node label f is a morphism $f : m \boxtimes \bar{m} \rightarrow U(x)$. We define the node label $f' : m \boxtimes \bar{m} \rightarrow I^{\mathcal{M}}$ for the loop graph after the **SV**-move to be the composition

$$f' := \frac{1}{\mathcal{D}_{\mathcal{A}} \mathcal{D}_{\mathcal{B}}} \Theta_{\mathcal{M}} \circ \tilde{\varphi} \circ f. \quad (4.11)$$

This completes the description of the **SV**-move.

The proof that the move **SV** is a move of invariance is the content of Section 4.2.5.

Fun – FUNCTORIALITY Given a bimodule equivalence $F : {}_{\mathcal{A}}\mathcal{M}_{\mathcal{B}} \xrightarrow{\cong} {}_{\mathcal{A}}\mathcal{N}_{\mathcal{B}}$, we can replace a defect line labeled by $m \in {}_{\mathcal{A}}\mathcal{M}_{\mathcal{B}}$ with a defect line labeled by $F(m) \in {}_{\mathcal{A}}\mathcal{N}_{\mathcal{B}}$. F also induces new ray- and node labels. Let us write

$$U(x) = x_{(\mathcal{R})} \boxtimes x_{(\mathcal{M})} \quad \text{and} \quad U(y) = y_{(\overline{\mathcal{M}})} \boxtimes y_{(\mathcal{R})} \quad (4.12)$$

for the ray labels x and y . That F is a bimodule functor ensures that the objects

$$x_{(\mathcal{R})} \boxtimes F(x_{(\mathcal{M})}) \quad \text{and} \quad F(y_{(\overline{\mathcal{M}})}) \boxtimes y_{(\mathcal{R})} \quad (4.13)$$

have balancings, together with which they form appropriate post-move ray labels that we denote, in a slight abuse of notation, by $F(x)$ and $F(y)$. The total node spaces before and after the move are of the form

$$\begin{aligned} & \cdots \otimes_{\mathcal{M}} \langle m, x_{(\mathcal{M})} \rangle \otimes_{\overline{\mathcal{M}}} \langle \bar{m}, y_{(\overline{\mathcal{M}})} \rangle \otimes \cdots \quad \text{and} \\ & \cdots \otimes_{\mathcal{N}} \langle F(m), F(x_{(\mathcal{M})}) \rangle \otimes_{\overline{\mathcal{N}}} \langle \overline{F(m)}, F(y_{(\overline{\mathcal{M}})}) \rangle \otimes \cdots \end{aligned} \quad (4.14)$$

Clearly, F defines a linear map between these two spaces, which provides new node labels $F(f), F(g)$.

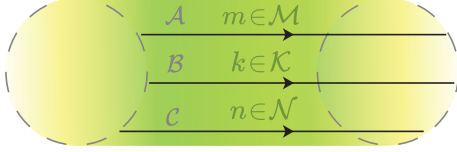
$$\begin{array}{ccc} \Sigma & & \Sigma' \\ \begin{array}{c} \text{A} \\ m \in \mathcal{M} \\ \text{B} \\ f \quad \quad \quad g \\ x \quad \quad \quad y \end{array} & \xrightarrow{\text{Fun}} & \begin{array}{c} \text{A} \\ F(m) \in \mathcal{N} \\ \text{B} \\ F(f) \quad \quad \quad F(g) \\ F(x) \quad \quad \quad F(y) \end{array} \end{array} \quad (4.15)$$

The proof that the move **Fun** is a move of invariance is the content of Section 4.2.6.

G – *HYPOTHESIZED: GLUE BOUNDARIES / FACTORIZATION* This move is only hypothesized, and we will not prove that it is an invariance of the evaluation. Nevertheless, it is conceptually relevant in pointing out how the generality of extruded graphs, in particular the possibility to consider surfaces of higher genus, could be used in practical ways, see Remark 5.15.

The **G**-move is a move between an extruded graph as on the left-hand side of (4.16) and a linear combination of extruded graphs (discussed in Remark 3.11) as on the right-hand side of the picture (4.16).

Σ



$$\xrightarrow{\mathbf{G}} \sum_{\mathbf{x}} \Sigma' \quad (4.16)$$

The coat of the region Σ is topologically an annulus: it is the mantle of a cylinder, with several (but at least one) defect lines going from one cap to the other. Applying the **G**-move to an extruded graph at a region Σ amounts to cutting the cylinder into two segments, each containing a node. As mentioned, the result is a linear combination of extruded graphs. Accordingly, we write the resulting region Σ' as a linear combination

$$\Sigma' = \sum_{\mathbf{x} \in \mathcal{M} \square \mathcal{N} \square \mathcal{K} \square} \Sigma_{\mathbf{x}}'. \quad (4.17)$$

Here, \mathbf{x} runs over a set of representatives of simple objects in the relative Deligne product of the cyclically ordered bimodule categories appearing in Σ . Topologically, all of the $\Sigma_{\mathbf{x}}'$ are equal; they only differ in their algebraic labeling. As can be seen on the right-hand side in (4.16), the **G**-move, in the process of cutting the cylinder Σ , adds two new nodes, whose node spaces are in duality. These nodes are present in each of the $\Sigma_{\mathbf{x}}'$, therein denoted $L_{\mathbf{x}}$ and $\bar{L}_{\mathbf{x}}$, and are assigned ray categories $\mathbb{T}^{\mathbf{R}}(L_{\mathbf{x}}) = \mathcal{M} \square \mathcal{N} \square \mathcal{K} \square$ and $\mathbb{T}^{\mathbf{R}}(\bar{L}_{\mathbf{x}}) = \bar{\mathcal{K}} \square \bar{\mathcal{N}} \square \bar{\mathcal{M}} \square$, respectively. The rays of the region $\Sigma_{\mathbf{x}}'$ are labeled by \mathbf{x} and $\bar{\mathbf{x}}$, which are objects in these ray categories.

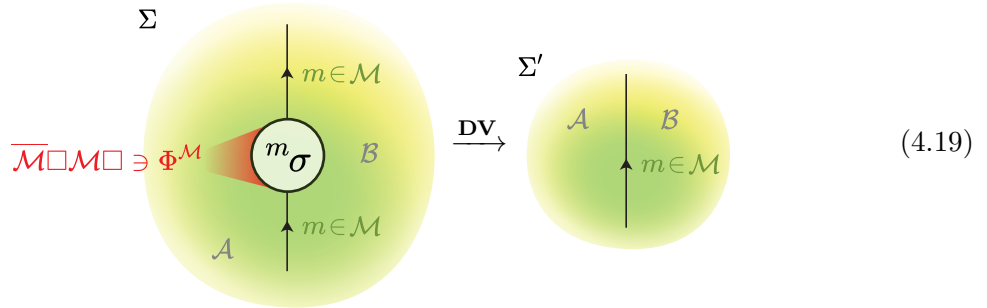
As was justified in Remark 3.11, we equip the nodes $L_{\mathbf{x}}$ and $\bar{L}_{\mathbf{x}}$ not with individual node labels, but with a vector in the tensor product of node spaces $N_{\mathbf{x}}(L_{\mathbf{x}})(\bar{m} \otimes \bar{n} \otimes \bar{k})$ and $N_{\bar{\mathbf{x}}}(\bar{L}_{\mathbf{x}})(m \otimes n \otimes k)$:

$$\star \langle m \otimes n \otimes k, U(\mathbf{x}) \rangle \otimes \star \langle U(\mathbf{x}), m \otimes n \otimes k \rangle \in N_{\mathbf{x}}(L_{\mathbf{x}})(\bar{m} \otimes \bar{n} \otimes \bar{k}) \otimes N_{\bar{\mathbf{x}}}(\bar{L}_{\mathbf{x}})(m \otimes n \otimes k). \quad (4.18)$$

Note that this is not a pure vector, but an instance of the kind of Sweedler notation introduced in Section 2.4. We will not provide a proof that this move is an invariance.

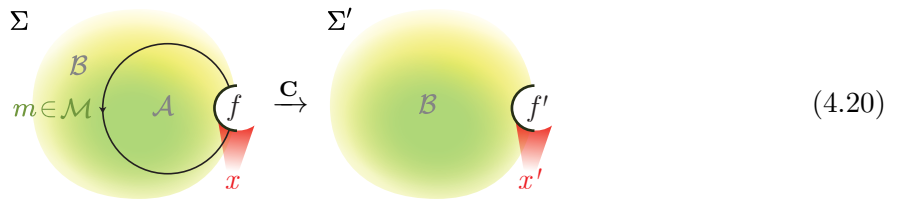
In addition to these elementary moves, we will show the following composite moves to be invariances:

DV – DISSOLVE VERTEX A node with precisely two adjacent defect lines, one ingoing and one outgoing, both labeled by the same object $m \in \mathcal{M}$, which moreover has an attached ray labeled by $\Phi^{\mathcal{M}}$, may be labeled with the vector $\text{sil}(\text{id}_m) = \sigma^m$. (This equality was shown in (2.183).) If this is indeed the node label, the node can be removed, such that only a continuous, m -labeled defect line remains.



The proof that the move **DV** is a move of invariance is the content of Section 4.3.1.

L – LOOP MOVE A loop attached to a node can be removed. Note that this is only possible when at least one other defect line is attached to the node, as otherwise, the move would result in a node without defect lines, which is not allowed.



The ray label x' is given by the contraction $x' = \Phi^{\mathcal{M}} \bullet_{\overline{\mathcal{M}} \square \mathcal{M}} x$. Beware that in general, x and x' live in non-equivalent ray categories – the cosilent object $\Phi^{\mathcal{M}}$ is a unit with respect to the contraction $\bullet_{\mathcal{M}}$, not $\bullet_{\overline{\mathcal{M}} \square \mathcal{M}}$. Concretely, if $U(x) = x_{(\overline{\mathcal{M}} \square \mathcal{M})} \boxtimes x_{(\mathcal{R})}$, where $x_{(\mathcal{R})}$ is a rest term, we have

$$U(x') = \overline{\mathcal{M}} \square \mathcal{M} \langle x_{(\overline{\mathcal{M}} \square \mathcal{M})}, \Phi^{\mathcal{M}} \rangle \otimes x_{(\mathcal{R})} \cong \mathcal{A} \langle x_{(\overline{\mathcal{M}})}, x_{(\mathcal{M})} \rangle \otimes x_{(\mathcal{R})}. \quad (4.21)$$

The last isomorphism involves the subspace ${}^{\mathcal{A}}\langle x_{(\overline{\mathcal{M}})}, x_{(\mathcal{M})} \rangle$ of the hom-space introduced in Lemma 2.31. The isomorphism

$$\text{sil}^{-1} : \overline{\mathcal{M}} \boxtimes \mathcal{M} \langle x_{(\overline{\mathcal{M}})} \boxtimes x_{(\mathcal{M})}, \mathbb{1}_{\mathcal{M}} \rangle \cong \mathcal{M} \langle x_{(\overline{\mathcal{M}})}, x_{(\mathcal{M})} \rangle \quad (4.22)$$

from (2.181) restricts to the subspaces involved in (4.21). Thus, we can specify the post-move node label f' as a morphism $f' : n \rightarrow {}^{\mathcal{A}}\langle x_{(\overline{\mathcal{M}})}, x_{(\mathcal{M})} \rangle \otimes x_{(\mathcal{R})}$, where n stands for the labels of the other defect lines attached to the node. Let us write $f = f_{(\overline{\mathcal{M}})} \otimes f_{(\mathcal{M})} \otimes f_{(\mathcal{R})}$, where

$$f_{(\overline{\mathcal{M}})} : x_{(\overline{\mathcal{M}})} \rightarrow m, \quad f_{(\mathcal{M})} : m \rightarrow x_{(\mathcal{M})}, \quad \text{and} \quad f_{(\mathcal{R})} : n \rightarrow x_{(\mathcal{R})}. \quad (4.23)$$

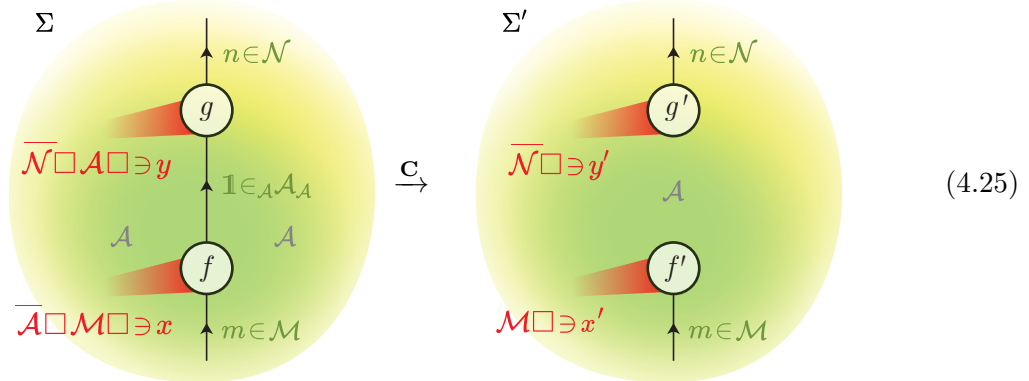
Then f' is given as

$$f' := r(f_{(\mathcal{M})} \circ f_{(\overline{\mathcal{M}})}) \otimes f_{(\mathcal{R})}, \quad (4.24)$$

where $r : \mathcal{M} \langle x_{(\overline{\mathcal{M}})}, x_{(\mathcal{M})} \rangle \rightarrow {}^{\mathcal{A}}\langle x_{(\overline{\mathcal{M}})}, x_{(\mathcal{M})} \rangle$ is the retraction from (2.155).

The proof that the move **L** is a move of invariance is the content of Section 4.3.2.

DE – DISSOLVE EDGE An edge which is *transparent* – that is, labeled by the regular bimodule category \mathcal{A} , and moreover labeled by the monoidal unit $\mathbb{1} \in \mathcal{A}$, can be removed (or inserted) between two nodes as shown in (4.25).



More precisely, let $x' \in Z_{\mathcal{A}}(\mathcal{M})$ and $y' \in Z_{\mathcal{A}}(\overline{\mathcal{N}})$ be objects in the centers of the \mathcal{A} - \mathcal{A} -bimodule categories \mathcal{M} and $\overline{\mathcal{N}}$. As such, x' and y' are appropriate ray labels for the rays of the post-move region Σ' . Before the move, the rays of the region Σ must be labeled with objects in the ray categories $\overline{\mathcal{A}} \square \mathcal{M} \square = Z_{\mathcal{A}}(\overline{\mathcal{A}} \square \mathcal{M})$ and $\overline{\mathcal{N}} \square \mathcal{A} \square = Z_{\mathcal{A}}(\overline{\mathcal{N}} \square \mathcal{A})$. We denote the (partial) forgetful functors $Z_{\mathcal{A}}(\overline{\mathcal{A}} \square \mathcal{M}) \rightarrow \overline{\mathcal{A}} \square \mathcal{M}$ and $Z_{\mathcal{A}}(\overline{\mathcal{N}} \square \mathcal{A}) \rightarrow \overline{\mathcal{N}} \square \mathcal{A}$ by \tilde{U} . The equivalence of bimodule categories $\overline{\mathcal{N}} \cong \overline{\mathcal{N}} \square \mathcal{A}$ from (2.134) extends to an equivalence of linear categories $Z_{\mathcal{A}}(\overline{\mathcal{N}}) \cong Z_{\mathcal{A}}(\overline{\mathcal{N}} \square \mathcal{A})$ because $Z_{\mathcal{A}}(-)$ is a 2-functor from bimodule categories to linear categories [FSS17, Prop. 3.7]. The ray label y in the region Σ is the image of y' under this equivalence, and x is defined similarly. The precise form (2.136) of the equivalence shows that

$$\tilde{U}(x) = \overline{\mathbb{1}} \boxtimes U(x') \quad \text{and} \quad \tilde{U}(y) = U(y') \boxtimes \mathbb{1}, \quad (4.26)$$

and applying the complete forgetful functors, we find using (2.108) that

$$U(x) = \int_a \bar{a} \boxtimes a U(x') \quad \text{and} \quad U(y) = \int_a U(y') a^* \boxtimes a. \quad (4.27)$$

On the fourth level of labels in the region Σ' , the node labels

$$f' : m \rightarrow U(x') \quad \text{and} \quad g' : \bar{n} \rightarrow U(y') \quad (4.28)$$

are used to define the node labels $f : \bar{\mathbb{1}} \boxtimes m \rightarrow \int_a \bar{a} \boxtimes a U(x')$, $g : \bar{n} \boxtimes \mathbb{1} \rightarrow \int_a U(y') a^* \boxtimes a$ of Σ . It suffices to give the simple components ${}^a f$, ${}^a g$ of f and g . Due to Schur's lemma, all simple components except for ${}^{\mathbb{1}} f$ and ${}^{\mathbb{1}} g$ are zero. Thus setting

$${}^{\mathbb{1}} f := \text{id}_{\bar{\mathbb{1}}} \boxtimes f' \quad \text{and} \quad {}^{\mathbb{1}} g := g' \boxtimes \text{id}_{\mathbb{1}} \quad (4.29)$$

defines f and g . Moreover, this shows that the associations $f' \mapsto f$ and $g' \mapsto g$ define isomorphisms between the node spaces of Σ' and Σ .

The proof that the move **DE** is a move of invariance is the content of Section 4.3.3.

IH – INTERNAL HOM-MOVE Commonly in graphical notations, internal hom objects of a module category ${}_{\mathcal{A}}\mathcal{M}$ are drawn as two parallel lines of opposite orientation, labeled by objects $m, n \in \mathcal{M}$, which together represent the object ${}_{\mathcal{A}}[m, n]$ in \mathcal{A} , as introduced in (2.49). In emphasize that the two lines labeled by m and n combine into a single object, they are, in pictures, held together by "clasps and bubbles" [BS11] or form "zippers" [Sch13b].

Within extruded graphs, parallel lines labeled by objects in module categories may appear, but they do not represent internal hom objects. The **IH**-move shows that nevertheless, there is no risk of misinterpretation, because replacing such a pair of parallel defect lines with a single defect line labeled by an internal hom object is a move of invariance. In particular, clasps-and-bubbles and zippers are not needed in extruded graphs.

Given a traced bimodule category ${}_{\mathcal{A}}\mathcal{M}_{\mathcal{B}}$ with objects $m, n \in \mathcal{M}$, the **IH**-move locally looks as in (4.30). The labels are discussed in the following.

On the left-hand side of (4.30), x and y are ray labels in the appropriate ray categories for the nodes – only part of the nodes are shown, and only parts of the ray labels are relevant for the move: those belonging to the defect lines labeled by \mathcal{M} . We thus write

$$U'(x) = x_{(\mathcal{R})} \boxtimes x_{(\mathcal{M} \square \bar{\mathcal{M}})} \quad \text{and} \quad U'(y) = y_{(\mathcal{M} \square \bar{\mathcal{M}})} \boxtimes y_{(\mathcal{R})}, \quad (4.31)$$

where U' forgets all balancings except for the balancing between \mathcal{M} and $\overline{\mathcal{M}}$. Similarly, the node spaces are given by a tensor product of vector spaces, where each tensorand corresponds to a defect line, so it is possible to give the node labels in factorized form, where

$$f : \overline{m} \boxtimes n \rightarrow U(x_{(\mathcal{M} \square \overline{\mathcal{M}})}) \quad \text{and} \quad g : \overline{n} \boxtimes m \rightarrow U(y_{(\mathcal{M} \square \overline{\mathcal{M}})}) \quad (4.32)$$

belong to the defect lines pictured, and $f_{\mathbb{R}}, g_{\mathbb{R}}$ belong to the other defect lines.

After the move, on the right-hand side of (4.30), the two \mathcal{M} -labeled defect lines have merged into a single defect line labeled by the regular bimodule category ${}_{\mathcal{A}}\mathcal{A}_{\mathcal{A}}$. The object label for the defect line is the internal hom object ${}_{\mathcal{A}}[n, m]$. The internal hom of \mathcal{M} with respect to the left acting category \mathcal{A} extends to a \mathcal{A} - \mathcal{A} -bimodule functor ${}_{\mathcal{A}}[-] : {}_{\mathcal{A}}\mathcal{M} \square_{\mathcal{B}} \overline{\mathcal{M}}_{\mathcal{A}} \rightarrow {}_{\mathcal{A}}\mathcal{A}_{\mathcal{A}}$ [Sch13a, Eq. 6.14]. The bimodule nature of this functor ensures that the objects

$$x_{(\mathbb{R})} \boxtimes {}_{\mathcal{A}}[x_{(\mathcal{M} \square \overline{\mathcal{M}})}] \quad \text{and} \quad {}_{\mathcal{A}}[y_{(\mathcal{M} \square \overline{\mathcal{M}})}] \boxtimes y_{(\mathbb{R})} \quad (4.33)$$

come equipped with balancings and thus define objects in the ray categories. These balanced objects are, by abuse of notation, labeled ${}_{\mathcal{A}}[x]$ and ${}_{\mathcal{A}}[y]$ in (4.30).

By the adjunction (2.111), the morphisms f and g correspond to morphisms $\tilde{f} : n \square \overline{m} \rightarrow x_{(\mathcal{M} \square \overline{\mathcal{M}})}$ and $\tilde{g} : m \square \overline{n} \rightarrow y_{(\mathcal{M} \square \overline{\mathcal{M}})}$. To these morphisms, the functor ${}_{\mathcal{A}}[-]$ can be applied. This is what is meant by the notation ${}_{\mathcal{A}}[\tilde{f}], {}_{\mathcal{A}}[\tilde{g}]$ in (4.30).

Remark 4.3. Recall from Remark 3.20 that the structure of a bimodule trace is not necessary in order to define the evaluation of extruded graphs. It is, however, necessary for the validity of the **IH**-move. To see this, note that the symmetry of the move implies another move, which differs from **IH** in that the orientation of the defect line on the right-hand side of (4.30) is reversed, and the roles of m and n are exchanged. Combining these two moves amounts to the statement that the dual of ${}_{\mathcal{A}}[n, m]$ is ${}_{\mathcal{A}}[m, n]$. Such an isomorphism, subject to coherence conditions, is just a bimodule trace on \mathcal{M} [Sch15, Cor. 5.26].

The proof that the move **IH** is a move of invariance is the content of Section 4.3.4.

With the list of elementary and composite moves complete, we are ready to formulate the next theorem, which states that the moves leave the evaluation invariant.

Theorem 4.4. *The moves **C**, **EF**, **DE**, **DV**, **SV**, **Fun**, and **IH** defined above are moves of invariance for the evaluation $|-|$ of extruded graphs from Definition 3.17.*

The proof of Theorem 4.4 is the content of Sections 4.2 and 4.3. But first, let us note that Theorem 4.4 implies the following uniqueness result:

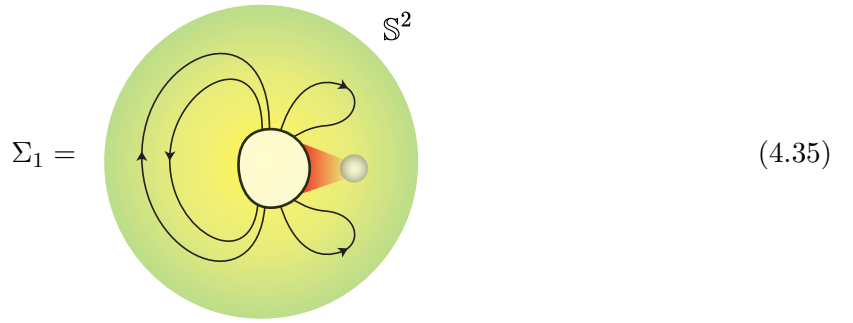
Theorem 4.5. *The evaluation procedure $|-|$ defined in Definition 3.17 is the unique map from the set of extruded graphs on the sphere \mathbb{S}^2 to \mathbb{K} such that loop graphs are evaluated to traces as in Theorem 3.28, and which is invariant under the moves **OR**, **C**, **EF**, and **SV**.*

Proof. We consider any evaluation procedure $||-||$ which evaluates loop graphs as in Theorem 3.28 and for which the moves **OR**, **C**, **EF**, and **SV** are moves of invariance. We then show that $||\Sigma|| = |\Sigma|$ for an extruded graph Σ on \mathbb{S}^2 .

The network of n defect lines and k nodes on the coat of Σ form a connected graph with n edges and k vertices. Any connected graph has a spanning tree, that is, a subgraph without cycles which contains all vertices of the original graph [Hat01, Prop. 1A.1]. We pick such a spanning tree, and in it an edge. Note that this edge is not a loop. We may thus apply the contraction move **C** to the corresponding defect line in Σ , obtaining an extruded graph Σ' with $(n - 1)$ defect lines and $(k - 1)$ nodes. Since **C** is by assumption a move of invariance with respect to the evaluation procedure $||-\|$, we find $||\Sigma|| = ||\Sigma'||$. This step is repeated until we arrive at an extruded graph Σ_1 with only a single node, which still satisfies

$$||\Sigma|| = ||\Sigma_1||. \quad (4.34)$$

As depicted in (4.35) below, the defect lines of Σ_1 , all starting and ending at the unique node, form a bouquet of circles embedded on \mathbb{S}^2 , which remains the underlying surface of Σ_1 .



There is at least one contractible defect line in Σ_1 . To see this, pick a point $p \in \mathbb{S}^2$ away from the defect lines. Each defect line defines two subsets of the sphere: The connected components of the complement of the defect line and the node. The point p must lie in one of these connected subsets; we call the subset which does not contain p the *region associated with the defect line*. We say that a defect line \mathcal{M} *encloses* another defect line \mathcal{N} iff the region associated with \mathcal{N} is a subset of the region associated with \mathcal{M} . It is clear that the set of defect lines with the relation "being enclosed" form a finite partially ordered set. As such, it has a minimal element, which is a contractible defect line.

We pick a contractible defect line, and apply the loop move **L**, erasing the defect line. This step is repeated until only one defect line is left. As we will see below (Section 4.3.2), the **L**-move can be realized as a composition of **C**, **OR**, and **EF**-moves. Thus, the evaluation $||-\|$ is invariant under **L**.

The resulting extruded graph is a lasso graph Q , and still, the evaluation $||-\|$ remains unchanged: $||\Sigma|| = ||Q||$. Finally, using that the **SV**-move is an invariance of the evaluation $||-\|$, we transform the lasso graph into a loop graph O such that $||\Sigma|| = ||O||$.

However, we also assumed that loop graphs are evaluated under $||-\|$ according to Theorem 3.28. This means that the alternative evaluation and the evaluation $||-\|$ defined in Section 3 agree on loop graphs. We thus find

$$||\Sigma|| = ||O|| = |O| = |\Sigma|. \quad (4.36)$$

Hence, $||-\| = |-\|$ as a function on extruded graphs on the sphere. \square

4.2 ELEMENTARY MOVES

This is the first of two sections that comprise the proof of Theorem 4.4. For some moves, we have to prove the invariance property by directly using Definition 3.17, the definition of the evaluation procedure. These moves are called elementary. Other moves can be obtained as compositions of elementary moves, and we will treat them in Section 4.3.

4.2.1 PROOF STRATEGY FOR ELEMENTARY MOVES

The discussion of most of the elementary moves in the subsequent sections follows a general pattern, which we outline here.

Recall that the definitions of the various moves at the beginning of Section 4 involved a linear map between node spaces

$$\psi : N_x(m) \rightarrow N_{x'}(m'), \quad (4.37)$$

which describes the change in node labels. Note that here, m and x stand for a collection of defect and ray labels before the move, and m' and x' stand for their counterparts after the move.

In order to show that a move is an invariance, we consider the diagram (4.38) below. Some arrows that appear therein are yet to be defined.

$$\begin{array}{ccccc}
 N_x(m) & \xrightarrow{N_x(m\tau)} & \mathbb{T}^{\mathbb{P}} & \xrightarrow{\pi} & \mathbb{T} & \searrow \varphi \\
 \downarrow \psi & & \downarrow \Psi^{\mathbb{P}} & & \downarrow \Psi & \nearrow \varphi' \\
 N_{x'}(m') & \xrightarrow{N_{x'}(m'\tau)} & \mathbb{T}^{\mathbb{P}'} & \xrightarrow{\pi'} & \mathbb{T}' & \searrow \varphi'
 \end{array} \quad (4.38)$$

We first explain how the commutativity of the outer paths implies that we have a move of invariance at hand. By Definition 3.17, the composition on the upper edge of (4.38) is the evaluation procedure before the move, and the bottom path is the evaluation procedure *after* the move, using the post-move labels obtained from pre-move labels via the map ψ . Thus, if the outer paths in this diagram are the same maps, the move is an invariance.

We will deduce the commutativity of the outer paths in (4.38) from the commutativity of the cells. To this end, we now discuss the arrows $\Psi^{\mathbb{P}}$ and Ψ .

Since $\mathbb{T}^{\mathbb{P}}$ is a coend with structure morphisms $N_x(m\tau)$, there is a unique linear map $\Psi^{\mathbb{P}} : \mathbb{T}^{\mathbb{P}} \rightarrow \mathbb{T}^{\mathbb{P}'}$ such that the left square in (4.38) commutes. For each particular move, we will see that by a corresponding result of [FSS22], the linear map $\Psi^{\mathbb{P}}$ between pre-block spaces restricts to an isomorphism Ψ of the block spaces:

$$\begin{array}{ccc}
 \mathbb{T} & \hookrightarrow & \mathbb{T}^{\mathbb{P}} \\
 \downarrow \Psi & & \downarrow \Psi^{\mathbb{P}} \\
 \mathbb{T}' & \hookrightarrow & \mathbb{T}^{\mathbb{P}'}.
 \end{array} \quad (4.39)$$

This isomorphism Ψ provides a post-move label φ' for the core, such that $\varphi' = \varphi \circ (\Psi)^{-1}$, hence the triangular cell on the right side of (4.38) commutes as well.

The last step in order to show that the move we consider is an invariance is to check the commutativity of the middle square in (4.38). The meaning of this square is that the map Ψ^P , which *restricts* to Ψ on the subspace $T \subset T^P$, also *descends* to the quotient T . This condition will have to be checked for each move individually. To this end, we note the following lemma, which is just a reiteration of Lemma 2.19.

Lemma 4.6. *The commutativity of the diagram*

$$\begin{array}{ccc} T^P & \xrightarrow{h} & T^P \\ \downarrow \Psi^P & & \downarrow \Psi^P \\ T^{P'} & \xrightarrow{h'} & T^{P'} \end{array}, \quad (4.40)$$

involving the holonomy idempotents h, h' instead of the projectors π, π' implies the commutativity of the middle square in (4.38).

Thus, when proving that a move is an invariance, our task is to check that (4.40) commutes.

Remark 4.7. In light of Remark 3.5, it should be noted that using results of [FSS22] to deduce the existence of a map Ψ which satisfies (4.39) is not necessary and only serves a comparative reason. Indeed, by Lemma 2.19, the commutativity of (4.40) implies the existence of a unique map Ψ which makes both (4.39) and the middle cell in (4.38) commute.

We now turn to the study of individual moves, aiming to prove Theorem 4.4.

4.2.2 OR – ORIENTATION REVERSAL

The **OR**-move is easily seen to be an invariance.

In the introductory discussion in Section 4, we have already seen that the node spaces before and after the move can be identified, and we can indeed view them as equal without loss of generality, by assuming that the acting categories \mathcal{A} and \mathcal{B} are strictly pivotal. Consequently, also the pre-block spaces are equal. Explicitly, using (3.20), they are of the form

$$T^P = \mathcal{M} \langle y_{(\overline{\mathcal{M}})}, x_{(\mathcal{M})} \rangle \otimes \cdots = \overline{\mathcal{M}} \langle x_{(\overline{\mathcal{M}})}, y_{(\mathcal{M})} \rangle \otimes \cdots = T^{P'}. \quad (4.42)$$

That this identification of pre-block spaces restrict to an isomorphism of block spaces was observed in [FSS22, Prop. 4.24].

We must now show that the diagram (4.40) commutes. Unraveling the definition of the two holonomy idempotents h for Σ and h' for Σ' reveals that $h = h'$. This is because in the holonomy balancing (3.24), say for the domain \mathcal{A} , the balancing

$$\mathcal{M}\langle a^*y_{(\overline{\mathcal{M}})}, x_{(\mathcal{M})} \rangle \otimes \cdots \cong \mathcal{M}\langle y_{(\overline{\mathcal{M}})}, ax_{(\mathcal{M})} \rangle \otimes \cdots \quad (4.43)$$

appears as a composition factor. This balancing is the same for both $\mathbb{T}^{\mathbb{P}}$ and $\mathbb{T}^{\mathbb{P}'}$. A similar statement hold for the domain B

4.2.3 C – CONTRACTION

The second move for which we show the invariance property is the contraction move, which, as described in Section 4.1, allows us to transform two nodes, connected by a defect line, into a single node, thereby dissolving the defect line.

The map $\Psi^{\mathbb{P}}$ between pre-block spaces is constructed from the map $\psi : g \otimes f \mapsto g \circ_m f$ using the universal coend property of pre-block spaces:

$$\begin{array}{ccc} N_{x,y}(k, m, l) & \xrightarrow{N_{x,y}(k,m,l\tau)} & \mathbb{T}^{\mathbb{P}} \\ \downarrow \psi & & \downarrow \Psi^{\mathbb{P}} \\ N_{x \bullet_{\mathcal{M}} y}(k, l) & \xrightarrow{N_{x \bullet_{\mathcal{M}} y}(k,l\tau)} & \mathbb{T}^{\mathbb{P}'} \end{array} \quad (4.44)$$

The fact that $\Psi^{\mathbb{P}}$ restricts to a map Ψ between block spaces as in (4.39) is the content of [FSS22, Lemma 4.39].

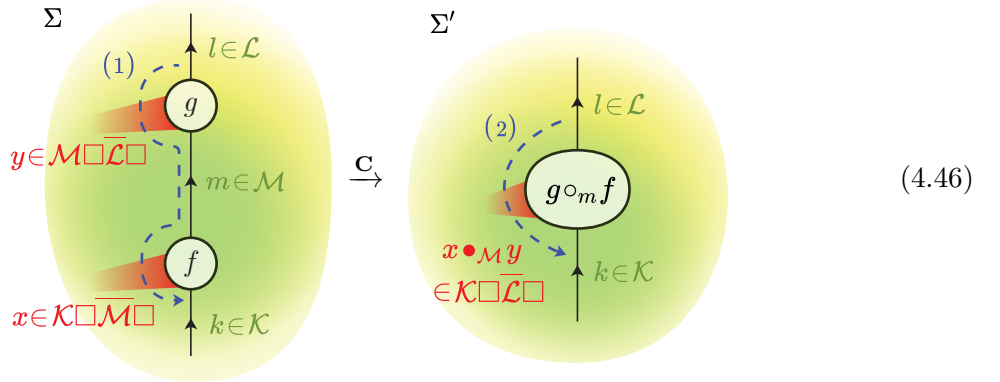
Following the general proof strategy outlined in Section 4.2.1, we now need to check that all cells of the diagram (4.38), which here takes the form

$$\begin{array}{ccccc} N_{x,y}(k, m, l) & \xrightarrow{N_{x,y}(k,m,l\tau)} & \mathbb{T}^{\mathbb{P}} & \xrightarrow{\pi} & \mathbb{T} & \searrow \varphi \\ \downarrow \psi & & \downarrow \Psi^{\mathbb{P}} & & \downarrow \Psi & \\ N_{x \bullet_{\mathcal{M}} y}(k, l) & \xrightarrow{N_{x \bullet_{\mathcal{M}} y}(k,l\tau)} & \mathbb{T}^{\mathbb{P}'} & \xrightarrow{\pi'} & \mathbb{T}' & \nearrow \varphi' \\ & & & & & \searrow \varphi' \\ & & & & & \mathbb{K} \end{array} \quad (4.45)$$

commute for the move **C**.

As mentioned in Section 4.2.1, the left square in (4.45) commutes by construction, see (4.44). In order to check the commutativity of the middle square in (4.38), we need to prove that the two composition factors of the holonomy operations h and h' corresponding to the paths from k

to l agree. These paths are labeled as (1) and (2) in the picture (4.46) below.



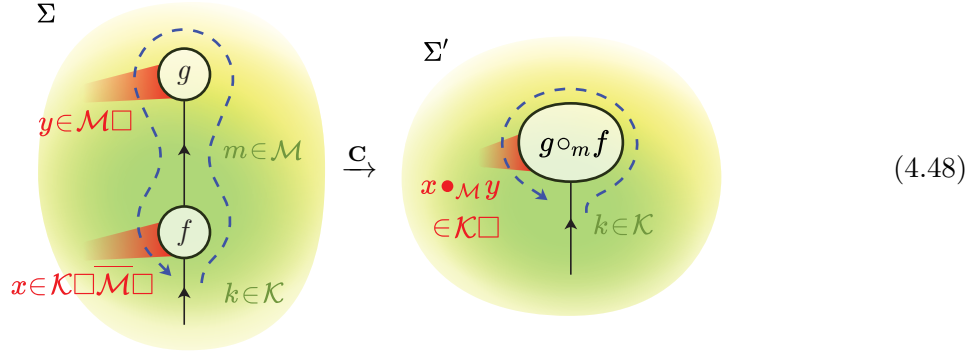
As we learned in Lemma 4.6, it is indeed sufficient to check this for the *idempotent* holonomy operations, as in (4.40). We perform the check only for the holonomy with respect to the domain \mathcal{A} ; the argument for the \mathcal{B} -holonomy is similar. Specifically, the following diagram (4.47) needs to commute, in which the left vertical column composes to the path (1) in the picture (4.46), and the right vertical column composes to the path (2). For convenience, only the relevant parts of the pre-block functors are written out: there coends over the variables l and k are omitted in (4.47).

$$\begin{array}{ccc}
f^n \langle n \boxtimes \bar{l}a, U(y) \rangle \otimes \langle k \boxtimes \bar{n}, U(x) \rangle & \xrightarrow{\Psi^p} & \langle k \boxtimes \bar{l}a, U(x \bullet_{\mathcal{M}} y) \rangle \\
\downarrow & & \downarrow \\
f^n \langle n \boxtimes \bar{l}, U(y)a^* \rangle \otimes \langle k \boxtimes \bar{n}, U(x) \rangle & \longrightarrow & \langle k \boxtimes \bar{l}, U(x \bullet_{\mathcal{M}} y)a^* \rangle \\
\downarrow & & \downarrow \\
f^n \langle n \boxtimes \bar{l}, a^*U(y) \rangle \otimes \langle k \boxtimes \bar{n}, U(x) \rangle & & \\
\downarrow & & \\
f^n \langle an \boxtimes \bar{l}, U(y) \rangle \otimes \langle k \boxtimes \bar{n}, U(x) \rangle & & \\
\downarrow & & \\
f^n \langle n \boxtimes \bar{l}, U(y) \rangle \otimes \langle k \boxtimes \bar{n}a, U(x) \rangle & & \\
\downarrow & & \\
f^n \langle n \boxtimes \bar{l}, U(y) \rangle \otimes \langle k \boxtimes \bar{n}, U(x)a^* \rangle & & \\
\downarrow & & \downarrow \\
f^n \langle n \boxtimes \bar{l}, U(y) \rangle \otimes \langle k \boxtimes \bar{n}, a^*U(x) \rangle & \longrightarrow & \langle k \boxtimes \bar{l}, a^*U(x \bullet_{\mathcal{M}} y) \rangle \\
\downarrow & & \downarrow \\
f^n \langle n \boxtimes \bar{l}, U(y) \rangle \otimes \langle ak \boxtimes \bar{n}, U(x) \rangle & \longrightarrow & \langle ak \boxtimes \bar{l}, U(x \bullet_{\mathcal{M}} y) \rangle
\end{array}
\tag{4.47}$$

In the above diagram, the commutativity of the top and bottom squares is trivial. The large cell commutes by definition of $x \bullet_{\mathcal{M}} y$, as can be seen by unraveling the definition (2.191) of the contraction operation.

The proof for the one-sided case is completely analogous, only that here, only a single domain is adjacent to the $(m \in \mathcal{M})$ -labeled defect line, and hence the following paths need to be compared

for the holonomy operation:



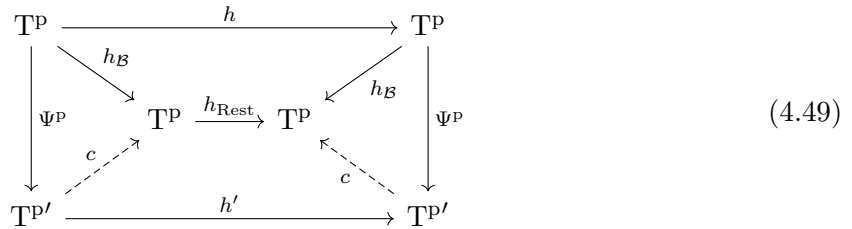
This completes the proof that the move **C** is an invariance.

4.2.4 **EF** – EDGE FUSION

As described in Section 4.1, the edge fusion move allows use to merge parallel defect lines which share start and end nodes. We proceed to show that **EF** is a move of invariance, following the proof strategy outlined in Section 4.2.1.

Accordingly, the map $\Psi^{\mathcal{P}} : \mathbb{T}^{\mathcal{P}} \rightarrow \mathbb{T}^{\mathcal{P}'}$ between pre-block spaces is constructed from ψ using the universal coend property of pre-block spaces. This means that $\Psi^{\mathcal{P}}$ is unique such that the left square in (4.38) commutes. That the map $\Psi^{\mathcal{P}}$ restricts to an isomorphism Ψ between block spaces has been proven in [FSS22, Theorem 4.43].

We are left to show that the square (4.40) (which is the outer square in (4.49) below) commutes for the move **EF**. This implies, by Lemma 4.6, that **EF** is an invariance. To this end, we note that the holonomy idempotent on Σ factorizes into commuting idempotents $h = h_{\text{Rest}} \circ h_{\mathcal{B}}$, where $h_{\mathcal{B}}$ is the holonomy idempotent with respect to the \mathcal{B} -labeled domain in Σ . Thus, $h_{\mathcal{B}} \circ h = h_{\text{Rest}} \circ h_{\mathcal{B}}$. The square (4.40) assumes, with a subdivision, the following form.



We have to find an injective map c such that all smaller cells in (4.49) which involve c commute, and show that the remaining small cell at the top of (4.49) commutes. This then implies commutativity of the outer square. For convenience, we reproduce the picture (4.5) illustrating

the regions Σ and Σ' .

$$(4.50)$$

As a map out of the coend

$$\mathrm{TP}' = \int^{k \in \mathcal{M} \square \mathcal{N}} \langle \bar{k} \boxtimes \dots, U'(x) \rangle \otimes \langle k \boxtimes \dots, U'(y) \rangle, \quad (4.51)$$

c is given by its components c^k , which are the composition

$$\begin{aligned} c^k &: \langle \bar{k} \boxtimes \dots, U'(x) \rangle \otimes \langle k \boxtimes \dots, U'(y) \rangle \\ &\xrightarrow[\text{forget } \mathcal{B}\text{-balancing}]{U} \langle \bar{k}_{(\mathcal{N})} \boxtimes \bar{k}_{(\mathcal{M})} \boxtimes \dots, U(x) \rangle \otimes \langle k_{(\mathcal{M})} \boxtimes k_{(\mathcal{N})} \boxtimes \dots, U(y) \rangle \\ &\xrightarrow[\text{coend structure morphisms}]{\sigma^{k_{(\mathcal{M})}} \sigma^{k_{(\mathcal{N})}}} \int^{q \in \mathcal{M}} \int^{r \in \mathcal{N}} \langle \bar{r} \boxtimes \bar{q} \boxtimes \dots, U(x) \rangle \otimes \langle q \boxtimes r \boxtimes \dots, U(y) \rangle = \mathrm{TP}. \end{aligned} \quad (4.52)$$

Here we used the form of Sweedler notation for the forgetful functor from (2.146), writing $U(k) = k_{(\mathcal{M})} \boxtimes k_{(\mathcal{N})}$. To see that $c : \mathrm{TP}' \rightarrow \mathrm{TP}$ is injective, note that under the isomorphisms $\mathrm{TP}' \cong \langle x_{(\mathcal{M} \square \mathcal{N})}, y_{(\mathcal{M} \square \mathcal{N})} \rangle \otimes \dots$ and $\mathrm{TP} \cong \langle x_{(\mathcal{M})} \boxtimes x_{(\mathcal{N})}, y_{(\mathcal{M})} \boxtimes y_{(\mathcal{N})} \rangle \otimes \dots$, that we encountered in Remark 3.6, the map c corresponds to the subspace inclusion, meaning that the following diagram commutes:

$$\begin{array}{ccc} \mathrm{TP}' & \xrightarrow{\cong} & \langle x_{(\mathcal{M} \square \mathcal{N})}, y_{(\mathcal{M} \square \mathcal{N})} \rangle \otimes \dots \\ \downarrow c & & \downarrow \text{subspace inclusion} \\ \mathrm{TP} & \xrightarrow{\cong} & \langle x_{(\mathcal{M})} \boxtimes x_{(\mathcal{N})}, y_{(\mathcal{M})} \boxtimes y_{(\mathcal{N})} \rangle \otimes \dots \end{array} \quad (4.53)$$

This can be checked explicitly, using the form of the isomorphism sil from Section 2.15. Thus c is monic, and the outer square in the diagram (4.49) commutes if all the cells commute.

Commutativity of the top square in (4.49) is easily seen. To verify that the bottom square commutes, recall that the holonomy idempotents h' and h_{Rest} are defined as a composition of individual holonomy idempotents for each domain except for \mathcal{B} – these domains can be identified across Σ and Σ' . On the other hand, the linear map c affects only the algebraic data associated with the domain \mathcal{B} . It thus commutes with the holonomy idempotents for the other domains.

This leaves us with the relevant parts of the diagram (4.49): the triangles on the left and the right, which happen to be equal. Hence, we check whether

$$c \circ \Psi^{\mathcal{P}} = h_{\mathcal{B}}. \quad (4.54)$$

For computing purposes, we are interested in the components $\mathbf{qr}c^{\mathbf{k}}$ of c (recall from (4.52) that c is a map into a double coend), for simple objects $\mathbf{k} \in \mathcal{M} \square \mathcal{N}$, $\mathbf{q} \in \mathcal{M}$ and $\mathbf{r} \in \mathcal{N}$. They are, according to (2.37), given by:

$$\begin{aligned} \mathbf{qr}c^{\mathbf{k}} &\stackrel{(2.37)}{=} d_{\mathbf{q}} d_{\mathbf{r}} \mathbf{qr} \tau \circ \Theta_{\mathcal{M} \boxtimes \mathcal{N}}^{-1} \circ c^{\mathbf{k}} \\ &\stackrel{(4.52)}{=} d_{\mathbf{q}} d_{\mathbf{r}} \mathbf{qr} \tau \circ \Theta_{\mathcal{M} \boxtimes \mathcal{N}}^{-1} \circ \sigma^{U(\mathbf{k})} \circ U \\ &\stackrel{(2.47)}{=} d_{\mathbf{q}} d_{\mathbf{r}} \left\langle \star_{\langle \mathbf{k}(\mathcal{N}), \mathbf{r} \rangle} \boxtimes \star_{\langle \mathbf{k}(\mathcal{M}), \mathbf{q} \rangle} \boxtimes \cdots, U(x) \right\rangle \otimes \left\langle \star_{\langle \mathbf{q}, \mathbf{k}(\mathcal{M}) \rangle} \boxtimes \star_{\langle \mathbf{r}, \mathbf{k}(\mathcal{N}) \rangle} \boxtimes \cdots, U(y) \right\rangle \circ U \end{aligned} \quad (4.55)$$

Moreover, we would like to write out the components $\mathbf{k}(\Psi^{\mathbb{P}})^{\mathbf{ij}}$ for simple objects $\mathbf{i} \in \mathcal{M}$, $\mathbf{j} \in \mathcal{N}$ and $\mathbf{k} \in \mathcal{M} \square \mathcal{N}$, using the definition of ψ from (4.6). To this end, recall the isomorphisms $\text{adj}_{\mathbf{i} \boxtimes \mathbf{j}, U'(x)}^{\boxtimes}$ and $\text{adj}_{\mathbf{i} \boxtimes \mathbf{j}, U'(y)}^{\boxtimes}$ from (2.112) and (2.111) witnessing the induction adjunctions (2.110). We again use (2.37) to obtain the k -components of $\Psi^{\mathbb{P}}$. This leads to the following.

$$\begin{aligned} \mathbf{k}(\Psi^{\mathbb{P}})^{\mathbf{ij}} &= d_{\mathbf{k}} \mathbf{k} \tau \circ \Theta_{\mathcal{M} \square \mathcal{N}}^{-1} \circ \sigma^{\mathbf{i} \boxtimes \mathbf{j}} \circ \left(\text{id} \otimes \frac{\Theta_{\mathcal{B}}}{\mathcal{D}_{\mathcal{B}}} \right) \circ (\text{adj}_{\mathbf{i} \boxtimes \mathbf{j}, U'(x)}^{\boxtimes} \otimes \text{adj}_{\mathbf{i} \boxtimes \mathbf{j}, U'(y)}^{\boxtimes}) \\ &\stackrel{(2.47)}{=} d_{\mathbf{k}} \left\langle \star_{\langle \mathbf{i} \boxtimes \mathbf{j}, \mathbf{k} \rangle} \boxtimes \cdots, U'(x) \right\rangle \otimes \left\langle \star_{\langle \mathbf{k}, \mathbf{i} \boxtimes \mathbf{j} \rangle} \boxtimes \cdots, U'(y) \right\rangle \\ &\quad \circ \left(\text{id} \otimes \frac{\Theta_{\mathcal{B}}}{\mathcal{D}_{\mathcal{B}}} \right) \circ (\text{adj}_{\mathbf{i} \boxtimes \mathbf{j}, U'(x)}^{\boxtimes} \otimes \text{adj}_{\mathbf{i} \boxtimes \mathbf{j}, U'(y)}^{\boxtimes}) \end{aligned} \quad (4.56)$$

Knowing the components of c and of $\Psi^{\mathbb{P}}$, we write out the composition $c \circ \Psi^{\mathbb{P}}$ in components:

$$\begin{aligned} \mathbf{qr}(c \circ \Psi^{\mathbb{P}})^{\mathbf{ij}} &\stackrel{(2.40)}{=} \sum_{\mathbf{k}} \mathbf{qr}c^{\mathbf{k}} \circ \mathbf{k}(\Psi^{\mathbb{P}})^{\mathbf{ij}} \\ &= \sum_{\mathbf{k}} d_{\mathbf{q}} d_{\mathbf{r}} d_{\mathbf{k}} \left\langle \star_{\langle \mathbf{k}(\mathcal{N}), \mathbf{r} \rangle} \boxtimes \star_{\langle \mathbf{k}(\mathcal{M}), \mathbf{q} \rangle} \boxtimes \cdots, U(x) \right\rangle \otimes \left\langle \star_{\langle \mathbf{q}, \mathbf{k}(\mathcal{M}) \rangle} \boxtimes \star_{\langle \mathbf{r}, \mathbf{k}(\mathcal{N}) \rangle} \boxtimes \cdots, U(y) \right\rangle \\ &\quad \circ U \circ \left\langle \star_{\langle \mathbf{i} \boxtimes \mathbf{j}, \mathbf{k} \rangle} \boxtimes \cdots, U'(x) \right\rangle \otimes \left\langle \star_{\langle \mathbf{k}, \mathbf{i} \boxtimes \mathbf{j} \rangle} \boxtimes \cdots, U'(y) \right\rangle \\ &\quad \circ \left(\text{id} \otimes \frac{\Theta_{\mathcal{B}}}{\mathcal{D}_{\mathcal{B}}} \right) \circ (\text{adj}_{\mathbf{i} \boxtimes \mathbf{j}, U'(x)}^{\boxtimes} \otimes \text{adj}_{\mathbf{i} \boxtimes \mathbf{j}, U'(y)}^{\boxtimes}). \end{aligned} \quad (4.57)$$

According to (2.114) and (2.113), on vectors

$$\alpha = \int^i \int^j \overline{ij \alpha_{(1)}} \otimes ij \alpha_{(2)} \in \int^i \int^j \left\langle \bar{j} \boxtimes \bar{i} \boxtimes \cdots, U(x) \right\rangle \otimes \left\langle i \boxtimes j \boxtimes \cdots, U(y) \right\rangle = \text{TP}, \quad (4.58)$$

we have

$$\begin{aligned} &(\text{adj}_{\mathbf{i} \boxtimes \mathbf{j}, U'(x)}^{\boxtimes} \otimes \text{adj}_{\mathbf{i} \boxtimes \mathbf{j}, U'(y)}^{\boxtimes})(\overline{ij \alpha_{(1)}} \otimes ij \alpha_{(2)}) \\ &= \left(\int^{a \in \mathcal{B}} \overline{a \text{cobrev}_x} \circ a(\overline{ij \alpha_{(1)}}) a^* \right) \otimes \left(\int_{b \in \mathcal{B}} \text{brev}_y^b \circ b(ij \alpha_{(2)}) b^* \right). \end{aligned} \quad (4.59)$$

Making the substitution (4.59) in (4.57), we obtain

$$\begin{aligned}
\mathfrak{q}^{\mathbf{r}}(c \circ \Psi^{\mathbf{p}})(\alpha) &= \sum_{\mathbf{ij}} \mathfrak{q}^{\mathbf{r}}(c \circ \Psi^{\mathbf{p}})^{\mathbf{ij}}(\overline{\mathbf{ij}\alpha_{(1)}} \otimes \mathbf{ij}\alpha_{(2)}) \\
&= \sum_{\mathbf{kij}} \frac{d_{\mathbf{q}}d_{\mathbf{r}}d_{\mathbf{k}}}{\mathcal{D}_{\mathcal{B}}} \left(\int^{a \in \mathcal{B}} \frac{\overline{a \text{cobrev}_x} \circ a(\overline{\mathbf{ij}\alpha_{(1)}})a^* \circ \star_{\langle \mathbf{i} \boxtimes \mathbf{j}, \mathbf{k} \rangle} \circ (\star_{\langle \mathbf{k}_{(\mathcal{M})}, \mathbf{r} \rangle} \boxtimes \star_{\langle \mathbf{k}_{(\mathcal{M})}, \mathbf{q} \rangle}) \right) \\
&\quad \otimes \left(\int^{b \in \mathcal{B}} d_b \text{brev}_y^b \circ b(\mathbf{ij}\alpha_{(2)})b^* \circ \star_{\langle \mathbf{k}, \mathbf{i} \boxtimes \mathbf{j} \rangle} \circ (\star_{\langle \mathbf{q}, \mathbf{k}_{(\mathcal{M})} \rangle} \boxtimes \star_{\langle \mathbf{r}, \mathbf{k}_{(\mathcal{N})} \rangle}) \right). \tag{4.60}
\end{aligned}$$

The expression (4.60) describes the simple components $\mathfrak{q}^{\mathbf{r}}(c \circ \Psi^{\mathbf{p}})(\alpha)$ of a vector $(c \circ \Psi^{\mathbf{p}})(\alpha) \in \mathbb{T}^{\mathbf{p}}$. In order to prove (4.54), we wish to compare this to the vector $h_{\mathcal{B}}(\alpha) \in \mathbb{T}^{\mathbf{p}}$. It is, however, again more convenient to pass both of these vectors through the isomorphism (3.20). For $(c \circ \Psi^{\mathbf{p}})(\alpha)$, this has the effect of composing the tensor factors in (4.60), and to sum over simple objects \mathbf{q} and \mathbf{r} . We thus obtain:

$$\begin{aligned}
&\sum_{\mathbf{krqij}} \frac{d_{\mathbf{q}}d_{\mathbf{r}}d_{\mathbf{k}}}{\mathcal{D}_{\mathcal{B}}} \left(\int^{b \in \mathcal{B}} d_b \text{brev}_y^b \circ b(\mathbf{ij}\alpha_{(2)})b^* \right) \circ \star_{\langle \mathbf{k}, \mathbf{i} \boxtimes \mathbf{j} \rangle} \circ (\star_{\langle \mathbf{q}, \mathbf{k}_{(\mathcal{M})} \rangle} \boxtimes \star_{\langle \mathbf{r}, \mathbf{k}_{(\mathcal{N})} \rangle}) \\
&\quad \circ (\star_{\langle \mathbf{k}_{(\mathcal{M})}, \mathbf{q} \rangle} \boxtimes \star_{\langle \mathbf{k}_{(\mathcal{N})}, \mathbf{r} \rangle}) \circ \star_{\langle \mathbf{i} \boxtimes \mathbf{j}, \mathbf{k} \rangle} \circ \left(\int^{a \in \mathcal{B}} a(\mathbf{ij}\alpha_{(1)})a^* \circ a \text{cobrev}_x \right) \\
&\stackrel{(2.17)}{=} \sum_{\mathbf{kij}} \frac{d_{\mathbf{k}}}{\mathcal{D}_{\mathcal{B}}} \left(\int^{b \in \mathcal{B}} d_b \text{brev}_y^b \circ b(\mathbf{ij}\alpha_{(2)})b^* \right) \circ \star_{\langle \mathbf{k}, \mathbf{i} \boxtimes \mathbf{j} \rangle} \\
&\quad \circ \star_{\langle \mathbf{i} \boxtimes \mathbf{j}, \mathbf{k} \rangle} \circ \left(\int^{a \in \mathcal{B}} a(\mathbf{ij}\alpha_{(1)})a^* \circ a \text{cobrev}_x \right) \tag{4.61} \\
&\stackrel{(2.17)}{=} \sum_{\mathbf{ij}} \frac{1}{\mathcal{D}_{\mathcal{B}}} \left(\int^{b \in \mathcal{B}} d_b \text{brev}_y^b \circ b(\mathbf{ij}\alpha_{(2)})b^* \right) \circ \left(\int^{a \in \mathcal{B}} a(\mathbf{ij}\alpha_{(1)})a^* \circ a \text{cobrev}_x \right) \\
&\stackrel{(2.40)}{=} \sum_{\mathbf{bij}} \frac{d_{\mathbf{b}}}{\mathcal{D}_{\mathcal{B}}} \text{brev}_y^{\mathbf{b}} \circ \mathbf{b}(\mathbf{ij}\alpha_{(2)})\mathbf{b}^* \circ \mathbf{b}(\mathbf{ij}\alpha_{(1)})\mathbf{b}^* \circ \mathbf{b} \text{cobrev}_x \\
&= \sum_{\mathbf{bij}} \frac{d_{\mathbf{b}}}{\mathcal{D}_{\mathcal{B}}} \text{brev}_y^{\mathbf{b}} \circ \mathbf{b}(\mathbf{ij}\alpha_{(2)} \circ \mathbf{ij}\alpha_{(1)})\mathbf{b}^* \circ \mathbf{b} \text{cobrev}_x \\
&\stackrel{(2.179)}{=} \sum_{\mathbf{b}} \frac{d_{\mathbf{b}}}{\mathcal{D}_{\mathcal{B}}} \text{brev}_y^{\mathbf{b}} \circ \mathbf{b} \text{sil}^{-1}(\alpha) \mathbf{b}^* \circ \mathbf{b} \text{cobrev}_x.
\end{aligned}$$

We here denoted the isomorphism (3.20) by sil , as introduced in (2.179).

In order to compare this expression to the holonomy idempotent $h_{\mathcal{B}}$, we use that under the

isomorphism (3.20), $h_{\mathcal{B}}$ becomes the following, writing $\tilde{\alpha}$ for $\text{sil}^{-1}(\alpha)$:

$$\begin{array}{ccc}
\mathbb{T}^{\mathbb{P}} \cong \langle x_{(\mathcal{M})} \boxtimes x_{(\mathcal{N})}, y_{(\mathcal{M})} \boxtimes y_{(\mathcal{N})} \rangle \otimes \cdots & & \tilde{\alpha} \\
\downarrow & & \downarrow \\
\int^b \langle x_{(\mathcal{M})} \boxtimes bb^* x_{(\mathcal{N})}, y_{(\mathcal{M})} \boxtimes y_{(\mathcal{N})} \rangle \otimes \cdots & & \frac{1}{\mathcal{D}_{\mathcal{B}}} \int^b \tilde{\alpha} \circ (\text{ev}^b U(x)) \\
\downarrow & & \downarrow \\
\int^b \langle x_{(\mathcal{M})} \boxtimes bb^* x_{(\mathcal{N})}, y_{(\mathcal{M})} \boxtimes y_{(\mathcal{N})} \rangle \otimes \cdots & & \int^b \frac{d_b}{\mathcal{D}_{\mathcal{B}}} \tilde{\alpha} \circ (\text{ev}^b U(x)) \\
\downarrow & & \downarrow \\
\int^b \langle x_{(\mathcal{M})} b^* \boxtimes bx_{(\mathcal{N})}, y_{(\mathcal{M})} \boxtimes y_{(\mathcal{N})} \rangle \otimes \cdots & & \int^b \frac{d_b}{\mathcal{D}_{\mathcal{B}}} \tilde{\alpha} \circ (\text{ev}^b U(x)) \circ (b \text{br}_{b^*}^{x-1}) \\
& & = \int^b \frac{d_b}{\mathcal{D}_{\mathcal{B}}} \tilde{\alpha} \circ (\text{brev}_x^b) \\
\downarrow & & \downarrow \\
\int^b \langle x_{(\mathcal{M})} \boxtimes bx_{(\mathcal{N})}, y_{(\mathcal{M})} b \boxtimes y_{(\mathcal{N})} \rangle \otimes \cdots & & \int^b \frac{d_b}{\mathcal{D}_{\mathcal{B}}} (\tilde{\alpha} b) \circ (\text{brev}_x^b) \circ (bU(x) {}_b\text{coev}) \\
& & = \int^b \frac{d_b}{\mathcal{D}_{\mathcal{B}}} (\tilde{\alpha} b) \circ (\text{br}_b^x) \\
\downarrow & & \downarrow \\
\int^b \langle x_{(\mathcal{M})} \boxtimes bx_{(\mathcal{N})}, y_{(\mathcal{M})} \boxtimes by_{(\mathcal{N})} \rangle \otimes \cdots & & \int^b \frac{d_b}{\mathcal{D}_{\mathcal{B}}} (\text{br}_b^{y-1}) \circ (\tilde{\alpha} b) \circ (\text{br}_b^x) \\
\downarrow & & \downarrow \\
\int^b \langle x_{(\mathcal{M})} \boxtimes b^* bx_{(\mathcal{N})}, y_{(\mathcal{M})} \boxtimes y_{(\mathcal{N})} \rangle \otimes \cdots & & \int^b \frac{d_b}{\mathcal{D}_{\mathcal{B}}} (\text{ev}^{b^*} U(y)) \circ (\text{br}_b^{y-1}) \circ (b^* \tilde{\alpha} b) \circ (b^* \text{br}_b^x) \\
& & = \int^b \frac{d_b}{\mathcal{D}_{\mathcal{B}}} (\text{brev}_y^{b^*}) \circ (b^* \tilde{\alpha} b) \circ (b^* \text{br}_b^x) \\
\downarrow & & \downarrow \\
\langle x_{(\mathcal{M})} \boxtimes x_{(\mathcal{N})}, y_{(\mathcal{M})} \boxtimes y_{(\mathcal{N})} \rangle \otimes \cdots \cong \mathbb{T}^{\mathbb{P}} & & \sum_{\mathbf{b}} \frac{d_{\mathbf{b}}}{\mathcal{D}_{\mathcal{B}}} (\text{brev}_y^{\mathbf{b}^*}) \circ (\mathbf{b}^* \tilde{\alpha} \mathbf{b}) \circ (\mathbf{b}^* \text{br}_{\mathbf{b}}^x) \circ ({}_b\text{coev } U(x)) \\
& & = \sum_{\mathbf{b}} \frac{d_{\mathbf{b}}}{\mathcal{D}_{\mathcal{B}}} (\text{brev}_y^{\mathbf{b}^*}) \circ (\mathbf{b}^* \tilde{\alpha} \mathbf{b}) \circ ({}_b\text{cobrev}_x).
\end{array} \tag{4.62}$$

This expression is equal to the result of the calculation (4.61), proving that $(c \circ \Psi^{\mathbb{P}})(\alpha) = h_{\mathcal{B}}(\alpha)$ for all $\alpha \in \mathbb{T}^{\mathbb{P}}$. Thus the outer paths in the diagram (4.49) commute, and the move is invariant.

4.2.5 SV – SUBSIDE VERTEX

Recall the illustration of the **SV**-move from (4.7):

$$\tag{4.63}$$

We denote the lasso graph on the left-hand side of (4.63) by Q , and the loop graph on the right-hand side by O . From Lemma 3.23, we know that

$$|Q| = \varphi(r(f \circ_m \tau)). \quad (4.64)$$

Writing the linear form φ in terms of a trace, as in (4.10), we obtain

$$|Q| = \mathrm{Tr}_{\mathbb{T}\mathbb{R}}(\tilde{\varphi} \circ r(f \circ_m \tau)). \quad (4.65)$$

This can be written out further using the second result (3.47) of Lemma 3.23.

$$|Q| = \mathrm{Tr}_{\mathbb{T}\mathbb{R}} \left(\int^n \sum_{\mathbf{a}} \frac{d_{\mathbf{a}} d_n}{\mathcal{D}_{\mathcal{A}}} \tilde{\varphi} \circ \mathrm{brev}_x^{\mathbf{a}^*} \circ (\mathbf{a}^* f \mathbf{a}) \circ (\star_{\langle n, \mathbf{a}^* m \rangle} \boxtimes \star_{\langle \mathbf{a}^* m, n \rangle}) \right). \quad (4.66)$$

We now turn our attention to the loop graph O on the right-hand side of (4.63). The idea is to view O as a lasso graph, and to apply the same reasoning to it as we did to Q . Recall that the core label of O , $\Theta_{\mathcal{M}}^*$, was defined in (3.59) using the isomorphism

$$\widetilde{\Theta_{\mathcal{M}}^*} := \mathcal{D}_{\mathcal{A}} \mathcal{D}_{\mathcal{B}} \Theta_{\mathcal{M}}^{-1} \quad (4.67)$$

as $\Theta_{\mathcal{M}}^* := \mathrm{Tr}_{\mathbb{T}\mathbb{R}}(\widetilde{\Theta_{\mathcal{M}}^*} \circ -)$. Invoking Lemma 3.23 and the definition (4.11) of the node label $f' = \frac{1}{\mathcal{D}_{\mathcal{A}} \mathcal{D}_{\mathcal{B}}} \Theta_{\mathcal{M}} \circ \tilde{\varphi} \circ f$, we obtain the following formula the evaluation of the loop graph:

$$|O| = \mathrm{Tr}_{\mathbb{T}\mathbb{R}} \left(\widetilde{\Theta_{\mathcal{M}}^*} \circ r(f' \circ_m \tau) \right) = \frac{1}{\mathcal{D}_{\mathcal{A}} \mathcal{D}_{\mathcal{B}}} \mathrm{Tr}_{\mathbb{T}\mathbb{R}} \left(\widetilde{\Theta_{\mathcal{M}}^*} \circ r(\Theta_{\mathcal{M}} \circ \tilde{\varphi} \circ f \circ_m \tau) \right). \quad (4.68)$$

More explicitly, using (3.47), this becomes

$$\begin{aligned} |O| &= \frac{1}{\mathcal{D}_{\mathcal{A}} \mathcal{D}_{\mathcal{B}}} \mathrm{Tr}_{\mathbb{T}\mathbb{R}} \left(\int^n \sum_{\mathbf{a}} \frac{d_{\mathbf{a}} d_n}{\mathcal{D}_{\mathcal{A}}} \widetilde{\Theta_{\mathcal{M}}^*} \circ \mathrm{brev}_{\mathbb{F}^{\mathcal{M}}}^{\mathbf{a}^*} \circ (\mathbf{a}^* \Theta_{\mathcal{M}} \mathbf{a}) \circ (\mathbf{a}^* \tilde{\varphi} \mathbf{a}) \circ (\mathbf{a}^* f \mathbf{a}) \circ (\star_{\langle n, \mathbf{a}^* m \rangle} \boxtimes \star_{\langle \mathbf{a}^* m, n \rangle}) \right) \\ &= \frac{1}{\mathcal{D}_{\mathcal{A}} \mathcal{D}_{\mathcal{B}}} \mathrm{Tr}_{\mathbb{T}\mathbb{R}} \left(\int^n \sum_{\mathbf{a}} \frac{d_{\mathbf{a}} d_n}{\mathcal{D}_{\mathcal{A}}} \widetilde{\Theta_{\mathcal{M}}^*} \circ \Theta_{\mathcal{M}} \circ \mathrm{brev}_{\mathbb{F}^{\mathcal{M}}}^{\mathbf{a}^*} \circ (\mathbf{a}^* \tilde{\varphi} \mathbf{a}) \circ (\mathbf{a}^* f \mathbf{a}) \circ (\star_{\langle n, \mathbf{a}^* m \rangle} \boxtimes \star_{\langle \mathbf{a}^* m, n \rangle}) \right) \\ &\stackrel{(4.67)}{=} \mathrm{Tr}_{\mathbb{T}\mathbb{R}} \left(\int^n \sum_{\mathbf{a}} \frac{d_{\mathbf{a}} d_n}{\mathcal{D}_{\mathcal{A}}} \mathrm{brev}_{\mathbb{F}^{\mathcal{M}}}^{\mathbf{a}^*} \circ (\mathbf{a}^* \tilde{\varphi} \mathbf{a}) \circ (\mathbf{a}^* f \mathbf{a}) \circ (\star_{\langle n, \mathbf{a}^* m \rangle} \boxtimes \star_{\langle \mathbf{a}^* m, n \rangle}) \right) \\ &= \mathrm{Tr}_{\mathbb{T}\mathbb{R}} \left(\int^n \sum_{\mathbf{a}} \frac{d_{\mathbf{a}} d_n}{\mathcal{D}_{\mathcal{A}}} \tilde{\varphi} \circ \mathrm{brev}_x^{\mathbf{a}^*} \circ (\mathbf{a}^* f \mathbf{a}) \circ (\star_{\langle n, \mathbf{a}^* m \rangle} \boxtimes \star_{\langle \mathbf{a}^* m, n \rangle}) \right). \end{aligned} \quad (4.69)$$

In the second and the last identity, we used that $\Theta_{\mathcal{M}}$ and $\tilde{\varphi}$ are morphisms of balanced objects, which allowed us to commute them with the brev-morphism. Comparison with (4.66) shows that $|Q| = |O|$, hence the move **SV** is an invariance of the evaluation.

4.2.6 Fun – FUNCTORIALITY

In the usual way, the morphism between node spaces defines a morphism Ψ^P between pre-block spaces:

$$\begin{array}{ccc}
 \langle m, x_{(\mathcal{M})} \rangle \otimes \langle \bar{m}, y_{(\bar{\mathcal{M}})} \rangle & \xrightarrow{F} & \langle F(m), F(x_{(\mathcal{M})}) \rangle \otimes \langle \overline{F(m)}, F(y_{(\bar{\mathcal{M}})}) \rangle \\
 \downarrow \sigma^m & & \downarrow \sigma^{F(m)} \\
 \int^n \langle n, x_{(\mathcal{M})} \rangle \otimes \langle \bar{n}, y_{(\bar{\mathcal{M}})} \rangle & \xrightarrow{\Psi^P} & \int^n \langle n, F(x_{(\mathcal{M})}) \rangle \otimes \langle \bar{n}, F(y_{(\bar{\mathcal{M}})}) \rangle
 \end{array} \tag{4.70}$$

Because F is an equivalence, Ψ^P is an isomorphism. Verifying that the square (4.40) commutes is straightforward and similar to how the other moves were proved.

4.3 COMPOSITE MOVES

This section is the second and final part of the proof of Theorem 4.4. The remaining moves do not have to be proved by explicitly using the definition of the evaluation procedure, but can be obtained as compositions of moves we already know to be invariances.

4.3.1 DV – DISSOLVE VERTEX

We begin by redrawing the picture (4.19) in a slightly larger region, this time involving another node labeled by f , adjacent to the upper m -labeled defect line. This is only possible if the two m -labeled defect lines featured on the left-hand side of (4.19) are indeed different, i.e. they do not form a loop. But if they did form a loop, then the extruded graph on the right-hand side of (4.19) would feature a loop without a node, which is not allowed in extruded graphs. Hence, another node f must exist.

The **DV**-move can be viewed as a **C**-move: On the left-hand side of (4.71), one can contract the upper (or equivalently the lower) m -labeled defect line; this eliminates the middle node. We need to check that the changes in the labels reflect the changes prescribed by the move **C**. For the ray label x , this amounts to verifying that there is an isomorphism

$$x \cong_{\Phi^{\mathcal{M}}} \bullet_{\mathcal{M}} x, \tag{4.72}$$

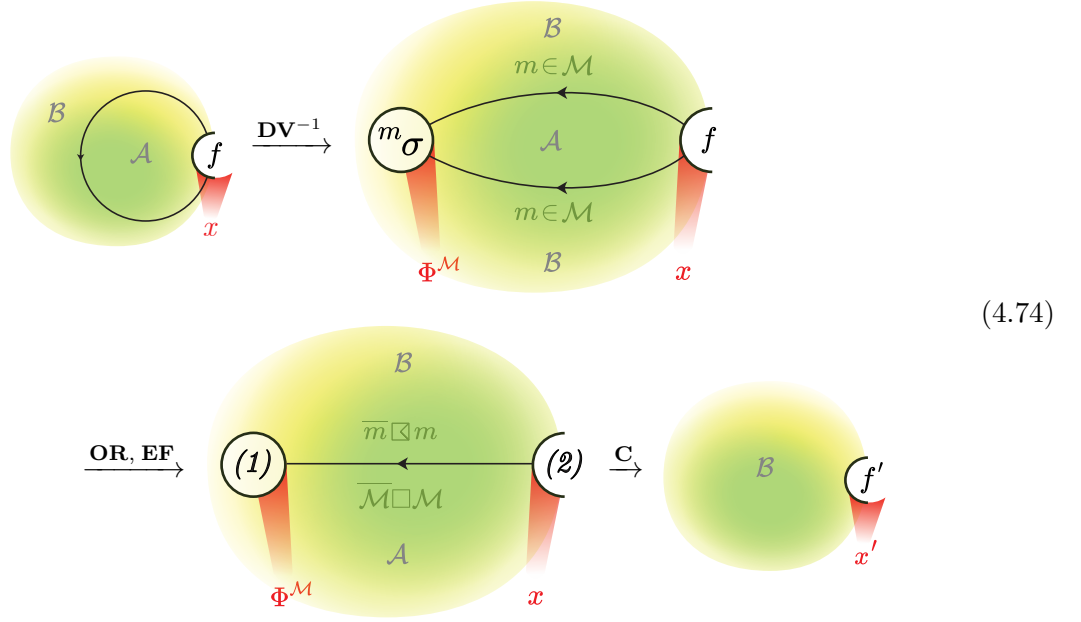
and for the node label f , we need to show that under this isomorphism, the following assignment is made:

$$f \mapsto \text{sil}(\text{id}_{\mathcal{M}}) \circ_m f. \quad (4.73)$$

This follows from Remark 2.38.

4.3.2 L – LOOP MOVE

The **L**-move is obtained as the following composition of moves. The ray- and node labels are described in detail below.



First, we apply an inverse **DV**-move to the loop, which splits it into two \mathcal{M} -labeled defect lines and creates a new node, with cosilent ray and node label $\sigma^m : \bar{m} \boxtimes m \rightarrow \int^{k \in \mathcal{M}} \bar{k} \boxtimes k$. Next, we flip the orientation of one of the \mathcal{M} -labeled defect lines using the **OR**-move, so that both point away from the f -labeled node. The **EF**-move then merges the two defect lines into one, labeled by $\bar{m} \boxtimes m \in \overline{\mathcal{M}} \boxtimes \mathcal{M}$. This leaves the nodes (1) and (2) in (4.74) with labels obtained by passing through the appropriate adjunctions, as explained in (4.6). Explicitly, the node (1) has the label

$$\text{adj}_{\bar{m} \boxtimes m, \Phi^{\mathcal{M}}}^{\boxtimes}(\sigma^m) \circ \Theta_{\mathcal{A}} : \bar{m} \boxtimes m \rightarrow \Phi^{\mathcal{M}}, \quad (4.75)$$

while the node (2) is labeled by

$$\left(\frac{1}{\mathcal{D}_{\mathcal{A}}} \text{adj}_{\bar{m} \boxtimes m, x_{(\overline{\mathcal{M}} \boxtimes \mathcal{M})}}^{\boxtimes} (f_{(\overline{\mathcal{M}})} \otimes f_{(\mathcal{M})}) \right) \otimes f_{(\mathcal{R})} : \overline{\bar{m} \boxtimes m} \rightarrow x_{(\overline{\mathcal{M}} \boxtimes \mathcal{M})} \boxtimes x_{(\mathcal{R})}. \quad (4.76)$$

In the last step, we use the (one-sided version of the) **C**-move to absorb node (1) into node (2). This results in the ray label $x' = \Phi^{\mathcal{M}} \bullet_{\overline{\mathcal{M}} \boxtimes \mathcal{M}} x$ as described in (4.21). The newly obtained node's

label is given, according to (4.4), by the contraction of the node labels (4.75) and (4.76) in the sense of (2.204). Working this out, we obtain the expression

$$\left(\frac{1}{\mathcal{D}_{\mathcal{A}}} \text{adj}_{\overline{m} \boxtimes m, \Phi^{\mathcal{M}}}^{\boxtimes}(\sigma^m) \circ \Theta_{\mathcal{A}} \circ \text{adj}_{\overline{m} \boxtimes m, x_{(\overline{\mathcal{M}} \square \mathcal{M})}}^{\boxtimes}(f_{(\overline{\mathcal{M}})} \otimes f_{(\mathcal{M})}) \right) \otimes f_{(\mathcal{R})} \quad (4.77)$$

for the node label, which we recognize from (2.120) to be equal to

$$r \left(\sigma^m \circ (f_{(\overline{\mathcal{M}})} \otimes f_{(\mathcal{M})}) \right) \otimes f_{(\mathcal{R})}, \quad (4.78)$$

where $r : \overline{\mathcal{M}} \boxtimes \mathcal{M} \langle x_{(\overline{\mathcal{M}})} \boxtimes x_{(\mathcal{M})}, \mathbf{I}^{\mathcal{M}} \rangle \rightarrow \overline{\mathcal{M}} \square \mathcal{M} \langle x_{(\overline{\mathcal{M}} \square \mathcal{M})}, \Phi^{\mathcal{M}} \rangle$ denotes the retraction from Lemma 2.23. Using that

$$\text{sil}^{-1}(\sigma^m \circ (f_{(\overline{\mathcal{M}})} \otimes f_{(\mathcal{M})})) = f_{(\mathcal{M})} \circ f_{(\overline{\mathcal{M}})} : x_{(\overline{\mathcal{M}})} \rightarrow x_{(\mathcal{M})}, \quad (4.79)$$

and that by Remark 2.37, the retraction r from Lemma 2.23 gets mapped, under the isomorphism sil^{-1} , to the retraction r from Lemma 2.31 in the sense that

$$\begin{array}{ccc} \overline{\mathcal{M}} \boxtimes \mathcal{M} \langle x_{(\overline{\mathcal{M}})} \boxtimes x_{(\mathcal{M})}, \mathbf{I}^{\mathcal{M}} \rangle & \xrightarrow{\text{sil}^{-1}} & \mathcal{M} \langle x_{(\overline{\mathcal{M}})}, x_{(\mathcal{M})} \rangle \\ \downarrow r & & \downarrow r \\ \overline{\mathcal{M}} \square \mathcal{M} \langle x_{(\overline{\mathcal{M}} \square \mathcal{M})}, \Phi^{\mathcal{M}} \rangle & \longrightarrow & \mathcal{M} \langle x_{(\overline{\mathcal{M}})}, x_{(\mathcal{M})} \rangle \end{array} \quad (4.80)$$

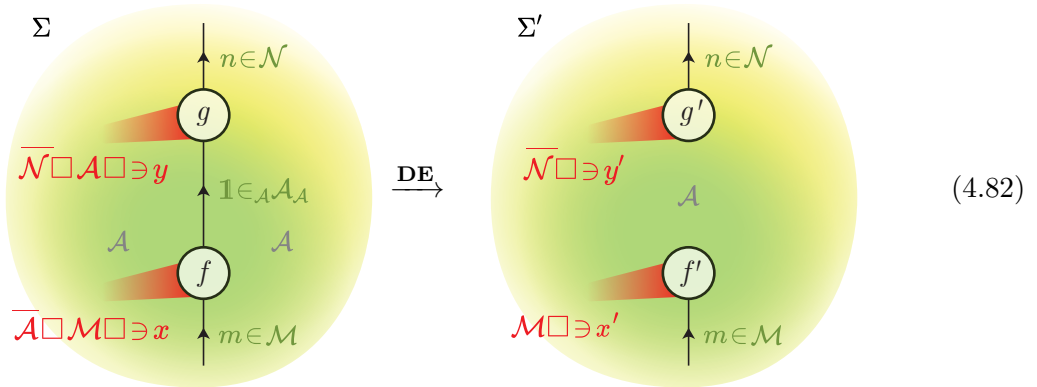
commutes, we can deduce that the node label, as a map

$$n \rightarrow \mathcal{M} \langle x_{(\overline{\mathcal{M}})}, x_{(\mathcal{M})} \rangle \otimes x_{(\mathcal{R})}, \quad (4.81)$$

is given by $f' = r(f_{(\mathcal{M})} \circ f_{(\overline{\mathcal{M}})})$, as stated in (4.24).

4.3.3 DE – DISSOLVE EDGE

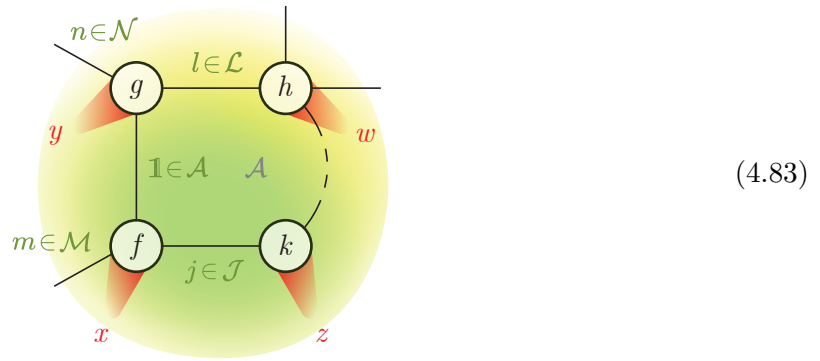
Recall the illustration of the **DE**-move from (4.25):



As a first step, we remark that the $(\mathbf{1} \in \mathcal{A})$ -labeled defect line in the left-hand side of (4.82) is adjacent to two domains – the left and right \mathcal{A} -labeled domains are indeed distinct. This is the

case because otherwise, the move would produce a non-contractible domain on the right-hand side of (4.82), which is not allowed in extruded graphs.

We focus on one of the domains adjacent to the $(\mathbb{1} \in \mathcal{A})$ -labeled defect line; let us pick the right one. A possibility for how this domain may look like is illustrated below.



We are interested in the counterclockwise neighbor of the $(\mathbb{1} \in \mathcal{A})$ -labeled defect line adjacent to the node g : in (4.83), this is the defect line labeled by $l \in \mathcal{L}$. This defect line is also adjacent to the \mathcal{A} -labeled domain we selected for our argument. It may or may not be a loop.

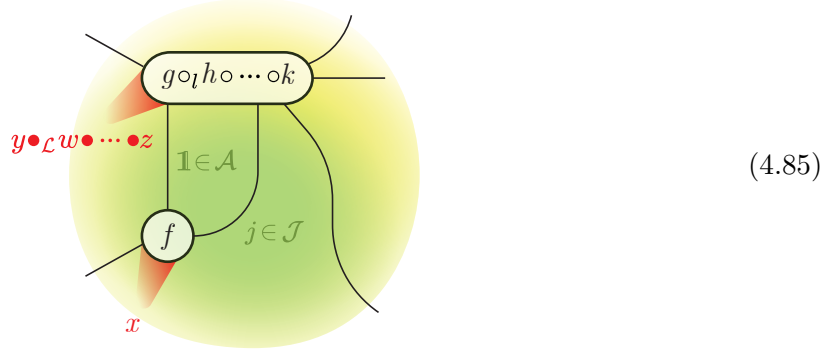
If it is a loop, then it encircles some area, as highlighted in (4.84) below.



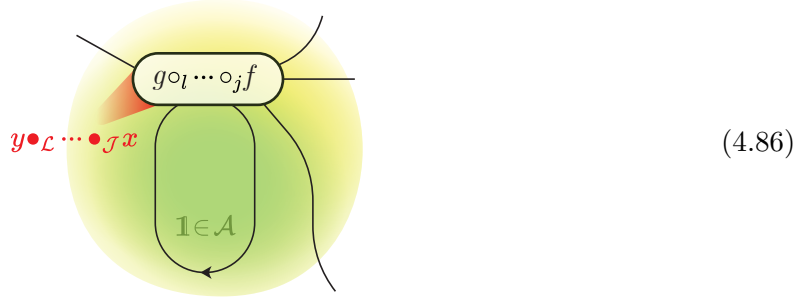
The contents of this area can be absorbed into the node currently labeled by g through a sequence of moves – this is very similar to the proof of Theorem 4.5. Then, once the loop is contractible, we apply the move **L**, dissolving the defect line in the process.

If the $(l \in \mathcal{L})$ -labeled defect line is not a loop, then we apply the contraction move **C**. In any case, the \mathcal{A} -labeled domain now has one adjacent defect line less. We repeat this procedure until

only one other defect line is left. We assume that it is labeled by $j \in \mathcal{J}$.



In the configuration we have now reached (4.85), we can once more apply the **C**-move to the ($j \in \mathcal{J}$)-labeled defect line. This results in a loop labeled by $1 \in \mathcal{A}$ as depicted in (4.86).



We recall the ray and node labels of (4.86). The image of the ray label $y \bullet_{\mathcal{L}} \dots \bullet_{\mathcal{J}} x$ under the forgetful functor can be written as

$$U(y \bullet_{\mathcal{L}} \dots \bullet_{\mathcal{J}} x) = V(x_{(\overline{\mathcal{J}})}, y_{(\mathcal{L})}) \otimes y_{(\overline{\mathcal{N}})} \boxtimes y_{(\mathcal{A})} \boxtimes x_{(\overline{\mathcal{A}})} \boxtimes x_{(\mathcal{M})} \boxtimes \dots, \quad (4.87)$$

where $V(x_{(\overline{\mathcal{J}})}, y_{(\mathcal{L})})$ is some vector space, built from the hom-spaces that appear in the definition (2.197) of the contraction, that is equipped with a balancing

$$V(x_{(\overline{\mathcal{J}})} a, y_{(\mathcal{L})}) \cong V(x_{(\overline{\mathcal{J}})}, a y_{(\mathcal{L})}), \quad a \in \mathcal{A}. \quad (4.88)$$

Recall from (4.27) that we assumed, without loss of generality, the following for the node labels x and y :

$$x_{(\overline{\mathcal{A}})} \boxtimes x_{(\mathcal{M})} = \int_a \bar{a} \boxtimes a x'_{(\mathcal{M})} \quad \text{and} \quad y_{(\overline{\mathcal{N}})} \boxtimes y_{(\mathcal{A})} = \int_a y'_{(\overline{\mathcal{N}})} a^* \boxtimes a. \quad (4.89)$$

The node label in (4.86) is given by the morphism

$$\begin{array}{ccccccc} \mathbb{K} & \otimes & \bar{n} & \boxtimes & \mathbf{1} & \boxtimes & \bar{\mathbf{1}} & \boxtimes & m & \boxtimes & \dots \\ \downarrow v & & \downarrow g_{(\overline{\mathcal{N}})} & & \downarrow g_{(\mathcal{A})} & & \downarrow f_{(\overline{\mathcal{A}})} & & \downarrow f_{(\mathcal{M})} & & \\ V(x_{(\overline{\mathcal{J}})}, y_{(\mathcal{L})}) & \otimes & \int_a \int_b y'_{(\overline{\mathcal{N}})} a^* & \boxtimes & a & \boxtimes & \bar{b} & \boxtimes & b x'_{(\mathcal{M})} & \boxtimes & \dots \end{array} \quad (4.90)$$

for an appropriate vector $v \in V(x_{(\overline{\mathcal{J}})}, y_{(\mathcal{L})})$ obtained from the various other node labels h, k, \dots , that we do not need to specify in more detail. With these data in mind, we apply the **L**-move in order to eliminate the $(\mathbf{1} \in \mathcal{A})$ -labeled loop. The resulting extruded graph has the following topology; the ray- and node labels are specified below.



The ray label of (4.91) is given by $\Phi_{\mathcal{A}} \bullet_{\mathcal{A} \square \overline{\mathcal{A}}} (y \bullet_{\mathcal{L}} \cdots \bullet_{\mathcal{J}} x)$. The appearance of the silent object as opposed to the cosilent object is explained as follows. Compared to (4.20), the loop we consider in (4.86) has opposite orientation. Thus, $\overline{\mathcal{A}}$, not \mathcal{A} , takes on the role of the bimodule category \mathcal{M} from (4.20) that labels the loop. We then use that $\Phi_{\overline{\mathcal{A}}} = \Phi_{\mathcal{A}}$. Importantly, this identification between an end and a coend is only a formal switch of perspective between a category and its opposite, and does not involve the isomorphism $\Theta_{\mathcal{A}}$ obtained from the pivotal structure. We know from (4.21) that without balancings, this objects can be expressed as

$$\begin{aligned}
U(\Phi_{\mathcal{A}} \bullet_{\mathcal{A} \square \overline{\mathcal{A}}} (y \bullet_{\mathcal{L}} \cdots \bullet_{\mathcal{J}} x)) &= {}_{\mathcal{A} \square \overline{\mathcal{A}}} \langle (y \bullet_{\mathcal{L}} \cdots \bullet_{\mathcal{J}} x)_{(\mathcal{A} \square \overline{\mathcal{A}})}, \Phi_{\mathcal{A}} \rangle \otimes y_{(\overline{\mathcal{N}})} \boxtimes x_{(\mathcal{M})} \boxtimes \cdots \\
&\cong {}_{\mathcal{A} \square \overline{\mathcal{A}}} \langle (y \bullet_{\mathcal{L}} \cdots \bullet_{\mathcal{J}} x)_{(\mathcal{A} \square \overline{\mathcal{A}})}, \mathbf{1} \boxtimes \overline{\mathbf{1}} \rangle \otimes y_{(\overline{\mathcal{N}})} \boxtimes x_{(\mathcal{M})} \boxtimes \cdots \\
&\cong {}_{\mathcal{A} \boxtimes \overline{\mathcal{A}}} \langle x_{(\overline{\mathcal{A}})} \boxtimes y_{(\mathcal{A})}, \mathbf{1} \boxtimes \overline{\mathbf{1}} \rangle \otimes y_{(\overline{\mathcal{N}})} \boxtimes x_{(\mathcal{M})} \boxtimes \cdots \\
&\cong \int_{a,b} V(x_{(\overline{\mathcal{J}})}, y_{(\mathcal{L})}) \otimes {}_{\mathcal{A} \boxtimes \overline{\mathcal{A}}} \langle b \boxtimes a, \mathbf{1} \boxtimes \overline{\mathbf{1}} \rangle \otimes y'_{(\overline{\mathcal{N}})} a^* \boxtimes b x'_{(\mathcal{M})} \boxtimes \cdots \\
&\cong V(x_{(\overline{\mathcal{J}})}, y_{(\mathcal{L})}) \otimes y'_{(\overline{\mathcal{N}})} \boxtimes x'_{(\mathcal{M})} \boxtimes \cdots
\end{aligned} \tag{4.92}$$

To get from the first to the second line in (4.92), we used that the silent object of a tensor category can be expressed using the induction functor \boxtimes from (2.108). Then, in the third line, we applied the adjunction (2.112). At this point, we can use our knowledge about the object $U(y \bullet_{\mathcal{L}} \cdots \bullet_{\mathcal{J}} x)$ from (4.89). We could not have plugged in (4.89) earlier, because we do not have an explicit description of the term $(y \bullet_{\mathcal{L}} \cdots \bullet_{\mathcal{J}} x)_{(\mathcal{A} \square \overline{\mathcal{A}})}$ – the warning expressed in Remark 2.30 applies here. Finally, the last step in (4.92) is performed using the Yoneda lemma in the form (2.169).

Part of the data of the node label for (4.91) is, according to (4.24), the morphism

$$r \left((g \circ_l \cdots \circ_j f)_{(\mathcal{A} \boxtimes \overline{\mathcal{A}})} \right) \in {}_{\mathcal{A} \square \overline{\mathcal{A}}} \langle (y \bullet_{\mathcal{L}} \cdots \bullet_{\mathcal{J}} x)_{(\mathcal{A} \square \overline{\mathcal{A}})}, \Phi_{\mathcal{A}} \rangle, \tag{4.93}$$

where r denotes the retraction from Lemma 2.23. An explicit calculation reveals that in our case, the image of this vector pushed through the first two isomorphisms in (4.92) is given by

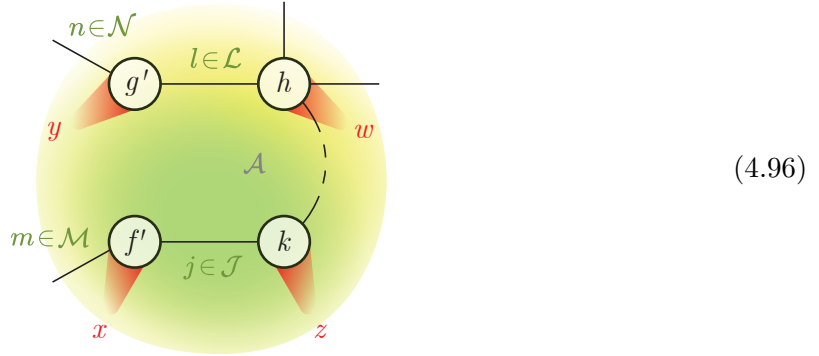
$$f_{(\overline{\mathcal{A}})} \otimes g_{(\mathcal{A})} \in {}_{\mathcal{A} \boxtimes \overline{\mathcal{A}}} \langle x_{(\overline{\mathcal{A}})} \boxtimes y_{(\mathcal{A})}, \mathbf{1} \boxtimes \overline{\mathbf{1}} \rangle. \tag{4.94}$$

This implies that the node label of (4.91) is given by

$$\begin{array}{ccccccc} \mathbb{K} & \otimes & \bar{n} & \boxtimes & m & \boxtimes & \dots \\ \downarrow v & & \downarrow g'_{(\bar{\mathcal{N}})} & & \downarrow f'_{(\mathcal{M})} & & \\ V(x_{(\bar{\mathcal{J}})}, y_{(\mathcal{L})}) & \otimes & y'_{(\bar{\mathcal{N}})} & \boxtimes & x'_{(\mathcal{M})} & \boxtimes & \dots \end{array}, \quad (4.95)$$

where f' and g' are as in (4.28).

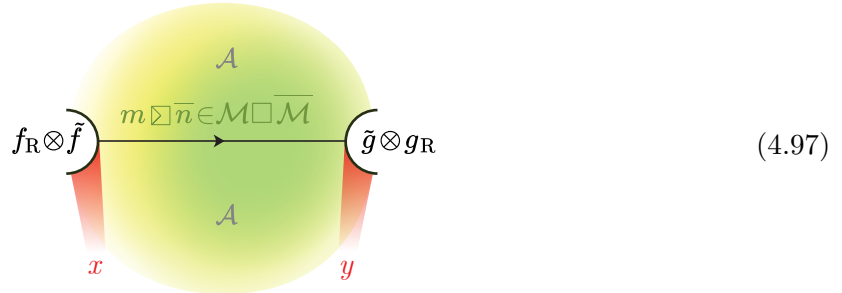
At this point, we take a step back and consider the post-move region, redrawn in our situation here:



All the moves we applied to get from (4.83) to (4.91) can, in the exact same way, be applied to (4.96); except that now, we do not need to apply the **L**-move, because the $(1 \in \mathcal{A})$ -labeled defect line was never present. It is easy to verify that under this sequence of moves, the region (4.96) transforms into the same region (4.91) we obtained before, with the same ray- and node labels that we just computed. This means we have succeeded in writing the move **DE** as a composition of elementary moves.

4.3.4 **IH** – INTERNAL HOM-MOVE

Applying the **OR**-move and the **EF**-move to the left-hand side of (4.30) results in a single defect line:



We now apply the move **C** to both (4.97) and the right-hand side of (4.30) and compare the resulting extruded graphs, which we call Σ and Σ' , respectively.

The label of the, now unique, ray in Σ , the contracted version of (4.97), is given by $x \bullet_{\mathcal{M} \boxtimes \overline{\mathcal{M}}} y$. Recall from (2.192) that

$$U(x \bullet_{\mathcal{M} \boxtimes \overline{\mathcal{M}}} y) = {}_{\mathcal{M} \boxtimes \overline{\mathcal{M}}} \langle y_{(\mathcal{M} \boxtimes \overline{\mathcal{M}})}, x_{(\mathcal{M} \boxtimes \overline{\mathcal{M}})} \rangle \otimes x_{(\mathcal{R})} \boxtimes y_{(\mathcal{R})}. \quad (4.98)$$

The node of Σ is labeled by $f_{\mathcal{R}} \otimes (g \circ_m \boxtimes_{\overline{\mathcal{N}}} f) \otimes g_{\mathcal{R}}$.

On the other hand, after applying \mathbf{C} to the right-hand side of (4.30), we are left with Σ' , which contains a single ray labeled by $\mathcal{A}[x] \bullet_{\mathcal{B} \mathcal{A}} \mathcal{A}[y]$, with node label $f_{\mathcal{R}} \otimes (\mathcal{A}[\tilde{g}] \circ_{\mathcal{A}[n, m]} \mathcal{A}[\tilde{f}]) \otimes g_{\mathcal{R}}$. Note that the underlying labeled defect surfaces of Σ and Σ' are equal: both only consist of a single ray, whose ray categories are the same. The linear map ${}_{\mathcal{M} \boxtimes \overline{\mathcal{M}}} \langle y_{(\mathcal{M} \boxtimes \overline{\mathcal{M}})}, x_{(\mathcal{M} \boxtimes \overline{\mathcal{M}})} \rangle \rightarrow \mathcal{A} \langle \mathcal{A}[y_{(\mathcal{M} \boxtimes \overline{\mathcal{M}})}], \mathcal{A}[x_{(\mathcal{M} \boxtimes \overline{\mathcal{M}})}] \rangle$ that comes with the functoriality of $\mathcal{A}[-]$ defines a morphism $U(x \bullet_{\mathcal{M} \boxtimes \overline{\mathcal{M}}} y) \rightarrow U(\mathcal{A}[x] \bullet_{\mathcal{B} \mathcal{A}} \mathcal{A}[y])$ which respects the balancings, and thus is a morphism between the ray labels $\eta : x \bullet_{\mathcal{M} \boxtimes \overline{\mathcal{M}}} y \rightarrow \mathcal{A}[x] \bullet_{\mathcal{B} \mathcal{A}} \mathcal{A}[y]$. As the block spaces for different ray labels on a given labeled defect surface assemble into a functor, the map η between two ray labels defines a map between block spaces $\mathbb{T}(\eta) : \mathbb{T} \rightarrow \mathbb{T}'$. In order to construct a post-move core label φ' from the label φ of the core of Σ , we use a retraction of the linear map $T(\eta)$. The existence of such a retraction is inherited from the fact that

$$\mathcal{A}[-] : {}_{\mathcal{M} \boxtimes \overline{\mathcal{M}}} \langle y_{(\mathcal{M} \boxtimes \overline{\mathcal{M}})}, x_{(\mathcal{M} \boxtimes \overline{\mathcal{M}})} \rangle \rightarrow \mathcal{A} \langle \mathcal{A}[y_{(\mathcal{M} \boxtimes \overline{\mathcal{M}})}], \mathcal{A}[x_{(\mathcal{M} \boxtimes \overline{\mathcal{M}})}] \rangle \quad (4.99)$$

admits a retraction γ , which can be constructed as follows. Note that a morphism $t : y_{(\mathcal{M} \boxtimes \overline{\mathcal{M}})} \rightarrow x_{(\mathcal{M} \boxtimes \overline{\mathcal{M}})}$ is a morphism of unbalanced objects $t : y_{(\mathcal{M})} \boxtimes y_{(\overline{\mathcal{M}})} \rightarrow x_{(\mathcal{M})} \boxtimes x_{(\overline{\mathcal{M}})}$ that satisfies a property. The simple objects of the Deligne product $\mathcal{M} \boxtimes \overline{\mathcal{M}}$ are of the form $\mathbf{m} \boxtimes \overline{\mathbf{n}}$, where \mathbf{m} and $\overline{\mathbf{n}}$ are simples in \mathcal{M} , which is why the collection of morphisms

$$\tilde{t}_{\mathbf{m}, \overline{\mathbf{n}}, j, i} := \star \langle x_{(\mathcal{M})} \boxtimes x_{(\overline{\mathcal{M}})}, \mathbf{m} \boxtimes \overline{\mathbf{n}} \rangle_{, i} \circ t \circ \star \langle \mathbf{m} \boxtimes \overline{\mathbf{n}}, y_{(\mathcal{M})} \boxtimes y_{(\overline{\mathcal{M}})} \rangle_{, j} \quad (4.100)$$

uniquely determines the morphism t . As endomorphisms of simple objects, the $\tilde{t}_{\mathbf{m}, \overline{\mathbf{n}}, j, i}$ are multiples of the identity, and thus correspond to scalars

$$t_{\mathbf{m}, \overline{\mathbf{n}}, j, i} = \frac{1}{d_{\mathbf{m}} d_{\overline{\mathbf{n}}}} \text{Tr}_{\mathcal{M} \boxtimes \overline{\mathcal{M}}}(\tilde{t}_{\mathbf{m}, \overline{\mathbf{n}}, j, i}), \quad (4.101)$$

which can be thought of as the matrix elements of t .

These matrix elements can be recovered from $\mathcal{A}[t]$ by observing that if $\tilde{t}_{\mathbf{m}, \overline{\mathbf{n}}, j, i}$ is a multiple of the identity, then so is

$$\mathcal{A}[\tilde{t}_{\mathbf{m}, \overline{\mathbf{n}}, j, i}] = \mathcal{A}[\star \langle x_{(\mathcal{M})} \boxtimes x_{(\overline{\mathcal{M}})}, \mathbf{m} \boxtimes \overline{\mathbf{n}} \rangle_{, i}] \circ \mathcal{A}[t] \circ \mathcal{A}[\star \langle \mathbf{m} \boxtimes \overline{\mathbf{n}}, y_{(\mathcal{M})} \boxtimes y_{(\overline{\mathcal{M}})} \rangle_{, j}]. \quad (4.102)$$

We thus find

$$t_{\mathbf{m}, \overline{\mathbf{n}}, j, i} = \frac{1}{d_{\mathcal{A}[\mathbf{n}, \overline{\mathbf{m}}]}} \mathcal{A}[\star \langle x_{(\mathcal{M})} \boxtimes x_{(\overline{\mathcal{M}})}, \mathbf{m} \boxtimes \overline{\mathbf{n}} \rangle_{, i}] \circ \mathcal{A}[t] \circ \mathcal{A}[\star \langle \mathbf{m} \boxtimes \overline{\mathbf{n}}, y_{(\mathcal{M})} \boxtimes y_{(\overline{\mathcal{M}})} \rangle_{, j}], \quad (4.103)$$

and deduce that a retraction to $\mathcal{A}[-]$ can, in terms of matrix elements, be defined for a morphism $u : \mathcal{A}[y_{(\mathcal{M} \square \overline{\mathcal{M}})}] \rightarrow \mathcal{A}[x_{(\mathcal{M} \square \overline{\mathcal{M}})}]$ by

$$\gamma(u)_{\mathbf{m}, \overline{\mathbf{n}}, j, i} = \frac{1}{d_{\mathcal{A}[\mathbf{n}, \mathbf{m}]}} \mathcal{A}[\star \langle x_{(\mathcal{M})} \boxtimes x_{(\overline{\mathcal{M}})}, \mathbf{m} \boxtimes \overline{\mathbf{n}} \rangle, i] \circ u \circ \mathcal{A}[\star \langle \mathbf{m} \boxtimes \overline{\mathbf{n}}, y_{(\mathcal{M})} \boxtimes y_{(\overline{\mathcal{M}})} \rangle, j]. \quad (4.104)$$

The retraction γ induces a retraction $\tilde{\gamma} : \mathbb{T}' \rightarrow \mathbb{T}$ of $\mathbb{T}(\eta)$, which allows us to define $\varphi' := \varphi \circ \tilde{\gamma}$ for the post-move core label. This implies that the move is an invariance.

Remark 4.8. The morphism γ can be defined in a more conceptual way, but showing that it is a retraction is then more tedious. This involves noting that the right adjoint of $\mathcal{A}[-]$ denoted by \mathbf{coev} in [Sch13a, Lem. 6.2.2] is also a left adjoint. Then γ is defined as the composition

$$\begin{aligned} \mathcal{A} \langle \mathcal{A}[y_{(\mathcal{M} \square \overline{\mathcal{M}})}], \mathcal{A}[x_{(\mathcal{M} \square \overline{\mathcal{M}})}] \rangle &\rightarrow \mathcal{A} \langle \mathbf{coev}(\mathcal{A}[y_{(\mathcal{M} \square \overline{\mathcal{M}})}]), \mathbf{coev}(\mathcal{A}[x_{(\mathcal{M} \square \overline{\mathcal{M}})}]) \rangle \\ &\rightarrow \mathcal{M} \square \overline{\mathcal{M}} \langle y_{(\mathcal{M} \square \overline{\mathcal{M}})}, x_{(\mathcal{M} \square \overline{\mathcal{M}})} \rangle \end{aligned} \quad (4.105)$$

using the unit and counit of the adjunctions.

This completes the proof of Theorem 4.4.

5 TOWARDS A TURAEV-VIRO TFT WITH DEFECTS

The main motivation for the notion of an extruded graph, together with the evaluation procedure defined in Section 3, is that they are a critical ingredient in the definition of a state-sum model with defects in all codimensions, whose union is not necessarily a manifold. While the definition of such a state-sum model (or, more precisely, its independence of auxiliary data) beyond the sketch provided in Section 5.4 exceeds the scope of this work, we demonstrate in this section that in a special case, the evaluation of extruded graphs reduces to a known evaluation procedure used for the definition of known state-sum models.

The special case we are interested in are extruded graphs whose underlying surfaces are spheres, with a restriction on the algebraic labels: All domains are labeled by the same spherical fusion category \mathcal{A} , and all edges are labeled by the regular bimodule category ${}_{\mathcal{A}}\mathcal{A}_{\mathcal{A}}$. We do not restrict labels of the third and fourth level: the object labels on the defect lines, ray labels and node labels. We call extruded graphs of this type *monochromatic*.

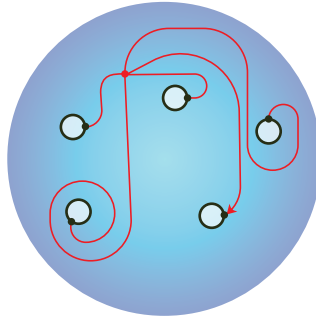
This restriction of algebraic data to a single spherical fusion category \mathcal{A} and no non-trivial bimodule categories fits into the context of the Turaev-Viro state-sum model on \mathcal{A} as described in [BK10; TV17]. This is a 3-dimensional TFT defined on a cobordism category in which the cobordisms are decorated with embedded ribbons, labeled by objects of the Drinfeld center $Z_{\mathcal{A}}(\mathcal{A})$. In order to define the TFT, a scalar must be assigned to what we will call a *spiked ball* in Definition 5.1: a closed 3-ball with $Z_{\mathcal{A}}(\mathcal{A})$ -labeled lines embedded in the interior and an \mathcal{A} -labeled graph on the boundary. This evaluation procedure involves, as a first step, projecting the interior lines onto the surface of the ball, such that we obtain a graph on \mathbb{S}^2 with strands labeled either by objects of \mathcal{A} or $Z_{\mathcal{A}}(\mathcal{A})$, with crossings allowed between strands of different

types. Such a combined graph Γ is called a *knotted \mathcal{A} -net in \mathbb{S}^2* in the language of [TV17], and the associated invariant is denoted $\mathbb{F}_{\mathcal{A}}(\Gamma) \in \mathbb{K}$.

After recalling some necessary background in Section 5.1, the goal of Section 5.2 is to first show how the evaluation of extruded graphs introduced in this paper can be used to define *another* evaluation procedure for spiked balls. Then, we will show that both evaluation procedures produce the same numerical invariant. This fact will serve as justification that extruded graphs, together with their evaluation procedure, are the correct generalization of spiked balls needed when defining a state-sum model with defects in all codimensions. In Section 5.3, we will briefly see that extruded graphs and their evaluation are closely related to yet another type of diagram used in a state-sum model with defects: The *polygon diagrams* introduced by Meusburger [Meu22]. We end with an outlook on how a Turaev-Viro-type TFT could be defined using the theory of extruded graphs in Section 5.4.

5.1 THE LEGO-TEICHMÜLLER GAME

In order to understand the block spaces for monochromatic extruded graphs, we need to recall some details of the so-called *Lego-Teichmüller Game* (LTG) from [MS89; BK00]. Let \mathcal{S} be a compact oriented surface of genus 0, possibly with boundary (hence a sphere with a finite number of holes), together with a choice of distinguished point on each boundary component. Such a surface is called an *extended surface* (of genus 0, the only case we consider here) [BK00]. A *marking* on an extended surface is a graph $M \subset \mathcal{S}$ embedded in \mathcal{S} of the following form: M has a unique vertex in the interior of \mathcal{S} , its other vertices are the distinguished points on the boundary of \mathcal{S} . M has one edge for each boundary component of \mathcal{S} , connecting the distinguished point on that boundary component to the unique vertex in the interior of \mathcal{S} . In addition, one of the edges of the marking M is distinguished; in the picture (5.1), which illustrates an example for an extended surface with a marking, this edge is drawn as an arrow.



(5.1)

Given a (finite, semisimple) ribbon category \mathcal{C} (that is, a braided tensor category with duals and a twist, see [EGNO15, Sec. 8.10]), let us label each boundary component of a marked extended surface with n boundary components ($n \geq 0$) with an object $c_i \in \mathcal{C}$ ($1 \leq i \leq n$). The marking graph on the extended surface provides a cyclic order on the boundary components (and hence on the objects c_i), which together with the distinguished edge becomes even a linear order in the obvious way: The boundary component adjacent to the distinguished edge of the marking is set as the first element in the order, and from hereon, we order the other edges, progressing

in clockwise cyclic fashion around the distinguished vertex of the marking. To such a marked extended surface (\mathcal{S}, M) with labels (c_\bullet) , we assign the vector space

$$\tau(\mathcal{S}, M, c_\bullet) := c\langle \mathbb{1}, c_1 \otimes \cdots \otimes c_n \rangle. \quad (5.2)$$

Of course, a different marking M' on \mathcal{S} can result in a different order for the objects (c_\bullet) . The orders for the markings M and M' are related by a permutation σ , such that

$$\tau(\mathcal{S}, M', c_\bullet) = c\langle \mathbb{1}, c_{\sigma(1)} \otimes \cdots \otimes c_{\sigma(n)} \rangle. \quad (5.3)$$

Using the braiding for \mathcal{C} , one can construct many different isomorphisms between the vector spaces $\tau(\mathcal{S}, M, c_\bullet)$ and $\tau(\mathcal{S}, M', c_\bullet)$. In order to construct a vector space that is independent of the choice of marking, however, a clique is needed. (Recall that a clique is a category with a unique isomorphism between any two objects.) While the set of vector spaces associated with different markings is not suitable as the set of objects for this clique, the set of markings itself is: The morphisms between markings are given by a set of moves between markings, taken up to relations between the moves. The fact that markings and moves-up-to-relations form a clique is proved in [BK00, Thm. 4.9], and was previously stated in [MS89]. As such, we may define the vector space

$$\tau(\mathcal{S}, c_\bullet) := \lim_M \tau(\mathcal{S}, M, c_\bullet). \quad (5.4)$$

Since $\tau(\mathcal{S}, c_\bullet)$ is defined using only the combinatorial structure of the markings on \mathcal{S} , it does not depend on the extended surface \mathcal{S} beyond its isomorphism class. We therefore denote

$$\tau_n(c_\bullet) := \tau(\mathcal{S}, c_\bullet) \quad (5.5)$$

for any extended surface \mathcal{S} with n boundary components and an unordered set of n objects of \mathcal{C} labeling the boundary components c_\bullet . The vector spaces $\tau_n(c_\bullet)$ are called *conformal blocks*.

5.2 RELATING EXTRUDED GRAPHS TO KNOTTED NETS

We define the notion of a spiked ball mentioned in the beginning of this section.

Definition 5.1. A *spiked ball* R colored by a spherical fusion category \mathcal{A} consists of a solid closed 3-ball R with embedded structure as follows: On the boundary ∂R of the 3-ball, which is a 2-sphere, a string diagram (an \mathcal{A} -colored graph in the sense of [TV17, Sec. 12.2.1]) is embedded, with strands labeled by objects of \mathcal{A} . Attached to some of the vertices are *spikes*: straight lines that stretch from a vertex on the boundary to the point $r \in R$ in the center of the ball. The spikes are labeled by objects of the Drinfeld center $Z_{\mathcal{A}}(\mathcal{A})$, and vertices that have attached spikes are called *spiked vertices*. As usual, we only consider *fine* spiked balls, meaning that the complement of the string diagram on the boundary is a disjoint union of disks.

On the boundary of R , the spiked vertices are labeled by vectors in spaces that can be thought of as cyclically symmetric hom-spaces. They are constructed as follows. Attached to a spiked vertex v is a spike, labeled by an object $x \in Z_{\mathcal{A}}(\mathcal{A})$. The adjacent edges on the boundary of R come with a cyclic order, and each with an orientation and an object $a_i \in \mathcal{A}$. For a given choice of a first edge in this cyclic order, we associate the hom-space

$${}_{\mathcal{A}}\langle a_1 \otimes \cdots \otimes a_{n-1} \otimes a_n, U(x) \rangle \quad (5.6)$$

if there are n many edges pointing towards the vertex. If an edge is pointing away from the vertex, the dual a_i^* of the corresponding object a_i is taken in its place. Using a combination of evaluation, coevaluation, and pivotality for \mathcal{A} , and the half-braiding for x , the covariant arguments in the hom-functor (5.6) can be cyclically permuted in the standard way, meaning there are canonical isomorphisms

$$\langle a_1 \otimes \cdots a_{n-1} \otimes a_n, U(x) \rangle \cong \langle a_n \otimes a_1 \otimes \cdots a_{n-1}, U(x) \rangle. \quad (5.7)$$

These isomorphisms are well understood, see e.g. [NS10]. Together with the permuted hom-spaces, they form a clique, and so we define

$$H(x, a_\bullet) := \lim_{\sigma} \langle a_{\sigma(1)} \otimes \cdots \otimes a_{\sigma(n)}, U(x) \rangle, \quad (5.8)$$

where σ runs over cyclic permutations. This is the vector space associated to the spiked vertex v . For a non-spiked vertex w , we replace x by the monoidal unit $\mathbf{1} \in Z_{\mathcal{A}}(\mathcal{A})$ in this construction. The vector spaces for non-spiked vertices are called *multiplicity modules* in [TV17, Sec. 12.1.3], and we will carry this name over to the more general spaces (5.8) for spiked vertices as well. (There is a difference between our convention and the one used in [TV17, Sec. 12.1.3]: The contravariant and the covariant arguments in the hom-functor (5.6) are exchanged.)

Finally, the central point $r \in R$ where all the spikes meet, is labeled by a vector in the dual of the vector space $\tau_k(x_\bullet)^*$ from (5.5), if there are k many spikes labeled by a collection x_\bullet of objects of $Z_{\mathcal{A}}(\mathcal{A})$.

The following picture is an illustration of a spiked ball:



In (5.9), the string diagram on ∂R is black, and the spikes are drawn in red. They point to the center r of the 3-ball.

Remark 5.2. Usually, to evaluate a diagram involving strands labeled by objects in a ribbon category such as $Z_{\mathcal{A}}(\mathcal{A})$ embedded into 3-dimensional space, these strands need to have ribbon structure, or equivalently, a framing. This is unnecessary in spiked balls because the spikes are straight lines pointing to the center of R . They can be equipped with a standard framing.

We would like to be able to identify spiked balls and monochromatic extruded graphs.

Observation 5.3. Let Σ be a monochromatic extruded graph on the sphere, meaning that all domains are labeled by the same spherical fusion category \mathcal{A} , and all defect lines are labeled by the regular bimodule category ${}_{\mathcal{A}}\mathcal{A}_{\mathcal{A}}$. Spiked balls and monochromatic extruded graphs have the same types of labels:

1. There is a distinguished set of equivalences between the ray category for any ray of Σ and the center $Z_{\mathcal{A}}(\mathcal{A})$: The ray category associated to any node L (with $n > 0$ adjacent defect lines) of a monochromatic extruded graph is of the form

$$\mathbb{T}^{\text{R}}(L) = \mathcal{A}^{\epsilon_1} \square \mathcal{A}^{\epsilon_2} \square \cdots \square \mathcal{A}^{\epsilon_n} \square, \quad (5.10)$$

where $\epsilon_i \in \{+, -\}$ are signs used to denote the opposed categories $\overline{\mathcal{A}} = \mathcal{A}^-$, $\mathcal{A} = \mathcal{A}^+$, depending on the orientation of the adjacent defect lines. The pivotal structure on the category \mathcal{A} furnishes an equivalence $\overline{\mathcal{A}} \cong \mathcal{A}$, which provides a distinguished equivalence

$$\mathbb{T}^{\text{R}}(L) \cong \mathcal{A} \square \mathcal{A} \square \cdots \square \mathcal{A} \square. \quad (5.11)$$

As mentioned in Section 2.12, the expression (5.11) is a 3-trace over a composition of 1-morphisms in a tricategory. As such, several structure morphisms can be used to obtain equivalences $\mathbb{T}^{\text{R}}(L) \cong Z_{\mathcal{A}}(\mathcal{A})$. It follows from the coherence theorem for 3-traces [FSS17, Prop. 5.4] that there is a distinguished natural isomorphism between any two of these equivalences, such that the equivalences, together with the natural isomorphisms, form a clique.

In order to avoid making explicit choices, we denote by

$$\mu_L : \mathbb{T}^{\text{R}}(L) \cong Z_{\mathcal{A}}(\mathcal{A}) \quad (5.12)$$

the limit of the clique of equivalences associated to the ray adjacent to a node L .

2. Let L be a node in Σ with adjacent ray labeled by $x \in \mathbb{T}^{\text{R}}(L)$, and adjacent defect lines labeled, in clockwise order, by objects $a_1, \dots, a_n \in \mathcal{A}$. Let us construct an isomorphism between the associated node space $\text{N}(L)$ and the multiplicity module $H(\mu_L(x), a_{\bullet})$ from (5.8).

As we saw in (5.11), the ray category is of the form

$$\mathbb{T}^{\text{R}}(L) \cong \mathcal{A}_1 \square \mathcal{A}_2 \square \cdots \square \mathcal{A}_n \square. \quad (5.13)$$

for n adjacent defect lines. In (5.13), we introduced subscripts for the various instances of $\mathcal{A} = \mathcal{A}_1 = \cdots = \mathcal{A}_n$ in order to keep track of which tensorand corresponds to which adjacent defect line. We continue to explicitly describe a sub-clique of the clique of equivalences $\mathbb{T}^{\text{R}}(L) \cong Z_{\mathcal{A}}(\mathcal{A})$ from part (1) of the observation. Given a relative Deligne product of k copies of \mathcal{A} , which is linearly ordered in the sense that one tensorand is chosen as the starting point, we consider the equivalence

$$\mathcal{A}_1 \square \cdots \square \mathcal{A}_{k-1} \square \mathcal{A}_n \square \rightarrow \mathcal{A}_1 \square \cdots \square \mathcal{A} \square, \quad (5.14)$$

obtained by applying the unitor $e : \mathcal{A}_{k-1} \square \mathcal{A}_n \rightarrow \mathcal{A}$ from (2.134) to the right-most two tensorands. (Recall that we do not take the relative Deligne product's associators into account.). Successively composing instances of the equivalence (5.14) produces n distinct equivalences $e_1, \dots, e_n : \mathbb{T}^{\text{R}}(L) \rightarrow Z_{\mathcal{A}}(\mathcal{A})$, one for each choice of starting point.

We denote the ray label by $x \in \mathbb{T}^{\mathbb{R}}(L)$. Recall that the nodespace is, in this case, given by

$$\mathbb{N}(L) = \mathbb{T}^{\mathbb{N}}(L) \langle a_1 \boxtimes \cdots \boxtimes a_n, U(x) \rangle, \quad (5.15)$$

where U denotes the forgetful functor $\mathcal{A}^{\square n} \rightarrow \mathcal{A}^{\boxtimes n}$, which forgets all n balancings. Depending on the signs ϵ_i from (5.10), some of the a_i should be replaced by their duals a_i^* , but we do not make this explicit in order not to overload notation. For our purposes, it is useful to consider the nodespace as a hom-space in the ray category rather than the node category, by passing through the adjunction (2.111):

$$\mathbb{N}(L) \cong \mathbb{T}^{\mathbb{R}}(L) \langle a_1 \boxtimes \cdots \boxtimes a_n \boxtimes, x \rangle. \quad (5.16)$$

In this form, it is clear that each equivalence e_1, \dots, e_n provides an isomorphism $\mathbb{N}(L) \cong Z_{\mathcal{A}}(\mathcal{A}) \langle e_i(a_1 \boxtimes \cdots \boxtimes a_n \boxtimes), e_i(x) \rangle$. Since we know from (2.135) that

$$e_i(a_1 \boxtimes \cdots \boxtimes a_n \boxtimes) = a_i \cdots a_n a_1 \cdots a_{i-1} \boxtimes \in Z_{\mathcal{A}}(\mathcal{A}), \quad (5.17)$$

we can once more use the adjunction (2.111), this time in reverse direction, to find an isomorphism

$$\mathbb{N}(L) \cong \mathcal{A} \langle a_i \cdots a_n a_1 \cdots a_{i-1}, U(e_i(x)) \rangle. \quad (5.18)$$

Here, the functor $U : Z_{\mathcal{A}}(\mathcal{A}) \rightarrow \mathcal{A}$ only forgets one balancing (namely, the half-braiding). If we combine the isomorphism (5.18) with the structure isomorphism of the limit (5.8), we obtain an isomorphism

$$\mathbb{N}(L) \cong H(\mu_L(x), a_{\bullet}). \quad (5.19)$$

A priori, this isomorphism is dependent on the choice of linear order we made on the set of adjacent defect lines. We will see in Proposition 5.4 that any such choice leads to the same isomorphism (5.19).

We will compare block spaces of monochromatic extruded graphs to the vector spaces $\tau_n(c_{\bullet})$ from (5.5) for spiked balls later, in Observation 5.6

Proposition 5.4. *The isomorphism $\mathbb{N}(L) \cong H(\mu_L(x), a_{\bullet})$ between the nodespace of a monochromatic extruded graph's node L and the multiplicity module $H(\mu_L(x), a_{\bullet})$ from (5.19) is independent of the choice of linear order imposed on the set of defect lines adjacent to L .*

Proof. The isomorphisms (5.18) turn the set of hom-spaces $\mathcal{A} \langle a_i \cdots a_n a_1 \cdots a_{i-1}, U(e_i(x)) \rangle$ into a clique, whose limit is the nodespace $\mathbb{N}(L)$. The canonical isomorphisms $e_i(x) \cong \mu_L(x)$, denoted by ν_i , furnish isomorphisms between the hom-spaces

$$\mathcal{A} \langle a_i \cdots a_n a_1 \cdots a_{i-1}, U(e_i(x)) \rangle \cong \mathcal{A} \langle a_i \cdots a_n a_1 \cdots a_{i-1}, U(\mu_L(x)) \rangle \quad (5.20)$$

The latter hom-spaces appeared in (5.8): Together with the morphisms (5.7), they also form a clique, whose limit is the multiplicity module $H(\mu_L(x), a_{\bullet})$. In order to deduce that the limits of these two cliques are related by a canonical isomorphism

$$\mathbb{N}(L) \cong H(\mu_L(x), a_{\bullet}), \quad (5.21)$$

we need to show that the set of isomorphisms (5.20) between objects of the cliques assemble into an isomorphism of cliques. Explicitly, this means that the diagram

$$\begin{array}{ccc}
\mathcal{A}\langle a_i \cdots a_n a_1 \cdots a_{i-1}, U(e_i(x)) \rangle & \xrightarrow{\nu_i \circ -} & \mathcal{A}\langle a_i \cdots a_n a_1 \cdots a_{i-1}, U(\mu_L(x)) \rangle \\
(5.18) \uparrow & & \downarrow (5.7) \\
\mathbf{N}(L) & & \\
(5.18) \downarrow & & \\
\mathcal{A}\langle a_j \cdots a_n a_1 \cdots a_{j-1}, U(e_j(x)) \rangle & \xrightarrow{\nu_j \circ -} & \mathcal{A}\langle a_j \cdots a_n a_1 \cdots a_{j-1}, U(\mu_L(x)) \rangle
\end{array} \tag{5.22}$$

needs to commute for all $i, j \in \{1, \dots, n\}$. It suffices to check this for the case $i = 1, j = 2$. For the proof, we consider the following diagram, which is described in detail below.

$$\begin{array}{ccccc}
& & \mathbf{N}(L) \cong \langle a_1 \boxtimes a_2 \boxtimes \cdots \boxtimes a_n \boxtimes, x \rangle & & \\
& & \swarrow -\text{obal}_1 & & \searrow -\text{obal}_2 \\
\langle a_1 a_2 \cdots a_n \boxtimes \mathbf{1} \boxtimes \cdots \boxtimes \mathbf{1} \boxtimes, x \rangle & \xrightarrow{-\text{obal}} & \langle \mathbf{1} \boxtimes a_2 \cdots a_n a_1 \boxtimes \cdots \boxtimes \mathbf{1} \boxtimes, x \rangle & & \\
\downarrow e_1 & & \swarrow e_1 & & \downarrow e_2 \\
& & \langle a_2 \cdots a_n a_1 \boxtimes, e_1(x) \rangle & & \\
\downarrow \text{adj} \boxtimes & & \swarrow -\circ e_1(\text{bal}) & & \downarrow \text{adj} \boxtimes \\
\langle a_1 a_2 \cdots a_n \boxtimes, e_1(x) \rangle & & \langle a_2 \cdots a_n a_1 \boxtimes, e_1(x) \rangle & & \langle a_2 \cdots a_n a_1 \boxtimes, e_2(x) \rangle \\
& & \swarrow -\circ e_1(\text{bal}) & & \swarrow \eta_x \circ - \\
& & \langle a_2 \cdots a_n a_1 \boxtimes, e_1(x) \rangle & & \langle a_2 \cdots a_n a_1, U(e_2(x)) \rangle \\
& & \downarrow \text{adj} \boxtimes & & \downarrow \text{adj} \boxtimes \\
\langle a_1 a_2 \cdots a_n, U(e_1(x)) \rangle & & \langle a_2 \cdots a_n a_1, U(e_1(x)) \rangle & & \langle a_2 \cdots a_n a_1, U(e_2(x)) \rangle \\
& & \swarrow (5.7) & & \swarrow U(\eta_x) \circ - \\
& & \langle a_2 \cdots a_n a_1, U(e_1(x)) \rangle & & \langle a_2 \cdots a_n a_1, U(\mu_L(x)) \rangle \\
& & \downarrow \nu_1 \circ - & & \downarrow \nu_2 \circ - \\
\langle a_1 a_2 \cdots a_n, U(\mu_L(x)) \rangle & \xrightarrow{(5.7)} & \langle a_2 \cdots a_n a_1, U(\mu_L(x)) \rangle & & \langle a_2 \cdots a_n a_1, U(\mu_L(x)) \rangle
\end{array} \tag{5.23}$$

Let us first discuss the morphisms that appear in the top triangle of the diagram (5.23). Recall that the functor $-\boxtimes-$ is balanced. From this balancing, we can construct an isomorphism

$$\begin{aligned}
a_1 \boxtimes a_2 \boxtimes \cdots \boxtimes a_n \boxtimes &\cong a_1 \boxtimes a_2 \boxtimes \cdots \boxtimes a_{n-1} a_n \boxtimes \mathbf{1} \boxtimes \cong \dots \\
&\cong a_1 \boxtimes a_2 \cdots a_n \boxtimes \cdots \boxtimes \mathbf{1} \boxtimes \cong a_1 a_2 \cdots a_n \boxtimes \mathbf{1} \boxtimes \cdots \boxtimes \mathbf{1} \boxtimes,
\end{aligned} \tag{5.24}$$

whose inverse we denote by bal_1 . Similarly, bal_2 is the inverse of the isomorphism

$$a_1 \boxtimes a_2 \boxtimes \cdots \boxtimes a_n \boxtimes \cong \mathbf{1} \boxtimes a_2 \boxtimes \cdots \boxtimes a_n a_1 \boxtimes \cong \dots \cong \mathbf{1} \boxtimes a_2 \cdots a_n a_1 \boxtimes \cdots \boxtimes \mathbf{1} \boxtimes. \tag{5.25}$$

We define $\text{bal} := \text{bal}_1 \circ \text{bal}_2^{-1}$ – this makes the topmost triangle of (5.23) commute – and remark that explicitly, bal is given by the composition

$$\begin{aligned} \mathbb{1} \boxtimes a_2 \cdots a_n a_1 \boxtimes \cdots \boxtimes \mathbb{1} \boxtimes &\cong a_2 \cdots a_n \boxtimes a_1 \boxtimes \cdots \boxtimes \mathbb{1} \boxtimes \cong a_2 \cdots a_n \boxtimes \mathbb{1} \boxtimes a_1 \boxtimes \cdots \boxtimes \mathbb{1} \boxtimes \\ &\cong a_2 \cdots a_n \boxtimes \mathbb{1} \boxtimes \cdots \boxtimes a_1 \boxtimes \cong a_1 a_2 \cdots a_n \boxtimes \mathbb{1} \boxtimes \cdots \boxtimes \mathbb{1} \boxtimes. \end{aligned} \quad (5.26)$$

In other words, the term $a_2 \cdots a_n$ gets balanced using just one balancing from left to right, while a_1 passes through all the other balancings in right-to-left direction.

With this at hand, we now explain why the commutativity of the outer paths of (5.23) is equivalent to the commutativity of (5.22): The isomorphism (5.18) appearing in (5.22) is equal to the composition $\text{adj}^{\boxtimes} \circ e_i$. Moreover, we have $e_i = e_i \circ (- \circ \text{bal}_i)$. This is because the equivalences e_i are constructed from the unitors (5.14), which map all balancings to the identity morphism (or, more precisely, to associators, which we assume to be the identity for \mathcal{A}). Thus, the first three arrows around the left and right side compose to instances of the morphism (5.18) for $i = 1$ and $i = 2$, respectively. So, proving that the boundary of (5.23) commutes implies the commutativity of (5.22).

We continue to inspect the cells of the diagram from top to bottom, and show that each one commutes. The commutativity of the cell (a) is a consequence of the functoriality of e_1 . New morphisms labeled η appear in the cell (b); η is the canonical natural isomorphism $\eta : e_2 \rightarrow e_1$, which is part of the clique from part (1) of the observation. Commutativity of (b) is an instance of the naturality of η . In order to see that the triangle to the left of (b) commutes, we observe that its vertical arrow is equal to the identity. The images of e_1 and e_2 of a \boxtimes -factorized object, such as $a_1 \boxtimes \cdots \boxtimes a_n \boxtimes$, differ only by a different bracketing of the terms. The isomorphism η relates these bracketings via associators, which we have assumed to be the identity. Thus, $\eta_{\mathbb{1} \boxtimes a_2 \cdots a_n a_1 \boxtimes \cdots \boxtimes \mathbb{1} \boxtimes} = \text{id}$, and the triangle commutes.

The cell (c) commutes because $\text{adj}^{\boxtimes} : \langle -, e_1(x) \rangle \rightarrow \langle -, U(e_1(x)) \rangle$ is an isomorphism of balanced functors, as mentioned in Remark 2.22. On the other hand, the cell (d) is just an instance of the naturality of adj^{\boxtimes} .

The cell (e) commutes because ν_1 is an isomorphism in the center of \mathcal{A} . Finally, the triangle in the bottom right of the diagram commutes because ν_i are the structure morphisms of the limit $\mu_L(x)$ of a clique in which η_x is a morphism.

We have now seen that all cells of the diagram (5.23), and hence its boundary, commute. This completes the proof of the proposition. \square

Observation 5.3, together with Proposition 5.4 provides us with an understanding of monochromatic ray- and node labels. In order to describe monochromatic core labels, we first need to understand how moves of invariance work for monochromatic extruded graphs. In the following, we already allow ourselves to consider monochromatic extruded graphs whose rays are labeled by objects in $Z_{\mathcal{A}}(\mathcal{A})$ and whose nodes are labeled by vectors in the appropriate multiplicity modules.

Lemma 5.5 (Monochromatic moves.). *The moves of invariance for extruded graphs from Section 4 can be expressed using the alternative system of labeling rays and nodes from Observation 5.3. We list some of them here:*

- The ordinary **OR**-move flips the direction of a defect line, thereby changing the bimodule category \mathcal{M} that labels it to its opposite $\overline{\mathcal{M}}$. The **OR**-move is thus not a move within the class of monochromatic extruded graphs, because it results in defect lines labeled by $\overline{\mathcal{A}}$, which is not allowed. When we speak of the monochromatic **OR**-move, we really mean the composition of the **OR**-move applied to an \mathcal{A} -labeled defect line with an instance of the **Fun**-move using the distinguished equivalence $\overline{\mathcal{A}} \cong \mathcal{A}$ that comes with the pivotal structure on \mathcal{A} . Concretely, the monochromatic **OR**-move replaces an $(a \in \mathcal{A})$ -labeled defect line with a defect line with opposite orientation, labeled by $a^* \in \mathcal{A}$.
- The monochromatic **C**-move takes the following form, where we label rays by objects $x, y \in Z_{\mathcal{A}}(\mathcal{A})$, and nodes by vectors in the appropriate multiplicity modules, as justified by Observation 5.3.

$$(5.27)$$

Here, the node label on the right-hand side of (5.27) is obtained as follows. The multiplicity modules $H(x, \dots, a^*)$ and $H(y, a, \dots)$ which are isomorphic to the respective node labels, come with structure isomorphisms

$$H(x, \dots, a^*) \cong \langle \dots a^*, U(x) \rangle \quad \text{and} \quad H(y, a, \dots) \cong \langle a \dots, U(y) \rangle. \quad (5.28)$$

We denote the images of f and g under these isomorphisms by f' and g' . By a form of generalized composition, these morphisms combine into the morphism

$$(5.29)$$

Again, the hom-space $\langle \dots, U(x \otimes y) \rangle$ is isomorphic to the multiplicity module $H(x \otimes y, \dots)$. The node label $g \circ_a f$ is defined as the image of the morphism (5.29) under this isomorphism.

- There is a monochromatic **EF**-move, which takes two parallel defect lines, labeled by $a, b \in \mathcal{A}$, and fuses them into a single defect line, labeled by $ab \in \mathcal{A}$, with the node labels changing in the obvious way.
- The monochromatic **DV**-move removes a node with a $(\mathbb{1} \in Z_{\mathcal{A}}(\mathcal{A}))$ -labeled ray with one incoming and one outgoing defect line, both labeled by $(a \in \mathcal{A})$, and node label $\text{ev}^a \in \langle aa^*, \mathbb{1} \rangle$.

- The loop move **L** can also easily be expressed in the monochromatic case: Assume that the node with an $(a \in \mathcal{A})$ -labeled loop is labeled by a vector f in the multiplicity module $H(x, a, a^*, \dots)$. By the usual yoga, we obtain a morphism f' from f in one of the concrete hom-spaces used to construct the multiplicity module. In order to perform the move **L** and remove the loop, f' needs to be replaced with the morphism

$$\begin{array}{c}
 \color{red}{x} \\
 | \\
 \boxed{f'} \\
 \begin{array}{c}
 | \quad | \quad | \\
 \color{black}{\curvearrowright} \\
 a
 \end{array}
 \end{array} \in \langle \dots, U(x) \rangle. \tag{5.30}$$

This morphism in turn defines a vector in the multiplicity module for the node without the loop. The ray label is left unchanged by this move.

Sketch of proof. There is nothing to be proved for the **OR**-move. The monochromatic **EF**-move is similarly obtained as a composition of the usual **EF**-move with the **Fun**-move for the unitor equivalence $e : \mathcal{A} \square \mathcal{A} \rightarrow \mathcal{A}$. For the other two moves, we need to check that switching from monochromatic labels to ordinary labels in the extruded graph, then performing the ordinary move, and then switching to monochromatic labels again, results in the change claimed by the lemma.

Concerning the monochromatic **C**-move, this amounts to verifying that the contraction operation on objects specializes to the monoidal product in $Z_{\mathcal{A}}(\mathcal{A})$ in the monochromatic case, and that the contraction operation for morphisms specializes to the generalized composition described in (5.29). This was discussed in Remark 2.39.

The monochromatic **DV** and **L**-move can, as in the non-monochromatic case, be expressed as a composition of monochromatic **OR**, **EF** and **C**-moves. One can check explicitly that this result in the moves as claimed. \square

With this at hand, we are in a position to relate the block spaces of monochromatic extruded graphs to the vector spaces from (5.5).

Observation 5.6. Let Σ be a monochromatic extruded graph on the sphere, as in Observation 5.3. Note that by cutting out the nodes from the coat of Σ , we obtain an extended surface. A marking M on this extended surface is said to be a *marking* on the extruded graph σ iff the marking is attached to the nodes away from the defect lines, the intersections between the defect lines and the marking are transversal, and the distinguished vertex of M does not lie on a defect line. Let us construct, for each marking M on Σ an isomorphism $t_M : \mathbb{T} \cong \tau(\Sigma, M, x_{\bullet})$.

To this end, we describe how the marking M on Σ defines a sequence of moves on Σ . Crucially, each move in this sequence comes with an isomorphism between the block spaces before and after the move. Our goal is to obtain an extruded graph Σ_M in this way, whose block space is related to $\tau(\Sigma, M, x_{\bullet})$ via a distinguished isomorphism.

When drawing pictures, we illustrate the extruded graph Σ by the following example, but keep

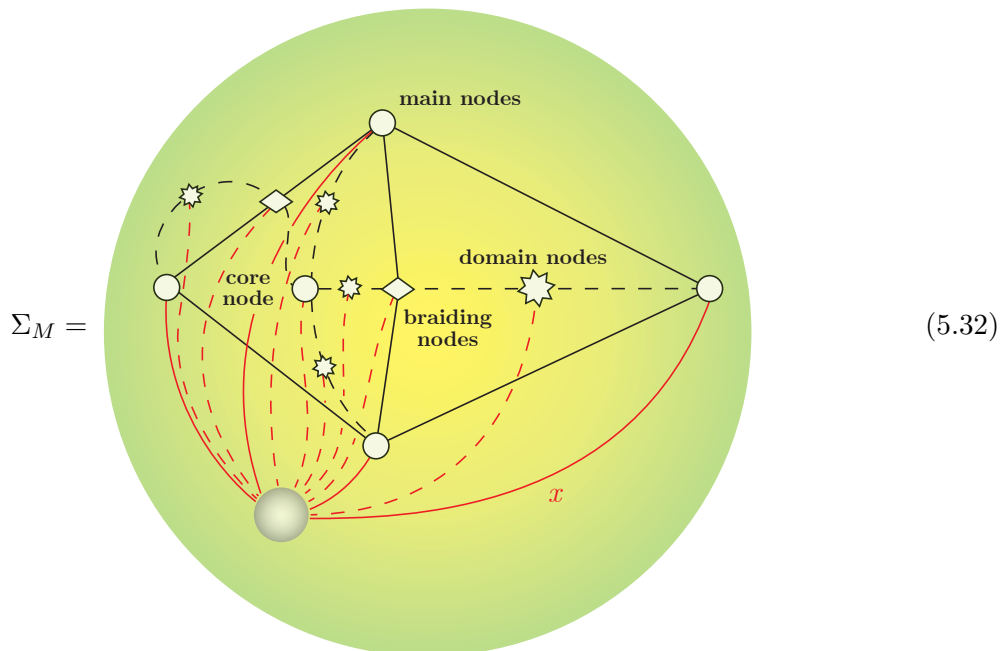
the argument general.



The first step is to apply a sequence of **DV**- and **DE**-moves to Σ , adding transparent defect lines and nodes in the following way: Recall that the marking M possesses a distinguished vertex. In the location of that vertex, we add a new node to Σ , which we call the *core node*. To the original nodes of Σ , we will from now on refer as *main nodes*.

We would like to add, for each edge of the marking M , a corresponding transparent defect line to Σ . To this end, we add a transparent node using the **DV**-move on the pre-existing defect lines wherever there would be a crossing between an edge of the marking and such new defect lines. We refer to these new nodes as *braiding nodes*. Now, we can add the new defect lines – as transparent lines, at first – using the **DE**-move between main nodes, braiding nodes, and the core node, retracing the edges of the marking. Accordingly, we call these defect lines *marking lines*. Note that the edges of the marking are segmented by the crossings. Each of these segments becomes an individual marking line.

Finally, we use the **DV**-move on every newly created marking line, adding another transparent node called a *domain node*. The resulting extruded graph Σ_M of this procedure is illustrated in (5.32), where we introduced the convention of drawing braiding nodes in a diamond shape and domain nodes in a star shape.



Recall how in the proof of Theorem 4.5, we used a choice of spanning tree for an extruded graph to sequentially contract all nodes into a single node using the **C**-move. We now recognize that the marking lines, together with all types of nodes, form a spanning tree for Σ_M . In addition, this spanning tree comes with a linear order on its marking lines, inherited from the order on the edges of the marking: Starting with the first edge of the marking, we enumerate the marking lines from the main node to the core node. We then proceed with the second edge of the marking, and so on. In this order, we apply the **C**-move to all marking lines, contracting them in the process, until we are left with an extruded graph Σ_1 with only a single node, as is done in the proof of Theorem 4.5. Unlike there, however, we here did not make any arbitrary choices in the moves that lead to Σ_1 .

From the monochromatic **C**-move described in Lemma 5.5, we know that the ray label for the ray of Σ_1 is given by $x_1 \otimes \cdots \otimes x_k$, if $x_1, \dots, x_k \in Z_{\mathcal{A}}(\mathcal{A})$ are the ray labels for the main nodes, in the linear order defined by the marking M . In the same fashion as in the proof of Theorem 4.5, the monochromatic **L**-move can be applied repeatedly to turn Σ_1 into a lasso graph Σ_Q . The ray label is not changed by this sequence of moves, so we end up with a lasso graph whose ray is labeled with $x_1 \otimes \cdots \otimes x_k \in Z_{\mathcal{A}}(\mathcal{A})$. The general results on lasso graphs from Section 3.4 provide us with a description of the block space for Σ_Q :

$$\begin{aligned} \mathrm{T}(\Sigma_Q) &\cong \overline{\mathcal{A}} \square_{\mathcal{A}} \square \left\langle \mathbb{1}_{\mathcal{A}}, e^{-1}(x_1 \otimes \cdots \otimes x_k) \right\rangle = \overline{\mathcal{A}} \square_{\mathcal{A}} \square \left\langle (\overline{\mathbb{1}} \boxtimes \mathbb{1}, \beta), e^{-1}(x_1 \otimes \cdots \otimes x_k) \right\rangle \\ &\cong Z_{\mathcal{A}}(\mathcal{A}) \left\langle e(\overline{\mathbb{1}} \boxtimes \mathbb{1}, \beta), x_1 \otimes \cdots \otimes x_k \right\rangle \cong Z_{\mathcal{A}}(\mathcal{A}) \langle \mathbb{1}, x_1 \otimes \cdots \otimes x_k \rangle = \tau(\Sigma, M, x_{\bullet}). \end{aligned} \quad (5.33)$$

Here, e denotes the unitor equivalence $e : \overline{\mathcal{A}} \square_{\mathcal{A}} \square \cong Z_{\mathcal{A}}(\mathcal{A})$, and β denotes the balancing of the object $\overline{\mathbb{1}} \boxtimes \mathbb{1} \in {}_{\mathcal{A}} \overline{\mathcal{A}} \square_{\mathcal{A}} \mathcal{A}$ with respect to the indicated bimodule structure. The last equality is the definition (5.2) of $\tau(\Sigma, M, x_{\bullet})$. The chain of morphisms (5.33), composed with the isomorphism

$$\mathrm{T} = \mathrm{T}(\Sigma) \cong \mathrm{T}(\Sigma_1) \cong \mathrm{T}(\Sigma_Q) \quad (5.34)$$

obtained from the moves, defines the isomorphisms $t_M : \mathrm{T} \cong \tau(\Sigma, M, x_{\bullet})$ mentioned at the start of the proof.

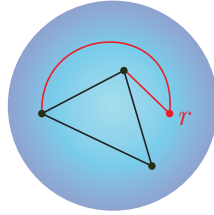
It should be noted that this statement is really not about extruded graphs, but about the block space of a monochromatic labeled defect sphere. We expect that different choices of markings M, M' lead to the same isomorphism $t_M = t_{M'}$, but for now this remains a conjecture.

Definition 5.7. Let R be a spiked ball. By a *marking* M on R , we mean a marking on the extended surface obtained from the surface $\partial R \cong \mathbb{S}^2$ of R by cutting out the vertices, which intersects the edges on the boundary of R only transversely.

If M is a marking on R , then a monochromatic extruded graph Σ_R on \mathbb{S}^2 can be constructed from (R, M) as follows. First, we modify R slightly: We add spikes labeled by the monoidal unit $\mathbb{1} \in Z_{\mathcal{A}}(\mathcal{A})$ until all vertices are spiked. This changes neither the multiplicity modules for the vertices, nor vector space τ_r for the point r in the center of R (up to more than a canonical isomorphism). The construction of the extruded graph Σ_R from the spiked ball R then amounts only to a change in vocabulary: Vertices become nodes, edges become defect lines, spikes become rays and the point $r \in R$ becomes the core. Observation 5.3 and Observation 5.6 then ensure that the algebraic labels can be transferred from the spiked ball to the extruded graph accordingly. We call Σ_R the extruded graph *associated to* the spiked ball R with marking M .

At most, the core label of Σ_R depend on the choice of marking.

Recall from [TV17, Sec. 15.3] that a (colored) knotted net in \mathbb{S}^2 is a string diagram drawn on the sphere, where some strands are labeled by objects of \mathcal{A} and others by objects of the Drinfeld center $Z_{\mathcal{A}}(\mathcal{A})$, as depicted, for example, in [TV17, Ex. 15.3.4]. The strands labeled by objects of the Drinfeld center are allowed to cross other strands at isolated points away from the coupons. We only consider knotted nets where all crossings are between one strand labeled by an object in the Drinfeld center, and one strand labeled by an object in \mathcal{A} . For these types of crossings, there is no distinction between over- and under-braidings. Both circular coupons (or equivalently, vertices), which are labeled by vectors in multiplicity modules, and rectangular coupons with distinguished inputs and outputs, labeled by appropriate morphisms, are allowed. The following picture gives an example of a knotted net:



(5.35)

Definition 5.8. A knotted net Γ is said to be a *projection* of a spiked ball R iff it can be obtained from R as follows:

- The edges and vertices of R are strands and (circular) coupons of Γ .
- There is one additional coupon in Γ , called the central coupon. For each spike in R , labeled by an object $x \in Z_{\mathcal{A}}(\mathcal{A})$, there is a strand in Γ , labeled by x as well, starting at the output of the central coupon and ending at the coupon corresponding to the vertex which the spike was attached to. We call these strands *spike-strands*. Spike-strands are allowed to cross other strands, but not other spike-strands or themselves.
- The spiked vertices in R are labeled by vectors in multiplicity modules $H(x, a_{\bullet})$ whose cliques consist of hom-spaces of the form $\langle U(x), a_1 \cdots a_i a_{i+1} \cdots a_n \rangle$. In contrast, the circular coupons of Γ are labeled, after passing through multiplicity modules $H(\mathbb{1}, \{a_{\bullet}, U(x)^*\})$, by hom-spaces of the form $\langle \mathbb{1}, a_1 \cdots a_i U(x)^* a_{i+1} \cdots a_n \rangle$. The position of $U(x)^*$ within the tensor product is determined by the location where the corresponding spike-strand attaches to the coupon; this is arbitrary. There is an isomorphism

$$H(x, a_{\bullet}) \cong \langle U(x), a_{i+1} \cdots a_n a_1 \cdots a_i \rangle \cong \langle \mathbb{1}, U(x)^* a_{i+1} \cdots a_n a_1 \cdots a_i \rangle \cong H(\mathbb{1}, \{a_{\bullet}, U(x)^*\}) \quad (5.36)$$

for each spiked vertex of R . We require that the labels of the spiked vertices of R are related to the labels of the circular coupons of Γ via these isomorphisms.

- The sphere underlying Γ , with the coupons that stem from spiked vertices in R cut out, is an extended surface. The central coupon and the spike-strands form a marking for this extended surface, with an appropriate labeling (x_{\bullet}) of strands by objects $x_i \in Z_{\mathcal{A}}(\mathcal{A})$, as in

Section 5.1. More precisely, to obtain a marked extended surface with labels, we label the boundary components (of coupons attached to a spike-strand) by the object in the Drinfeld center $Z_{\mathcal{A}}(\mathcal{A})$ that labels the adjacent spike-strand, and we collapse the rectangular central coupon to a point. Since all spike-strands are attached to the output of the central coupon, they are linearly ordered, and we select the left-most spike-strand as the distinguished edge for the marking.

Recall that the central point $r \in R$ is labeled by a vector in the space $\tau_k(x_{\bullet})$ from (5.5), if there are k many spikes. The marking we just introduced provides us with a canonical isomorphism

$$\tau_k(x_{\bullet}) \cong_{Z_{\mathcal{A}}(\mathcal{A})} \langle \mathbb{1}, x_1 \cdots x_n \rangle, \quad (5.37)$$

where the x_i are ordered according to the way the spike-strands are attached to the central coupon. We fix the label of the central coupon by requiring that this isomorphism relate the vector labeling the central point $r \in R$ to the label of the central coupon.

Note that there are, in general, multiple knotted nets Γ_R which are projections of R . Only when the spiked ball has no spikes can we speak of *the* projection Γ_R . As an example, consider that the knotted net (5.35) is a projection of the spiked ball (5.9). It is clear that a marking on a spiked ball R in the sense of Definition 5.7 defines a projection of R .

Remark 5.9. The concept of a spiked ball does not appear in [TV17]. In a sense, it is avoided there by formulating the theory in such a way that wherever a spiked ball would appear (e.g. in [TV17, Fig. 13.1, Sec. 15.5.1]), a canonical projection exists. This projection is then defined, skipping over the auxiliary notion of a spiked ball, which fits nevertheless quite natural into the theory.

Schematically, the relation between spiked balls, knotted nets, extruded graphs and their respective evaluations is as depicted in the following diagram, where the dotted arrows are defined for a choice of marking M for each spiked ball.

$$\begin{array}{ccc}
 & \{\text{spiked balls } R\} & \\
 \text{projection for marking } M \swarrow \cdots & & \cdots \searrow \text{associated to } (R, M) \\
 \{\text{knotted nets } \Gamma_R\} & & \{\text{extruded graphs } \Sigma_R\} \\
 \swarrow \text{evaluation } \mathbb{F}_{\mathcal{A}} & & \nwarrow \text{evaluation } |\cdot| \\
 & \mathbb{K} &
 \end{array} \quad (5.38)$$

The main result of this section is that the diagram (5.38) commutes for all choices of markings. This is first shown in Proposition 5.10 for spiked balls without spikes, and then, in Theorem 5.12, for general spiked balls. Indeed, projections and associated extruded graphs do not depend on a marking M for spiked balls without spikes, which is why no marking appears in the formulation of

Proposition 5.10 (Evaluating Spiked Balls without Spikes). *The evaluation of the extruded graph Σ_R associated to a spiked ball R without spikes is equal to the invariant of the knotted net Γ_R , which is the projection of R ,*

$$|\Sigma_R| = \mathbb{F}_{\mathcal{A}}(\Gamma_R). \quad (5.39)$$

Proof. We know that by Theorem 4.5, the extruded graph Σ_R can be evaluated using only the moves **OR**, **C**, **EF** and **SV**, as well as the formula for the evaluation of loop graphs from Theorem 3.28. Since the core label of Σ_R was transparent from the beginning (as the original spiked ball R is concentrated on the surface), we can even do without the **SV**-move. Analogous moves hold for knotted nets as well: The move **C** is translated to the move R_7 from [TV17, Sec. 15.4.6]. Similar moves to **OR** and **EF** for knotted nets are also obvious. We can thus apply a chain of these moves to the extruded graph Σ_R and to the knotted net Γ_R simultaneously, until we obtain, as in the proof of Theorem 4.5, a loop graph $\Sigma_{R'}$, and a knotted net $\Gamma_{R'}$ with a single coupon and a single strand. Their labels are still in correspondence: the defect line of $\Sigma_{R'}$ is labeled by the same object as the strand of $\Gamma_{R'}$, and the node label of $\Sigma_{R'}$ is the same as the coupon label of $\Gamma_{R'}$, after passing through the isomorphism for node spaces of monochromatic extruded graphs from Proposition 5.4. Since the moves used are invariances, the respective evaluations remain unchanged:

$$|\Sigma_R| = |\Sigma_{R'}|, \quad \mathbb{F}_{\mathcal{A}}(\Gamma_R) = \mathbb{F}_{\mathcal{A}}(\Gamma_{R'}). \quad (5.40)$$

The evaluation of loop graphs is discussed in Theorem 3.28, and the analogous result for knotted nets is found in [TV17, Ex. 15.4.2]. The respective evaluations agree. \square

Corollary 5.11. *Extruded graphs, in particular the generalized 6j-symbols described in Example 3.21, actually generalize the known 6j-symbols for spherical fusion categories.*

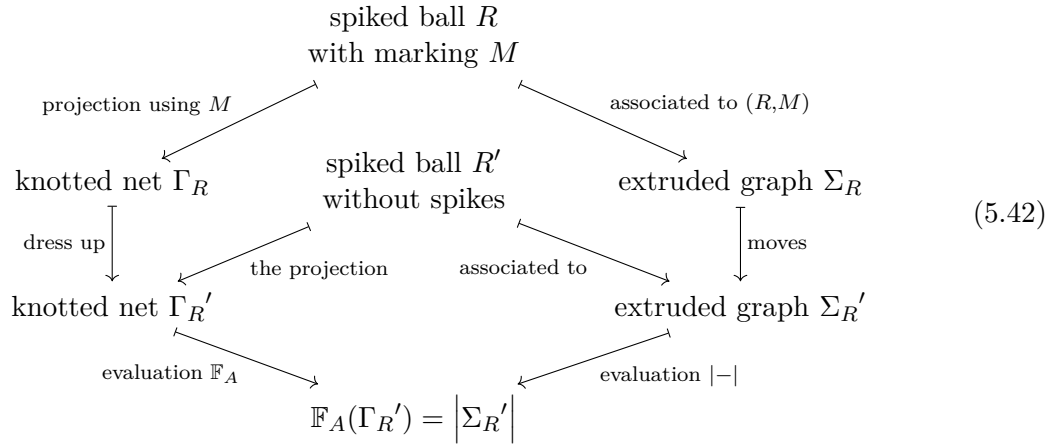
Theorem 5.12 (Evaluating Spiked Balls). *Let R be a spiked ball, and let M be a marking on R in the sense of Definition 5.7. The evaluation of the extruded graph Σ_R associated to (R, M) as defined in Definition 3.17 is equal to the invariant of the knotted net Γ_R which is a projection of R obtained from the marking M :*

$$|\Sigma_R| = \mathbb{F}_{\mathcal{A}}(\Gamma_R). \quad (5.41)$$

Proof. Let us first dress up the knotted net Γ_R to a knotted net $\Gamma_{R'}$ which leaves the invariant $\mathbb{F}_{\mathcal{A}}(\Gamma_R) = \mathbb{F}_{\mathcal{A}}(\Gamma_{R'})$ unchanged: We replace every crossing by a coupon labeled by an appropriate braiding morphism, see [TV17, Fig. 15.4]. Moreover, we assume that all vertices of R are spiked vertices. This is not a restriction: Adding transparent spikes labeled by $\mathbb{1} \in Z_{\mathcal{A}}(\mathcal{A})$ to non-spiked vertices does not change the associated extruded graph. It does change which knotted nets are projections of R , but only up to transparent strands, which have no effect on the evaluation.

The idea is to apply moves of invariance to the extruded graph Σ_R until it becomes an extruded graph $\Sigma_{R'}$ whose rays are transparent, and which resembles the knotted net $\Gamma_{R'}$ in the following sense: there exists a spiked ball R' without spikes such that $\Sigma_{R'}$ is the extruded graph associated to R' and such that $\Gamma_{R'}$ is the projection of R' . The situation can be summarized

diagrammatically:



The equality $\mathbb{F}_A(\Gamma_{R'}) = |\Sigma_{R'}|$ at the bottom of (5.42) holds by Proposition 5.10. Because the extruded graphs Σ_R and $\Sigma_{R'}$ are related by moves of invariance, they evaluate to the same scalar $|\Sigma_{R'}| = |\Sigma_R|$. Similarly, we will construct the knotted net $\Gamma_{R'}$ in such a way that $\mathbb{F}_A(\Gamma_R) = \mathbb{F}_A(\Gamma_{R'})$ holds. Combining these equalities, we find:

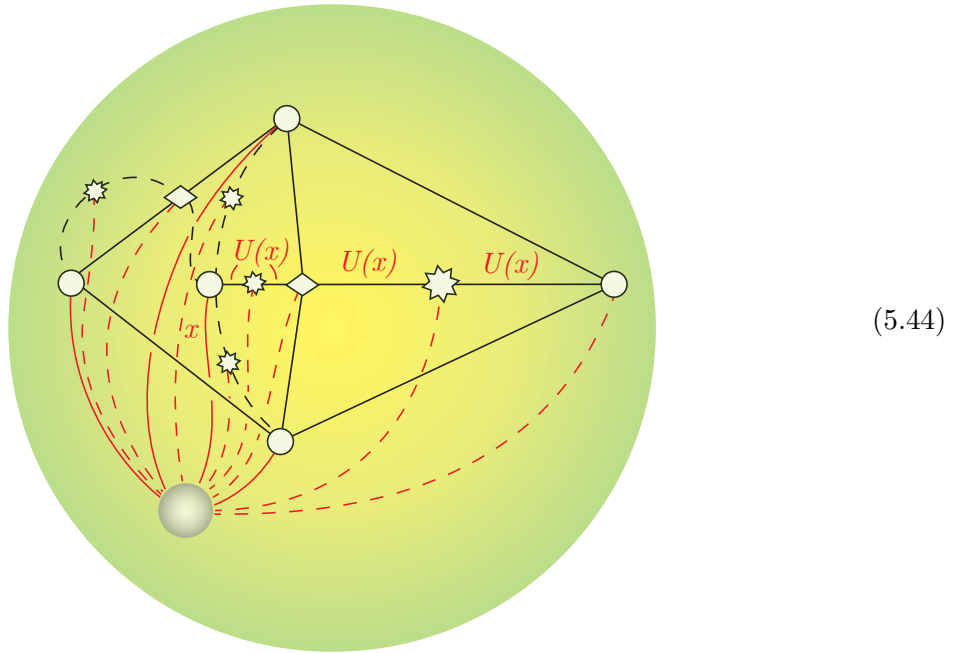
$$\mathbb{F}_A(\Gamma_R) = \mathbb{F}_A(\Gamma_{R'}) = |\Sigma_{R'}| = |\Sigma_R|, \tag{5.43}$$

which proves the theorem. Hence, we have to give a sequence of moves that transform Σ_R into $\Sigma_{R'}$. This is done in the remainder of this proof.

The marking M of the spiked ball R serves also as a marking for the extruded graph Σ_R , in the meaning discussed in Observation 5.6. We further follow Observation 5.6, by applying the chain of moves introduced there to Σ_R , using the marking M to transform it into the subdivided form (5.32). Recall that in this new extruded graph, we distinguish several types of nodes and defect lines, such as main nodes, braiding nodes, domain nodes, and the core node, as well as marking lines.

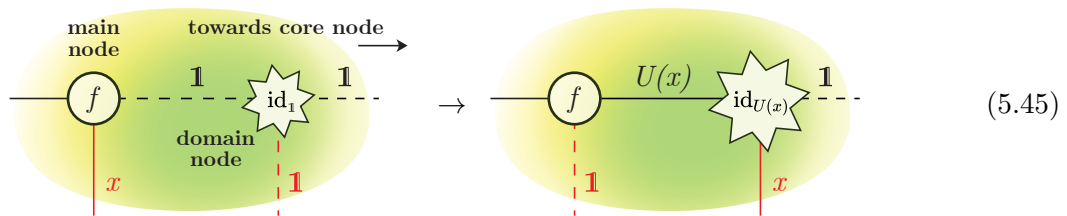
The next goal is to modify this subdivided graph such that all rays are transparent, except for the ray connecting the core node with the core. Note that from each of the main nodes, there is a path to the core node formed by a chain of marking lines. Using a sequence of moves specified below, it is possible to "reroute" the ray of a main node through this chain of marking lines and the core node, resulting in an extruded graph as depicted in (5.44). When comparing (5.44) to (5.32), note that previously, the ray connecting the chosen main node with the core was labeled by x . Now, in (5.44), this ray is labeled transparently, while the ray connecting the core node to the core carries the label x . The marking lines on the path from the core node to

the main node are now labeled by $U(x)$.



The moves needed to perform this rerouting of the x -labeled ray can all be seen to be invariances by applying the monochromatic **C**-move from Lemma 5.5 to both sides. We proceed to specify them.

First, we need to redirect the ray (labeled by x in the illustrations) of the main node that we consider through the first domain node encountered in the chain of marking lines leading to the core node. This leaves the main node with a transparent ray label. In the following pictures, note that we work with monochromatic labels for the rays and nodes, in the sense of Observation 5.3. In particular, the node labels are describes using morphisms in any of the concrete hom-spaces (5.6) that realize the multiplicity module; which one we choose is clear from the context.



Continuing along the chain of marking lines, the next node is either the core node or a braiding

node. For the case of a braiding node, the following move is used.

$$(5.46)$$

Behind every braiding node, in the direction towards the core node, there will be another domain node. The right-most braiding node in (5.46) is the same as the left-most node in (5.47). The node labels seem different, but we only chose to represent them in different instances of the hom-spaces (5.6). These hom-spaces are related by the isomorphism (5.7), which is the source of the half-braiding that appears in (5.47). Using different hom-spaces is necessary when checking that the respective moves (5.46) and (5.47) are invariances using the monochromatic **C**-move.

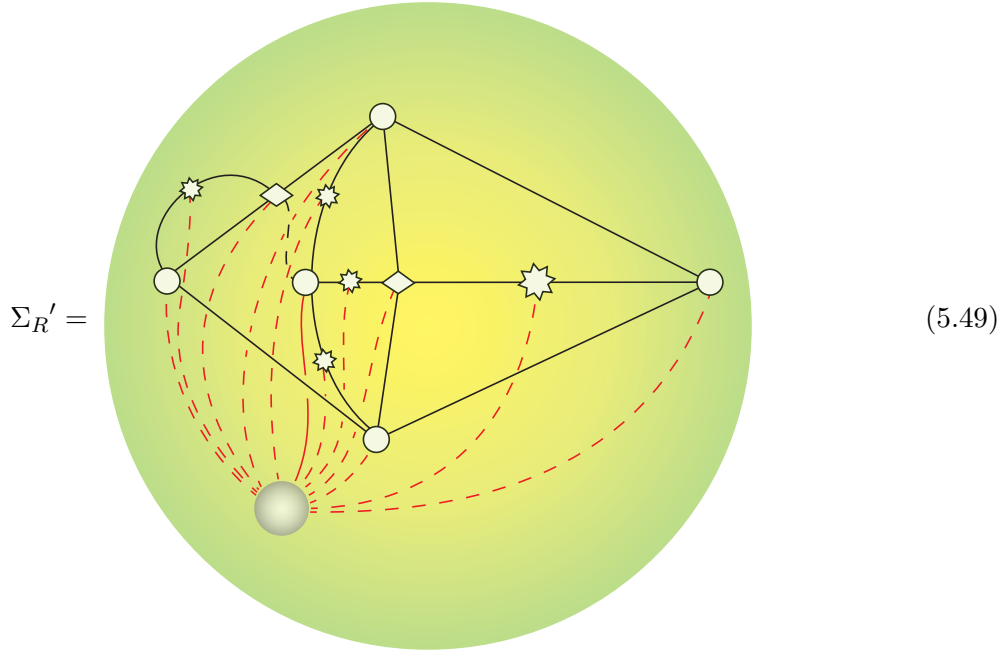
$$(5.47)$$

Finally, after repeating the moves (5.46) and (5.47) for some time, the last segment in the chain of marking lines involves a domain node and the core node. When completing this chain of moves for the first chain of marking lines, the core node's ray will be labeled by $y = \mathbb{1} \in Z_{\mathcal{A}}(\mathcal{A})$, but after that, the core node may have a non-trivial ray label y .

$$(5.48)$$

After applying the rerouting procedure to all main nodes, we are left with an extruded graph Σ_R' of the following form, in which all rays are transparent, except for the ray attached to the

core node.



The final change we would like to make is to raise the core data to the surface: By a generalized version of the **SV**-move, we can obtain an extruded graph where all rays are transparent, and where the core label is transparent, with the information that was previously stored in the core now being moved to the core node, and thus onto the coat. This is possible because the multiplicity module for the core node is isomorphic to the dual of the vector space τ_k from (5.5), which is the space of core labels.

It is clear that the extruded graph we obtained in this way and the knotted net Γ_R (after changing crossings to braidings, as mentioned before) are similar in the following sense: There is a spiked ball R' without spikes, such that Γ_R is the projection of R' , and such that the newly-constructed extruded graph is associated to R' . Hence, we may invoke Proposition 5.10, which completes the proof of Theorem 5.12. \square

5.3 RELATION TO POLYGON DIAGRAMS

In recent work by Meusburger [Meu22], so-called *polygon diagrams* were introduced in order to define a state-sum model with surface defects. In this section, we will briefly discuss how polygon diagrams and extruded graphs are related. We will see that polygon diagrams roughly correspond to extruded graphs on the sphere, whose only non-transparent defect lines are arranged in a circle.

Let \mathcal{A} and \mathcal{B} be spherical fusion categories, and consider a finite set of \mathcal{A} - \mathcal{B} -bimodule categories $\mathcal{M}_1, \dots, \mathcal{M}_k$. We consider an extruded graph Σ on the sphere, which has k many nodes, equipped with a cyclic order and connected with k many defect lines according to the order. We call the string of defect lines the *equator* of the extruded graph, and note that it splits the surface into two hemispheres, labeled by the spherical fusion categories \mathcal{A} and \mathcal{B} . Let us call the interior of these

two regions the monochromatic regions of Σ , because we allow for networks of monochromatic defect lines and nodes in the two hemispheres, which may connect to the nodes on the equator. The ray categories of the equatorial nodes are equivalent to categories of bimodule functors via the Eilenberg-Watts equivalences from Section 2.13. The ray categories for the nodes in the monochromatic areas are all equivalent to Drinfeld center of either \mathcal{A} or \mathcal{B} as a result of Proposition 5.4. We require all of them to be labeled by the monoidal unit $\mathbb{1}$. Then the block space of Σ is known to be the space of bimodule natural transformations between (compositions of) the bimodule functors that label the equatorial rays; see Example 3.10 for two equatorial nodes or [FSS22, Ex. 4.35] for the general case.

Let us now consider a polygon diagram as in [Meu22, Ex. 4.4]. From this, we can define an extruded graph of the form just described: The boundary of the polygon diagram becomes the equator. Recall that there are three overlaid graphs in interior of the polygon diagram: one for each acting category (solid black or gray lines in [Meu22]) and one (dashed lines in [Meu22]) labeled by functors. The sub-diagrams of the acting categories we project onto the corresponding hemispheres – they become the monochromatic parts of the extruded graph –, and the lines labeled by bimodule functors become the rays of the equatorial nodes. We restrict ourselves to only those polygon diagrams where all functor-labeled lines meet in a single vertex labeled by a (bimodule) natural transformation ν . If this is the case, then ν is an appropriate core label for the extruded graph.

Without going into much detail, we describe why evaluation of this extruded graph obtained from a polygon diagram is equal to evaluation of the polygon diagram itself, as defined in [Meu22, Def. 2.13]. This is similar to the proof of Theorem 5.12: we transform, in parallel, the extruded graph and the polygon diagram in question into an extruded graph (polygon diagram) with only a single node (vertex on the boundary of the polygon diagram) and a single ray (dashed line attached to the vertex). Each step of this transformation leaves the evaluation of both the extruded graph and the polygon diagram invariant. What we have obtained is a lasso graph. Having reduced the comparison between extruded graphs and polygon diagrams to this special case, the next result now shows that lasso graphs are indeed evaluated just like the corresponding polygon diagrams.

Proposition 5.13. *Let Q be a lasso graph as in (3.44), with the defect line labeled by an object $m \in {}_{\mathcal{A}}\mathcal{M}_{\mathcal{B}}$. Let $F : \mathcal{M} \rightarrow \mathcal{M}$ be a bimodule endofunctor of \mathcal{M} , pick a bimodule natural transformation $\nu : F \rightarrow \text{id}_{\mathcal{M}}$, and a morphism $f : m \rightarrow F(m)$.*

From these data we construct ray, core, and node labels for Q as follows. For the ray label, we choose $x := \text{coEW}_m(F)$, using the equivalence coEW_m from Section 2.13. Concerning the core label, note that there is a chain of isomorphisms

$$\text{Nat}_{\mathcal{A}|\mathcal{B}}(F, \text{id}_{\mathcal{M}}) = \text{Fun}_{\mathcal{A}|\mathcal{B}}(\mathcal{M}, \mathcal{M}) \langle F, \text{id}_{\mathcal{M}} \rangle \cong \langle x, \Phi^{\mathcal{M}} \rangle \cong \langle x, \Phi_{\mathcal{M}} \rangle \cong \langle \Phi_{\mathcal{M}}, x \rangle^* \cong \mathbb{T}^*. \quad (5.50)$$

The first equality is trivial, the second isomorphism is obtained by applying the functor coEW_m , the third isomorphism is post-composition with the isomorphism $\Theta_{\mathcal{M}}^{-1} : \Phi^{\mathcal{M}} \rightarrow \Phi_{\mathcal{M}}$, then we used (4.9), and finally, we recalled the explicit form of the block space of a lasso graph from (3.4). Let $\varphi \in \mathbb{T}^$ denote the image of ν under this chain of isomorphisms; this is the core label for*

Q . From the Yoneda lemma (2.169), we obtain a natural isomorphism Y between two functors $\text{Fun}(\mathcal{M}, \mathcal{M}) \rightarrow \text{vect}$:

$$Y_G : \langle m \boxtimes \bar{m}, \text{coEW}(G) \rangle \cong \langle m, G(m) \rangle. \quad (5.51)$$

We define the node label $\tilde{f} : m \boxtimes \bar{m} \rightarrow U(x)$ as $\tilde{f} := \mathcal{D}_A \mathcal{D}_B Y_F^{-1}(f)$.

We now claim: The evaluation $|Q|$ of the lasso graph Q with the specified labels is given by the scalar

$$|Q| = \text{Tr}_{\mathcal{M}}(\nu_m \circ f) \in \mathbb{K}. \quad (5.52)$$

Proof. By applying the **SV**-move to Q and then using Theorem 3.28, we know that

$$|Q| = \text{Tr}_{\mathcal{M}}(\text{sil}^{-1}(\varphi' \circ Y_F^{-1}(f))), \quad (5.53)$$

where $\varphi' \in \langle x, \Phi^{\mathcal{M}} \rangle$ is the image of the core label φ under the appropriate isomorphism $T^* \cong \langle x, \Phi^{\mathcal{M}} \rangle$, which is part of the chain of isomorphisms (5.50). In terms of the natural transformation ν , we have $\varphi' = \text{coEW}_m(\nu)$. Recognizing that $\text{sil}^{-1} = Y_{\text{id}_{\mathcal{M}}}$, we draw the following naturality diagram for Y ;

$$\begin{array}{ccc} \langle m \boxtimes \bar{m}, \text{coEW}(F) \rangle & \xrightarrow{Y_F} & \langle m, F(m) \rangle \\ \langle m \boxtimes \bar{m}, \text{coEW}(\nu) \rangle \downarrow =_{\varphi' \circ -} & & \downarrow \nu_m \circ - \\ \langle m \boxtimes \bar{m}, \text{coEW}(\text{id}_{\mathcal{M}}) \rangle & \xrightarrow{Y_{\text{id}_{\mathcal{M}}}} & \langle m, m \rangle \end{array} \quad (5.54)$$

Comparing the images of $Y_F^{-1}(f) : m \boxtimes \bar{m} \rightarrow \text{coEW}(F)$ under the two paths around the diagram (5.54), we find

$$\text{sil}^{-1}(\varphi' \circ Y_F^{-1}(f)) = Y_{\text{id}_{\mathcal{M}}}(\varphi' \circ \tilde{f}) = \nu_m \circ Y_F(\tilde{f}) = \nu_m \circ f. \quad (5.55)$$

Thus, the trace of the left-hand side of (5.55) is equal to the trace of the right-hand side, and the proof is done. \square

In particular, we find that our generalized 6j-symbols from Example 3.21 are a further generalization of what are called generalized 6j-symbols in [Meu22, Sec. 4.3]. To explain the appearance of the factor $\mathcal{D}_A \mathcal{D}_B$ in the definition of the node label \tilde{f} , recall from Remark 2.34 that we expect categorical dimensions to appear when keeping track of how traces change under the Eilenberg-Watts equivalences.

5.4 STATE-SUMS WITH DEFECTS

We are now in a position to sketch the construction of a state-sum model with defects in all dimensions. Since we are only laying out an idea, we have little aspiration to rigor in this section, and some terminology is left imprecise. The following is inspired by the construction of Turaev and Virelizier as laid out in [TV17].

Let Σ and Σ' be labeled defect surfaces as introduced in Section 3.1. We consider a 3-cobordism (M, D) with defects from Σ to Σ' , that is:

- an oriented 3-manifold M with boundary ∂M ,
- an orientation-preserving embedding of $\Sigma^{\text{op}} \amalg \Sigma$ into ∂M ; the image of this embedding is called the *gluing boundary* $\partial_g M$, and its complement in ∂M is called the *free boundary*,
- an oriented stratified 2-polyhedron D , see [TV17, Sec. 11.1.2], embedded in M , called the *defect structure*. It should respect the geometry of the cobordism:
 - The free boundary of M is a subset of D .
 - No interior of any 2-cells of D intersects the gluing boundary.
 - If the interior of an edge of D intersects the gluing boundary, then it is contained in it.

Moreover, the defect structure is labeled by the following algebraic data:

- The connected components of $M \setminus D$, called the *domains*, are labeled by spherical fusion categories, and
- the 2-cells of D are labeled by appropriate traced bimodule categories; 2-cells of D that lie in the free boundary are accordingly labeled by one-sided module categories.
- The orientation of each edge of D , together with the orientation of M , endows the set of adjacent (germs of) 2-cells with a cyclic order. We associate to the edge the balanced Deligne product of the bimodule categories that label the adjacent 2-cells using this cyclic order; note that this category is defined in a similar way as ray categories (3.8).¹ Each *internal* edge of D – meaning it is not contained in the gluing boundary – is labeled by an object from the associated category.
- Observe that there always exists a neighborhood U of any *internal* (meaning $v \notin \partial_g M$) vertex v of D which carries the structure of an extruded defect surface (i.e. an extruded graph without labels): The intersection of the 2-cells of D with the neighborhood's boundary ∂U are the defect lines, and the intersection of the edges of D with U are the rays of the extruded defect surface. Since the labels for the edges of D are suitable labels for the rays of the extruded defect lines, there is a block space \mathbb{T}_v associated with the core. We thus label the internal vertex v by a linear form $\varphi : \mathbb{T}_v \rightarrow \mathbb{K}$.

Notice that edges and vertices of D on the gluing boundary are not labeled. These fulfill a different role from the internal edges and vertices: The intersection of D with the gluing boundary equips the gluing boundary with the structure of a labeled defect surface. We require that this structure equals the one defined by the embedding of Σ and Σ' .

In the following, when we speak of "the cobordism M ", we really mean the pair (M, D) .

A state-sum TFT τ associates vector spaces to the defect surfaces Σ and Σ' and a linear map between these vector spaces to the defect 3-cobordism M . In order to state the definition however, we need to refine the defect structure D of M into a *skeleton* – this essentially means to add 2-cells labeled by regular bimodule categories, edges labeled by silent objects and vertices

¹The orientation of the edge, together with the orientation of M , also defines an orientation on each germ of each adjacent 2-cell. This orientation can be equal or opposite to the chosen orientation on the 2-cell. If the orientations are different, then we consider the *opposite* bimodule category in the relative Deligne product associated to the edge instead.

labeled by canonical vectors to D , thereby obtaining another defect structure \tilde{D} . We suppose that \tilde{D} is sufficiently fine in a sense we will not make precise here – certainly, we require that all domains of \tilde{D} are open balls. Since the refinement also affects the footprint of the defect structure on the gluing boundary, the newly obtained 3-cobordism \tilde{M} has as source and target defect surfaces $\tilde{\Sigma}$ and $\tilde{\Sigma}'$, which are refinements of Σ and Σ' in the sense of [FSS22, Defn. 5.15].

As an intermediate step, we construct a *pre-state-sum* $\tau^{\mathbb{P}}$ for sufficiently fine defect surfaces and defect 3-cobordisms, such as $\tilde{\Sigma}$, $\tilde{\Sigma}'$, and \tilde{M} . To the source component of the gluing boundary $\tilde{\Sigma}$, we assign the pre-block space $\tau^{\mathbb{P}}(\tilde{\Sigma}) = \mathbb{T}^{\mathbb{P}}(\tilde{\Sigma})$, and similarly for the target defect surface. Because the embedding of $\tilde{\Sigma}$ into $\partial\tilde{M}$ is orientation-reversing, the vector space associated with the gluing boundary of $\partial\tilde{M}$ is

$$\tau^{\mathbb{P}}(\partial_g\tilde{M}) = \mathbb{T}^{\mathbb{P}}(\tilde{\Sigma})^* \otimes \mathbb{T}^{\mathbb{P}}(\tilde{\Sigma}') \cong_{\text{vect}} \langle \mathbb{T}^{\mathbb{P}}(\tilde{\Sigma}), \mathbb{T}^{\mathbb{P}}(\tilde{\Sigma}') \rangle. \quad (5.56)$$

By a *coloring* of a 2-cell of \tilde{D} , we mean the choice of a (representative of an isomorphism class of a) simple object in the bimodule category with which the 2-cell is labeled. A choice of coloring for each 2-cell is called a coloring c of \tilde{D} . For a given coloring c of \tilde{D} , we now consider around each internal vertex v of \tilde{D} again a neighborhood Γ_v , which carries the structure of an extruded defect surface, with ray and core labels. In addition now, the coloring c provides Γ_v with object labels for the defect lines, so that Γ_v has well-defined node spaces. In the same way, the defect coloring determines labels for the defect lines of the gluing boundary. The tensor product over the total node spaces for all internal vertices v of \tilde{D} , and the node spaces of the incoming and outgoing defect surfaces $\tilde{\Sigma}$ and $\tilde{\Sigma}'$, is of particular importance to us:

$$\mathbb{N} := \mathbb{N}(\tilde{\Sigma})^* \otimes \mathbb{N}(\tilde{\Sigma}') \otimes \bigotimes_v \mathbb{N}(\Gamma_v), \quad (5.57)$$

where $\mathbb{N}(\Gamma_v)$ is the total nodespace of Γ_v as introduced in (3.15). The unordered tensor product (5.57) can be organized in another way, namely by edges instead of vertices. Either both end points of an internal edge e are internal vertices v_0 and v_1 , or one end point is an internal vertex v_0 , and the other lies on the gluing boundary. In any case, an internal edge defines two nodes: either a node n_0 of Γ_{v_0} and a node n_1 of Γ_{v_1} , or a node n_0 of Γ_{v_0} and a node n_1 of the defect surface $\partial_g\tilde{M}$. We define the *node space of an internal edge* e as $\mathbb{N}_e := \mathbb{N}(n_1) \otimes \mathbb{N}(n_2)$. This allows us to write the total node space \mathbb{N} arranged by internal edges:

$$\mathbb{N} = \bigotimes_e \mathbb{N}_e. \quad (5.58)$$

Let n_0, n_1 be the nodes associated to an internal edge e . Unraveling of the definition of the nodespaces $\mathbb{N}(n_0)$ and $\mathbb{N}(n_1)$ as hom-spaces (3.14) reveals that the bimodule traces on the labels for the 2-cells of \tilde{D} exhibit $\mathbb{N}(n_1)$ as the dual of $\mathbb{N}(n_0)$. This shows that the nodespace of an internal edge e can be expressed as

$$\mathbb{N}_e \cong \mathbb{N}(n_0) \otimes \mathbb{N}(n_0)^* \cong \mathbb{N}(n_1)^* \otimes \mathbb{N}(n_1), \quad (5.59)$$

and that there is a distinguished vector $\star_e \in \mathbb{N}_e$, which is obtained as a sum over elements of dual bases in either of the two expressions for \mathbb{N}_e in (5.59), as explained in Section 2.4. Because

the nodespace N can be built from the nodespaces of internal edges (5.58), the distinguished vectors \star_e in the nodespaces of internal edges assemble into a distinguished vector

$$\star := \bigotimes_e \star_e \in N \quad (5.60)$$

of the nodespace N .

On the other hand, the evaluation $|-|$ of extruded graphs from Definition 3.17 gives a linear form $|\Gamma_v| : N(\Gamma_v) \rightarrow \mathbb{K}$ for every internal vertex v . This allows us to identify a distinguished vector $|\tilde{M}, c|$ in the nodespace associated to the gluing boundary, which is the image of \star under the following map

$$\star \in \bigotimes_e N_e \stackrel{(5.58)}{=} N \stackrel{(5.57)}{=} N(\tilde{\Sigma})^* \otimes N(\tilde{\Sigma}') \otimes \bigotimes_v N(\Gamma_v) \xrightarrow{\text{id} \otimes \text{id} \otimes \bigotimes_v |\Gamma_v|} N(\tilde{\Sigma})^* \otimes N(\tilde{\Sigma}'). \quad (5.61)$$

So far, we have fixed a coloring c . In the next step, we will have to take the sum over all possible colorings, so we have to keep track of the way that the node spaces and the distinguished vector depend on c . Indeed, while $|\tilde{M}, c|$ depends on c as a whole, the nodespaces $N(\tilde{\Sigma})$ and $N(\tilde{\Sigma}')$ only depend on the coloring of those 2-cells of \tilde{D} that are adjacent to the respective gluing boundary components. We denote these sub-colorings of c by $c_{\tilde{\Sigma}}$ and $c_{\tilde{\Sigma}'}$, and add the dependence on the coloring as an index to the nodespaces:

$$|\tilde{M}, c| \in N_{c_{\tilde{\Sigma}}}(\tilde{\Sigma})^* \otimes N_{c_{\tilde{\Sigma}'}}(\tilde{\Sigma}'). \quad (5.62)$$

Observe that since a coloring assigns simple objects as labels for the defect lines of $\tilde{\Sigma}$ and $\tilde{\Sigma}'$, the direct sum over the node spaces for all colorings is just the pre-block space:

$$\text{TP}(\tilde{\Sigma}) = \bigoplus_{c_{\tilde{\Sigma}}} N_{c_{\tilde{\Sigma}}}(\tilde{\Sigma}) \quad \text{and} \quad \text{TP}(\tilde{\Sigma}') = \bigoplus_{c_{\tilde{\Sigma}'}} N_{c_{\tilde{\Sigma}'}}(\tilde{\Sigma}'). \quad (5.63)$$

Let us define a vector

$$t(\tilde{M}) := \left(\prod_{\substack{\text{domains } d \\ \text{not adj. to } \tilde{\Sigma}'}} \frac{1}{\mathcal{D}_{\mathcal{A}_d}} \right) \bigoplus_{c_{\tilde{\Sigma}}, c_{\tilde{\Sigma}'}} \frac{1}{\dim_1(c_{\tilde{\Sigma}'})} \sum_{c_{\text{int}}} \dim(c) |\tilde{M}, c| \in \text{TP}(\tilde{\Sigma})^* \otimes \text{TP}(\tilde{\Sigma}'), \quad (5.64)$$

where:

- The product over d runs over domains of \tilde{M} that are not adjacent to the target component of the gluing boundary $\tilde{\Sigma}'$.
- \mathcal{A}_d denotes the spherical fusion category that labels the domain d .
- $c_{\tilde{\Sigma}}$ and $c_{\tilde{\Sigma}'}$ run over colorings for the 2-cells of \tilde{D} adjacent to either part of the gluing boundary, while c_{int} runs over colorings of the 2-cells that are not adjacent to any gluing boundary. Together, they form a coloring $c = c_{\tilde{\Sigma}} \sqcup c_{\text{int}} \sqcup c_{\tilde{\Sigma}'}$ of \tilde{D} .

- Recall that 2-cells of \tilde{D} are labeled by traced bimodule categories, so that the objects a coloring assigns to a 2-cell have a dimension. As in [TV17, Eq. 13.1], the *dimension* $\dim(c)$ of a coloring c is the product of the dimensions of the objects $c(f)$ that c assigns to each 2-cell f of \tilde{D} , exponentially weighted by the Euler characteristic $\chi(f)$ of f :

$$\dim(c) := \prod_{\text{2-cells } f} d_{c(f)}^{\chi(f)}. \quad (5.65)$$

- The *contractible dimension* $\dim_1(c_{\tilde{\Sigma}'})$ is defined analogously, except that the Euler characteristic is not taken into account:

$$\dim_1(c_{\tilde{\Sigma}'}) := \prod_{\substack{\text{2-cells } f \\ \text{adjacent to } \tilde{\Sigma}'}} d_{c(f)}. \quad (5.66)$$

Since the dimensions of simple objects in a traced bimodule category are invertible, so is $\dim_1(c_{\tilde{\Sigma}'})$.

The vector $t(\tilde{M})$ from (5.64) corresponds, in the usual way, to a linear map $\tau^P(\tilde{M}) : \mathbb{T}^P(\tilde{\Sigma}) \rightarrow \mathbb{T}^P(\tilde{\Sigma}')$. We conjecture that τ^P is functorial in the sense that, given another sufficiently refined defect 3-cobordism $\tilde{N} : \tilde{\Sigma}' \rightarrow \tilde{\Sigma}''$, the linear map $\tau^P(\tilde{M} \sqcup_{\tilde{\Sigma}'} \tilde{N})$, which is associated to the defect 3-cobordism $\tilde{M} \sqcup_{\tilde{\Sigma}'} \tilde{N}$ obtained by gluing \tilde{M} and \tilde{N} along $\tilde{\Sigma}'$, is equal to the composition

$$\tau^P(\tilde{M} \sqcup_{\tilde{\Sigma}'} \tilde{N}) = \tau^P(\tilde{N}) \circ \tau^P(\tilde{M}). \quad (5.67)$$

The functoriality property (5.67) would generalize the known statement for the monochromatic case without free boundaries [TV17, Lem. 13.3], and in the presence of monochromatic free boundaries [Far20, Lem. 4.3.4]. The dimensions and normalization factors in (5.64) are chosen such that we expect these proofs to extend to (5.67).

Let us now suppose that \tilde{M}_1 and \tilde{M}_2 are two refinements of \tilde{M} , which are both defect 3-cobordisms $\tilde{M}_1, \tilde{M}_2 : \tilde{\Sigma} \rightarrow \tilde{\Sigma}'$ between the refinements $\tilde{\Sigma}, \tilde{\Sigma}'$ of Σ and Σ' . Then we obtain two linear maps $\tau^P(\tilde{M}_1), \tau^P(\tilde{M}_2) : \mathbb{T}^P(\tilde{\Sigma}) \rightarrow \mathbb{T}^P(\tilde{\Sigma}')$, with common source and target. In the monochromatic case, [TV17, Thm. 15.8] states that these maps are equal. We expect the same independence of the refinement to remain valid in our case:

$$\tau^P(\tilde{M}_1) = \tau^P(\tilde{M}_2). \quad (5.68)$$

If this is true, it immediately follows from the functoriality property (5.67) that the linear map $\tau^P(\tilde{\Sigma} \times [0, 1]) : \mathbb{T}^P(\tilde{\Sigma}) \rightarrow \mathbb{T}^P(\tilde{\Sigma})$ assigned to the cylinder over $\tilde{\Sigma}$ is an idempotent. We set

$$\tau(\tilde{\Sigma}) := \text{im } \tau^P(\tilde{\Sigma} \times [0, 1]). \quad (5.69)$$

and define $\tau(\tilde{M}) : \tau(\tilde{\Sigma}) \rightarrow \tau(\tilde{\Sigma}')$ as the restriction of $\tau^P(\tilde{M}) : \mathbb{T}^P(\tilde{\Sigma}) \rightarrow \mathbb{T}^P(\tilde{\Sigma}')$ to these subspaces. The assumed independence of the internal refinement (5.68) ensures that there is a distinguished isomorphism $\tau(\tilde{\Sigma}_1) \cong \tau(\tilde{\Sigma}_2)$ between the vector spaces associated to a pair of refinements $\tilde{\Sigma}_1, \tilde{\Sigma}_2$ of a defect surface Σ , and that these isomorphisms, considered for all refinements of Σ ,

assemble into a clique. This makes it possible to extend the construction of τ to defect surfaces Σ which may not be sufficiently fine:

$$\tau(\Sigma) := \lim_{\text{refinements } \tilde{\Sigma} \text{ of } \Sigma} \tau(\tilde{\Sigma}). \quad (5.70)$$

Moreover, we obtain a well-defined linear map $\tau(M) : \tau(\Sigma) \rightarrow \tau(\Sigma')$ for a defect 3-cobordism $M : \Sigma \rightarrow \Sigma'$.

This sketch of the construction of a topological field theory τ with defects is a natural extension of the definition of the Graph TQFT from [TV17]. Of course, much work is left to be done for the definition of τ to become well-defined: We have not made the category of defect 3-cobordisms precise enough: how which topologies exactly are allowed for the defect structures? Another vague term is that of *refinement* – it is unclear when a defect structure is *sufficiently fine*. Once these questions are answered, several theorems have to be proved. Namely, the functoriality property (5.67) has to be shown, along with the independence of $\tau^{\mathbb{P}}$ of the internal refinement (5.68). The latter property in particular appears challenging, and the proof of the corresponding statement in the monochromatic case [TV17, Thm. 15.8] is extensive. Notwithstanding these challenges, the results of the present thesis have brought us closer to giving a full definition of the state-sum model with defects τ . The evaluation of extruded graphs introduced in Definition 3.17 was prominently used in (5.61), and Theorem 5.12 ensures that our proposed evaluation at vertices specializes to the usual evaluation at vertices in the monochromatic case, as described in [TV17, Sec. 15.5.1].

Considering the state-sum model with defects τ also prompts questions on the relationship of τ to other TFT-like models. Given that the modular functor from [FSS22] was heavily used in the definition of extruded graphs, and that both it and τ use the same pre-block spaces as intermediate data for their definition, it is natural to expect a close connection. We therefore formulate

Conjecture 5.14. *The linear map $\tau^{\mathbb{P}}(\tilde{\Sigma} \times [0, 1]) : \mathbb{T}^{\mathbb{P}}(\tilde{\Sigma}) \rightarrow \mathbb{T}^{\mathbb{P}}(\tilde{\Sigma})$ is equal to the holonomy idempotent h from Definition 3.16, and thus its image is equal to the block space*

$$\tau(\tilde{\Sigma}) = \mathbb{T}(\tilde{\Sigma}). \quad (5.71)$$

To finalize this outlook, we end with a few remarks on further implications of extruded graphs and the state-sum model with defects.

Remark 5.15. The possibility to consider extruded graphs on higher-genus surfaces allows for the definition of another TFT η that assigns block spaces to defect surfaces. On a sufficiently refined defect 3-cobordism $M : \Sigma \rightarrow \Sigma'$, it is defined as follows. First, choose core labels α, β for the defect surfaces Σ, Σ' and fix a coloring c for the defect structure of M . This turns Σ and Σ' into extruded graphs, possibly of higher genus. They, together with the extruded graphs Γ_v for internal vertices v that we encountered in (5.57), have nodes which come in pairs determined by the edges of the defect structure. The two nodes of a pair are in such a duality as needed to apply the hypothesized move **G**. We would like to perform **G** on all such pairs. This is almost possible, with a caveat: Extruded graphs do not allow closed defect loops without a node. This is remedied by inserting a transparent vertex using **DV** whenever such a closed loop would

appear. We obtain an extruded graph Γ_c this way, which is still dependent on the coloring c . The association $\alpha \otimes \beta \mapsto |\Gamma_c|$ is a map $T(\Sigma) \otimes T(\Sigma')^* \rightarrow \mathbb{K}$, which corresponds to a linear map $\eta_c(M) : T(\Sigma) \rightarrow T(\Sigma')$. While different choices for the order in which the several instances of the moves **G** and **DV** were applied may result in different extruded graphs Γ_c , the fact that these moves are by Theorem 4.4 invariances implies that $\eta_c(M)$ is well-defined. Finally we define

$$\eta(M) := \left(\prod_{\substack{\text{domains } d \\ \text{not adj. to } \Sigma'}} \frac{1}{\mathcal{D}_{\mathcal{A}_d}} \right) \sum_c \frac{\dim(c)}{\dim_1(c_{\Sigma'})} \eta_c(M) : T(\Sigma) \rightarrow T(\Sigma'). \quad (5.72)$$

We refrain from showing here that η is functorial. If we assume Conjecture 5.14, then τ and η can be directly compared. We expect them to be equal,

$$\eta(M) = \tau(M), \quad (5.73)$$

which would imply that there exists a description of state-sum models (5.72) which uses the evaluation of a tubular neighborhood of the 1-skeleton of the defect structure of a 3-cobordism M , considered as an extruded graph.

Remark 5.16. A different description of a 3-dimensional state-sum TFT with defects in all codimensions was given in [Meu22]. This construction is indeed independent of the chosen triangulation. However, it is also more restrictive than our proposed model in that the defect structure is required to form a 2-manifold. In particular, no defect lines with more than two adjacent defect surfaces are allowed.

This makes it working with bimodule functors as opposed to objects in relative Deligne products as labels for defect lines manageable. Moreover, since vertices (0-dimensional defects) lie embedded in a surface, the adjacent defect lines are cyclically ordered. For this reason, polygon diagrams, as opposed to more general extruded graphs, are sufficient to describe their neighborhoods.

Another difference between to our proposed model is that the TFT from [Meu22] is based on a formulation of state-sum models that can be thought of as Poincaré-dual to our approach: Instead of a skeleton as an auxiliary structure, a triangulation (or a polytope complex in the sense of [BK10]) is used. In transitioning from a skeleton to a triangulation, the n -dimensional components of the skeleton become $(3 - n)$ -dimensional cells of the triangulation. This means we no longer evaluate at vertices, but at 3-cells; Edges, instead of faces, now have to be labeled by state-sum variables, and so on.

Crucially, however, this Poincaré-dualization should only be applied to the auxiliary structure of a skeleton – and not to the defect structure of a cobordism. This highlights a difference between the two models. In the formulation of [Meu22], defect structures and triangulations have to be treated as separate types of objects: The defect structure is part of the data of a cobordism, whereas a triangulation is auxiliary and serves only a technical purpose in the definition of the model. In our formulation, on the other hand, we expect to be able to view a skeleton as a sufficiently refined kind of defect structure. Defect structures and the auxiliary structures used to define the model are, fundamentally, of the same type. The auxiliary part of the defect structure is then the monochromatic substructure. This prompts the question: Do defect structures which

only differ by some monochromatic substructure evaluate to equal linear maps under a state-sum TFT? This relates to the next remark.

Remark 5.17. In our formulation of the state-sum model τ , the defect structure is taken as a rigid input datum, and there is no relation between different defect structures on a given 3-manifold. However, there are physical and mathematical reasons why we should consider defect structures related if they cannot be distinguished by τ . More precisely, τ defines an equivalence relation on the set of cobordisms $M : \Sigma \rightarrow \Sigma'$, generated by those local moves on defect structures that leave $\tau(M)$ invariant. Investigating the equivalence classes of cobordisms brings challenges for future work, such as answering the question: Can we give an explicit description of a generating set (comprising of local moves of defect structures) for this equivalence relation?

Remark 5.18. We already remarked on the close relation between extruded graphs and a graphical calculus for tricategories in Remark 3.3. There, we explained how extruded graphs could be viewed as 3-diagrams, and how the evaluation of extruded graphs could be obtained from the evaluation of 3-diagrams. Let us now reverse this reasoning, and try to find a way to use the evaluation of extruded graphs to define an evaluation of 3-diagrams by means of the proposed state-sum TFT τ , assuming Conjecture 5.14.

To this end, consider a defect 3-cobordism M whose underlying 3-manifold is a closed ball with a finite number of open balls removed from its interior. Declare the boundary sphere Σ' of the closed ball to be the target component of the 3-cobordism, and the remaining boundary (spheres $\Sigma_1, \dots, \Sigma_n$ in the interior) to be the source defect surface. Now pick a vector $\varphi_i \in T(\Sigma_i)$ for each connected component of the source defect surface. The defect 3-cobordism M , together with the φ_i , can be viewed as a kind of 3-diagram, which unlike the 3-diagrams considered in [BMS12] is not embedded in the standard cube $[0, 1]^3$, but in some closed ball. Instead of vertices, M has ball-shaped holes, which is an irrelevant difference. The labeling of the vertices on the other hand is a real difference: Without the ambient ("blackboard") framing of the standard cube, we cannot hope to assign 3-morphisms from concrete hom-spaces to vertices (or boundary components). Rather, we have to use the block space, which we think of as a symmetric version of the 3-morphism hom-spaces.

For the same reason, our version of a 3-diagram cannot be evaluated to a 3-morphism, but defines instead a vector in the block space for the target defect surface Σ' of M . Indeed, the TFT associates to M a linear map (we assume Conjecture 5.14)

$$T(M) : T(\Sigma_1) \otimes \cdots \otimes T(\Sigma_n) \rightarrow T(\Sigma'). \quad (5.74)$$

We declare $T(M)(\varphi_1 \otimes \cdots \otimes \varphi_n) \in T(\Sigma')$ to be the evaluation of the 3-diagram (M, φ_\bullet) . This evaluation is clearly isotopy invariant.

Let M' be the manifold obtained from M by collapsing the source defect surfaces into individual points. M' is topologically a closed ball. We expect that a homeomorphism $M' \cong [0, 1]^3$, which satisfies several non-singularity conditions, defines isomorphisms between each block space involved and a concrete hom-space, and thus defines a 3-diagram in the sense of [BMS12]. The evaluation of this 3-diagram can then be compared to the evaluation of (M, φ_\bullet) in our sense. It seems likely that they are equal or differ only by a normalization factor. If this is true, then the

evaluation of extruded graphs, which is essential in the definition of the TFT, facilitates the definition of an isotopy invariant evaluation of non-framed 3-diagrams in BiMod^{Tr} .

REFERENCES

- [BDSPV15] B. Bartlett, C. Douglas, C. Schommer-Pries, and J. Vicary. “Modular categories as representations of the 3-dimensional bordism 2- category” (2015). URL: <https://arxiv.org/abs/1509.06811>.
- [BK00] B. Bakalov and A. Kirillov Jr. “On the Lego-Teichmüller Game.” *Transformation Groups* 5(3) (2000), 207–244.
- [BK10] B. Balsam and A. Kirillov Jr. “Turaev-Viro Invariants as an Extended TQFT” (2010). URL: <http://arxiv.org/abs/1004.1533>.
- [BM21] N. Bortolussi and M. Mombelli. “(Co)ends for representations of tensor categories.” *Theory and Applications of Categories* 37.6 (2021), 144–188.
- [BMS12] J. W. Barrett, C. Meusburger, and G. Schaumann. “Gray categories with duals and their diagrams” (2012). URL: <https://arxiv.org/abs/1211.0529>.
- [BS11] J. Baez and M. Stay. “Physics, Topology, Logic and Computation: A Rosetta Stone.” *New Structures for Physics*. Ed. by Bob Coecke. Vol. 813. Lecture Notes in Physics. Springer Berlin, 2011, 95–174.
- [BW96] J. W. Barrett and B. W. Westbury. “Invariants of Piecewise-Linear 3-Manifolds.” *Trans. Amer. Math. Soc.* 348 (1996), 3997–4022.
- [Cos04] K. Costello. “Topological conformal field theories and Calabi-Yau categories” (2004). URL: <https://arxiv.org/abs/math/0412149>.
- [DSS20] C. L. Douglas, C. J. Schommer-Pries, and N. Snyder. “Dualizable tensor categories.” *Memoirs of the American Mathematical Society* (2020).
- [EGNO15] P. Etingof, S. Gelaki, D. Nikshych, and V. Ostrik. *Tensor Categories*. Vol. 205. Mathematical Surveys and Monographs. American Math. Soc., 2015.
- [ENOM10] P. Etingof, D. Nikshych, V. Ostrik, and E. Meir. “Fusion categories and homotopy theory.” *Quantum Topology* 1 (2010), 209–273.
- [Far20] J. Farnsteiner. “Generalized Frobenius-Schur Indicators as Turaev-Viro Invariants” (Sept. 2020).
- [FGJS22] J. Fuchs, C. Galindo, D. Jaklitsch, and C. Schweigert. “Spherical Morita contexts and relative Serre functors” (2022). URL: <https://arxiv.org/abs/2207.07031v2>.
- [FS22] J. Farnsteiner and C. Schweigert. “Frobenius–Schur indicators and the mapping class group of the torus.” *Lett Math Phys* 112 (2022), 39.
- [FSS17] J. Fuchs, G. Schaumann, and C. Schweigert. “A Trace for Bimodule Categories.” *Applied Categorical Structures* 25 (2017), 227–268.

- [FSS20a] J. Fuchs, G. Schaumann, and C. Schweigert. “Eilenberg-Watts calculus for finite categories and a bimodule Radford S^4 theorem.” *Trans. Amer. Math. Soc.* 373 (2020), 1–40.
- [FSS20b] J. Fuchs, G. Schaumann, and C. Schweigert. “Module Eilenberg-Watts calculus” (2020). URL: <https://arxiv.org/abs/2003.12514>.
- [FSS22] J. Fuchs, G. Schaumann, and C. Schweigert. “A modular functor from state sums for finite tensor categories and their bimodules.” *Theory and Applications of Categories* 38 (2022), 436–594.
- [FSV13] J. Fuchs, C. Schweigert, and A. Valentino. “Bicategories for Boundary Conditions and for Surface Defects in 3-d TFT.” *Commun. Math. Phys.* 321 (2013), 543–575.
- [FSY23] J. Fuchs, C. Schweigert, and Y. Yang. “String-net models for pivotal bicategories” (2023). URL: <https://arxiv.org/abs/2302.01468>.
- [Hat01] A. Hatcher. *Algebraic Topology*. Cambridge University Press, 2001.
- [Hum12] Ben Hummon. “Surface diagrams for gray-categories.” Phd Thesis, UC San Diego, 2012.
- [JS91] A. Joyal and R. Street. “The geometry of tensor calculus, I.” *Advances in Mathematics* 88.1 (1991), 55–112.
- [KK12] A. Kitaev and L. Kong. “Models for Gapped Boundaries and Domain Walls.” *Commun. Math. Phys.* 313 (2012), 351–373.
- [LFHSV21] L. Lootens, J. Fuchs, J. Haegeman, C. Schweigert, and F. Verstraete. “Matrix product operator symmetries and intertwiners in string-nets with domain walls.” *SciPost Phys.* 10 (2021), 053.
- [Mac71] S. MacLane. *Categories for the Working Mathematician*. Vol. 5. Graduate Texts in Mathematics. Springer, 1971.
- [Meu22] C. Meusburger. “State sum models with defects based on spherical fusion categories” (2022). URL: <https://arxiv.org/abs/2205.06874>.
- [MS89] G. Moore and N. Seiberg. “Classical and quantum conformal field theory.” *Comm. Math. Phys.* 123 (1989), 177–254.
- [NS07] S. Ng and P. Schauenburg. “Higher Frobenius-Schur Indicators for Pivotal Categories.” *Hopf Algebras and Generalizations, Contemp. Math.* 441 (2007), 63–90.
- [NS10] S. Ng and P. Schauenburg. “Congruence Subgroups and Generalized Frobenius-Schur Indicators.” *Commun. Math. Phys.* 300 (2010), 1–46.
- [PR68] G. Ponzano and T. Regge. “Semiclassical limit of Racah coefficients.” *Spectroscopic and group theoretical methods in physics*. Ed. by F. Bloch. North-Holland Publ. Co., 1968, 1–58.
- [Rie14] E. Riehl. *Categorical Homotopy Theory*. Cambridge University Press, 2014.
- [Sch13a] G. Schaumann. “Duals in Tricategories and in the Tricategory of Bimodule Categories.” Phd thesis. Friedrich-Alexander-Universität Erlangen-Nürnberg, Sept. 2013.

- [Sch13b] Gregor Schaumann. “Traces on module categories over fusion categories.” *Journal of Algebra* 379 (2013), 382–425.
- [Sch15] Gregor Schaumann. “Pivotal tricategories and a categorification of inner-product modules.” *Algebr Represent Theor* 19 (2015), 1407–1479.
- [Shi20] K. Shimizu. “Further Results on the Structure of (Co)Ends in Finite Tensor Categories.” *Applied Categorical Structures* 28 (2020), 237–286.
- [TV10] V. Turaev and A. Virelizier. “On two approaches to 3-dimensional TQFTs” (2010). URL: <https://arxiv.org/abs/1006.3501>.
- [TV17] V. Turaev and A. Virelizier. *Monoidal Categories and Topological Field Theory*. Vol. 322. Progress in Mathematics. Birkhäuser Basel, 2017.
- [TV92] V. G. Turaev and O. Y. Viro. “State Sum Invariants of 3-Manifolds and Quantum 6j-Symbols.” *Topology* 31 No. 4 (1992), 865–902.

